PG&E – PEER Directed Studies Program, Phase II

GOODNESS OF FIT IN SIMULATED NEAR-FAULT LONG PERIOD GROUND MOTIONS

FINAL REPORT

by

Robert Graves, Arben Pitarka, Nancy Collins, Paul Somerville
URS Greiner Woodward Clyde, Pasadena, CA

August 31, 1999

PG&E - PEER DIRECTED STUDIES PROGRAM, Phase II

GOODNESS OF FIT IN SIMULATED NEAR-FAULT LONG PERIOD GROUND MOTIONS

FINAL REPORT

August 31, 1999

Robert Graves, Arben Pitarka, Nancy Collins, Paul Somerville
URS Greiner Woodward Clyde, Pasadena, CA

INTRODUCTION

The objective of this project is to validate procedures for generating near-fault ground motions by simulating the ground motions of past earthquakes and comparing the results with the recorded ground motions. The period range of interest in this project is specified to be 0.125 Hz to 1.43 Hz (8 seconds to 0.7 seconds period). In this project, we have validated our simulation procedures against recordings of the five earthquakes listed in Table 1, which all have important near-fault recordings.

Near-fault ground motions have special characteristics (Somerville et al., 1997) which need to be considered in selecting procedures for quantifying the goodness of fit. First, the fault-normal component is systematically larger than the fault parallel component at periods longer than about 0.5 seconds. In characterizing near-fault ground motions for design, it is often appropriate to specify the fault normal and fault components separately. Accordingly, in validating a near-fault ground motion simulation procedure, it is appropriate to generate separate fault normal and fault parallel components and validate them against the corresponding recorded components. Second, the fault-normal component is often characterized by a coherent pulse of long-period motion. Unlike the case with most strong motion recordings which are predominantly stochastic, the waveform of this long-period is pulse is predominantly deterministic and is amenable to waveform modeling.

METHODS OF QUANTIFYING GOODNESS OF FIT

Based on the characteristics of near-fault ground motions described above, the methods that were selected to measure the goodness of fit between the recorded and simulated ground motions are as follows:

1. Response spectral ratio at 5% damping, measured by the natural logarithm of the difference between the recorded and simulated ground motions (Abrahamson et al., 1990). This is the conventional means of specifying design ground motions. It is sensitive to both the amplitude and the phasing of the ground motions, and is sensitive to a range of periods surrounding the specified ground motion period. Its value is 0 for a perfect fit, positive for underprediction, and negative for overprediction.

2. Fourier amplitude spectral ratio, measured by the natural logarithm of the difference between the recorded and simulated ground motions. This is the conventional means of quantifying spectral amplitudes in seismology. It is sensitive to absolute amplitude but insensitive to phase. Smoothing of the Fourier spectrum is required to give a meaningful estimate. Its value is 0 for a perfect fit, positive for underprediction, and negative for overprediction.

3. Cross correlation between the simulated and recorded ground motions. This provides a measure of the waveform fit, and is sensitive to phasing - the distribution of energy with time - but is insensitive to absolute amplitude. Its value lies in the range of 1 (perfect fit) to -1 (perfect anticorrelation). We use a window length of 15 seconds for the cross correlation.

4. Least squares fit, as measured by the equation

$$r^2 = (SRSS_{data} - SRSS_{residual}) / SRSS_{data}$$

where SRSS = square root of sum of squares, summed over the time series. We use a window length of 15 seconds for the cross correlation. The time series is the recorded time history for *data* and the difference between the recorded and simulated time histories for *residual*. This measure is sensitive to both absolute amplitude and phase. Its maximum value (for a perfect fit) is 1. For a null simulation, its value is zero, and it can have an unbounded negative value if the wave forms have negative correlation and very large differences in amplitude.

SIMULATION PROCEDURE

To simulate broadband time histories, the ground motions are computed separately in the short period and long period ranges, and then combined into a single broadband time history (Somerville et al., 1995; 1996). The use of different methods in these two period ranges is necessitated by the observation that ground motions have fundamentally different characteristics in these two period ranges. At long periods (longer than about 1 second), strong ground motions are deterministic in the sense that seismological models are capable of matching not only the spectral amplitudes but also the waveforms of recorded long period ground motions, once the rupture model of the earthquake and the seismic velocity structure of the region surrounding the earthquake are known. At short periods (shorter than about 1 second), strong ground motions become increasingly stochastic in nature. Seismological models are generally capable of matching the spectral amplitudes of the short period ground motions, but are generally not capable of matching the recorded waveforms. The transition from deterministic to stochastic behavior appears to be due to a transition from coherent source radiation and wave propagation conditions at long periods (over long dimensions) to incoherent source radiation and wave propagation conditions at short periods (over short dimensions). The two simulations are combined using matched filters at 1 Hz. For this study, we have used just the long period component of the broadband simulation procedure, because it almost spans the frequency range of interest in this study, which is 0.125 Hz to 1.43 Hz.

The Green's function method that we use to calculate the long period ground motions has a rigorous basis in theoretical and computational seismology (Helmberger, 1983). The earthquake source is represented as a shear dislocation on an extended fault plane, whose radiation pattern is accurately represented. Wave propagation is represented rigorously by Green's functions

computed for the seismic velocity structure which contains the fault and the site. These Green's functions contain both body waves and surface waves. The ground motion time history is calculated in the time domain using the elastodynamic representation theorem. This involves integration over the fault surface of the convolution of the slip time function on the fault with the Green's function for the appropriate depth and distance.

The near-fault strong motion recordings of the 1995 Kobe earthquake were strongly influenced by the basin edge effect due to the interaction of direct and diffracted waves at the edge of the Osaka basin (Pitarka et al., 1999). For this earthquake, at some stations it was necessary to use Green's functions calculated for a 3D velocity model using finite difference methods (e.g. Graves, 1996). For the other four earthquakes, the near-fault ground motions were not so strongly influenced by 3D velocity structure. In the 1994 Northridge earthquake, the deep structure of the Los Angeles basin had a strong influence on the ground motions recorded in the Los Angeles basin (Graves et al., 1999). These recordings do not contain forward rupture directivity effects, and so they were excluded from this study.

EARTHQUAKE RUPTURE MODELS AND CRUSTAL VELOCITY MODELS

In this study, we used earthquake rupture models derived by other investigators from the inversion of strong motion and other data. These rupture models are listed in Table 1 and analyzed in Somerville et al. (1999). The inversion process involves the calculation of Green's functions that represent the propagation of seismic waves between the source and the site. The degree to which we can accurately represent site effects in our simulations depends on the appropriateness of the shallow seismic velocity structures that were used in the rupture model inversions. The velocity models used in the simulations of the five events are listed in Tables 2 through 6.

For two of the five events analyzed, we consider that the velocity models used were quite realistic. In the 1979 Imperial Valley earthquake, all of the recording sites are on alluvium, and the Green's functions were calculated using a single seismic velocity model representing these uniform site conditions. We used this seismic velocity model to calculate the Green's functions used in our simulations. For the 1995 Kobe earthquake, the simulations at soil and rock sites were done using separate velocity models. In addition, Green's functions for a 3D basin velocity model were used to calculate the ground motions at sites located on the Osaka basin.

For the other three events analyzed, the velocity models used in the rupture model inversion may be less realistic. For the 1989 Loma Prieta earthquake, the inversion was based on a single seismic velocity model that is representative of rock site conditions. We used this seismic velocity model to simulate the ground motions on both rock and soil sites. In the 1994 Northridge earthquake, separate Green's functions for rock and soil sites were used in the inversion of the rupture model. We used the velocity model for rock sites to calculate the Green's functions for simulations on both rock and soil sites. It would have been preferable to use Green's functions calculated for separate rock and soil velocity models in simulations for the respective site categories. The rupture model of the 1992 Landers earthquake was generated using a seismic velocity having quite high surface velocity. We used separate velocity models for soil and rock conditions in our simulations for this earthquake. The only rock site that we modeled was the Lucerne recording.

RESULTS

The results of the validation studies are presented as sets of tables and figures for each earthquake. The table contains a summary of the goodness of fit measurements. These measurements are provided for individual stations, listed on the left hand column of the table. The median, standard deviation, and standard error of the mean of the stations are given at the bottom of the table. The first two columns show the maximum cross correlation between the recorded and simulated velocity time history, where each has been bandpass filtered with a 3 pole Butterworth filter in the frequency range of 0.125 Hz to 1.43 Hz. The first column shows the peak cross correlation for the fault normal component, and the second column shows the peak cross correlation for the fault parallel component in cases where the time lag for maximum cross correlation for the fault normal and fault parallel components are within 0.25 seconds of each other. We assume that the cross correlation lag of the dominant fault normal component is correct, and do not use the peak cross correlation of the fault parallel component if its lag is too different from that of the fault normal component. In most cases, only those recordings with strong forward rupture directivity effects and simple velocity waveforms have coincident peak cross correlations.

The third column show the minimum least squares fit for the fault normal component, and the fourth column shows the minimum least squares fit to the fault parallel component in cases where the time lag for minimum least squares for the fault normal and fault parallel components are within 0.25 seconds of each other. The least squares fit can be low even where the cross correlation is high if there are large differences in the amplitudes of the recorded and simulated waveforms. This is because the cross correlation is not sensitive to amplitude but the least squares measure is. In most cases, only those recordings with strong forward rupture directivity effects and simple velocity waveforms have coincident minimum least squares. In some cases, the least squares measure is less than zero, indicating a fit that is worse than a null simulation. These negative values arise from large discrepancies in amplitude and phase between the recorded and simulated ground motions. We do not find these results intuitively meaningful, because the simulations appear to be much better fits to the data than a null simulation, and have fairly high cross correlations.

The fifth and sixth columns show the natural logarithm of the difference between the recorded and simulated response spectrum, and the seventh and eighth columns show the natural logarithm of the difference between the recorded and simulated Fourier amplitude spectrum, averaged over the frequency range of 0.125 to 1.43 Hz. We used frequencies that were approximately evenly spaced in log frequency to give more weight to the longer periods. These values are shown separately for the fault normal and fault parallel components.

Following the table, the recorded and simulated velocity waveforms, bandpass filtered with a 3 pole Butterworth filter in the frequency range of 0.125 Hz to 1.43 Hz, are compared for each recording of the event. The comparisons for fault normal and fault parallel components are shown on separate pages. The recorded and simulated waveforms are aligned at the time lag that gives the maximum cross correlation for the fault normal component. The cross correlation and least squares values are given in the table described above.

The time history plots are followed by plots comparing the velocity response spectra and the Fourier amplitude spectra of the recorded and simulated velocity time histories, with one figure for each recording. Summary station by station plots of all recordings analyzed are first

presented, together with goodness of fit plots (showing bais and standard error) for the set of stations. These are followed by detailed plots of Fourier amplitude velocity spectra for each recording station. The figures on the left show the two spectra, and the figures on the right show the ratio of recorded to simulated motions. The top two plots show these comparisons separately for the fault normal and fault parallel components on a log-log scale. The bottom two plots show the same comparisons on a linear-linear scale.

TEST FOR DIRECTIVITY EFFECTS IN DATA AND SIMULATIONS

To evaluate the efficacy of the simulation procedure in predicting near-fault rupture directivity effects, we can examine whether the residuals between recorded and simulated ground motions have a trend that is related to rupture directivity. If a ground motion model (such as a conventional empirical attenuation relation) does not address rupture directivity effects, then this trend should be present in the residuals. If the simulation is effective in representing directivity effects, then this trend should not be present in the residuals.

We parameterize the rupture directivity effect by the directivity function X cos θ (for the strike-slip component of faulting) and Y cos ϕ (for the dip slip component of faulting), as shown in Figure 1, following Somerville et al. (1997). The angles θ and ϕ represent the angle between the fault plane and the line connecting the hypocenter to the site (θ is measured in the horizontal plane for strike-slip faulting and ϕ is measured in the vertical plane for dip-slip faulting). X and Y represent the fraction of the fault rupture that lies between the hypocenter and the site (X is measured along strike for strike-slip faulting and Y is measured up dip for dip-slip faulting). The form X cos θ and Y cos ϕ used in the directivity function is based on the assumption that directivity effects are influenced by two geometrical parameters. First, the smaller the angle between the direction of rupture propagation and the direction of waves travelling to the site, the larger the amplitude of the ground motion. Second, the larger the fraction of the fault rupture surface that lies between the hypocenter and the site, the larger the amplitude. This model was subsequently revised by Abrahamson (report to Caltrans, 1999) such that the directivity effect saturates for X and Y values larger than 0.4.

Of the four parameters we have used to measured goodness of fit in this study, only one (response spectral acceleration) is addressed in the rupture directivity model of Somerville et al. (1997) and in standard ground motion models. Accordingly, we have used response spectral acceleration at a fixed response spectral period as the parameter with which to analyze the effectiveness of the simulation procedure.

The figures show the results for the strike slip component of rupture directivity (X cos θ) on the left side, and the dip slip component of rupture directivity (Y cos ϕ) on the right side for a specified ground motion period. The top part of each figure shows the residuals between the recorded data and the empirical ground motion model of Abrahamson and Silva (1997). This model does not include the directivity function as a parameter. For all earthquakes, the residuals between the data and the Abrahamson and Silva (1997) model show a trend of increasing residual with increasing directivity function at some periods. This demonstrates that there are directivity effects in the data and that these effects have the trend expected from the model of directivity effects represented by the directivity function. The lower part of each figure shows the residuals between the data and our simulation results. These residuals do not have the trend that is present in the upper figure, indicating that the simulations are effective in modeling the directivity effects

that are present in the data.

REFERENCES

Abrahamson, N.A. and W.J. Silva (1997). Empirical response spectral attenuation relations for shallow crustal earthquakes, *Seismological Research Letters* 68, 94-127.

Abrahamson, N.A., P.G. Somerville, and C. Allin Cornell (1990). Uncertainty in numerical strong motion predictions, *Proc. 4th U.S. National Conference on Earthquake Engineering,* **1**, 407-416.

Graves, R. W., A. Pitarka, and P. G. Somerville (1998). Ground motion amplification in the Santa Monica area: effects of shallow basin edge structure, *Bull. Seism. Soc. Am.*, 88, 1224-1242.

Graves, R. W. (1966). Simulating seismic wave propagation in 3D elastic media using staggered-grid finite-differences, *Bull. Seism. Soc. Am.*, 86, 1091-1106.

Hartzell, S. H. and T. H. Heaton (1983). Inversion of strong ground motion and teleseismic waveform data for the fault rupture history of the 1979 Imperial Valley, California, earthquake, *Bull. Seism. Soc. Am.*, **73**, 1553-1583.

Helmberger, D.V. (1983). Theory and application of synthetic seismograms, in Earthquakes: Observation, Theory and Interpretation, Proc. Int. Sch. Phys. "Enrico Fermi" Course LXXXV, pp. 174-221, eds. Kanamori, H. and E. Boschi, North-Holland, Amsterdam.

Kamae, K., K. Irikura and A. Pitarka (1998). A technique for simulating strong ground motion using hybrid Green's functions, *Bull. Seism. Soc. Am.*, 88, 357-367.

Pitarka, A., P. Somerville, Y. Fukushima, T. Uetake, and K. Irikura (1999). Simulation of near-fault ground motion using hybrid Green's functions, submitted to BSSA.

Pitarka, A., K. Irikura, T. Iwata and H. Sekiguchi (1998). Three-dimensional simulation of the near-fault ground motion for the 1995 Hyogo-ken Nanbu (Kobe), Japan, earthquake. *Bull. Seism. Soc. Am.* 88, 428-440.

Somerville, P.G., K. Irikura, R. Graves, S. Sawada, D. Wald, N. Abrahamson, Y. Iwasaki, T. Kagawa, N. Smith and A. Kowada (1999). Characterizing earthquake slip models for the prediction of strong ground motion. *Seismological Research Letters* 70, 59-80.

Somerville, P.G., N.F. Smith, R.W. Graves, and N.A. Abrahamson (1997). Modification of empirical strong ground motion attenuation relations to include the amplitude and duration effects of rupture directivity, *Seismological Research Letters* 68, 199-222.

Somerville, P., C.K. Saikia, D. Wald, and R. Graves (1996). Implications of the Northridge earthquake for strong ground motions from thrust faults, *Bull. Seism. Soc. Am.*, 86, S115-S125.

Somerville, P.G., R.W. Graves, and C.K. Saikia (1995). Characterization of Ground Motions during the Northridge Earthquake of January 17, 1994. *Program to Reduce the Earthquake Hazards of Steel Moment Frame Buildings,* SAC Report 95-03.

Somerville, P.G., D.J. Wald, and N.F. Smith (1993). Prediction of the near-source ground accelerations of the Loma Prieta earthquake using a heterogeneous slip model. Unpublished manuscript.

Wald, D. J., D. V. Helmberger and T. H. Heaton (1991). Rupture model of the 1989 Loma Prieta earthquake from the inversion of strong motion and broadband teleseismic data, *Bull. Seism. Soc. Am.* **81**, 1540-1572.

Wald, D.J., and T.H. Heaton (1994). Spatial and temporal distribution of slip of the 1992 Landers, California earthquake, *Bull. Seism. Soc. Am.* **84**, 668-691.

Wald, D.J., T.H. Heaton, and K.W. Hudnut (1996). The slip history of the 1994 Northridge, California earthquake determined from strong motion, teleseismic, GPS and leveling data. *Bull. Seism. Soc. Am.* **86**, S49-S7

Table 1. Source Parameters of Earthquakes

Earthquake, Location	Date	Mech.	Mo x 10^{25} dyne-cm	Mw	Slip Model Reference
Imperial Valley, Ca.	1979.10.15	SS	5	6.43	Hartzell & Heaton, 1983
Loma Prieta, Ca.	1989.10.17	OB	30	6.95	Somerville et al., 1993; Wald et al., 1991
Landers, Ca.	1992.6.28	SS	75	7.22	Wald et al., 1994
Northridge, Ca.	1994.1.17	RV	11	6.66	Wald et al., 1996
Kobe, Japan	1995.1.17	SS	24	6.9	Pitarka et al.,1999 Kamae et al., 1998

Table 2

Imperial Valley: One-Dimensional Soil Velocity Model

Thickness (km)	Vp (km/s)	Vs (km/s)	Density (g/cm^3)	Qp	Qs
0.50	1.70	0.50	1.80	200	50
0.50	2.10	0.77	1.88	250	80
0.50	2.50	1.05	1.97	500	150
0.50	2.90	1.33	2.05	800	200
0.50	3.40	1.61	2.13	900	250
0.50	3.80	1.89	2.21	1000	300
0.50	4.20	2.16	2.30	1200	350
0.50	4.70	2.44	2.38	1500	500
0.50	5.10	2.72	2.46	1700	700
0.50	5.50	3.00	2.55	2000	800
3.0	5.60	3.14	2.70	2000	800
3.0	5.60	3.14	2.70	2000	800
0.5	7.20	4.16	2.80	2000	800
0.0	7.20	4.16	2.80	2000	800

Table 3

Loma Prieta Velocity Model

Vp (km/sec)	Vs (km/sec)	Density (g/cm^3)	Depth (km)
1.730	1.00	1.50	0.10
3.380	1.95	1.55	0.50
4.290	2.48	1.85	1.00
4.790	2.77	2.05	3.00
5.365	3.10	2.26	5.00
5.740	3.31	2.45	7.00
6.150	3.55	2.58	9.00
6.245	3.61	2.62	13.00
6.270	3.62	2.63	18.00
6.665	3.85	2.77	25.00
8.000	4.62	3.28	

Table 4

Landers: One-Dimensional Soil Velocity Model

Thickness (km)	Vp (km/s)	Vs (km/s)	Density (g/cm^3)	Qp	Qs
0.02	1.40	0.50	1:70	100	30
0.03	1.50	0.75	1.90	100	30
0.05	1.80	1.06	2.00	100	30
0.40	2.30	1.33	2.10	200	100
0.50	2.80	1.66	2.20	600	300
0.50	3.80	1.98	2.30	600	300
2.50	5.50	3.15	2.60	600	300
6.00	6.20	3.52	2.70	600	300
16.00	6.20	3.52	2.70	600	300
6.00	6.80	3.83	2.87	600	300
0.00	8.00	4.64	3.50	600	300

Landers: One-Dimensional Rock Velocity Model

Thickness (km)	Vp (km/s)	Vs (km/s)	Density (g/cm^3)	Qp	Qs
1.50	3.80	1.98	2.30	100	30
2.50	5.50	3.15	2.60	600	300
6.00	6.20	3.52	2.70	600	300
16.00	6.20	3.52	2.70	600	300
6.00	6.80	3.83	2.87	600	300
0.00	8.00	4.64	3.50	600	300

Table 5

Northridge Regional Velocity Structure

A. Rock Stations

Vp (km/sec)	Vs (km/sec)	Density (g/cm)	Thickness (km)	Depth (km)
1.9	1.0	2.1	0.5	0.0
4.0	2.0	2.4	1.0	0.5
5.5	3.2	2.7	2.5	1.5
6.3	3.6	2.8	23.0	4.0
6.8	3.9	2.9	13.0	27.0
7.8	4.5	3.3		40.0

B. Soil Stations

Vp (km/sec)	Vs (km/sec)	Density (g/cm)	Thickness (km)	Depth (km)
0.8	0.3	1.7	0.1	0.0
1.2	0.5	1.8	0.2	0.1
1.9	1.0	2.1	0.2	0.3
4.0	2.0	2.4	1.0	0.5
5.5	3.2	2.7	2.5	1.5
6.3	3.6	2.8	23.0	4.0
6.8	3.9	2.9	13.0	27.0
7.8	4.5	3.3		40.0

Table 6a

Kobe One-Dimensional Velocity Models

Site: KBU					
Depth (km)	Vp (km/s)	Vs (km/s)	Density (g/cm^3)	Qp	Qs
0.5	3.2	1.8	2.0	500	300
5.0	5.7	3.2	2.4	1000	400
>5.0	6.0	3.46	2.7	1000	500

Site: KOB					
Depth (km)	Vp (km/s)	Vs (km/s)	Density (g/cm^3)	Qp	Qs
0.06	1.5	0.45	1.9	150	80
0.2	1.7	0.55	2.0	150	80
0.4	1.8	0.65	2.0	150	80
0.6	1.9	1.1	2.2	300	170
5.0	5.7	3.2	2.4	1000	400
>5.0	6.0	3.46	2.7	1000	500

Site: MOT					
Depth (km)	Vp (km/s)	Vs (km/s)	Density (g/cm^3)	Qp	Qs
0.035	1.5	0.3	1.9	130	50
0.05	1.7	0.45	1.9	150	80
0.15	1.8	0.50	2.0	150	80
0.30	1.8	0.65	2.0	150	80
0.6	1.9	1.1	2.2	300	170
5.0	5.7	3.2	2.4	1000	400
>5.0	6.0	3.46	2.7	1000	500

Table 6b

Kobe Site: Takatori; 1D slice through3D velocity model

Vp (km/sec)	Vs (km/sec)	Density (g/cm^3)	Depth (km)
1.4	0.15	1.8	0.0
1.5	0.30	1.8	0.01
1.5	0.40	1.8	0.02
1.5	0.45	1.8	0.03
1.6	0.50	1.85	0.04
1.6	0.55	1.85	0.1
1.6	0.60	1.85	0.2
1.7	0.70	1.9	0.3
1.8	0.75	1.9	0.4
1.9	0.85	1.95	0.5
2.0	0.92	2.0	0.6
2.1	1.1	2.0	0.8
5.4	3.2	2.6	>1.0

Kobe, Landers, Loma Prieta, Northridge - Fault Normal

Spectral Acceleration at 5.0 sec

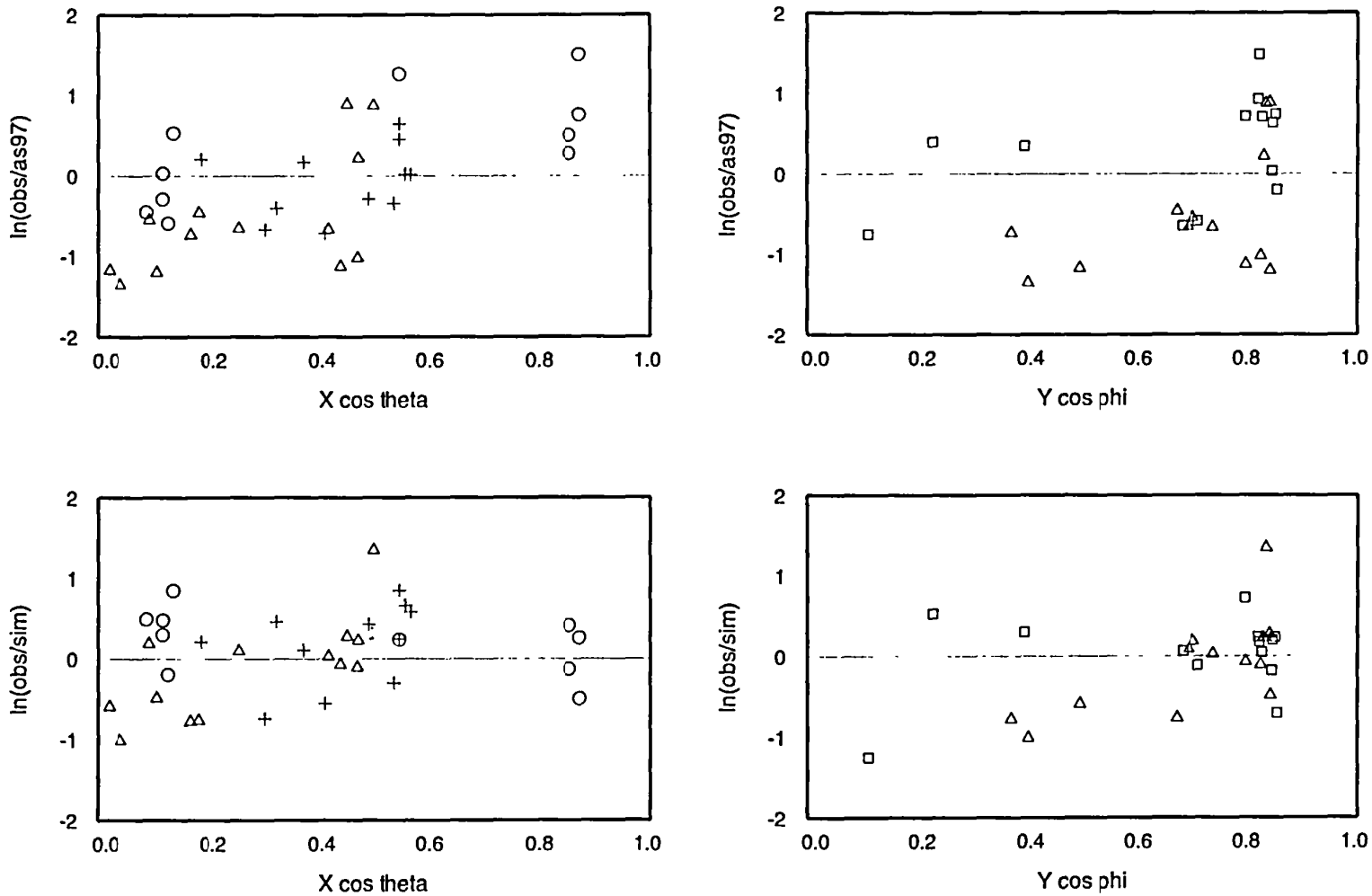

+ Kobe
○ Landers
△ Loma Prieta
□ Northridge

GMT Aug 25 11:16:45 1999 /u1/nancy/PEER-5/Comparisons

Kobe, Landers, Loma Prieta, Northridge - Fault Parallel

Spectral Acceleration at 5.0 sec

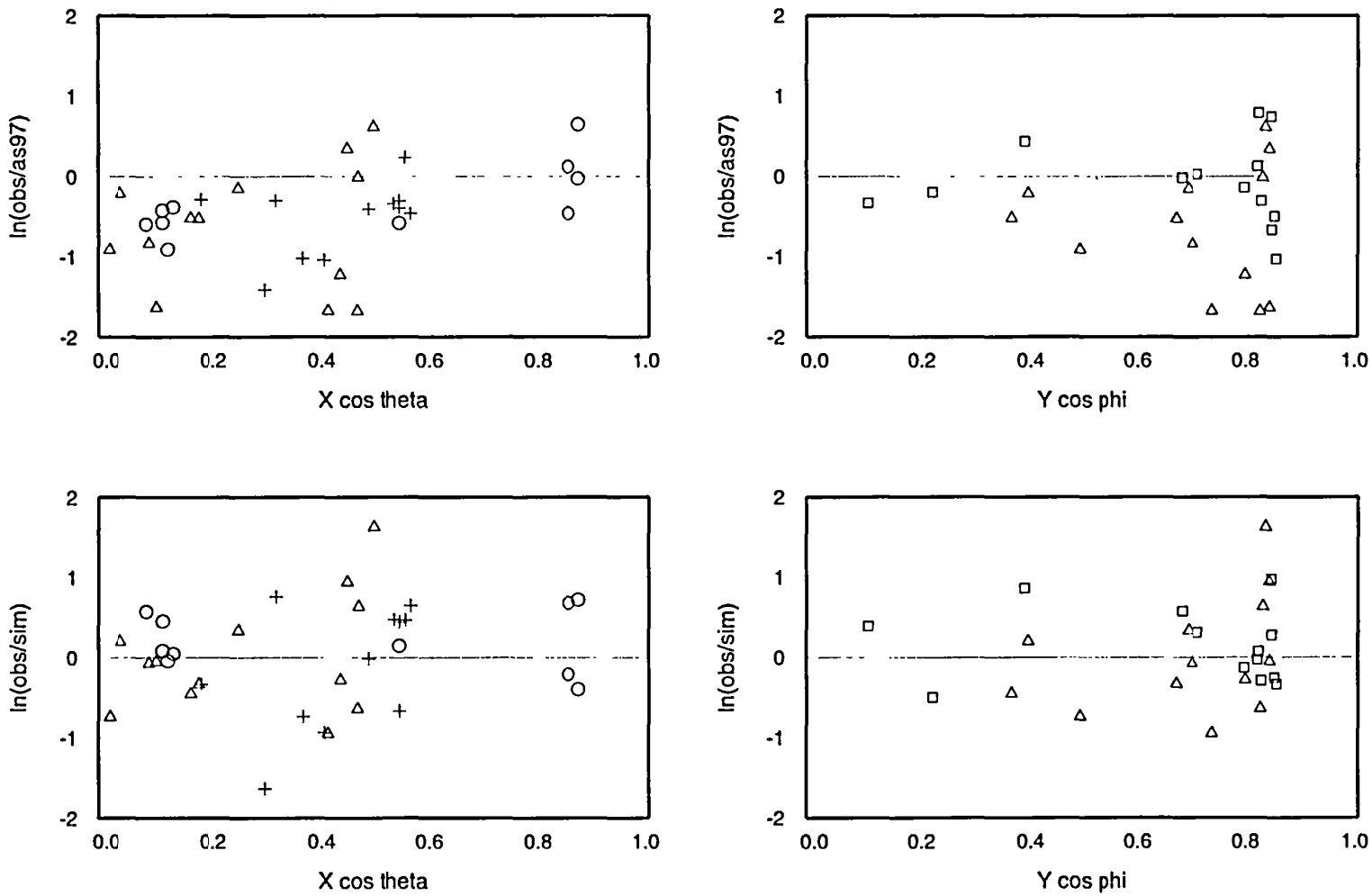

Kobe
Landers
Loma Prieta
Northridge

GMT Aug 25 11:16:57 1999 /u1/nancy/PEER-5/Comparisons

Kobe, Landers, Loma Prieta, Northridge - Fault Normal

Spectral Acceleration at 4.0 sec

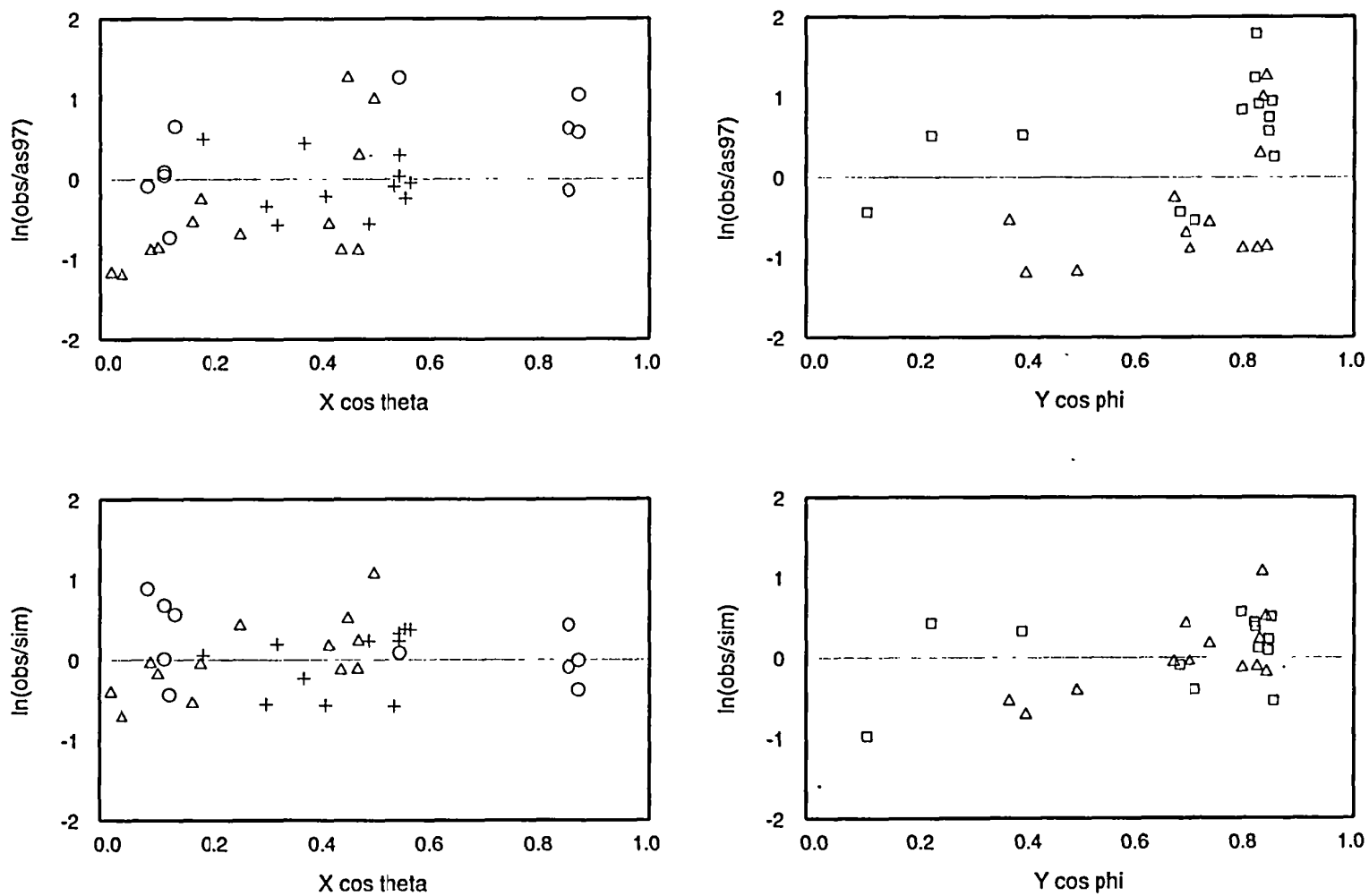

+ Kobe
○ Landers
△ Loma Prieta
□ Northridge

GMT Aug 25 11:17:11 1999 /u1/nancy/PEER-5/Comparisons

Kobe, Landers, Loma Prieta, Northridge - Fault Parallel

Spectral Acceleration at 4.0 sec

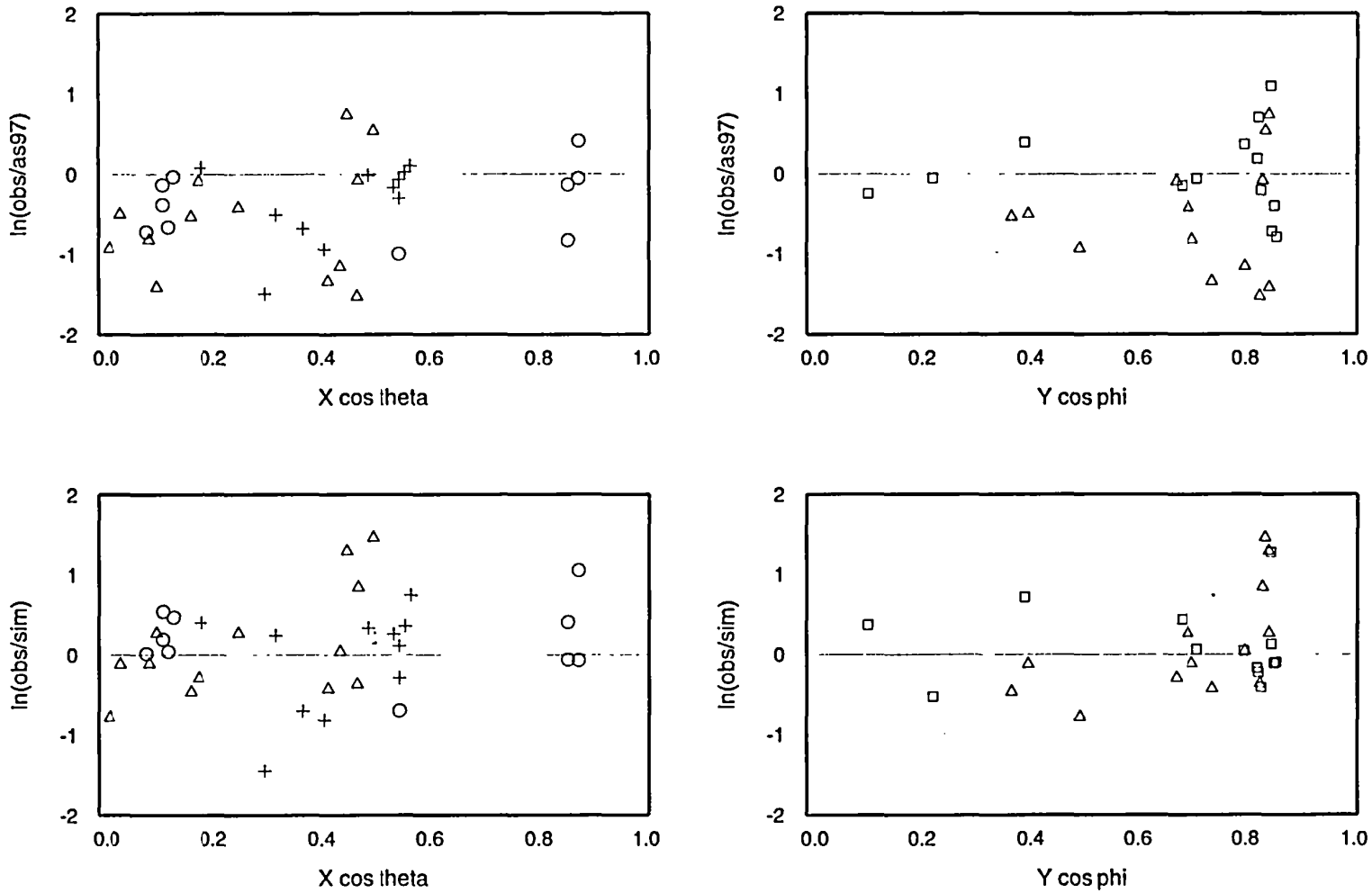

+ Kobe
○ Landers
△ Loma Prieta
□ Northridge

GMT Aug 25 11:17:24 1999 /u1/nancy/PEER-5/Comparisons

Kobe, Landers, Loma Prieta, Northridge - Fault Normal

Spectral Acceleration at 3.0 sec

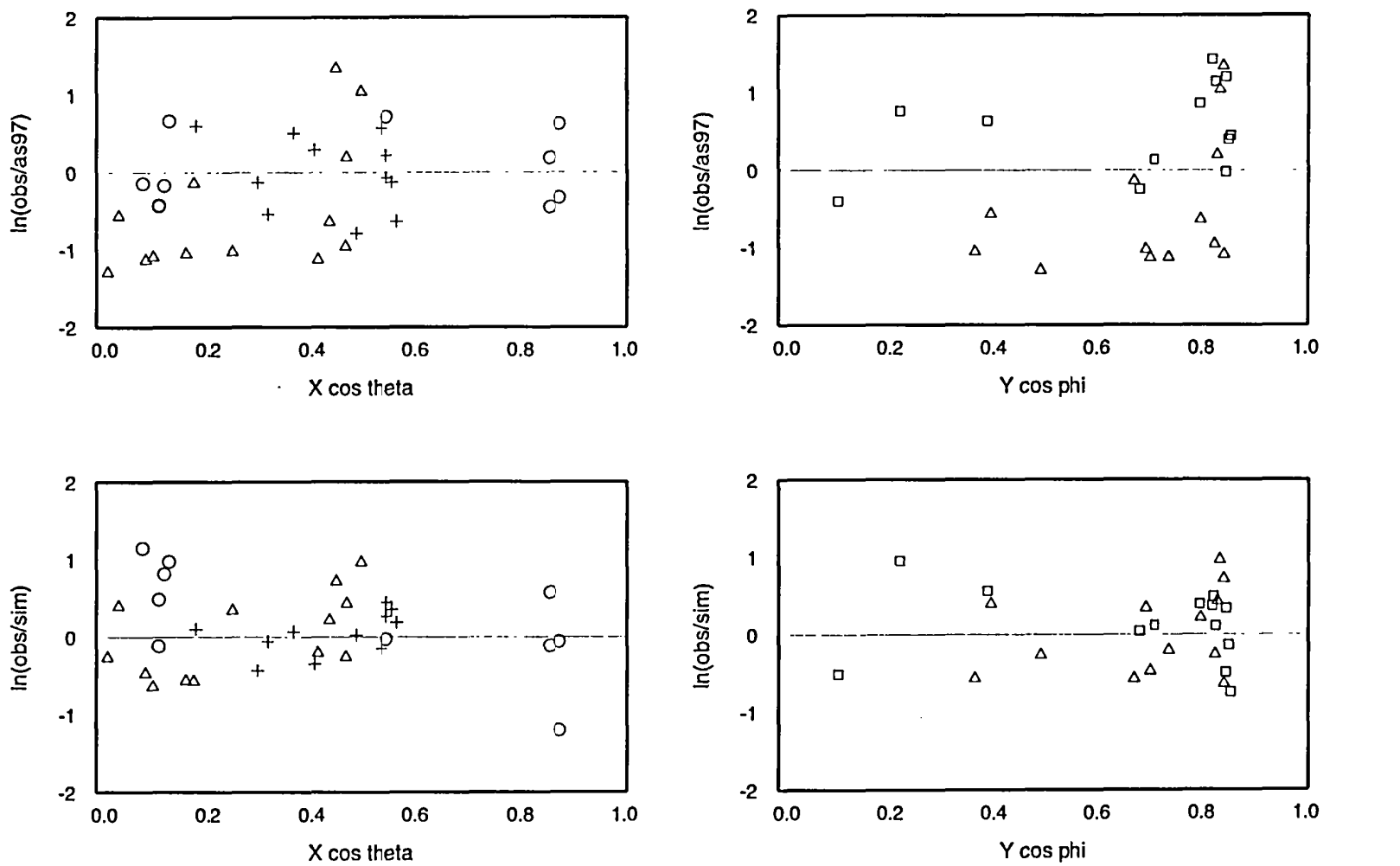

GMT Aug 25 11:17:37 1999 /u1/nancy/PEER-5/Comparisons

Kobe, Landers, Loma Prieta, Northridge - Fault Parallel

Spectral Acceleration at 3.0 sec

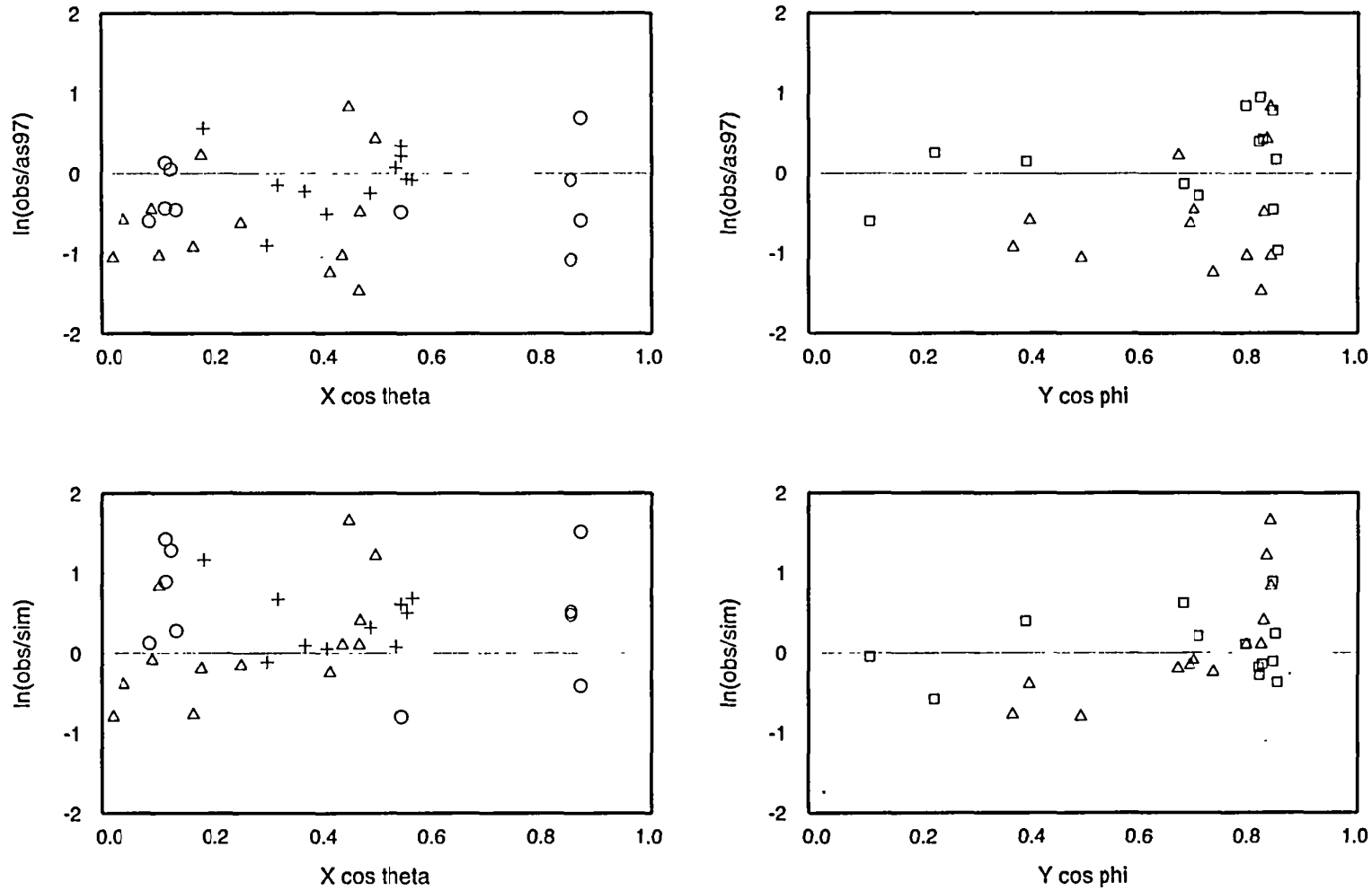

+ Kobe
○ Landers
△ Loma Prieta
□ Northridge

GMT Aug 25 11:17:50 1999 /u1/nancy/PEER-5/Comparisons

Kobe, Landers, Loma Prieta, Northridge - Fault Normal

Spectral Acceleration at 2.0 sec

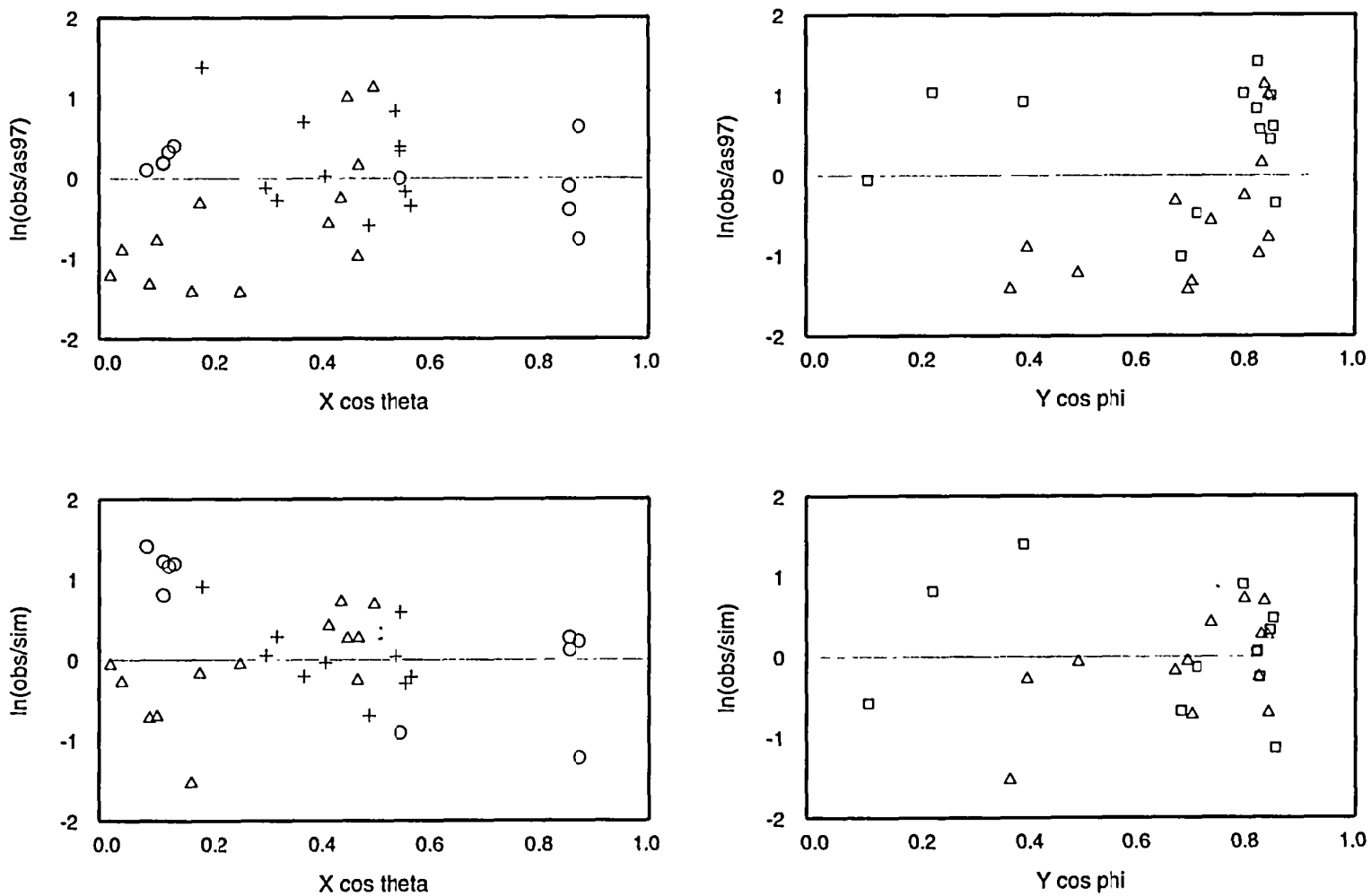

+ Kobe
O Landers
Δ Loma Prieta
□ Northridge

GMT Aug 25 11:18 04 1999 /u1/nancy/PEER-5/Comparisons

Kobe, Landers, Loma Prieta, Northridge - Fault Parallel

Spectral Acceleration at 2.0 sec

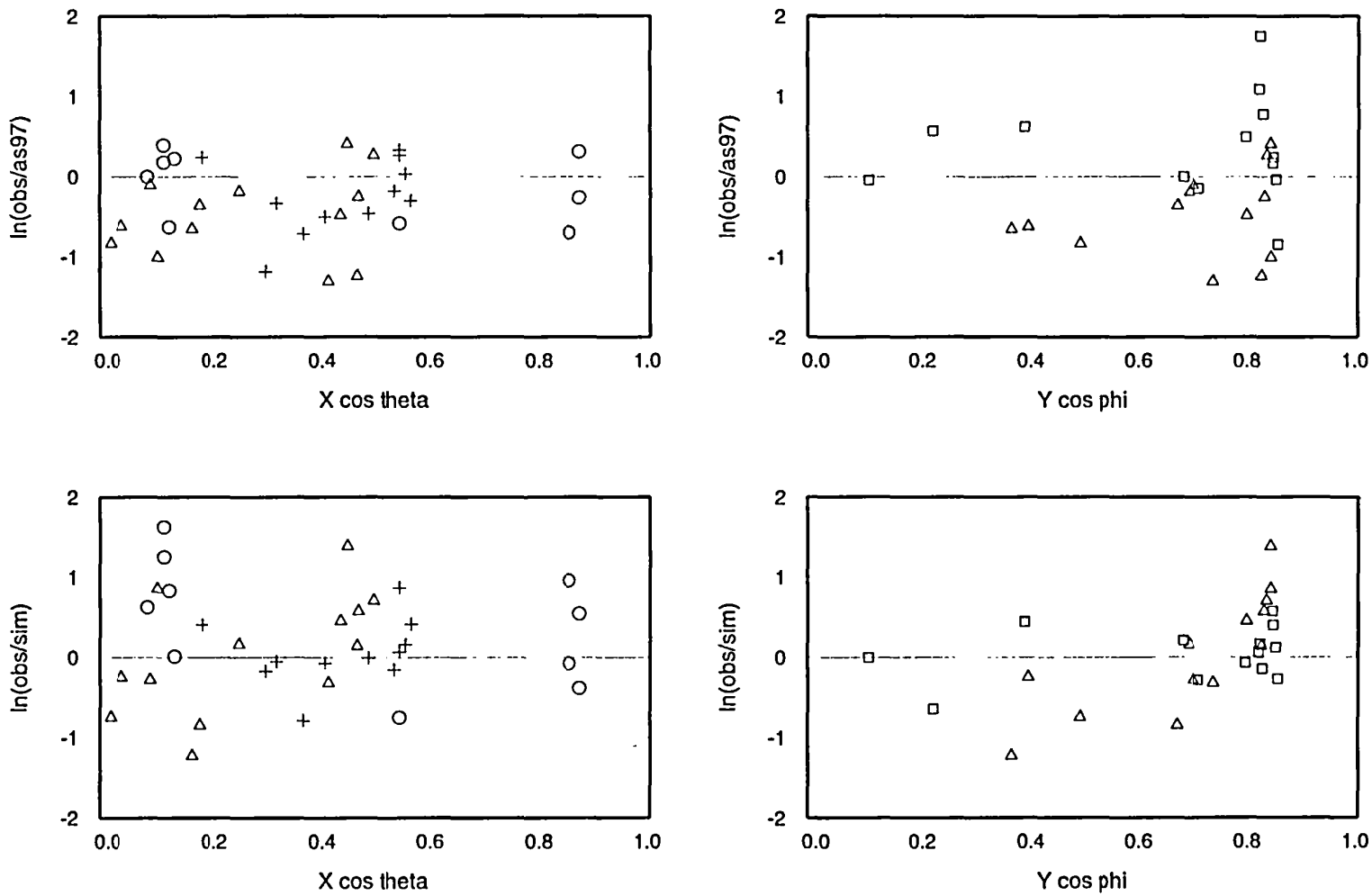

+ Kobe
○ Landers
△ Loma Prieta
□ Northridge

GMT Aug 25 11:18:18 1999 /u1/nancy/PEER-5/Comparisons

Kobe, Landers, Loma Prieta, Northridge - Fault Normal

Spectral Acceleration at 1.5 sec

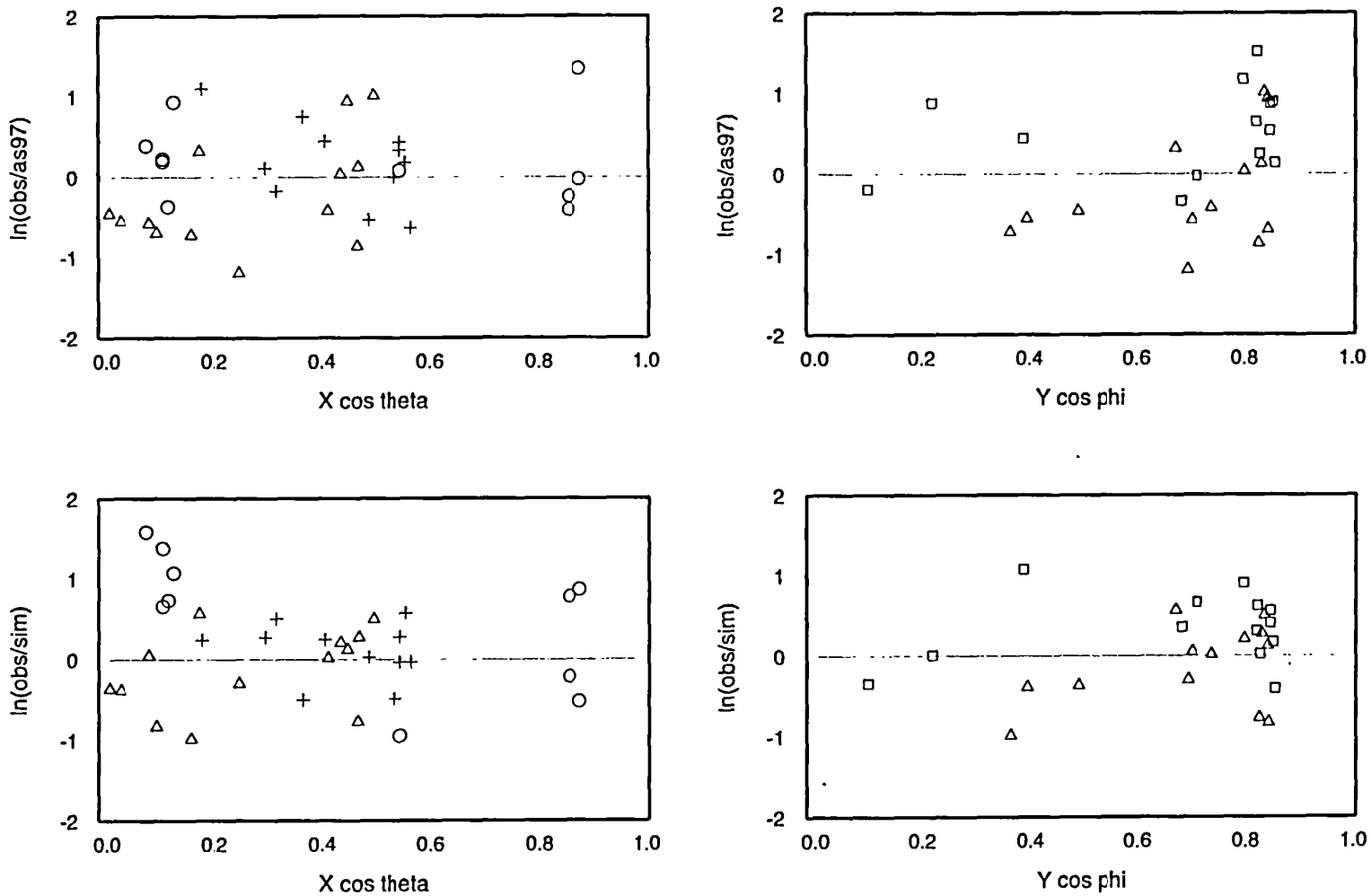

+ Kobe
○ Landers
△ Loma Prieta
□ Northridge

GMT Aug 25 11:18:31 1999 /u1/nancy/PEER-5/Comparisons

Kobe, Landers, Loma Prieta, Northridge - Fault Parallel

Spectral Acceleration at 1.5 sec

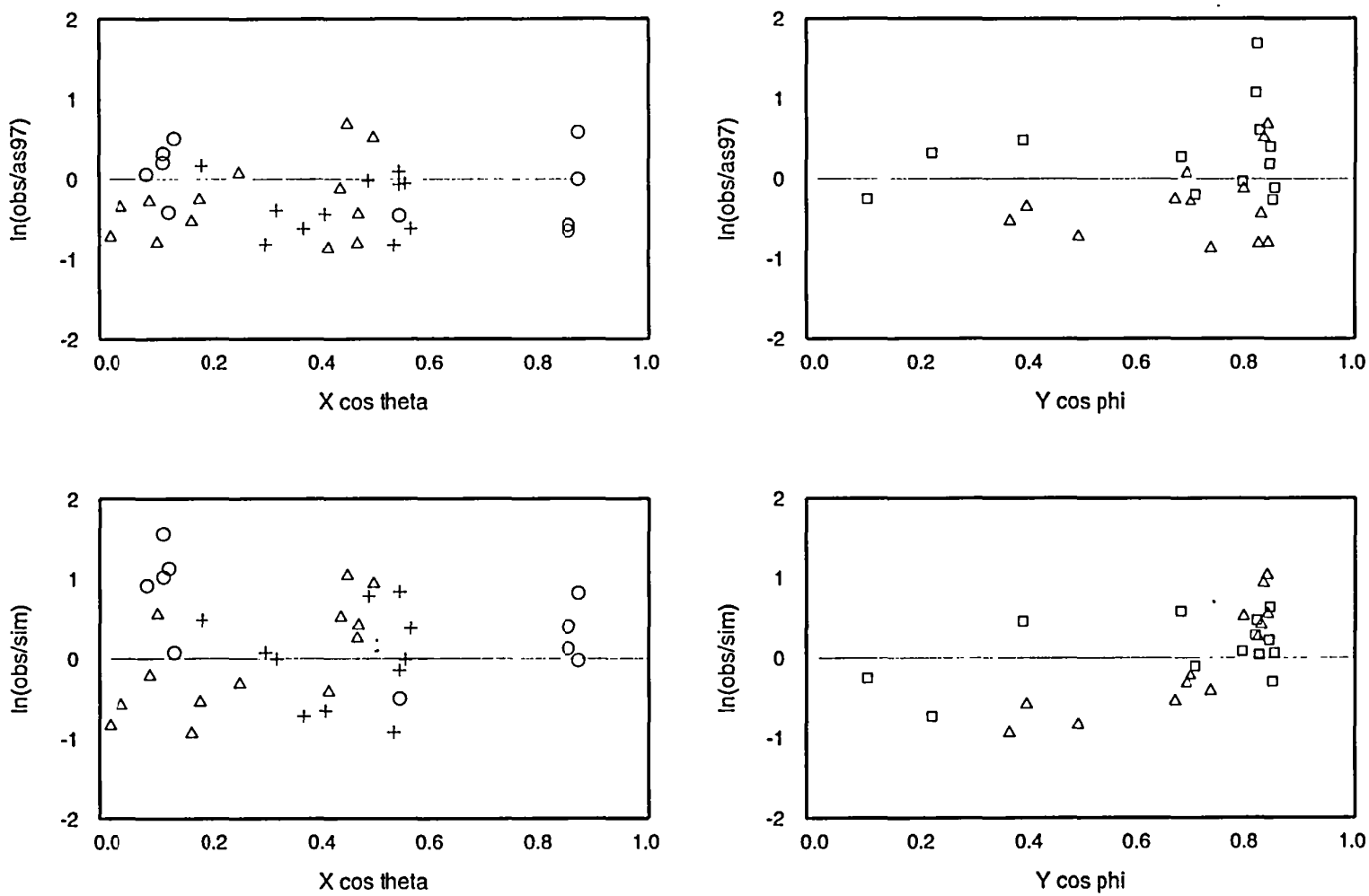

+ Kobe
○ Landers
△ Loma Prieta
□ Northridge

GMT Aug 25 11:18:44 1999 /u1/nancy/PEER-5/Comparisons

Kobe, Landers, Loma Prieta, Northridge - Fault Normal

Spectral Acceleration at 1.0 sec

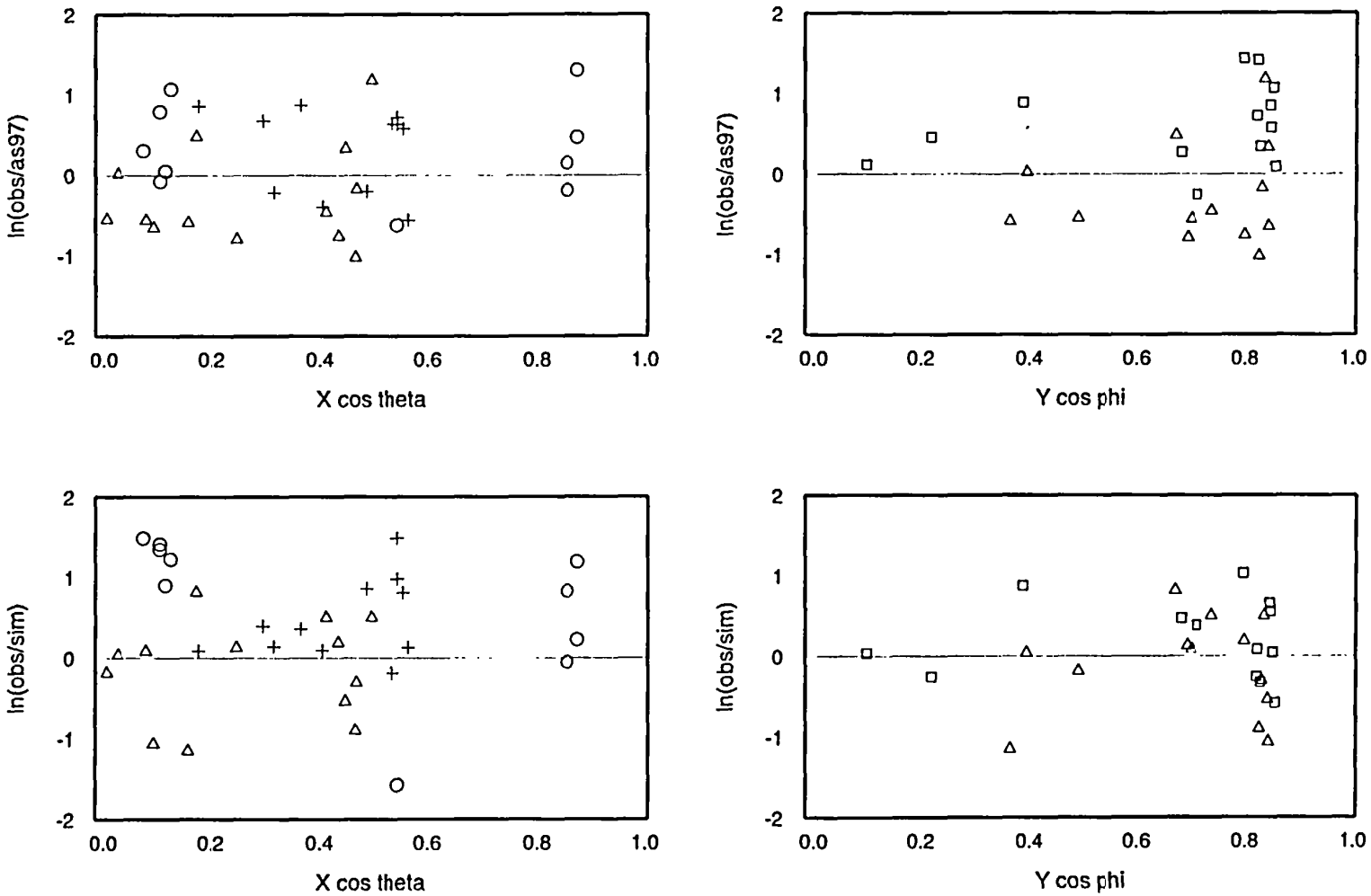

+ Kobe
○ Landers
△ Loma Prieta
□ Northridge

GMT Aug 25 11:18:57 1999 /u1/nancy/PEER-5/Comparisons

Kobe, Landers, Loma Prieta, Northridge - Fault Parallel

Spectral Acceleration at 1.0 sec

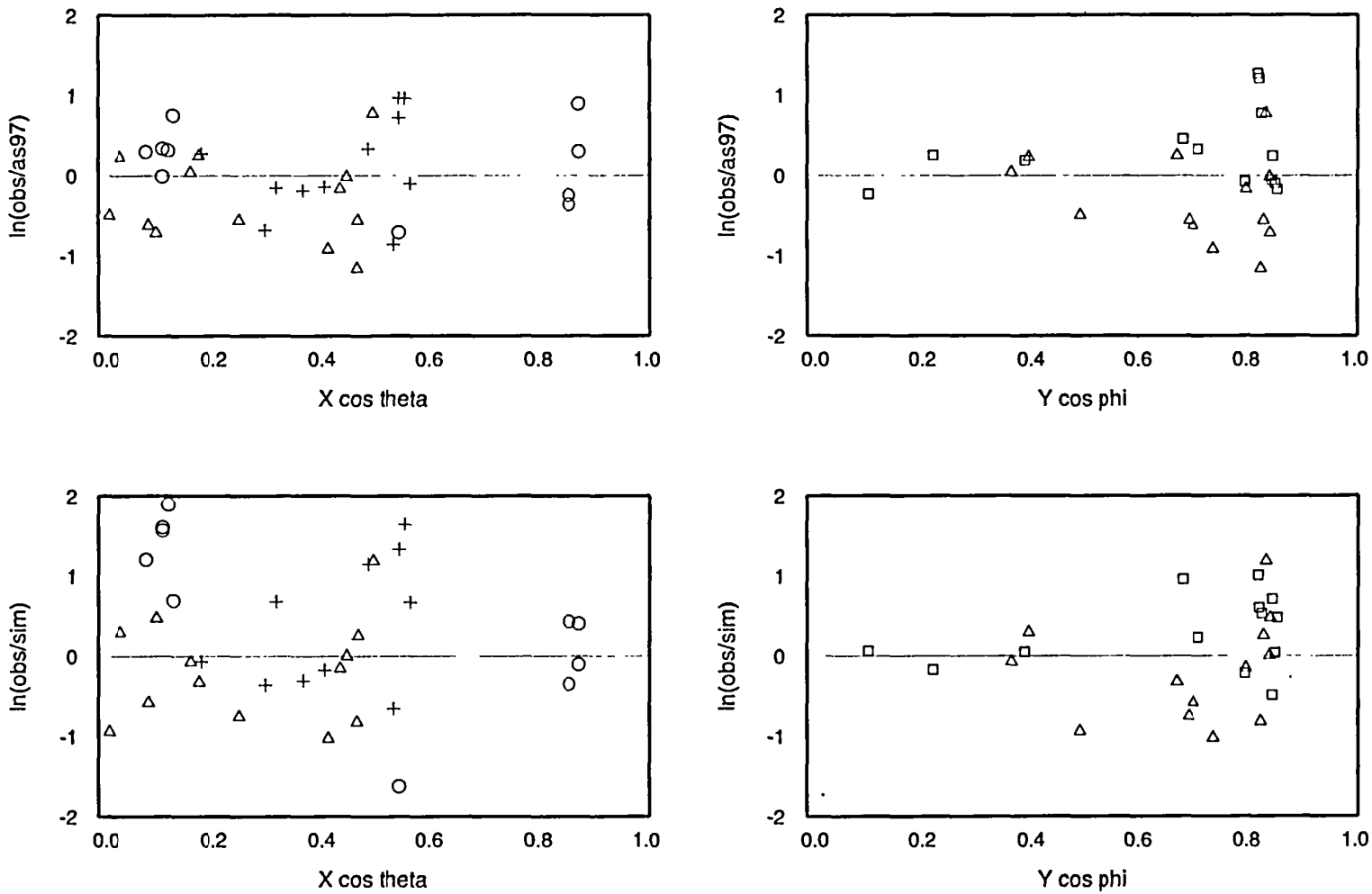

+ Kobe
○ Landers
△ Loma Prieta
□ Northridge

GMT Aug 25 11:19:10 1999 /u1/nancy/PEER-5/Comparisons

/u1/nancy/PEER-5/Loma/Comparisons/Tabulate
tableout

Station	Correlation FN	Correlation FP	Least Squares FN	Least Squares FP	Response Spectra FN	Response Spectra FP	Fourier Spectra FN	Fourier Spectra FP
andd	0.420		-0.044		0.043	-0.353	0.129	-0.206
bran	0.382		-0.018		0.428	-0.337	0.338	-0.307
capi	0.509		0.130		-0.266	-0.899	0.353	0.027
cldd	0.478		-0.027		-0.140	-0.323	-0.037	-0.189
cor	0.423		-0.682		-0.729	0.427	-0.395	0.638
gav	0.498		-0.475		-0.631	-0.298	-0.410	-0.224
gil6	0.615		0.173		0.207	-0.632	0.204	-0.497
gilb	0.680		0.261		0.047	0.041	-0.097	-0.120
hol	0.722		0.265		0.542	1.101	0.651	1.229
lgpc	0.705		0.290		0.009	0.638	-0.031	0.721
srtg	0.784	0.691	0.378	0.267	0.078	0.452	0.270	0.481
ucsc	0.461	0.323	-1.344	-0.779	-1.093	-0.612	-0.929	-0.737
waho	0.513		-0.007		-0.116	-0.049	-0.109	-0.024
Average	0.553	0.507	-0.085	-0.256	-0.125	-0.065	-0.005	0.061
Sigma	0.132		0.485		0.496	0.797	0.828	1.251
Sigma Mean	0.037		0.134		0.137	0.221	0.230	0.347

Loma Prieta - Fault Normal

Simulations and Data Band Pass Filtered 0.125-1.43 Hz

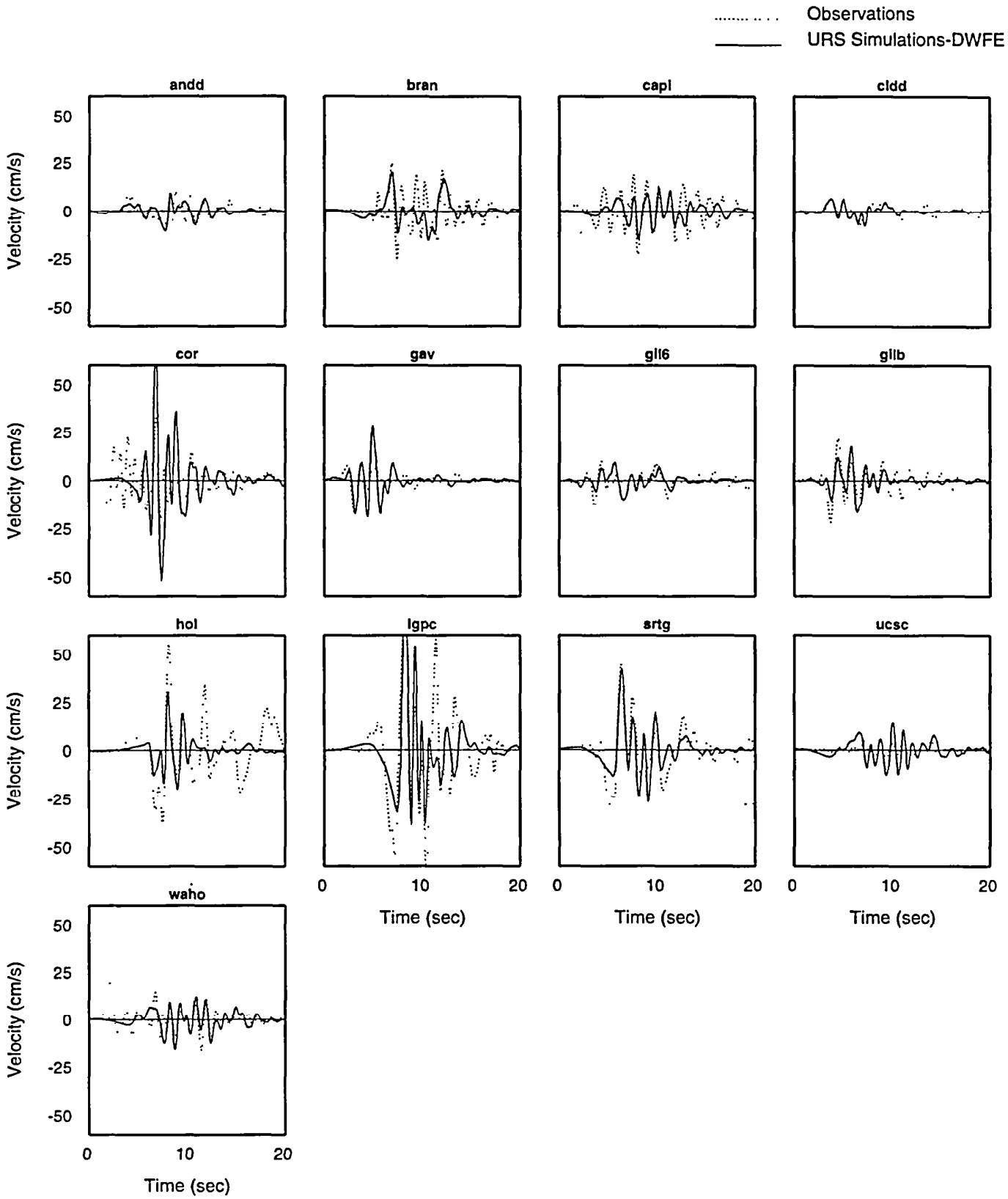

GMT Aug 31 10:46:37 1999 /u2/nancy/PEER-5/Loma/Comparisons

Loma Prieta - Fault Parallel

Simulations and Data Band Pass Filtered 0.125-1.43 Hz

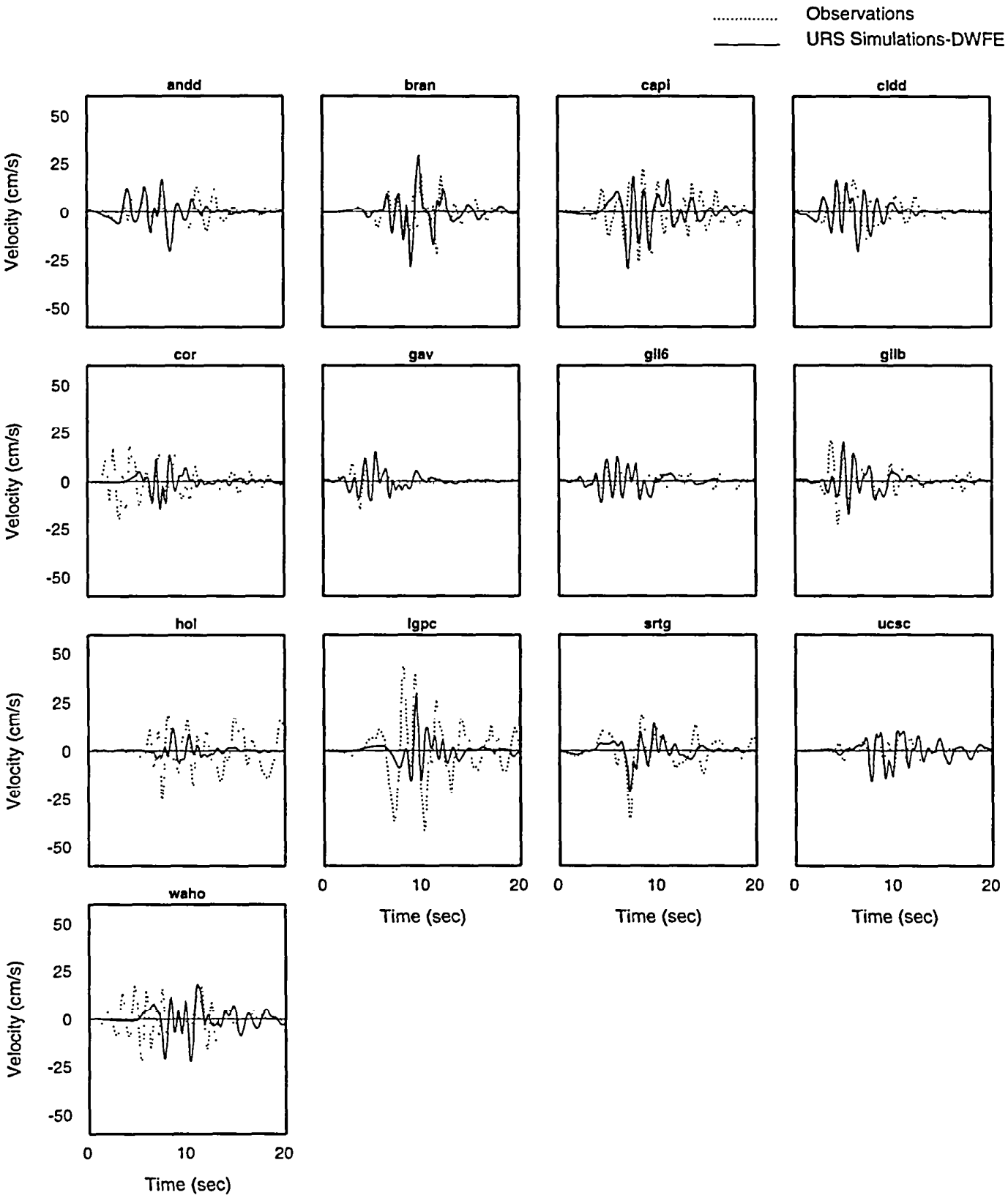

GMT Aug 31 10:47:11 1999 /u2/nancy/PEER-5/Loma/Comparisons

Loma Prieta - Fault Normal

Simulations and Data

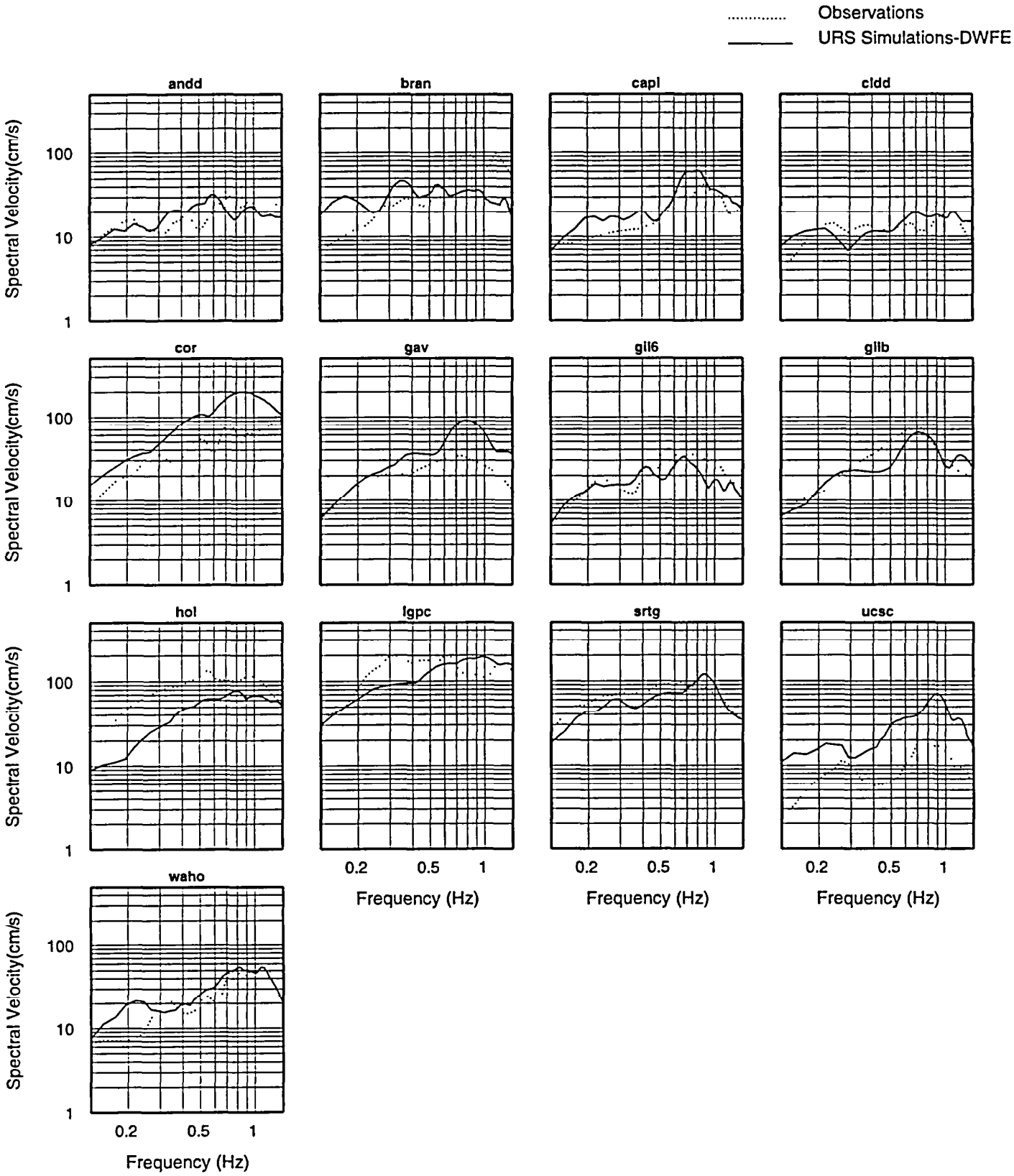

GMT Aug 31 15:19:01 1999 /u2/nancy/PEER-5/Loma/Comparisons

Loma Prieta - Fault Parallel

Simulations and Data

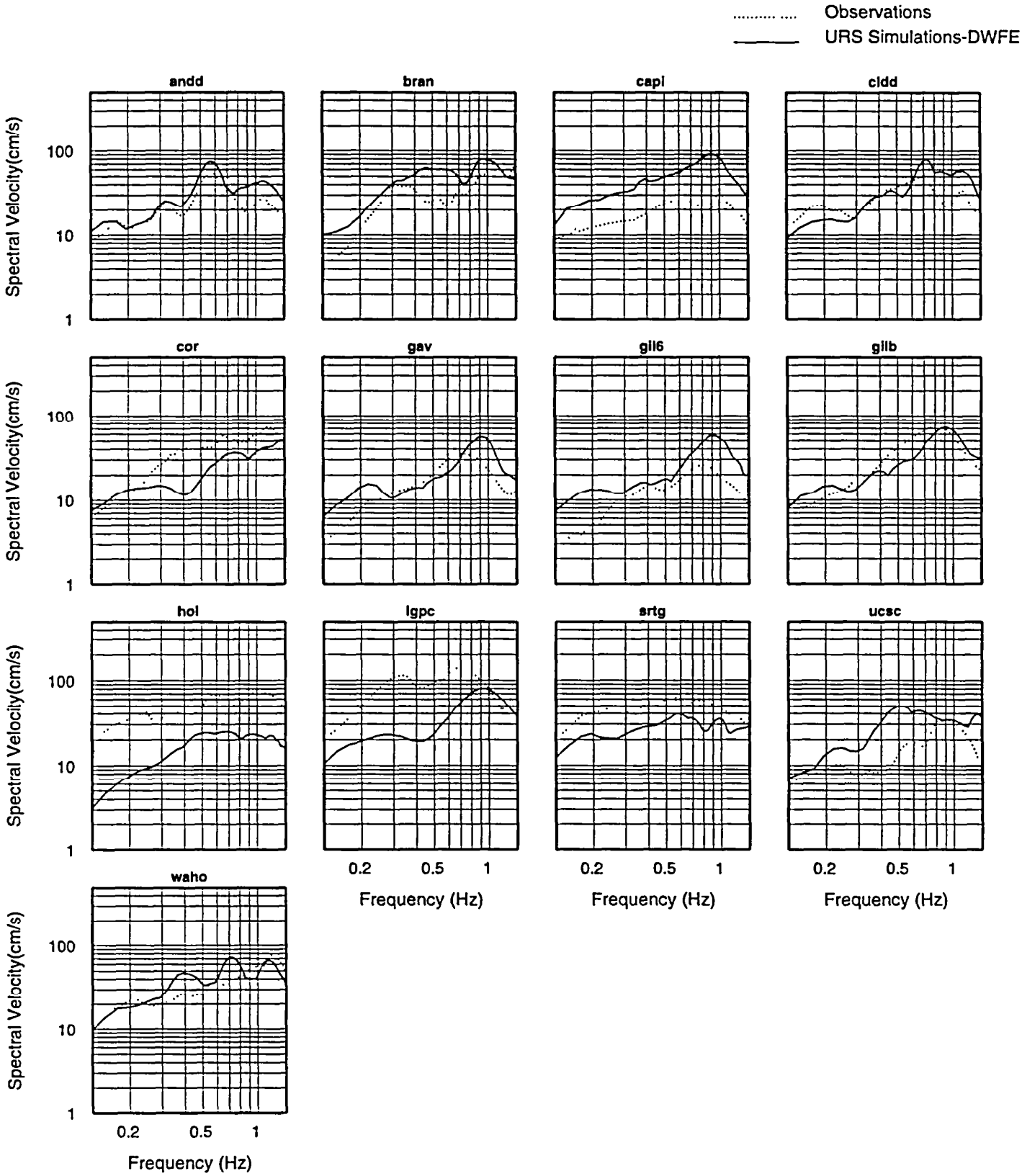

GMT Aug 31 15:19:17 1999 /u2/nancy/PEER-5/Loma/Comparisons

Loma Prieta - Fault Normal

Simulations and Data Band Pass Filtered 0.125-1.43 sec

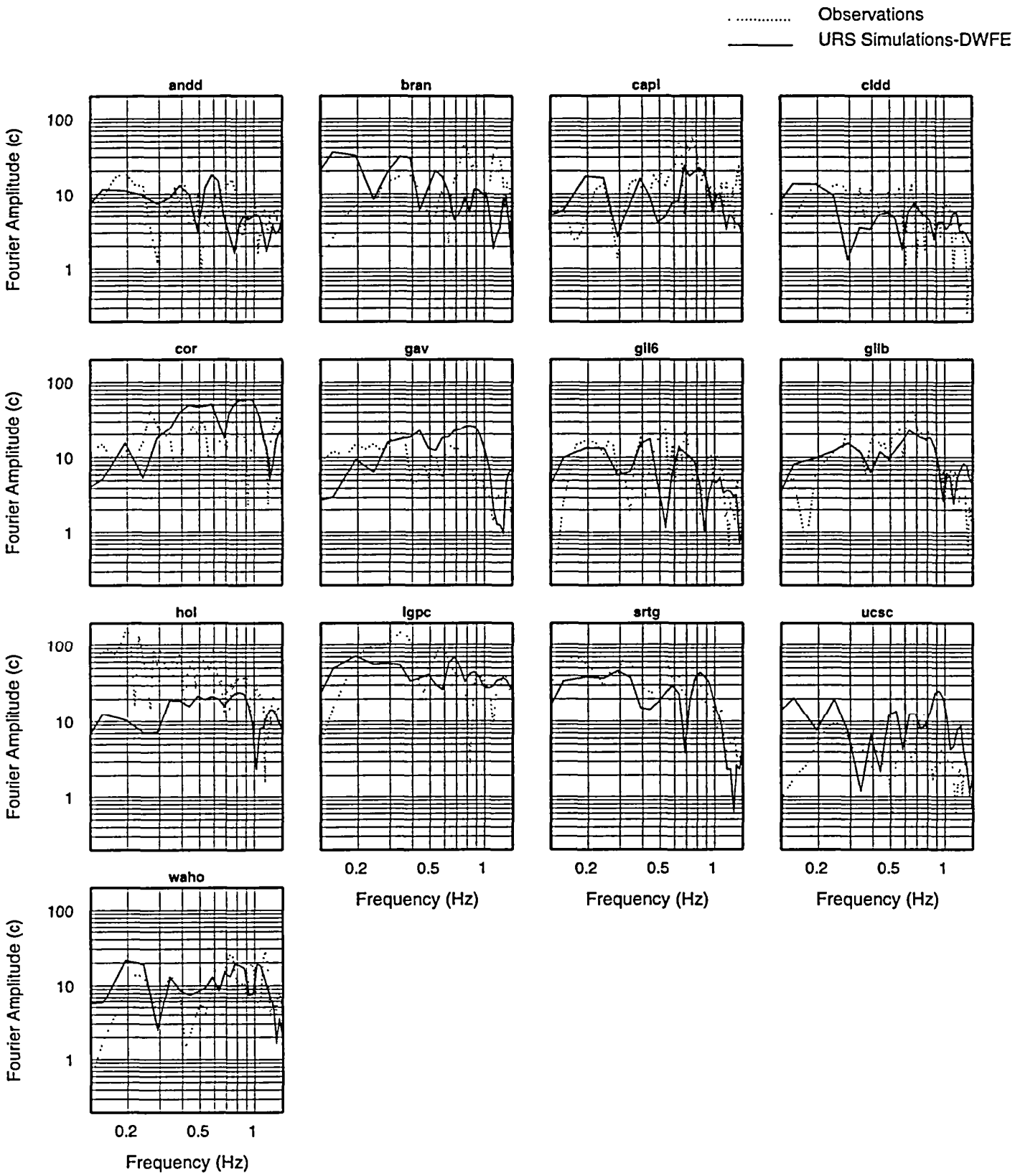

GMT Aug 31 15:23.42 1999 /u2/nancy/PEER-5/Loma/Comparisons

Loma Prieta - Fault Parallel

Simulations and Data Band Pass Filtered 0.125-1.43 sec

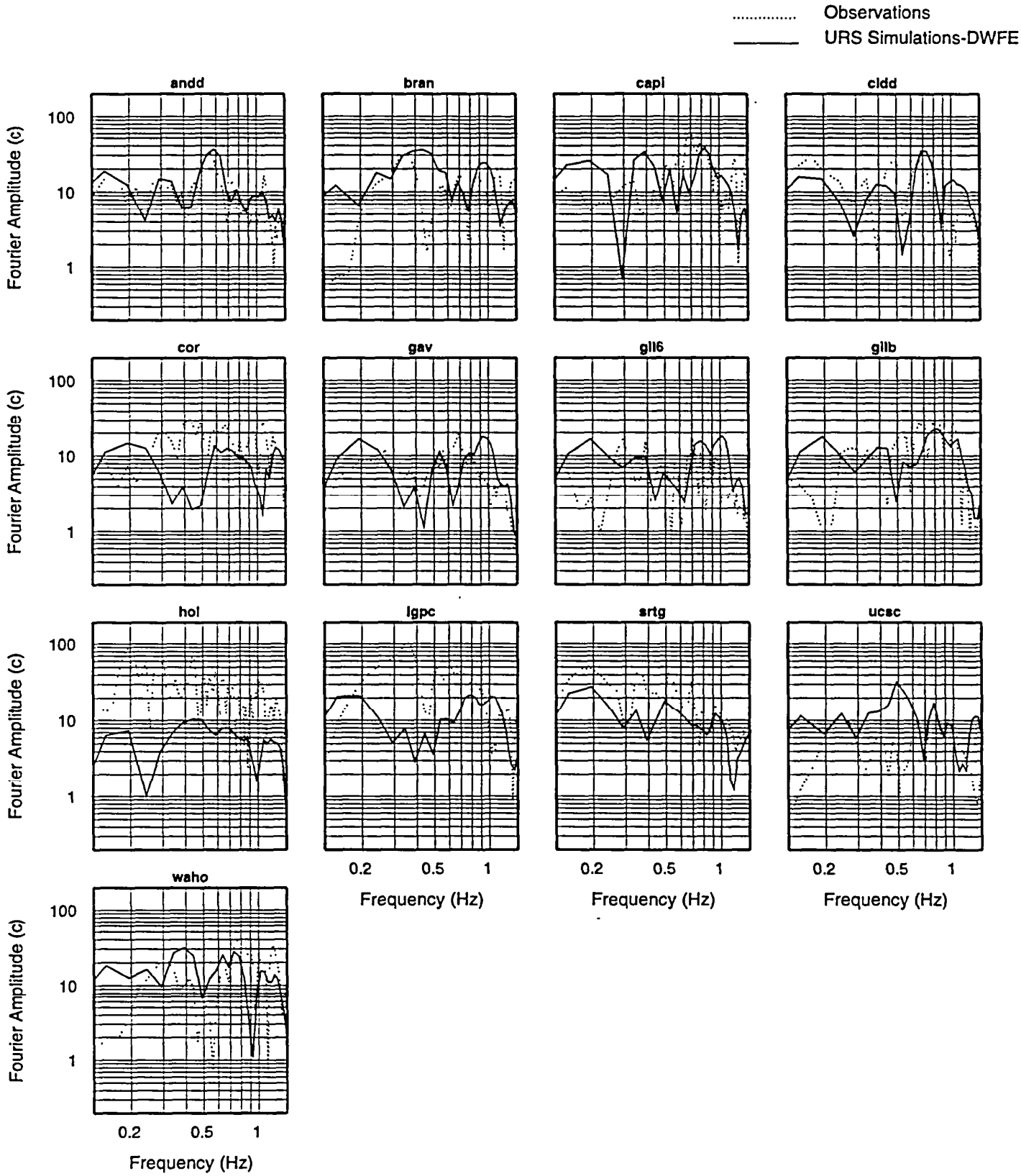

GMT Aug 31 15:23.59 1999 /u2/nancy/PEER-5/Loma/Comparisons

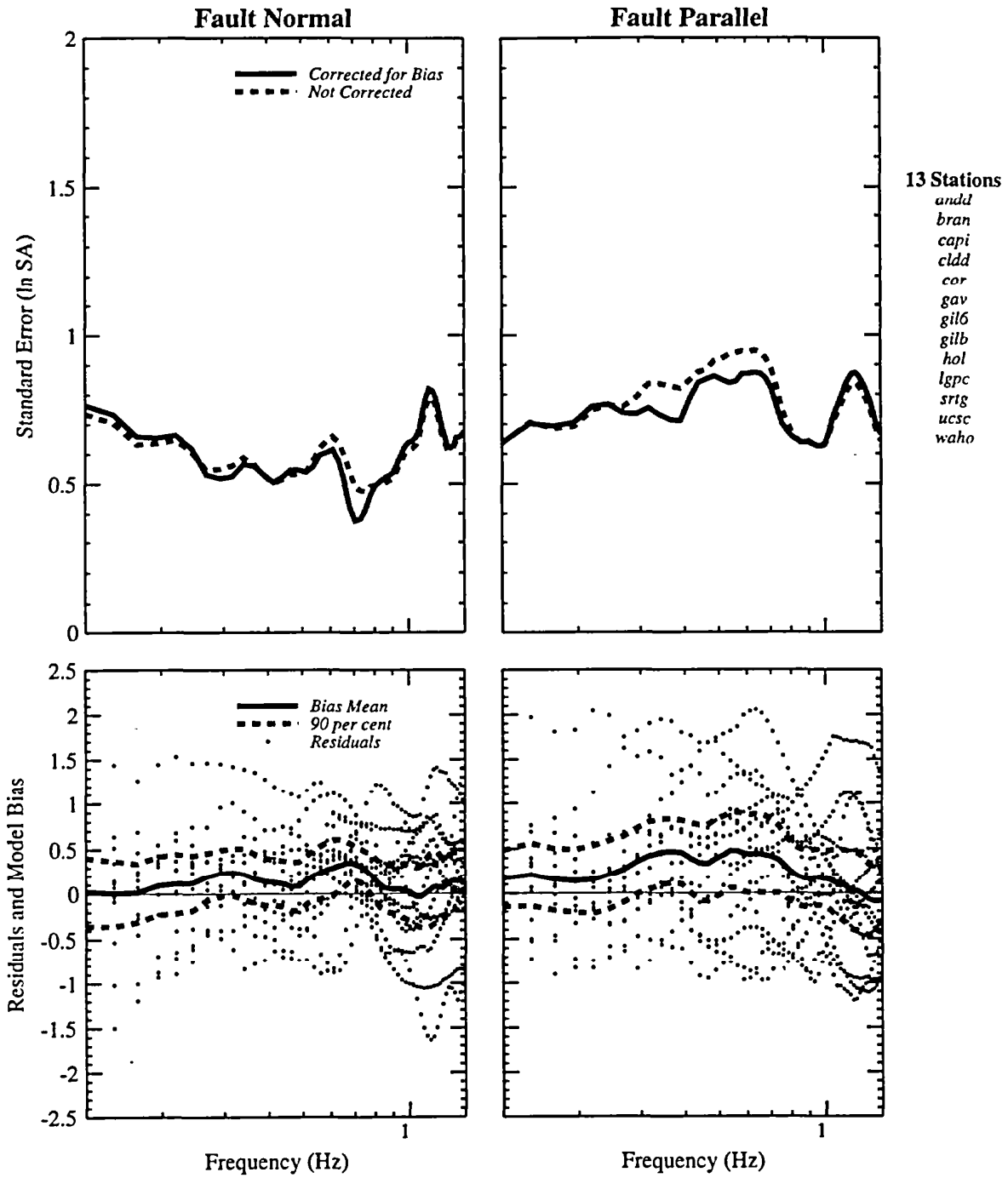

Loma Prieta Spectral Acceleration Goodness of Fit
Observed minus Synthetic (obs - sim)

nfsmith0 Tue Aug 31 13 39 26 PDT 1999
/u2/nancy/PEER-5/Loma/GoodFit/mplot_goodfit csh

Loma Prieta 10/17/89 - andd

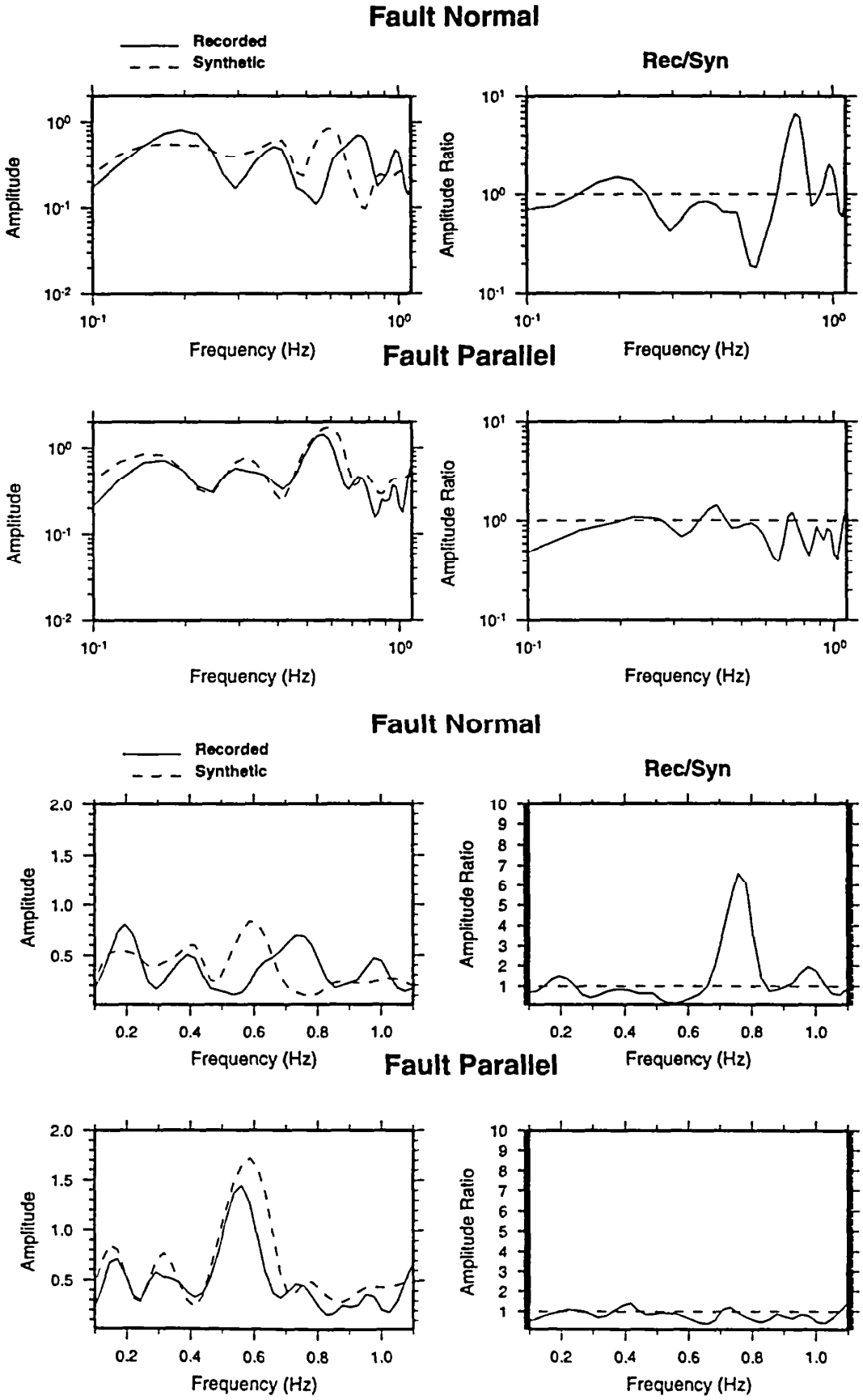

Loma Prieta 10/17/89 - bran

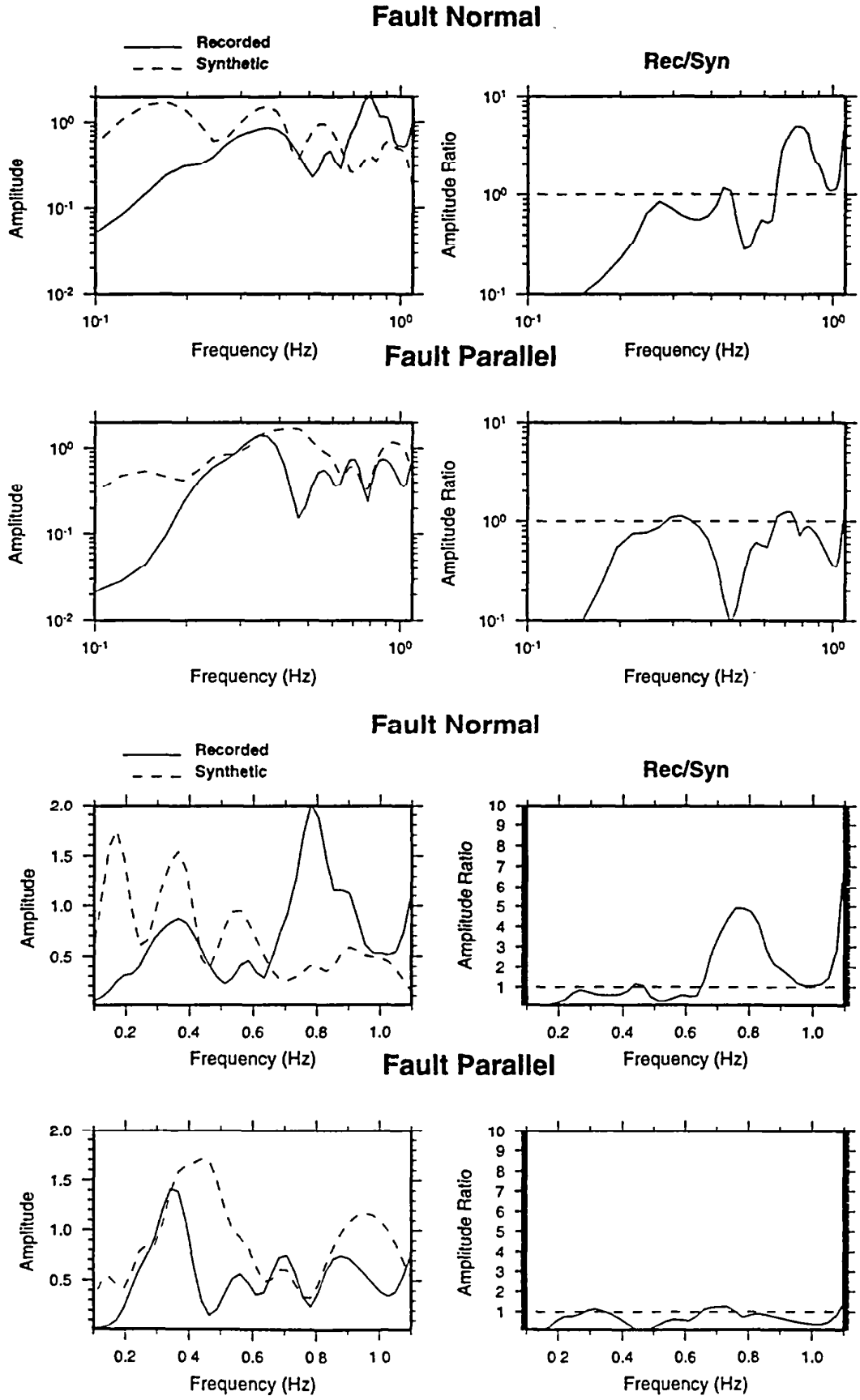

Loma Prieta 10/17/89 - capi

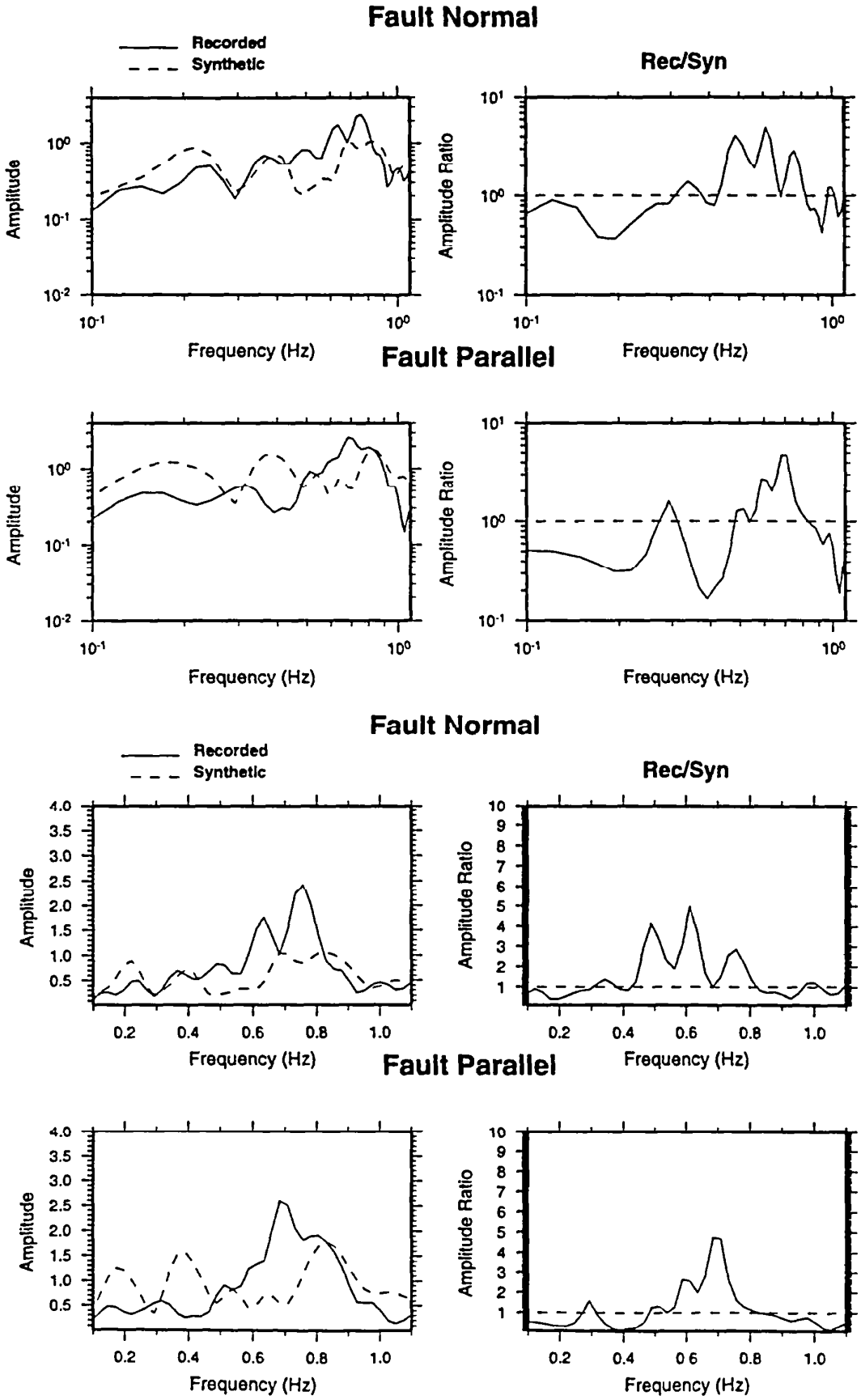

Loma Prieta 10/17/89 - cldd

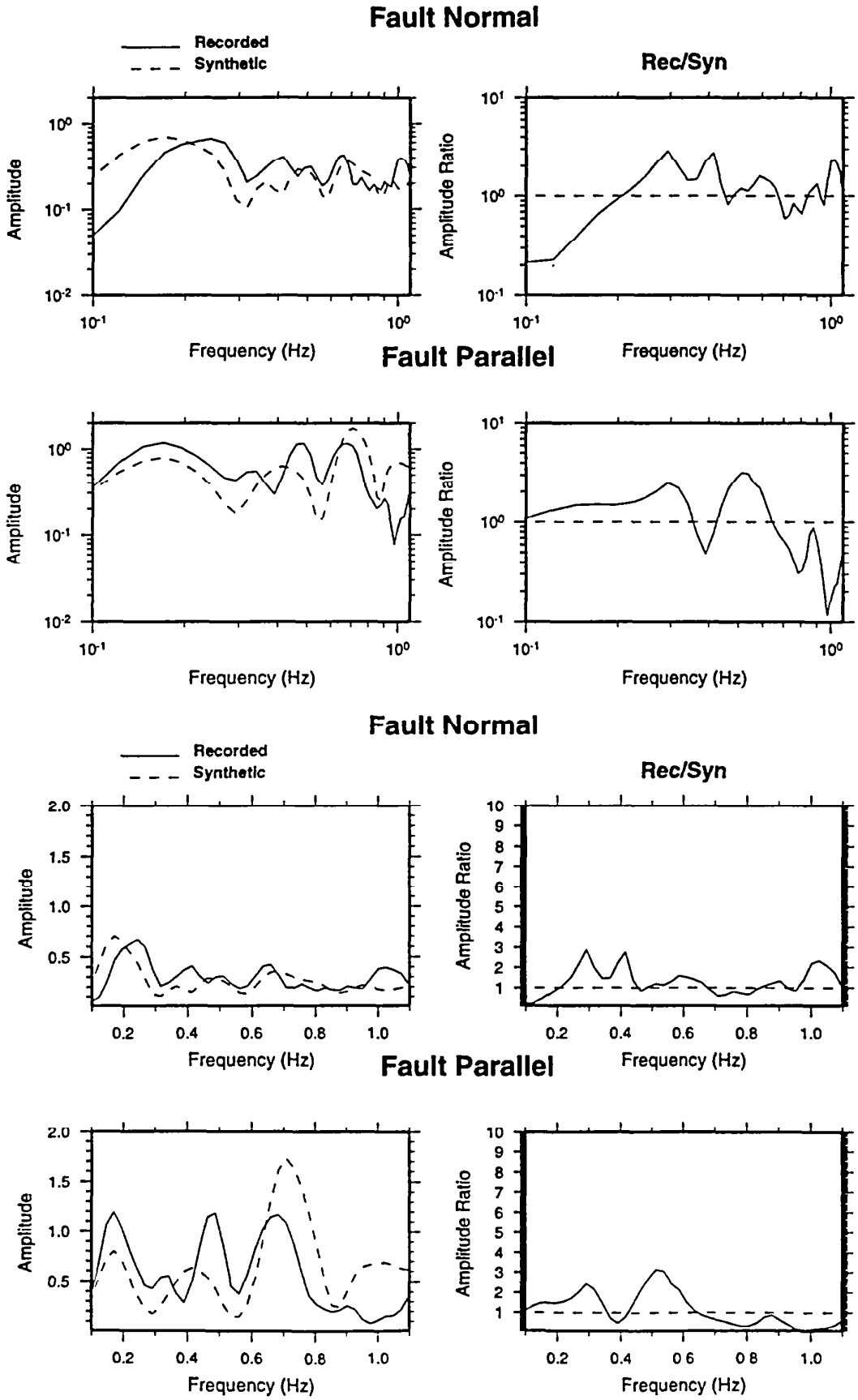

Loma Prieta 10/17/89 - cor

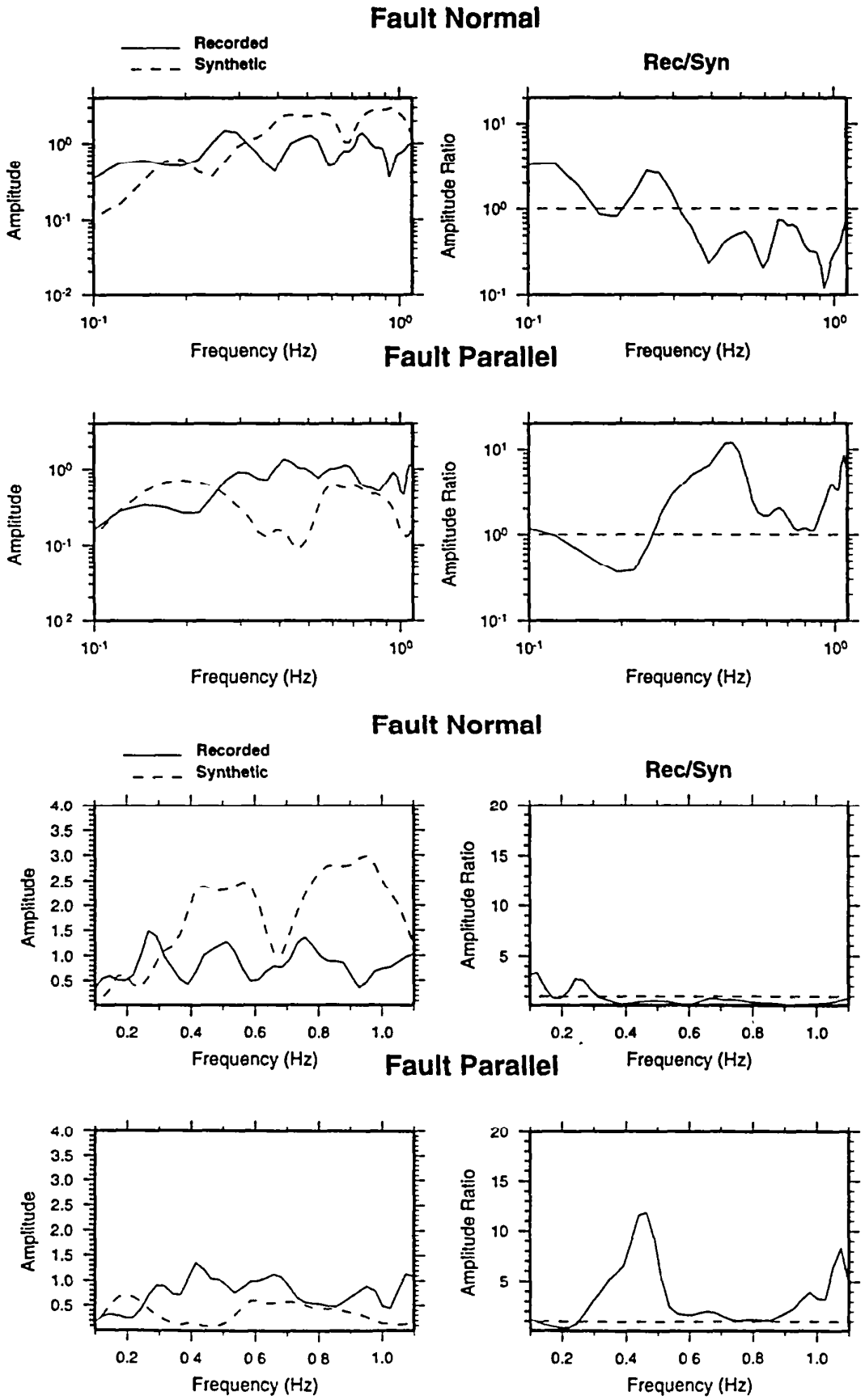

Loma Prieta 10/17/89 - gav

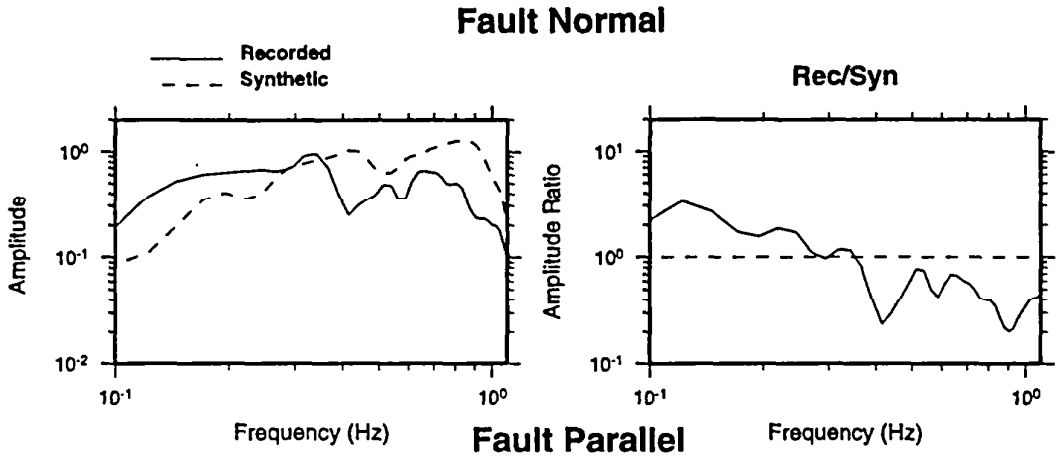

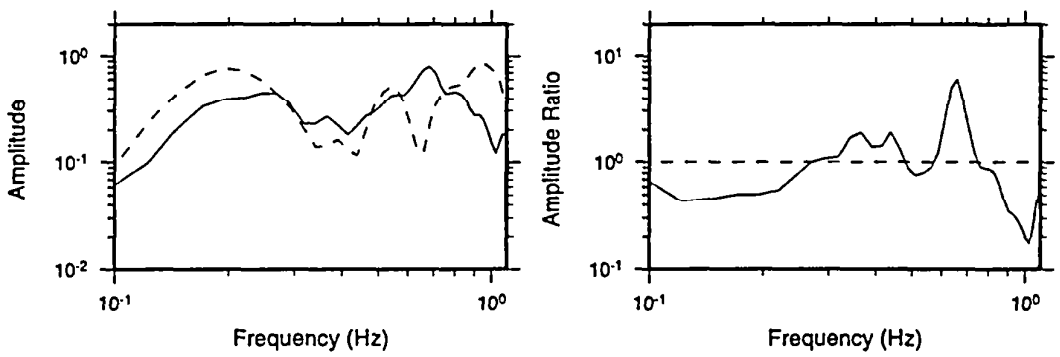

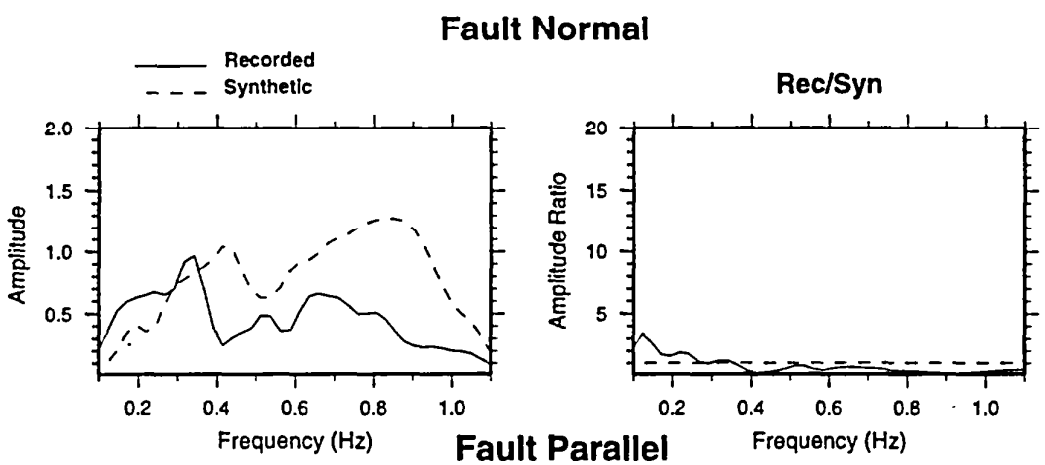

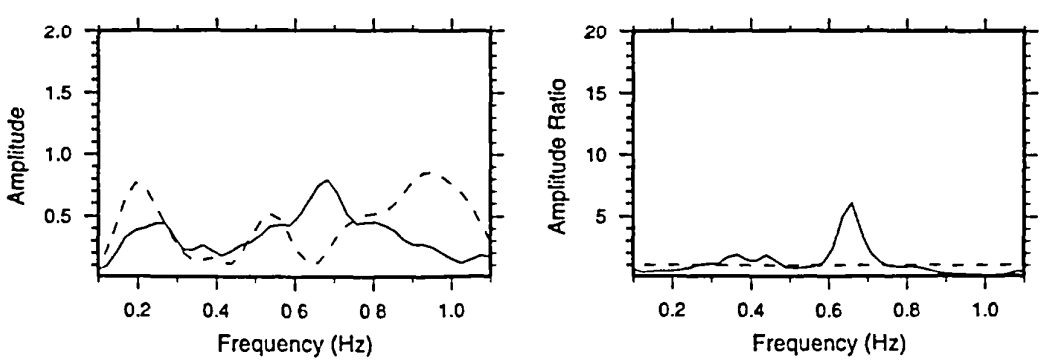

Loma Prieta 10/17/89 - gil6

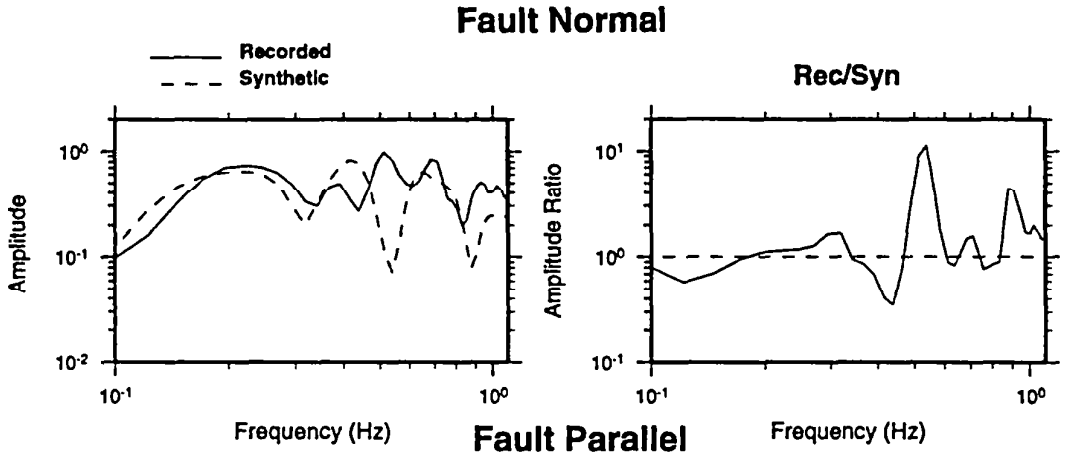

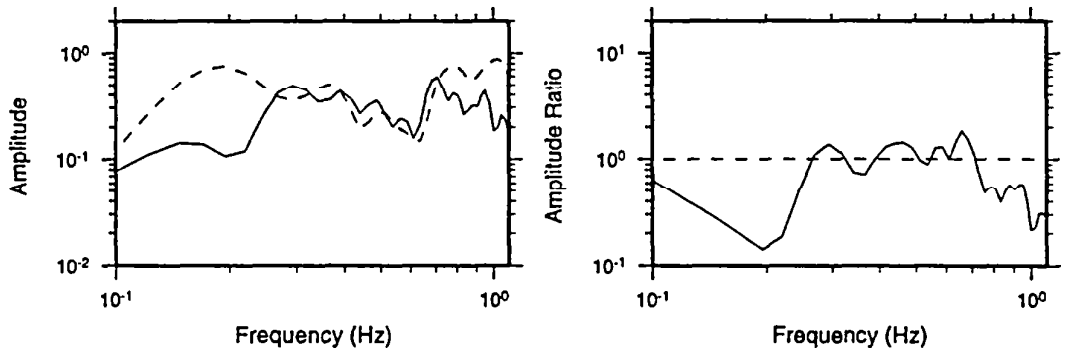

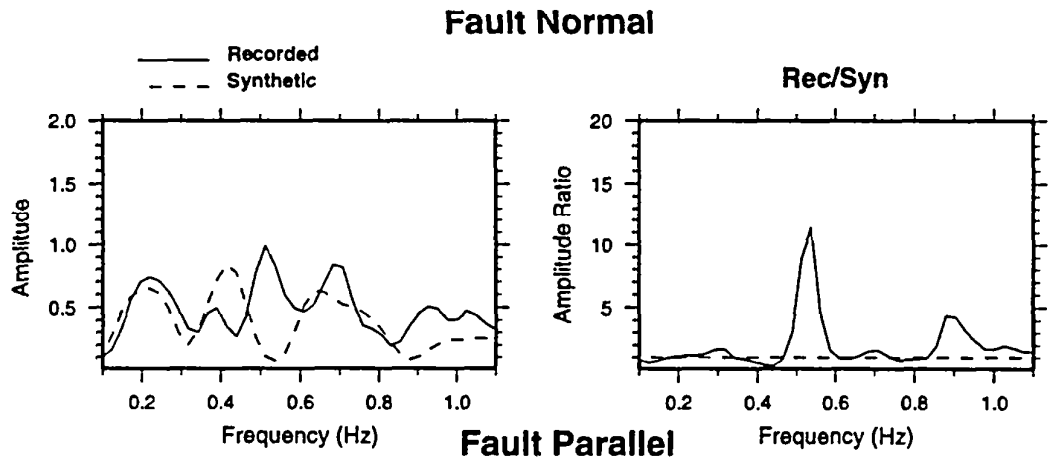

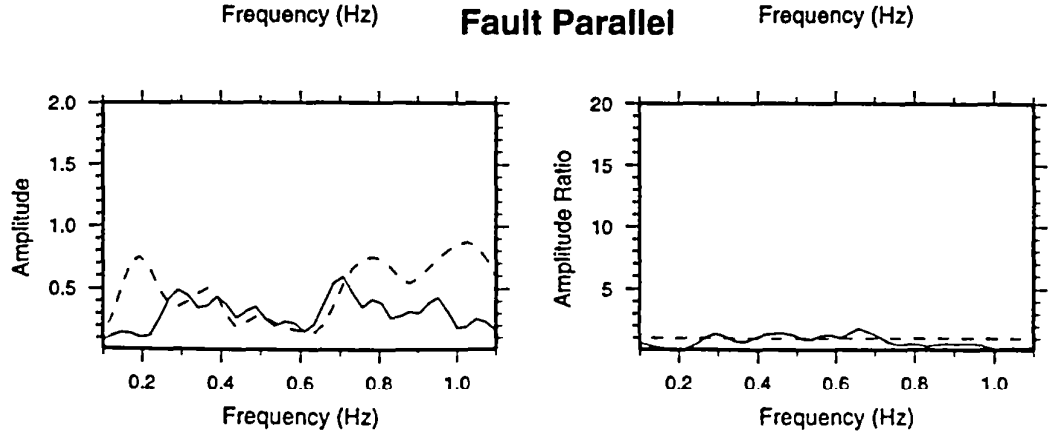

Loma Prieta 10/17/89 - gilb

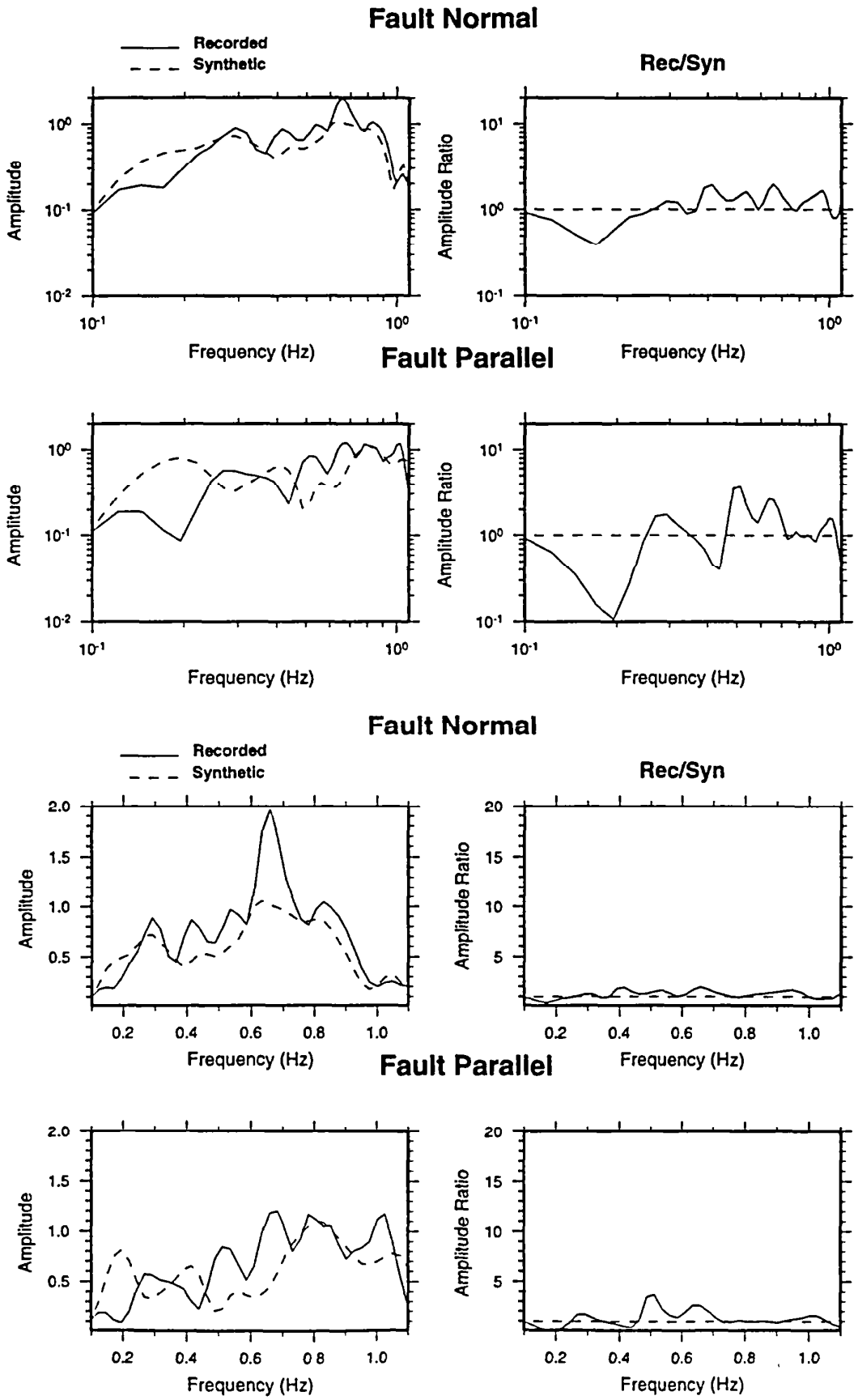

Loma Prieta 10/17/89 - hol

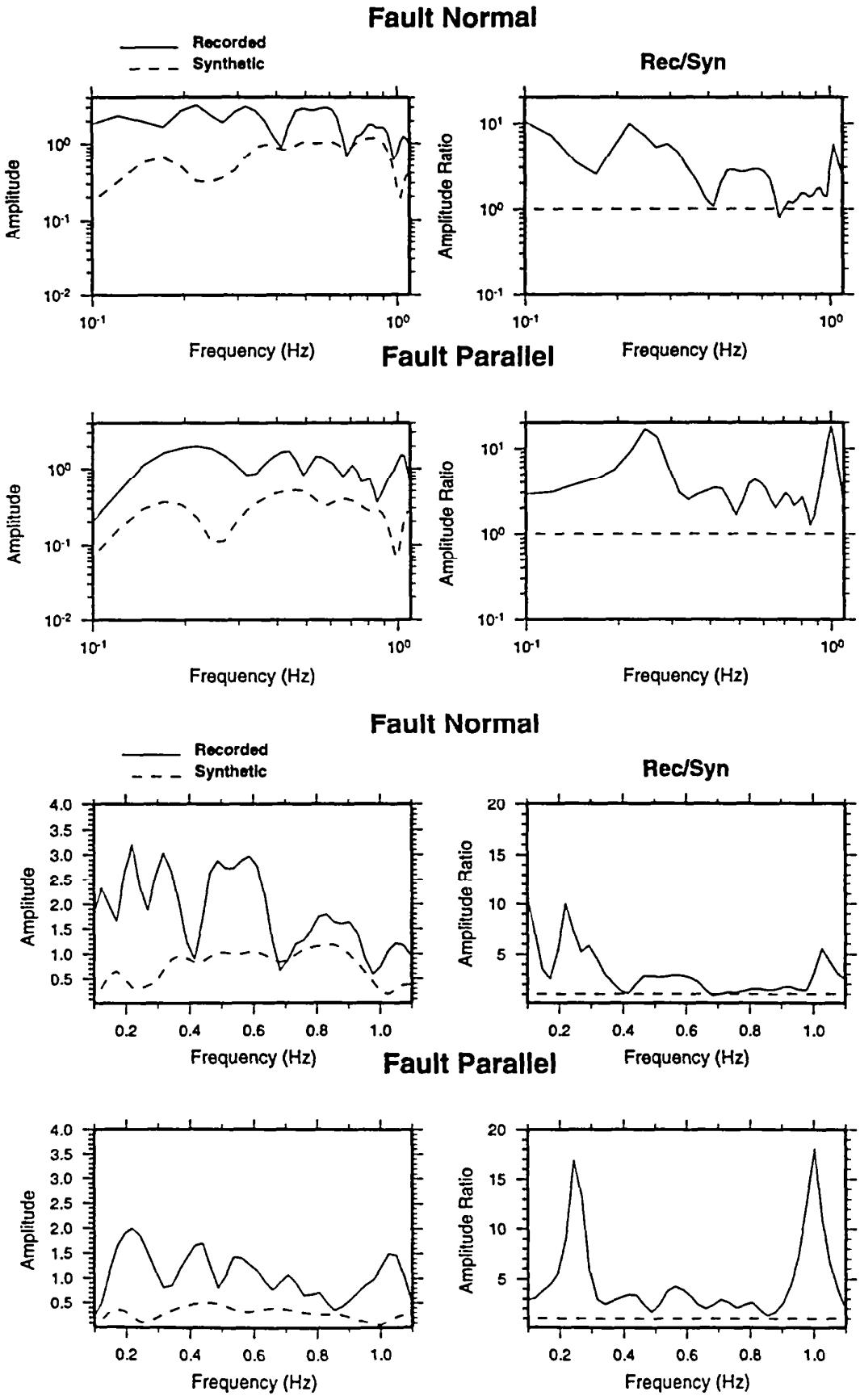

Loma Prieta 10/17/89 - lgpc

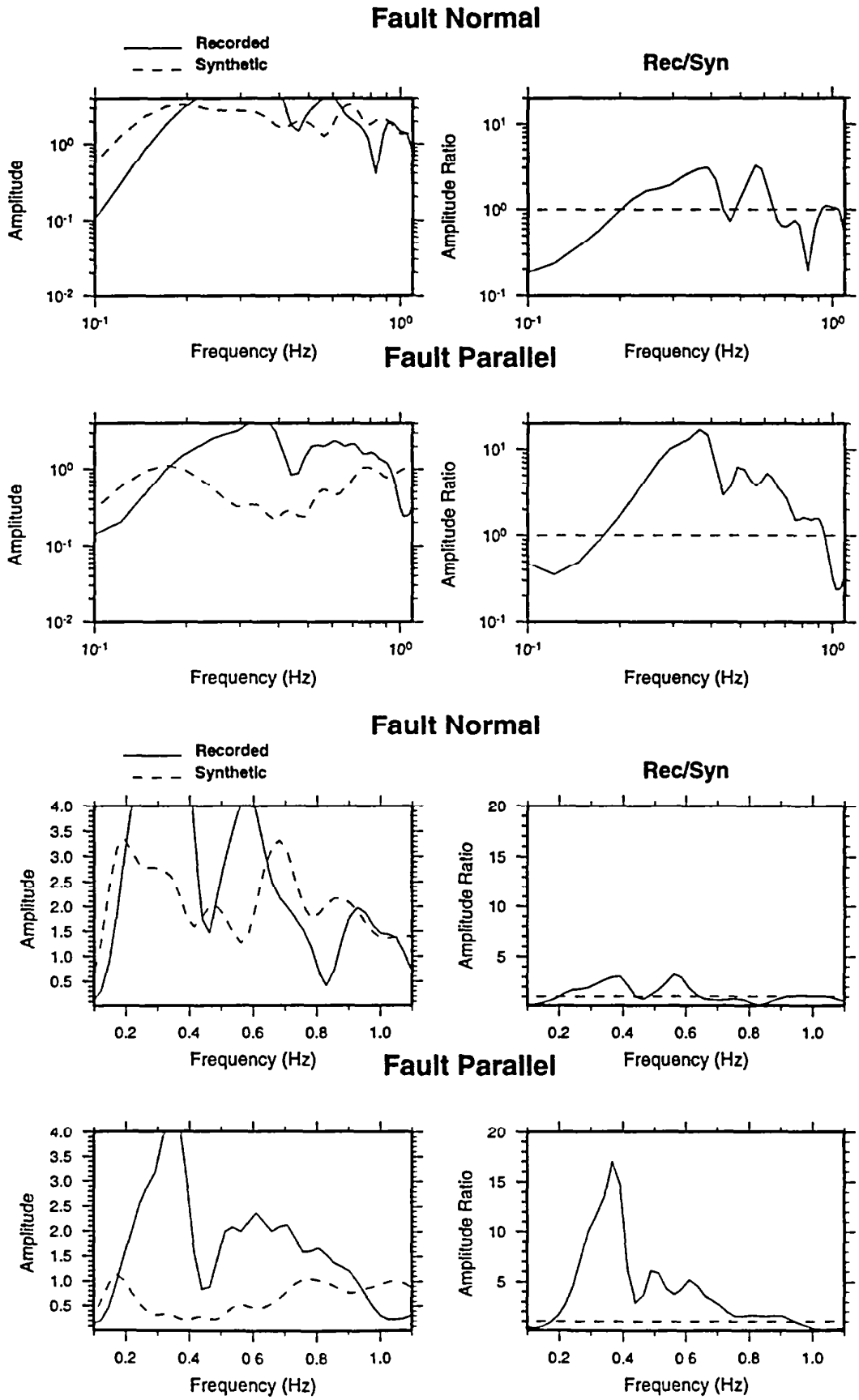

Loma Prieta 10/17/89 - srtg

Fault Normal

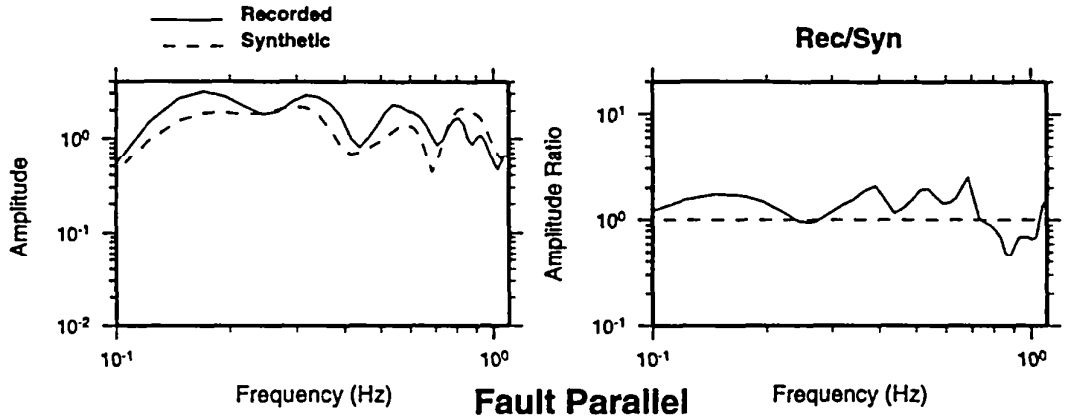

Fault Parallel

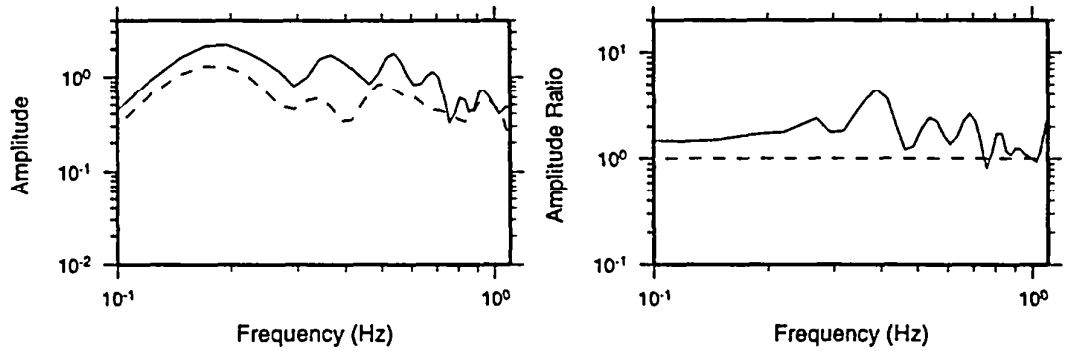

Fault Normal

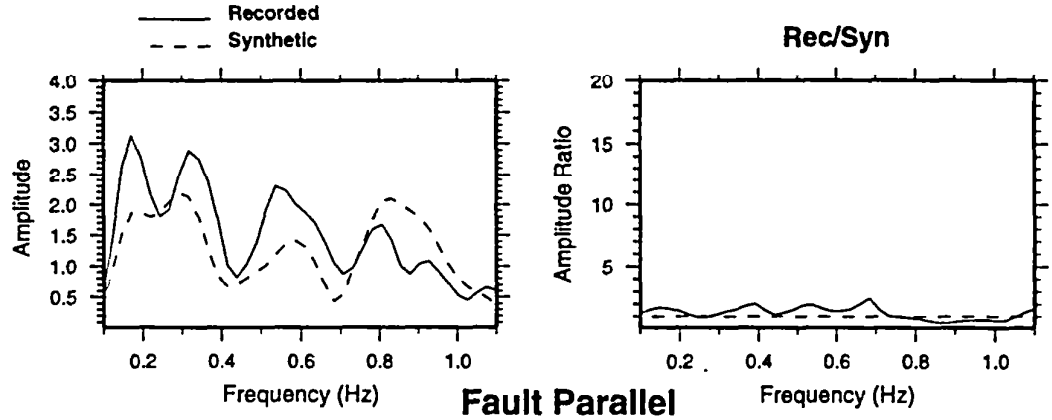

Fault Parallel

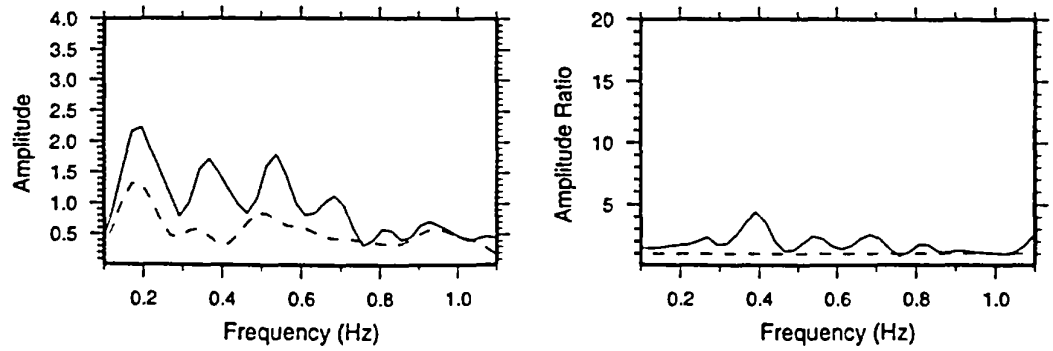

Loma Prieta 10/17/89 - ucsc

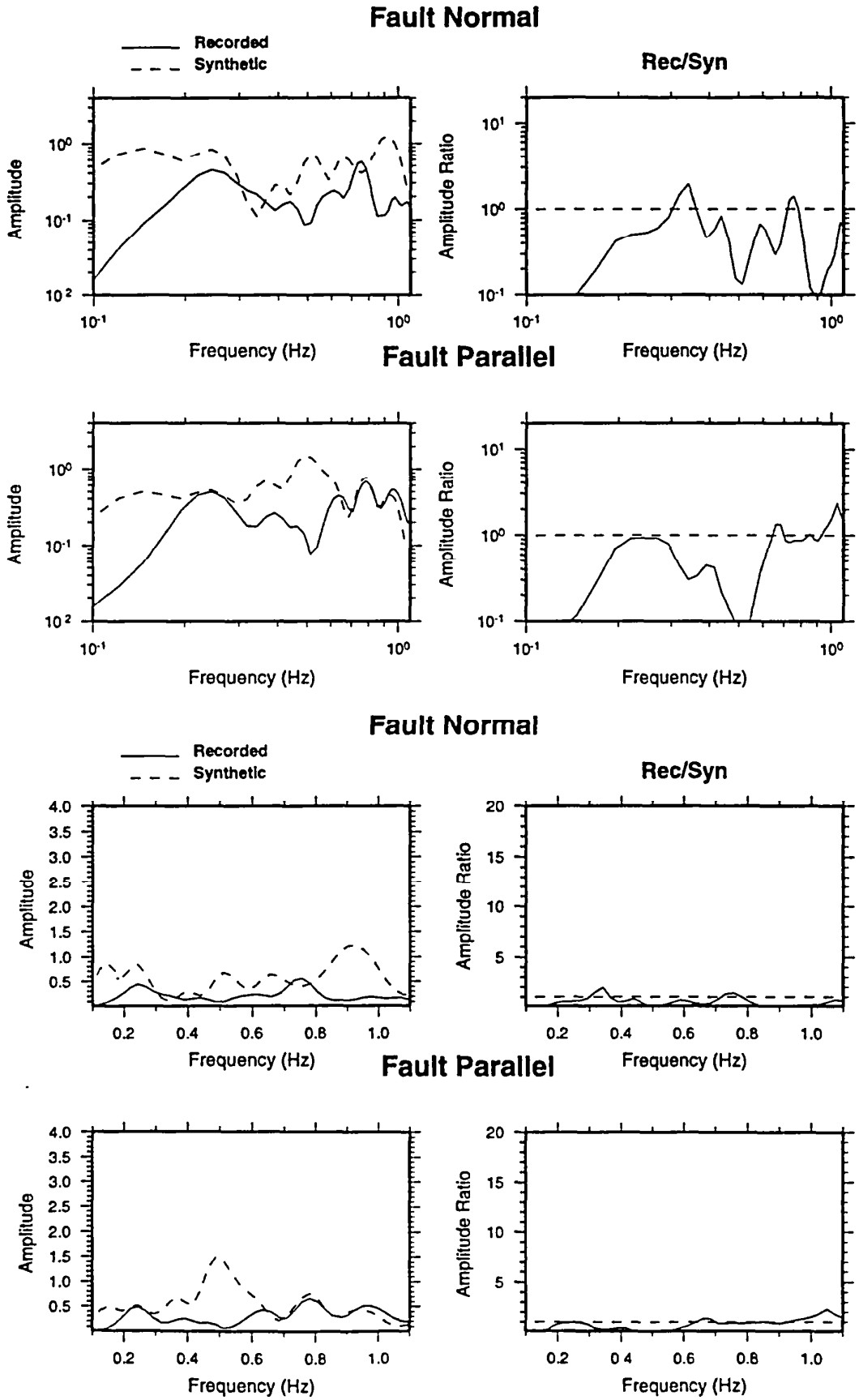

Loma Prieta 10/17/89 - waho

Fault Normal

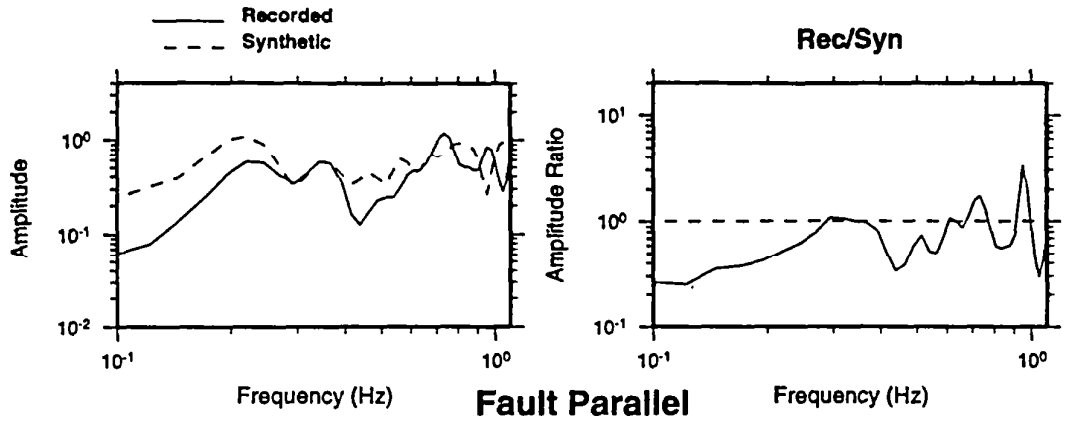

Fault Parallel

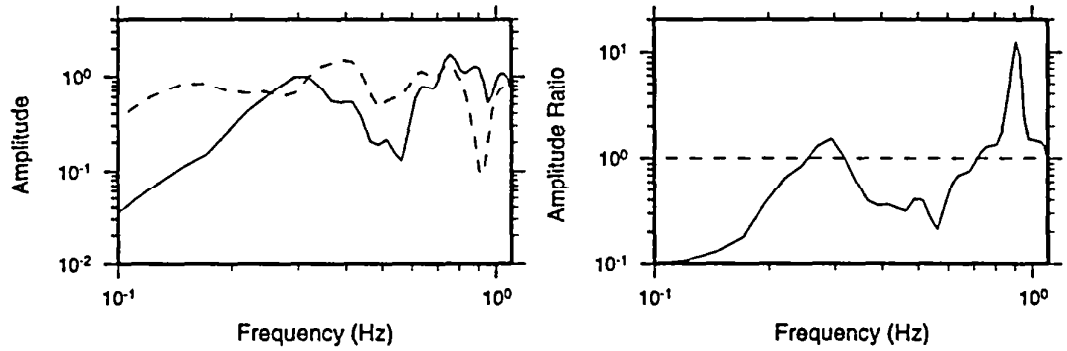

Fault Normal

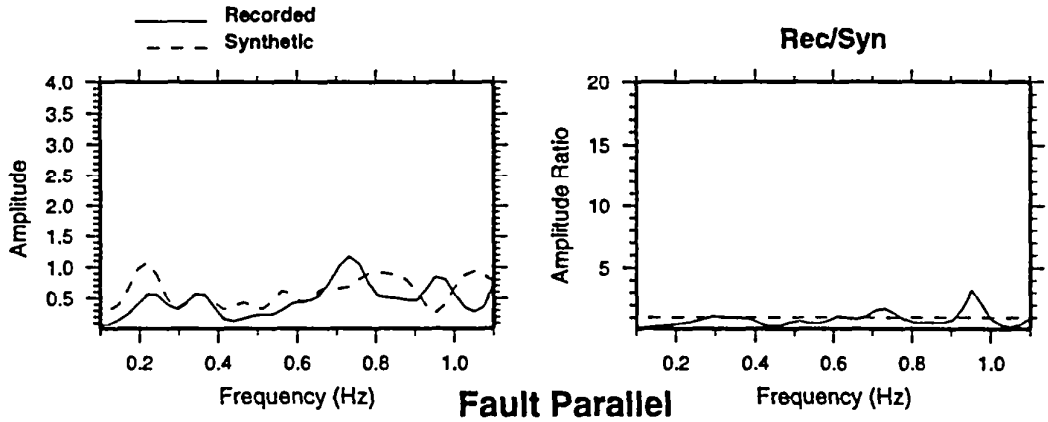

Fault Parallel

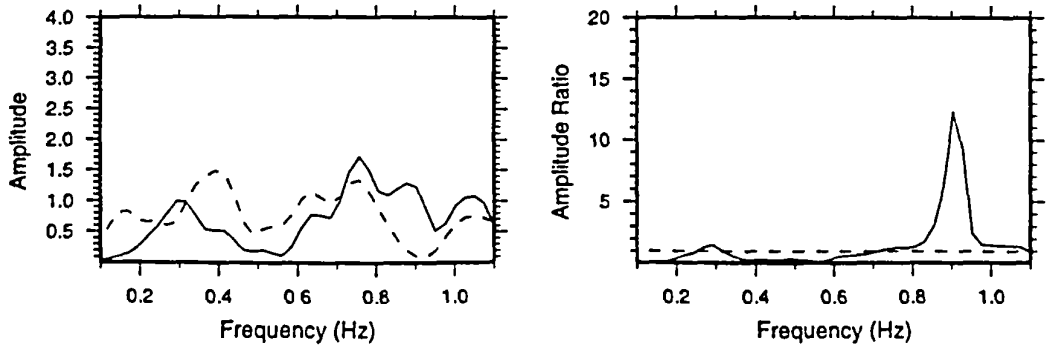

Loma Prieta - Fault Normal

SA at 7.0 sec

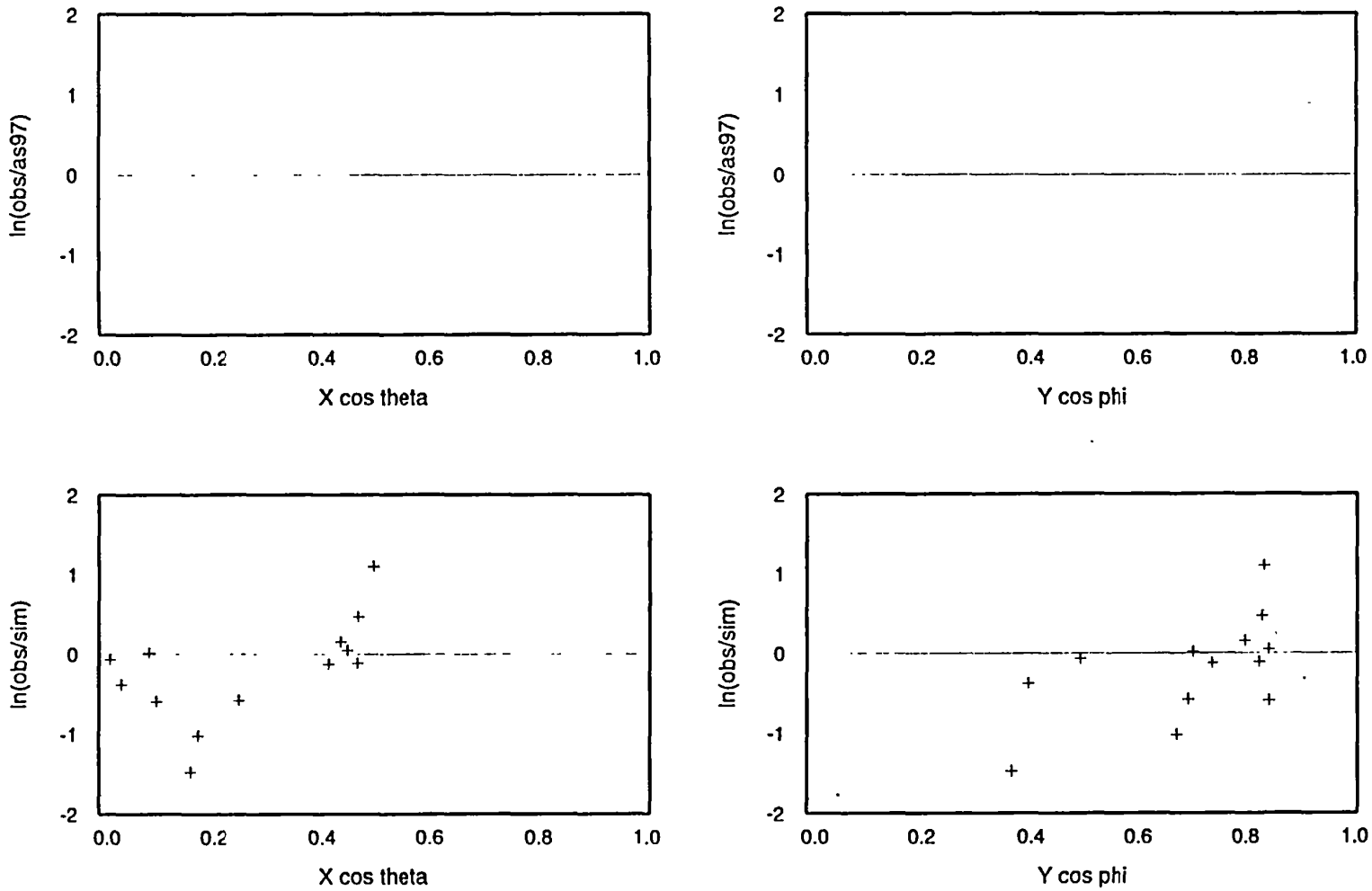

Loma Prieta - Fault Parallel

SA at 7.0 sec

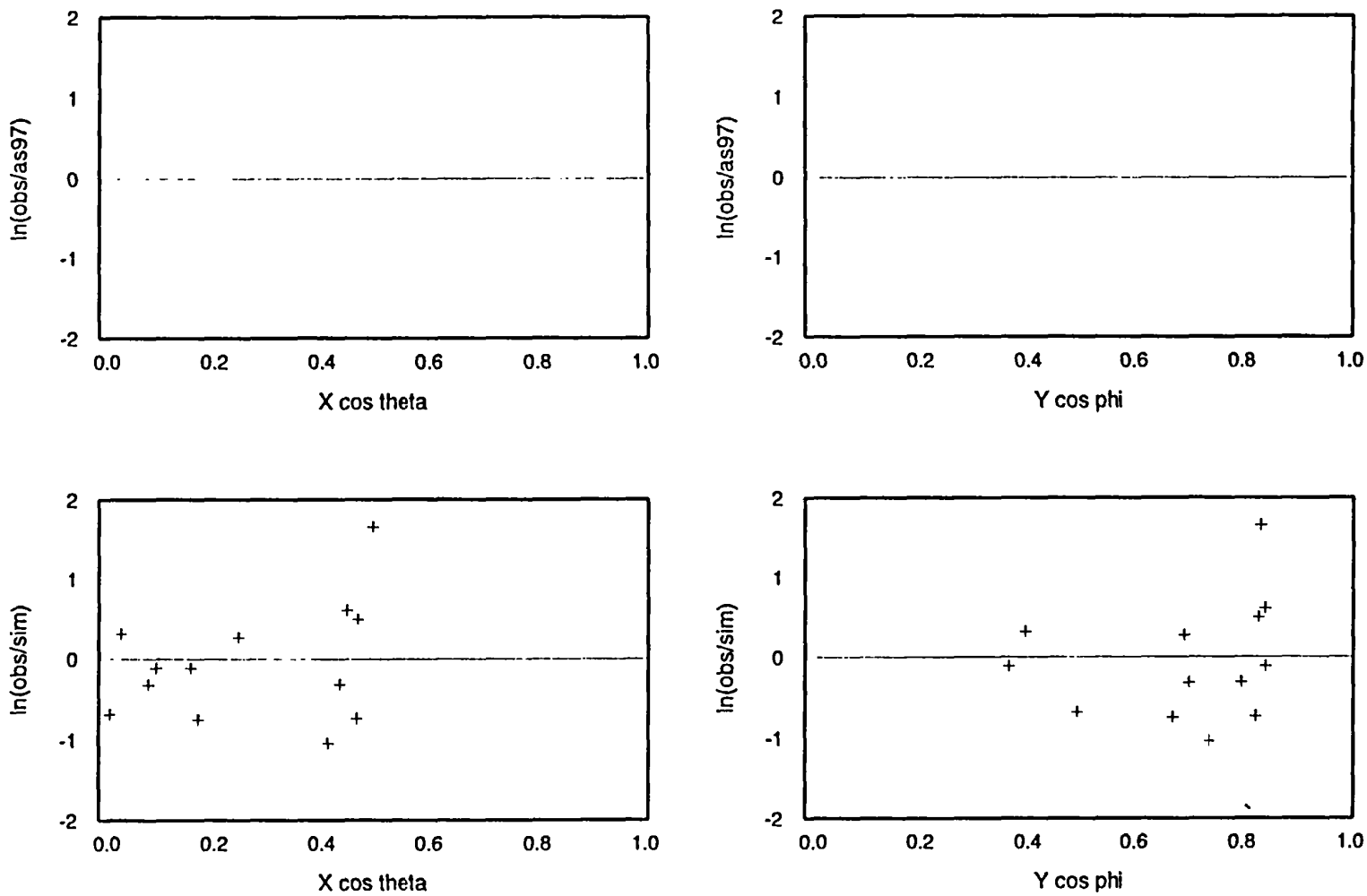

GMT Aug 24 14:54:07 1999 /u1/nancy/PEER-5/Loma/Comparisons/Resid_plots

Loma Prieta - Fault Normal

SA at 6.0 sec

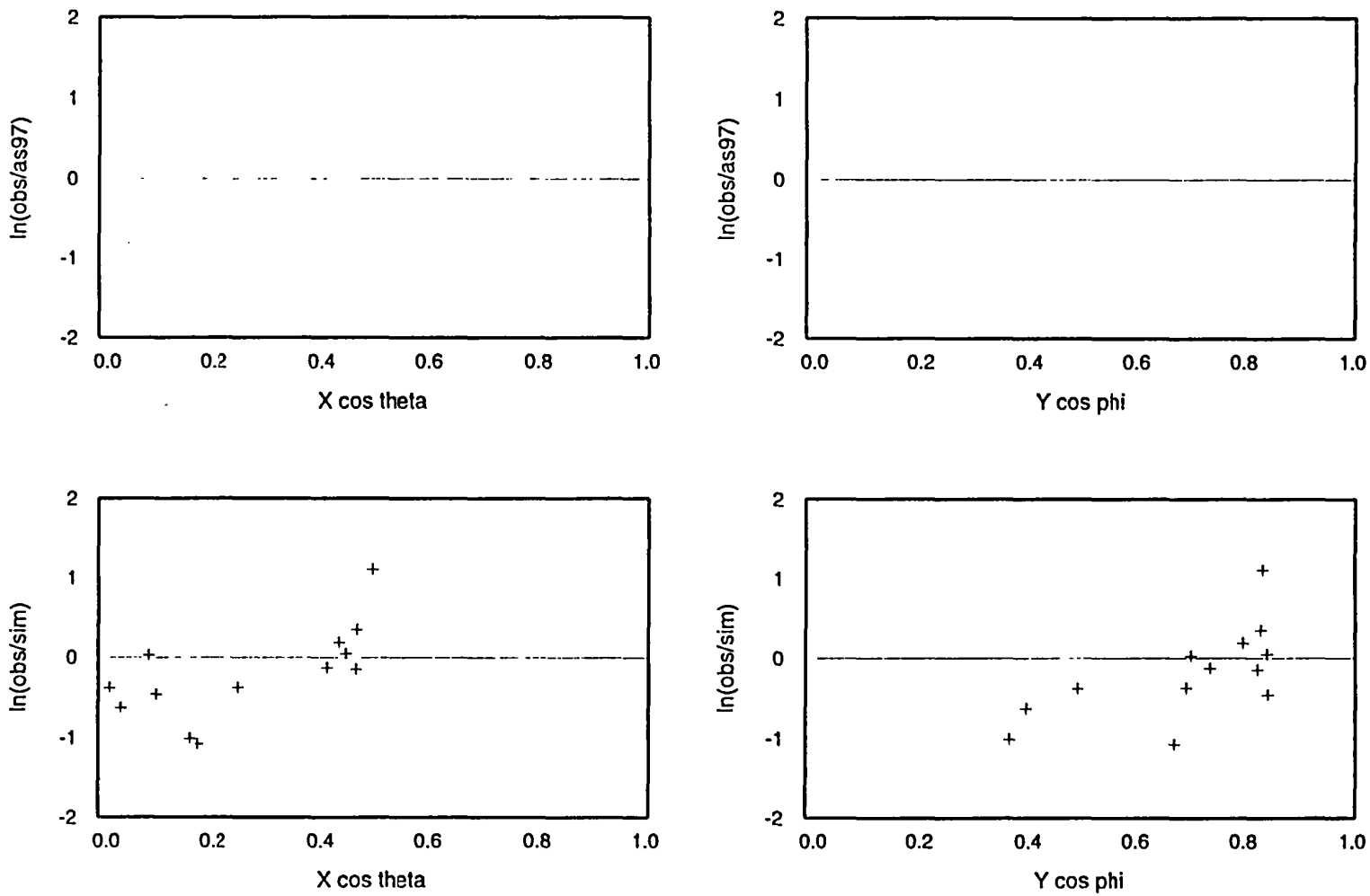

GMT Aug 24 14:54:21 1999 /u1/nancy/PEER-5/Loma/Comparisons/Resid_plots

Loma Prieta - Fault Parallel

SA at 6.0 sec

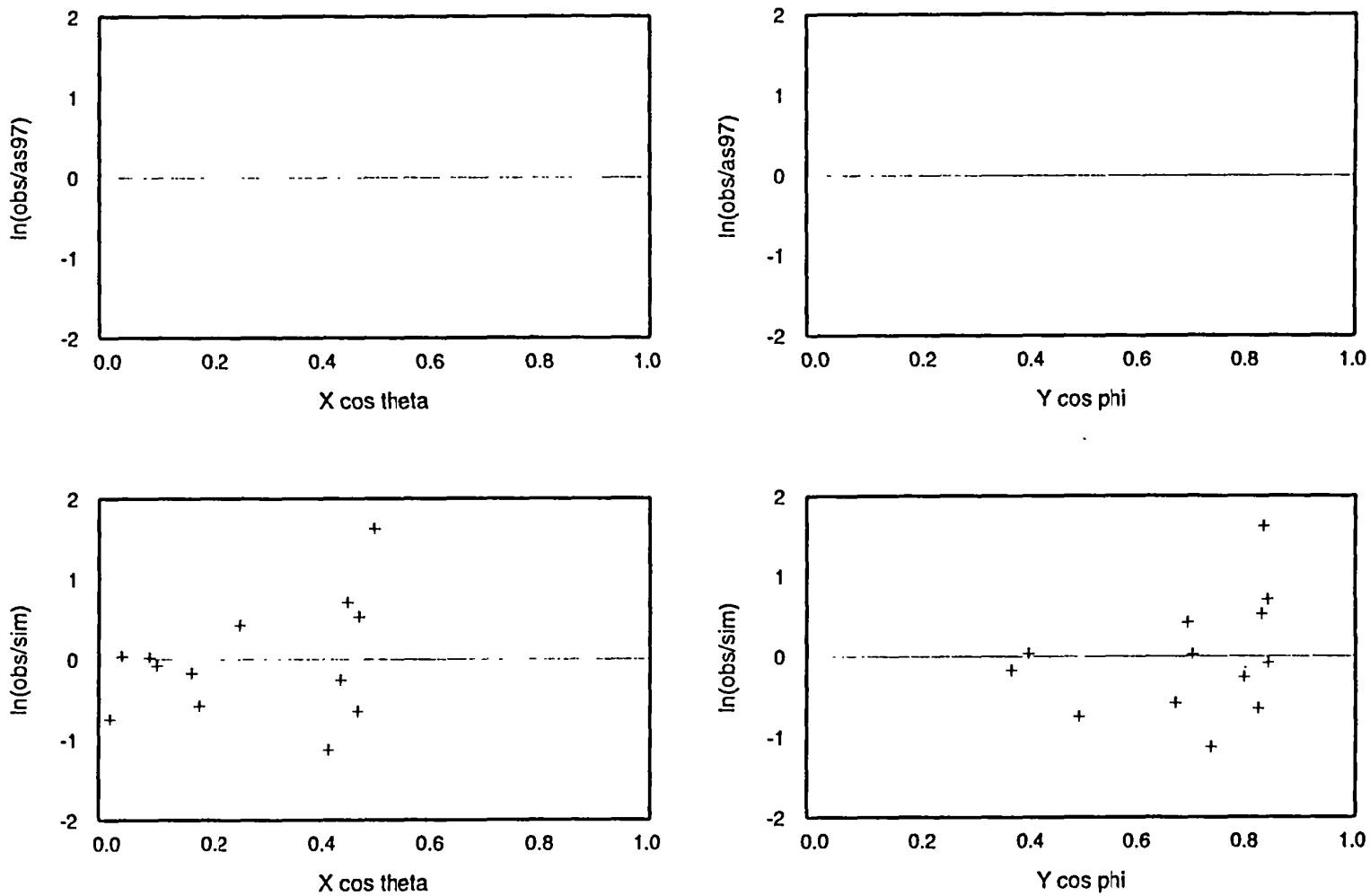

GMT Aug 24 14:54:34 1999 /u1/nancy/PEER-5/Loma/Comparisons/Resid_plots

Loma Prieta - Fault Normal

SA at 5.0 sec

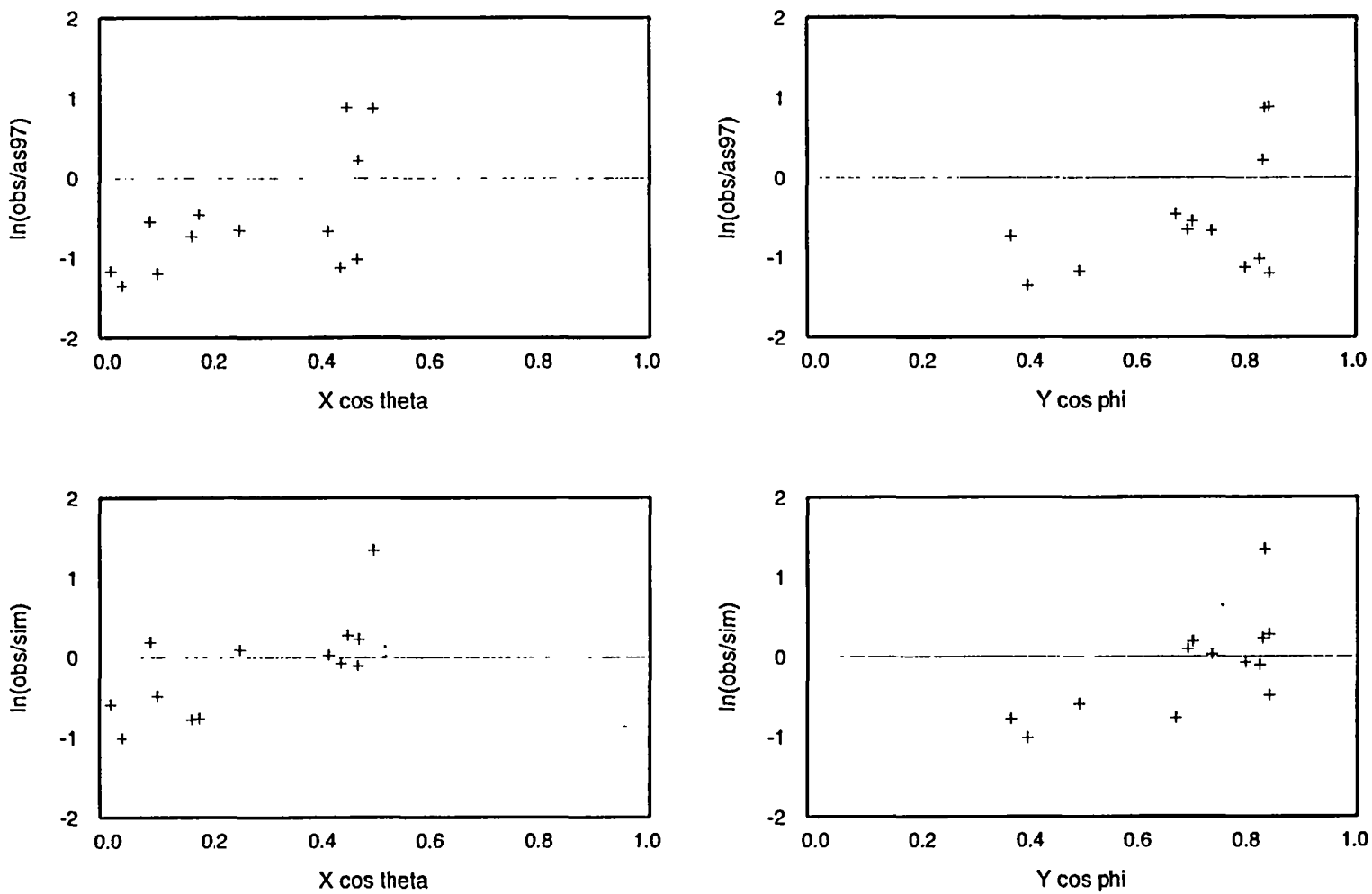

GMT Aug 24 14:54:49 1999 /u1/nancy/PEER-5/Loma/Comparisons/Resid_plots

Loma Prieta - Fault Parallel

SA at 5.0 sec

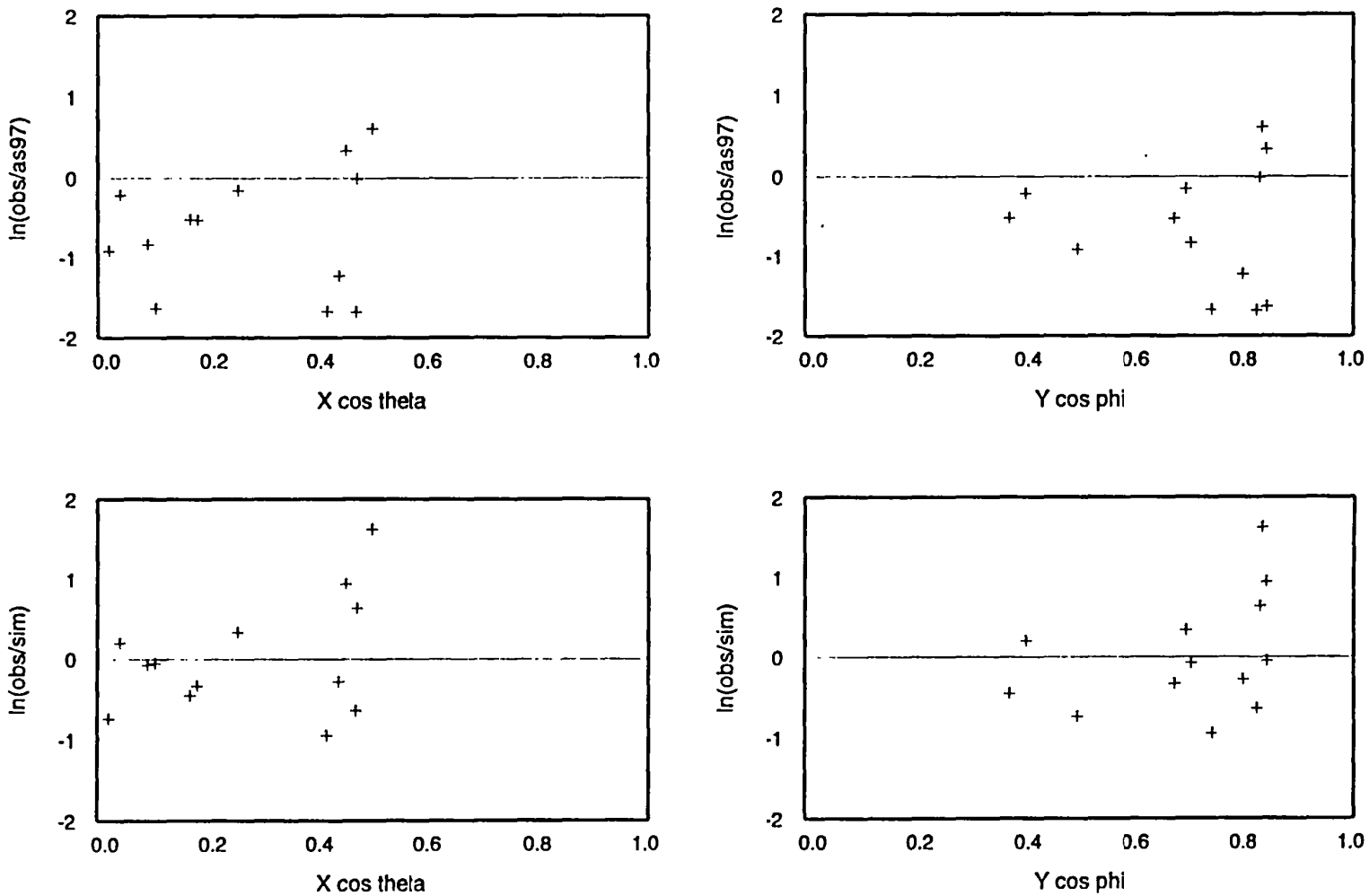

GMT Aug 24 14:55:02 1999 /u1/nancy/PEER-5/Loma/Comparisons/Resid_plots

Loma Prieta - Fault Normal

SA at 4.0 sec

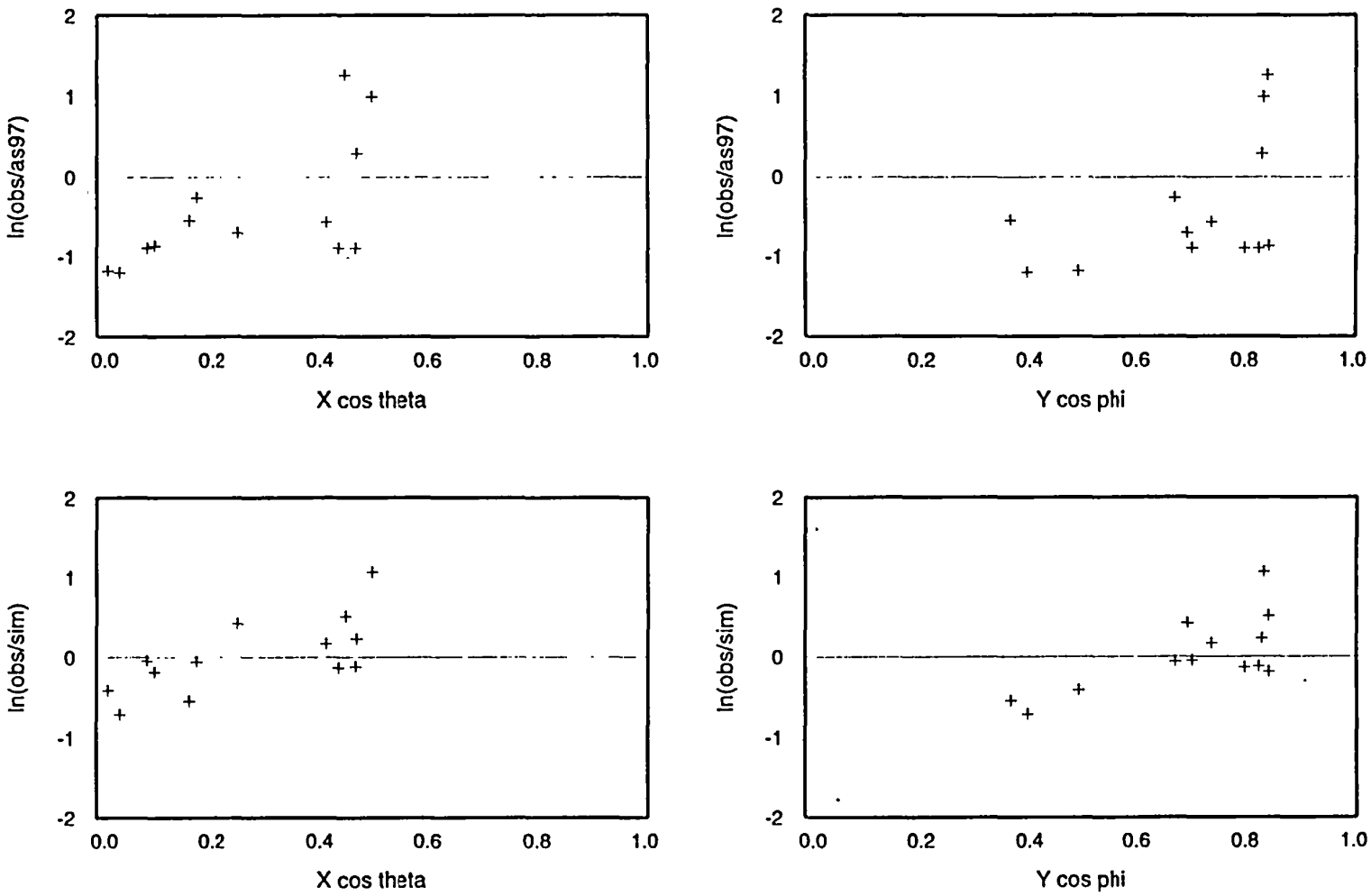

GMT Aug 24 14:55:17 1999 /u1/nancy/PEER-5/Loma/Comparisons/Resid_plots

Loma Prieta - Fault Parallel

SA at 4.0 sec

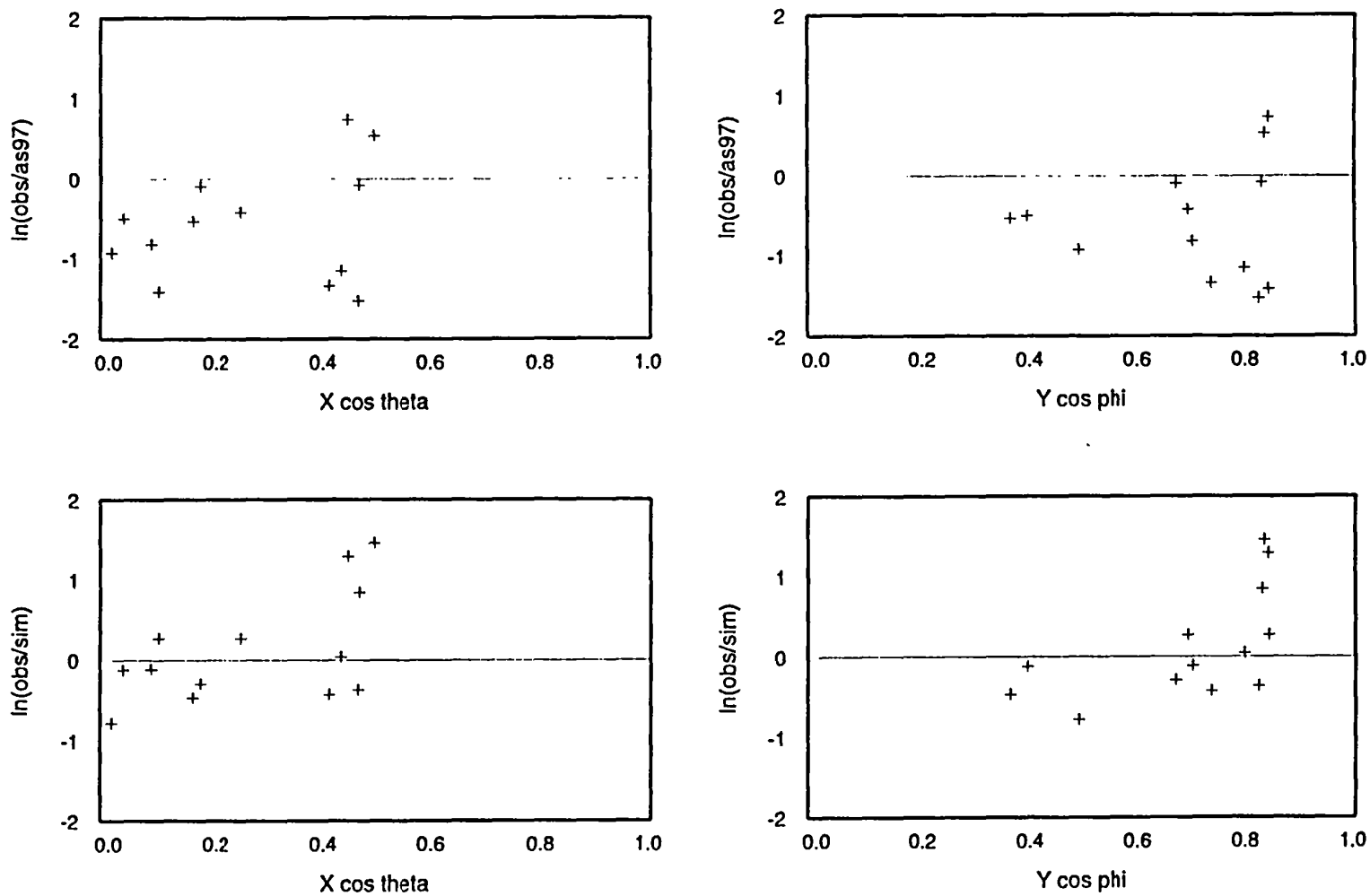

GMT Aug 24 14:55:30 1999 /u1/nancy/PEER-5/Loma/Comparisons/Resid_plots

Loma Prieta - Fault Normal

SA at 3.0 sec

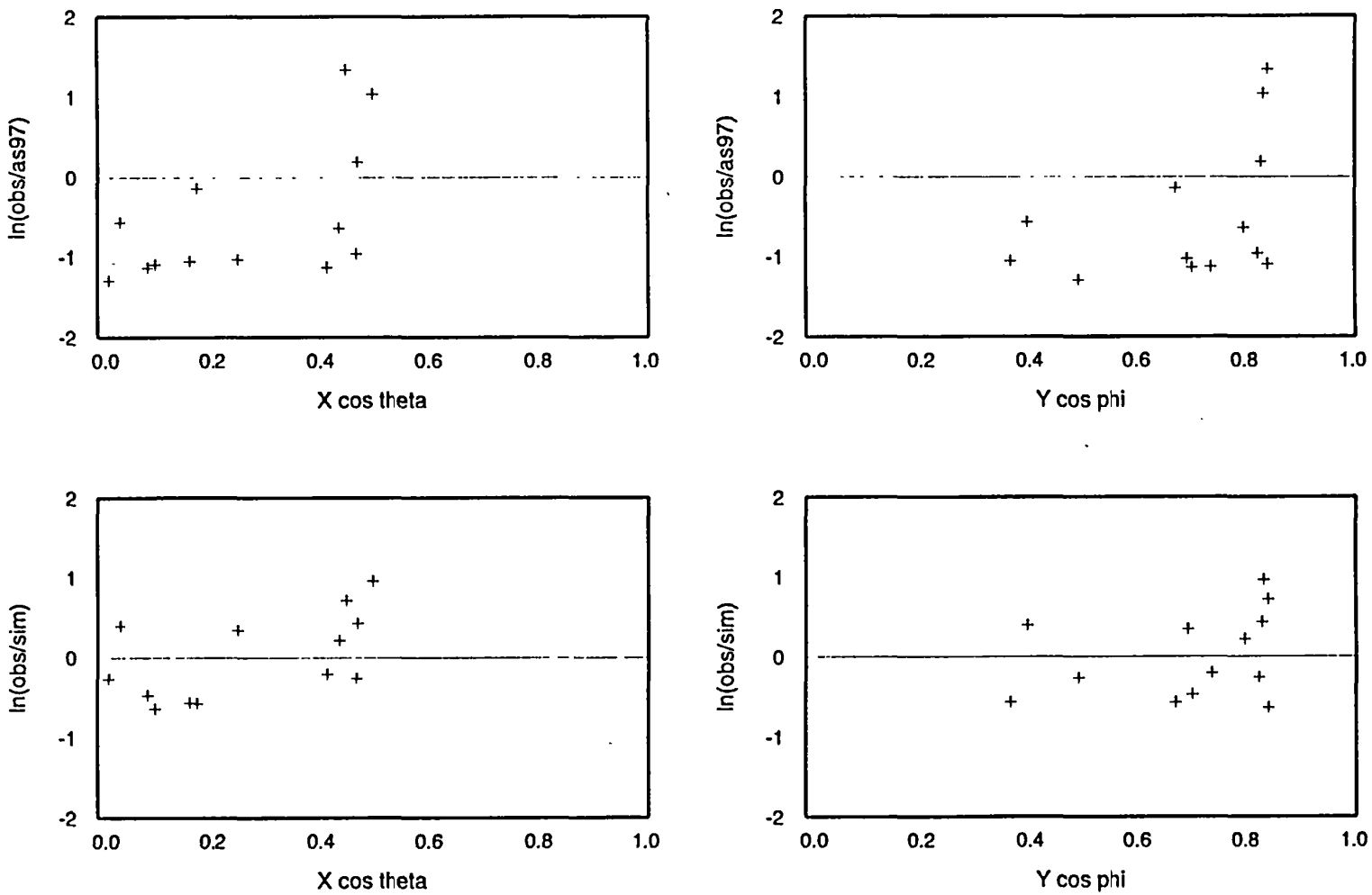

GMT Aug 24 14:55:43 1999 /u1/nancy/PEER-5/Loma/Comparisons/Resid_plots

Loma Prieta - Fault Parallel

SA at 3.0 sec

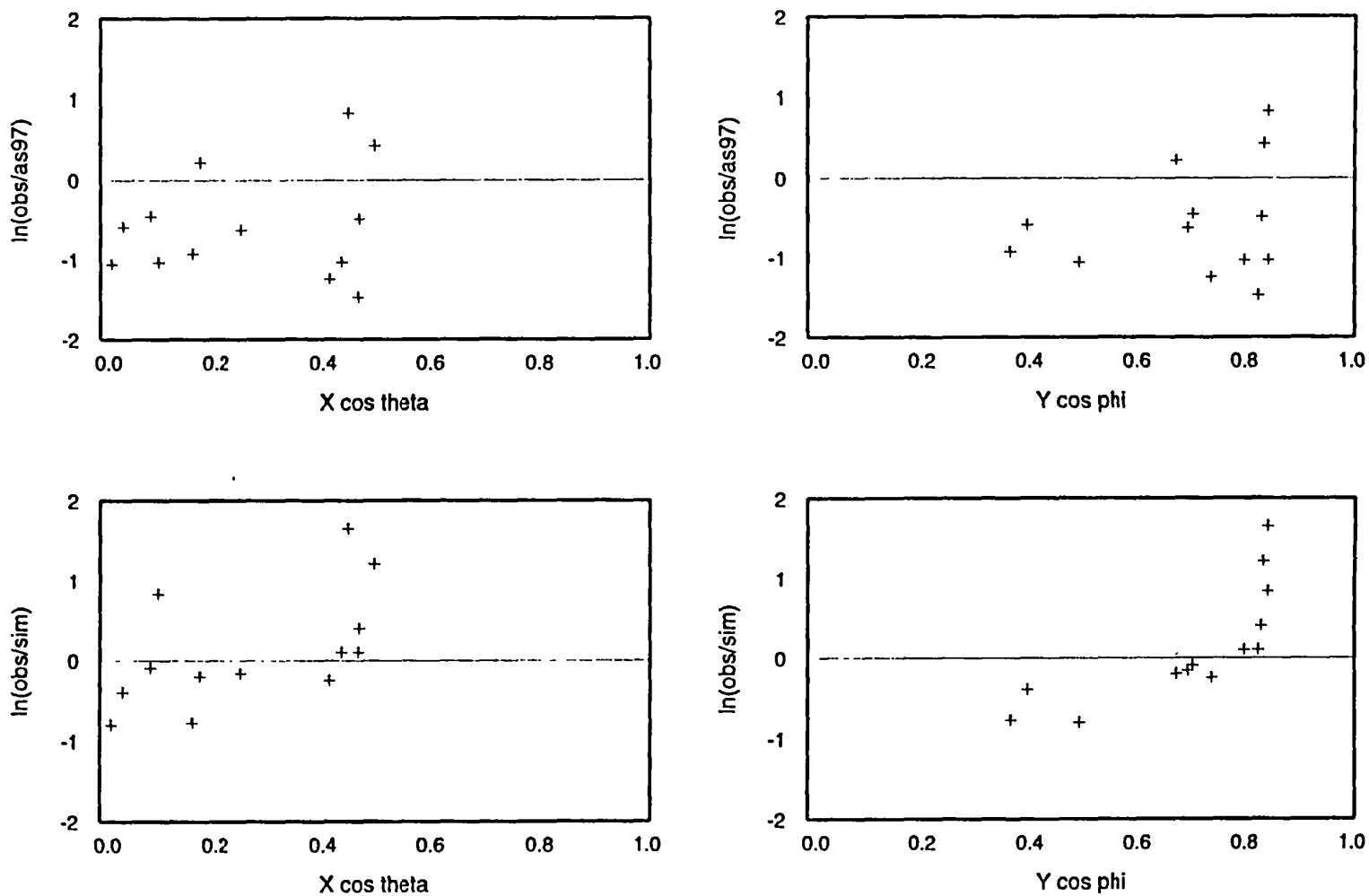

Loma Prieta - Fault Normal

SA at 2.0 sec

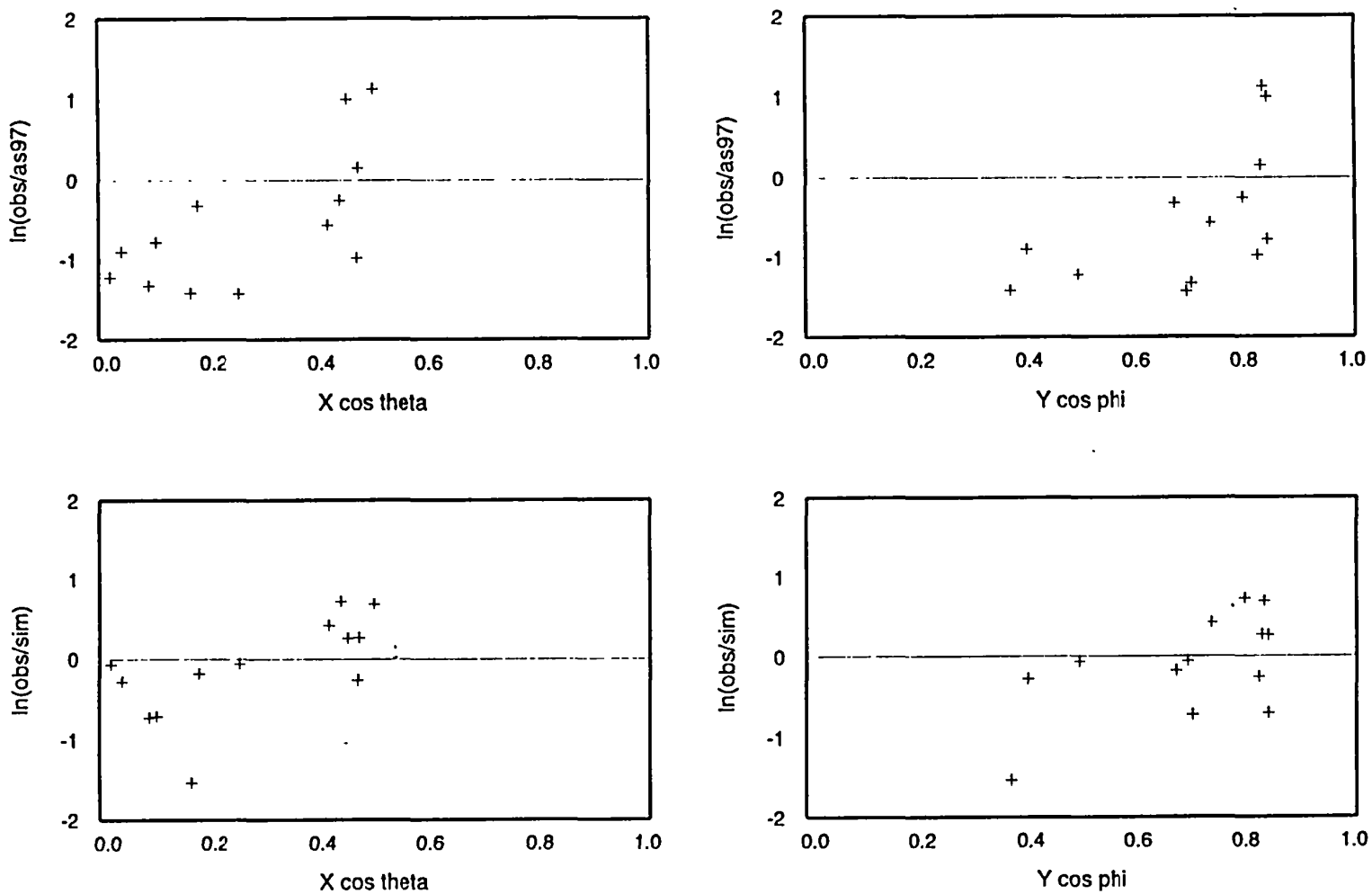

GMT Aug 24 14:57:46 1999 /u1/nancy/PEER-5/Loma/Comparisons/Resid_plots

Loma Prieta - Fault Parallel

SA at 2.0 sec

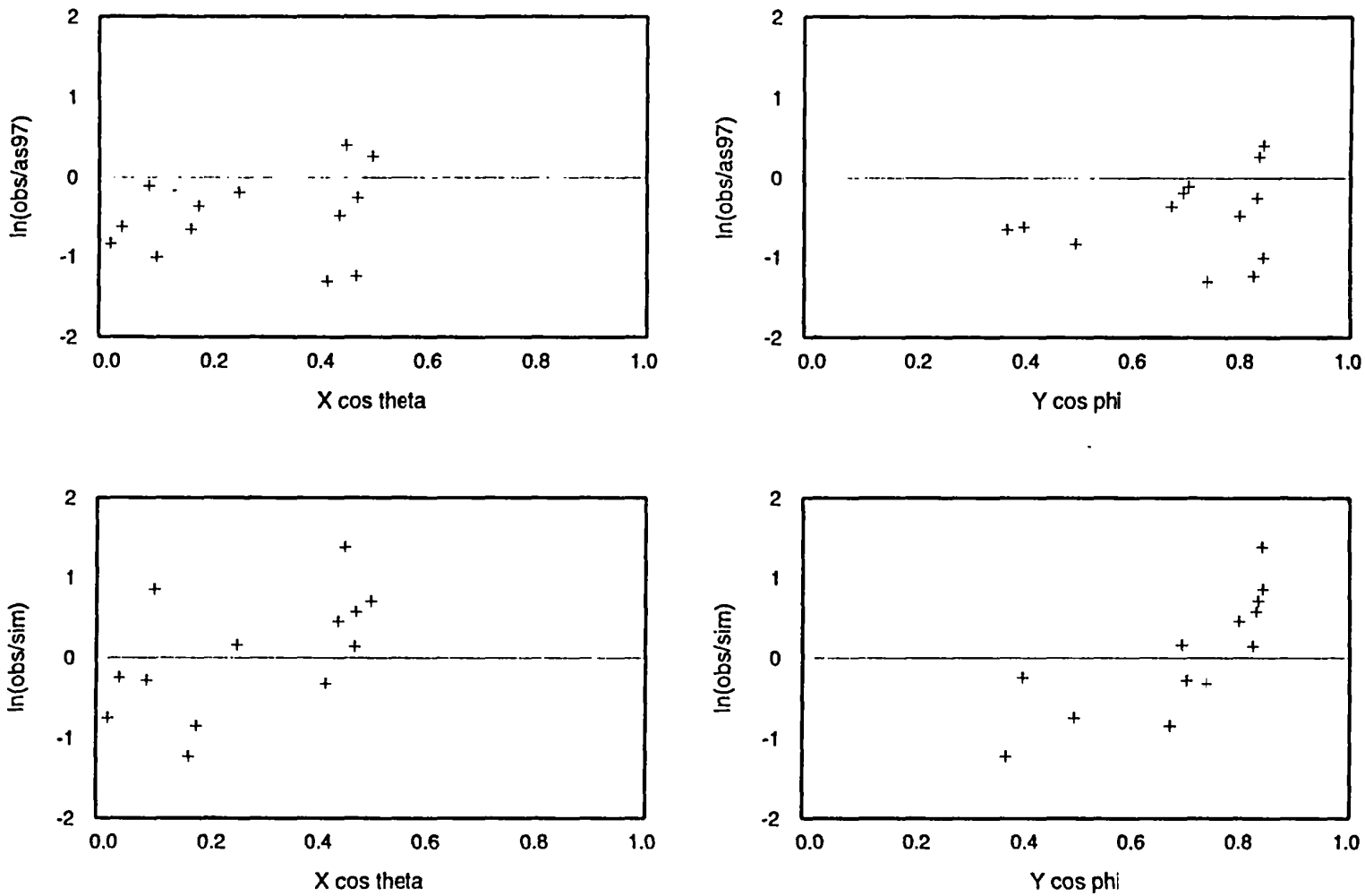

GMT Aug 24 14:57:58 1999 /u1/nancy/PEER-5/Loma/Comparisons/Resid_plots

Loma Prieta - Fault Normal

SA at 1.5 sec

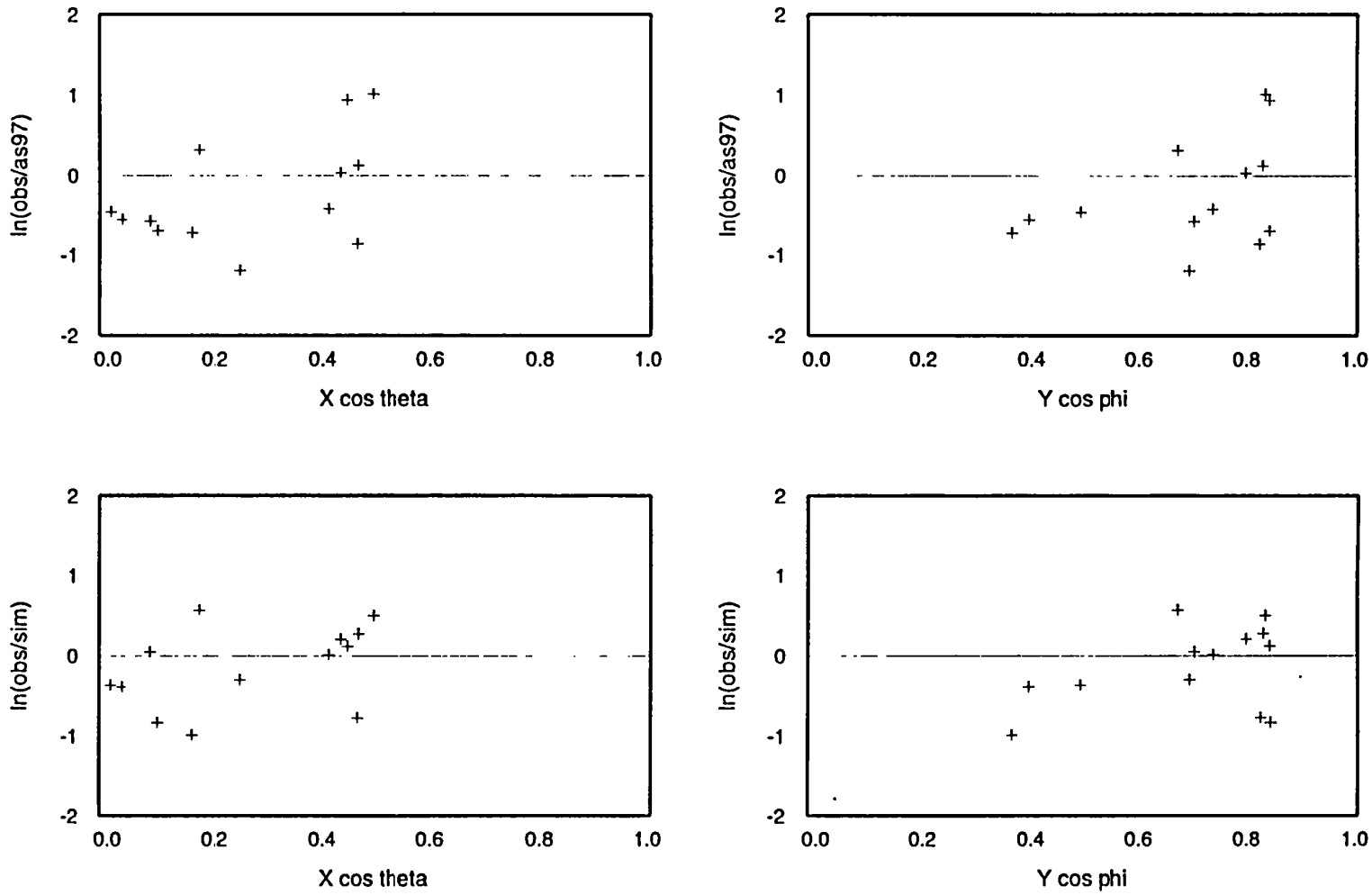

GMT Aug 24 14:58:10 1999 /u1/nancy/PEER-5/Loma/Comparisons/Resid_plots

Loma Prieta - Fault Parallel

SA at 1.5 sec

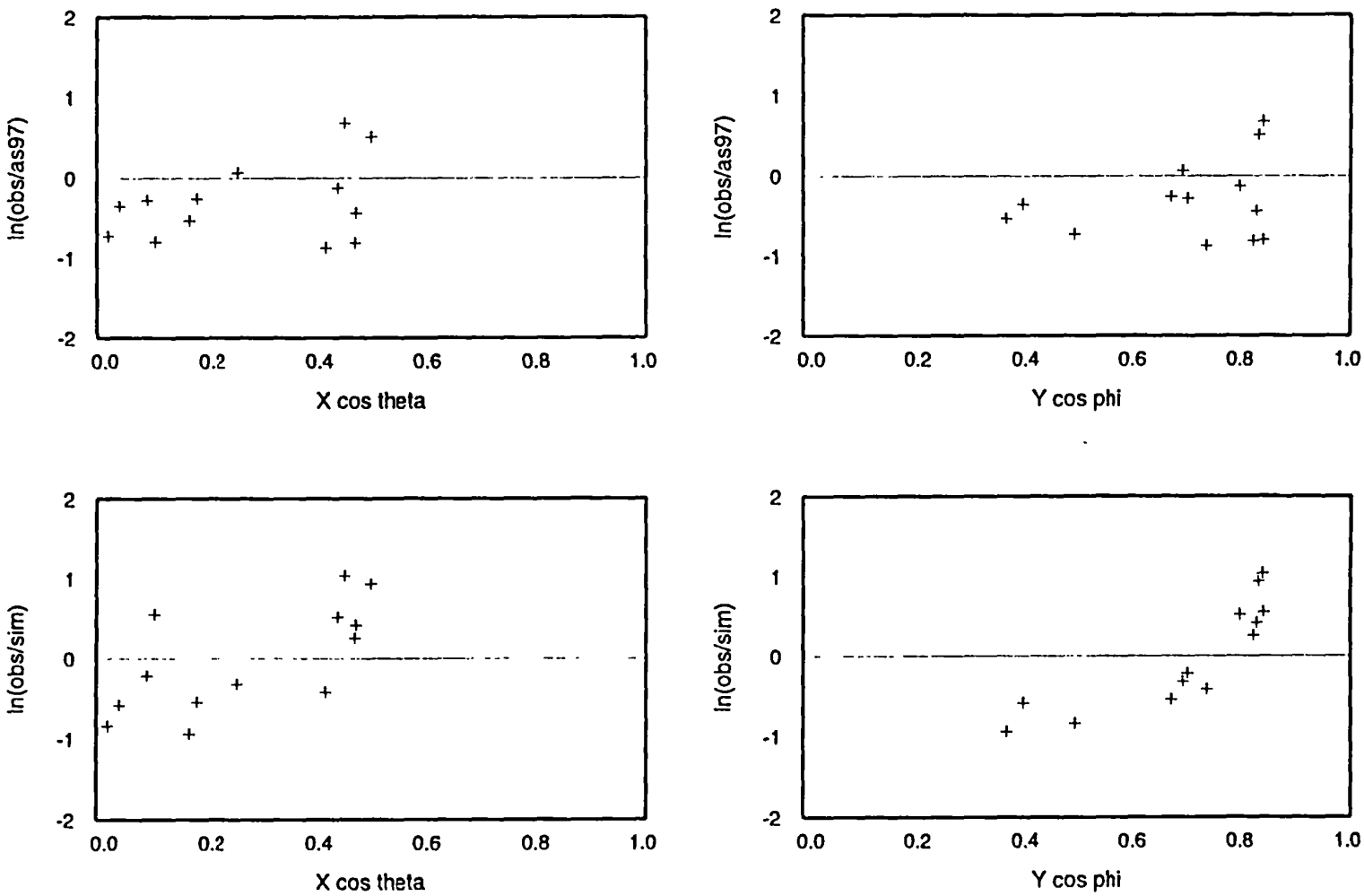

GMT Aug 24 14:58:22 1999 /u1/nancy/PEER-5/Loma/Comparisons/Resid_plots

Loma Prieta - Fault Normal

SA at 1.0 sec

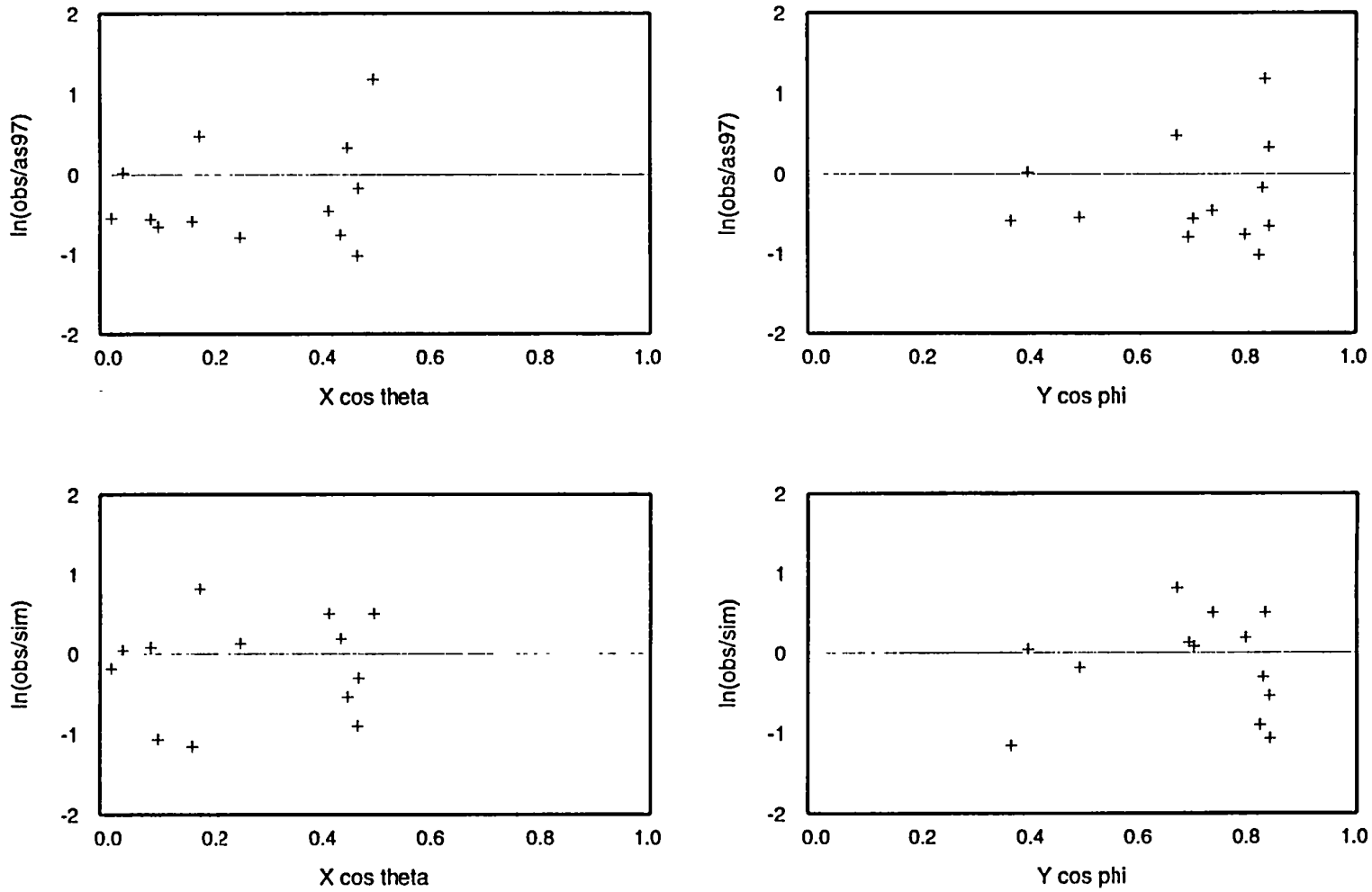

GMT Aug 24 14:58:35 1999 /u1/nancy/PEER-5/Loma/Comparisons/Resid_plots

Loma Prieta - Fault Parallel

SA at 1.0 sec

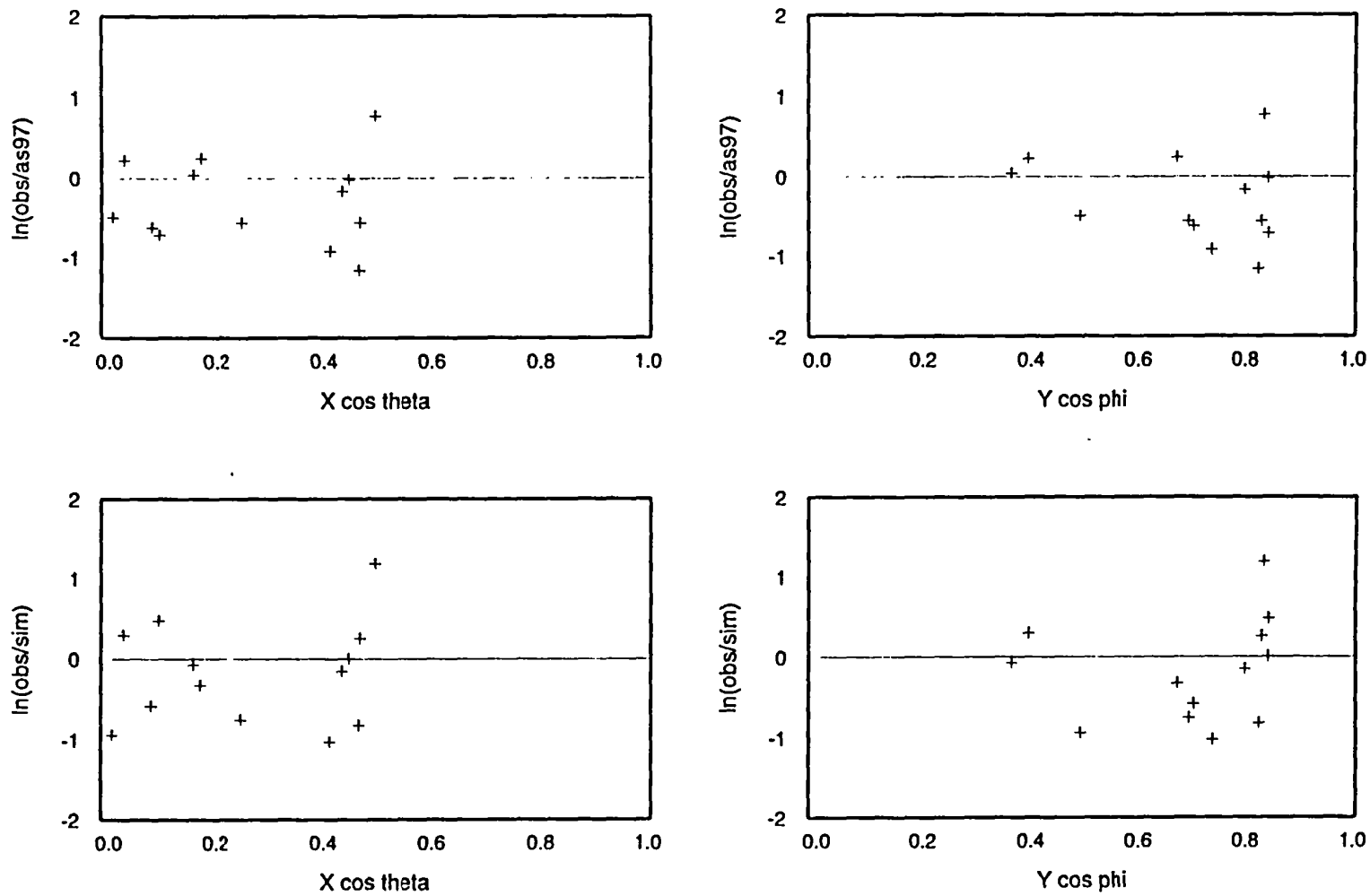

Station	Correlation FN	Correlation FP	Least Squares FN	Least Squares FP	Response Spectra FN	Response Spectra FP	Fourier Spectra FN	Fourier Spectra FP
bars	0.752		0.329		0.427	-0.044	0.377	0.153
cool	0.618		-0.155		-0.698	-0.224	-0.595	-0.253
dhsp	0.359		0.054		0.533	0.951	0.623	1.080
frti	0.618		0.181		0.073	0.705	-0.128	0.703
josh	0.311		0.029		1.032	0.336	0.994	0.423
lcss	0.622		-0.013		-0.475	-0.559	-0.679	-0.455
mvfs	0.273		0.038		1.080	0.780	1.041	0.929
nplm	0.374		0.055		0.962	1.132	0.965	1.179
plma	0.584		0.184		0.553	0.873	0.708	0.981
yerm	0.633		0.011		0.439	0.707	0.352	0.653
Average	0.514		0.071		0.393	0.466	0.366	0.539
Sigma	0.167		0.132		0.612	0.838	0.620	1.132
Sigma Mean	0.053		0.042		0.193	0.265	0.196	0.358

Landers - Fault Normal

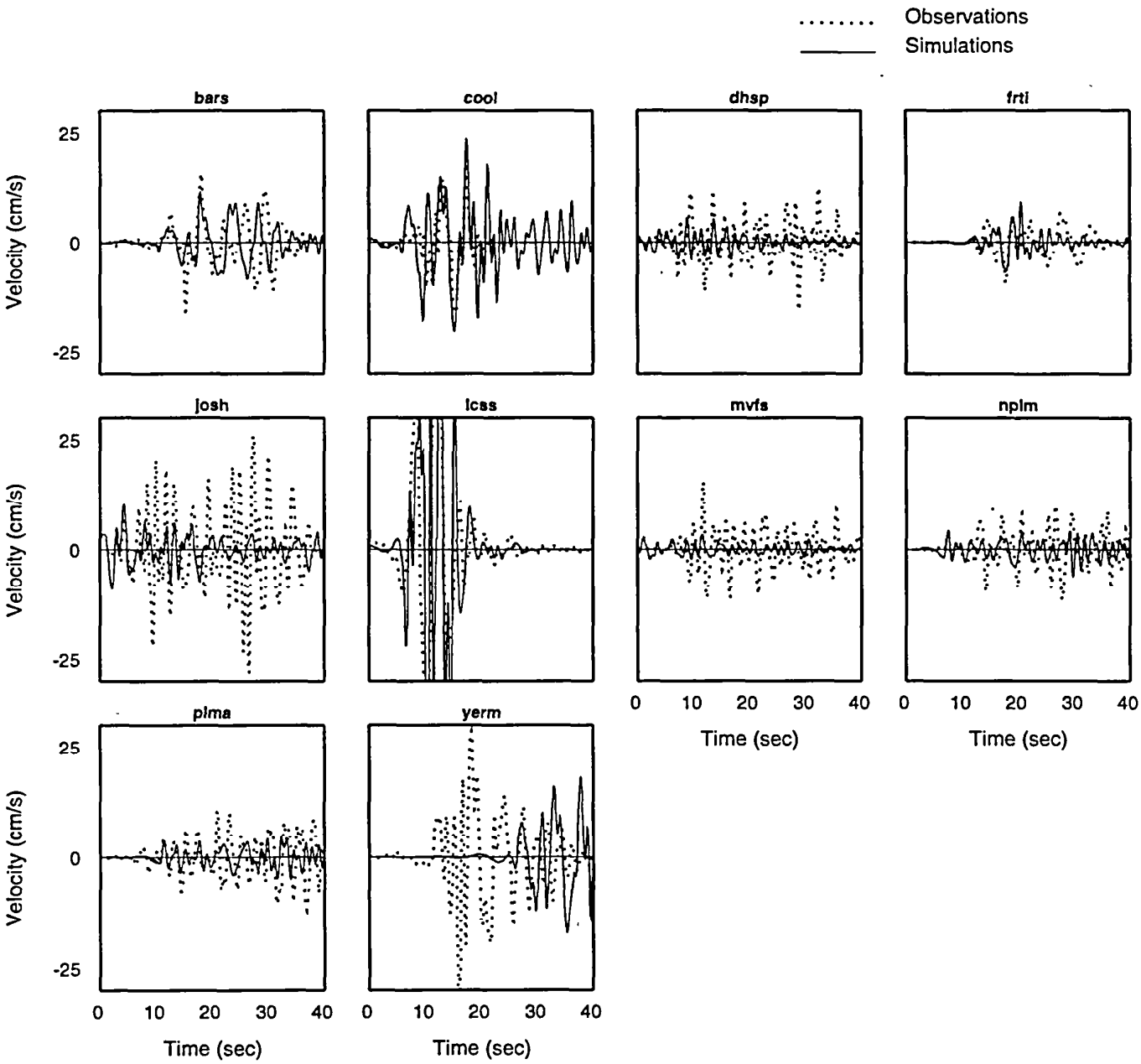

Landers - Fault Parallel

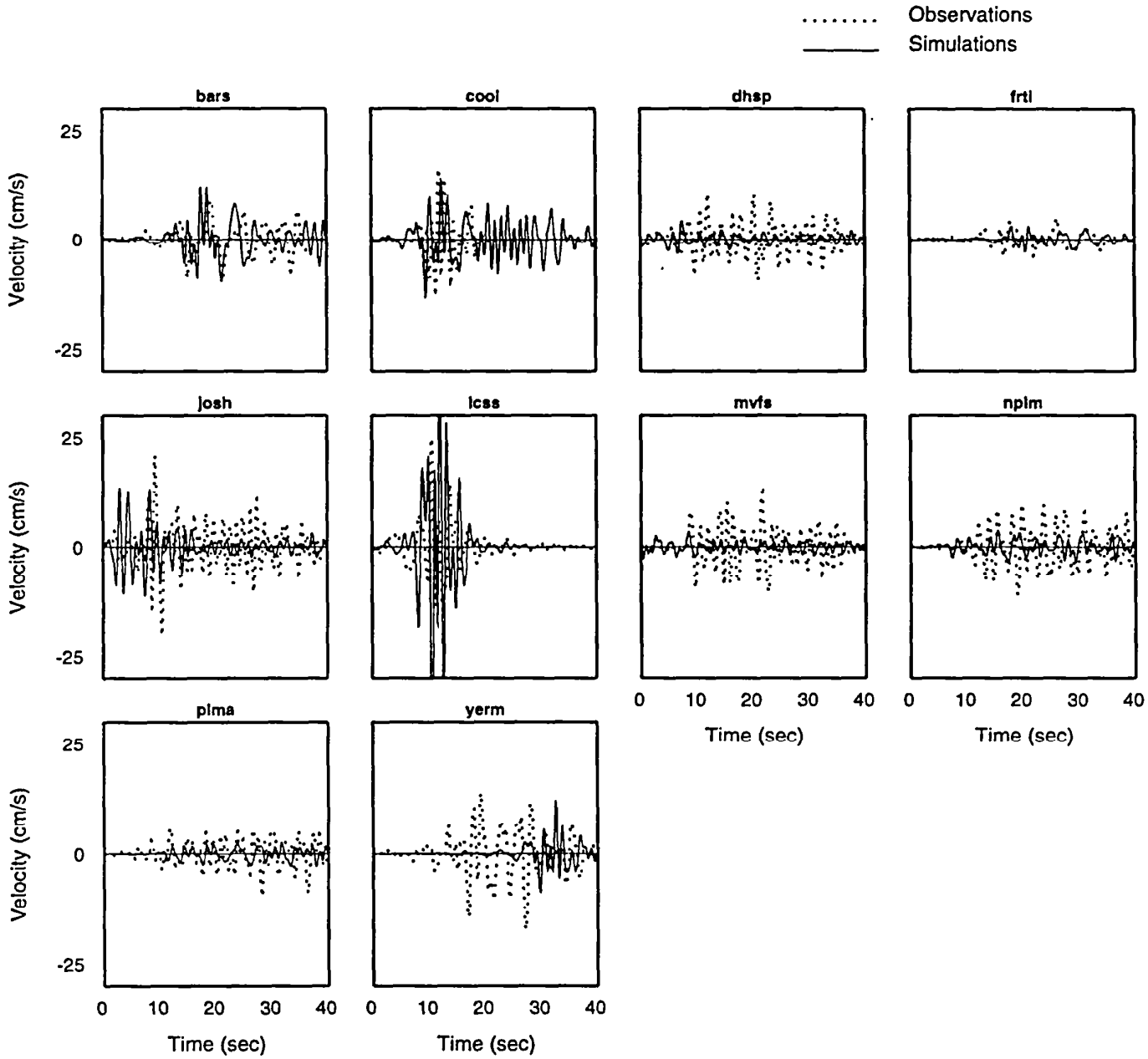

Landers - Fault Normal

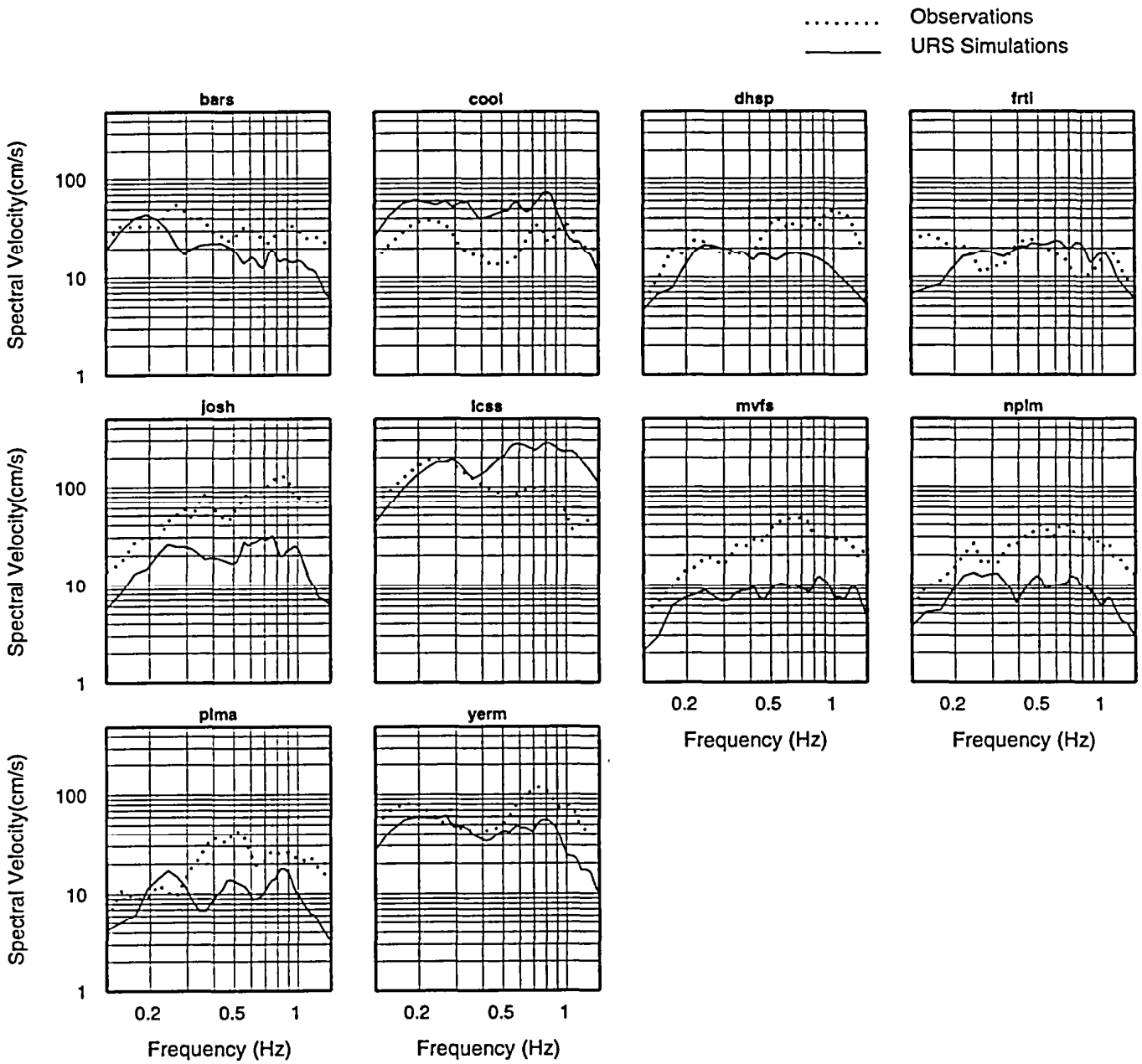

Landers - Fault Parallel

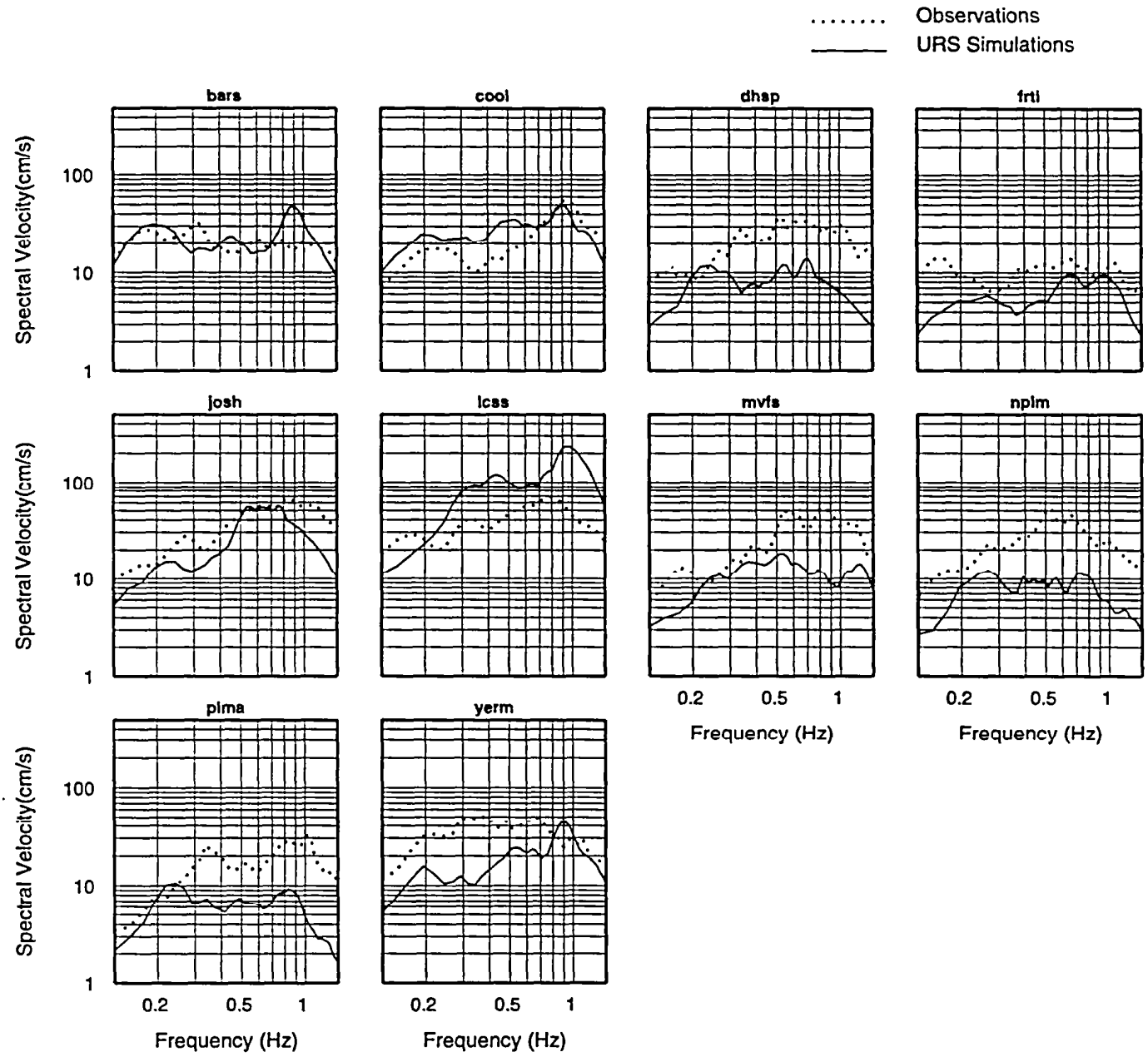

Landers - Fault Normal

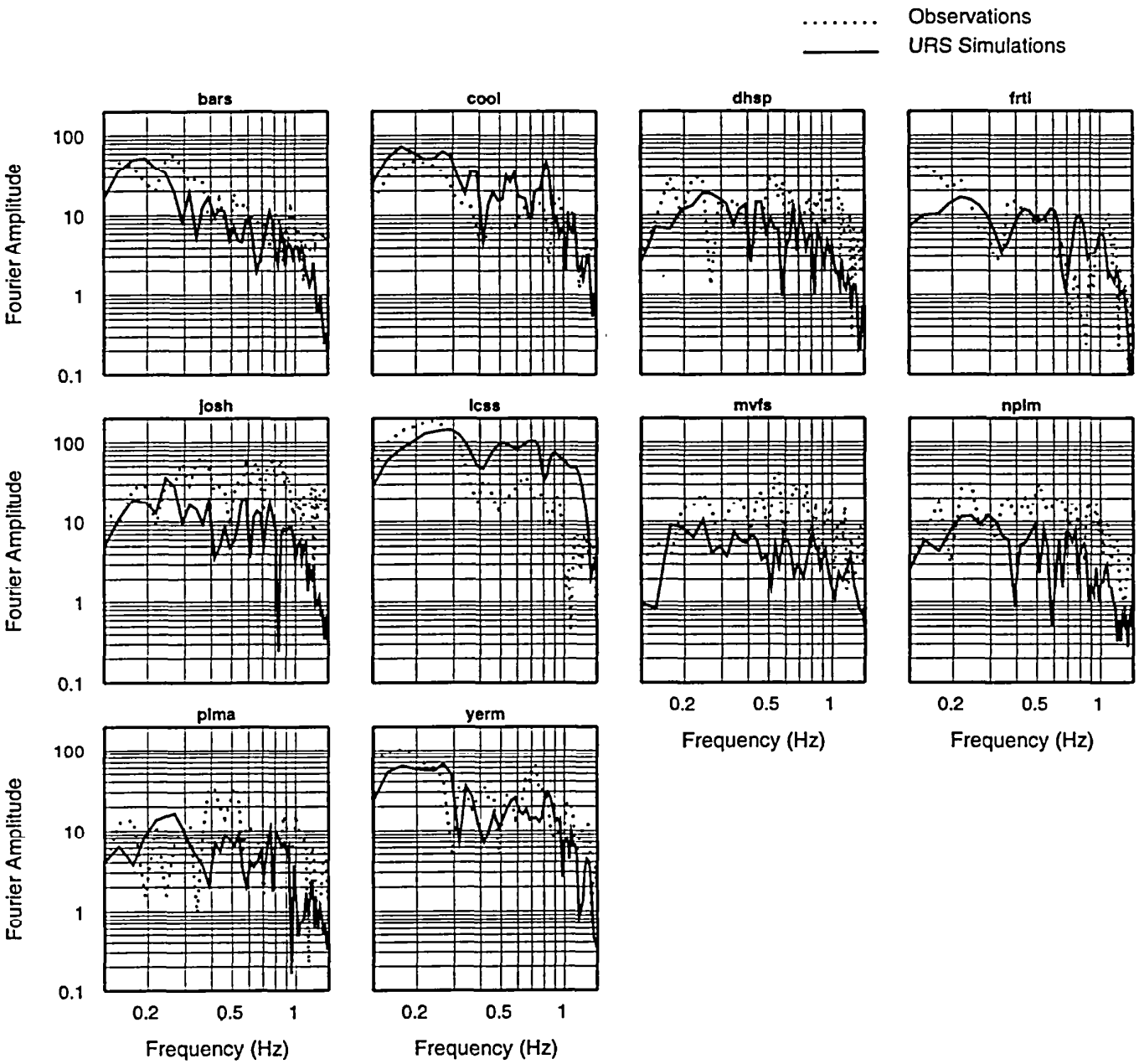

Landers - Fault Parallel

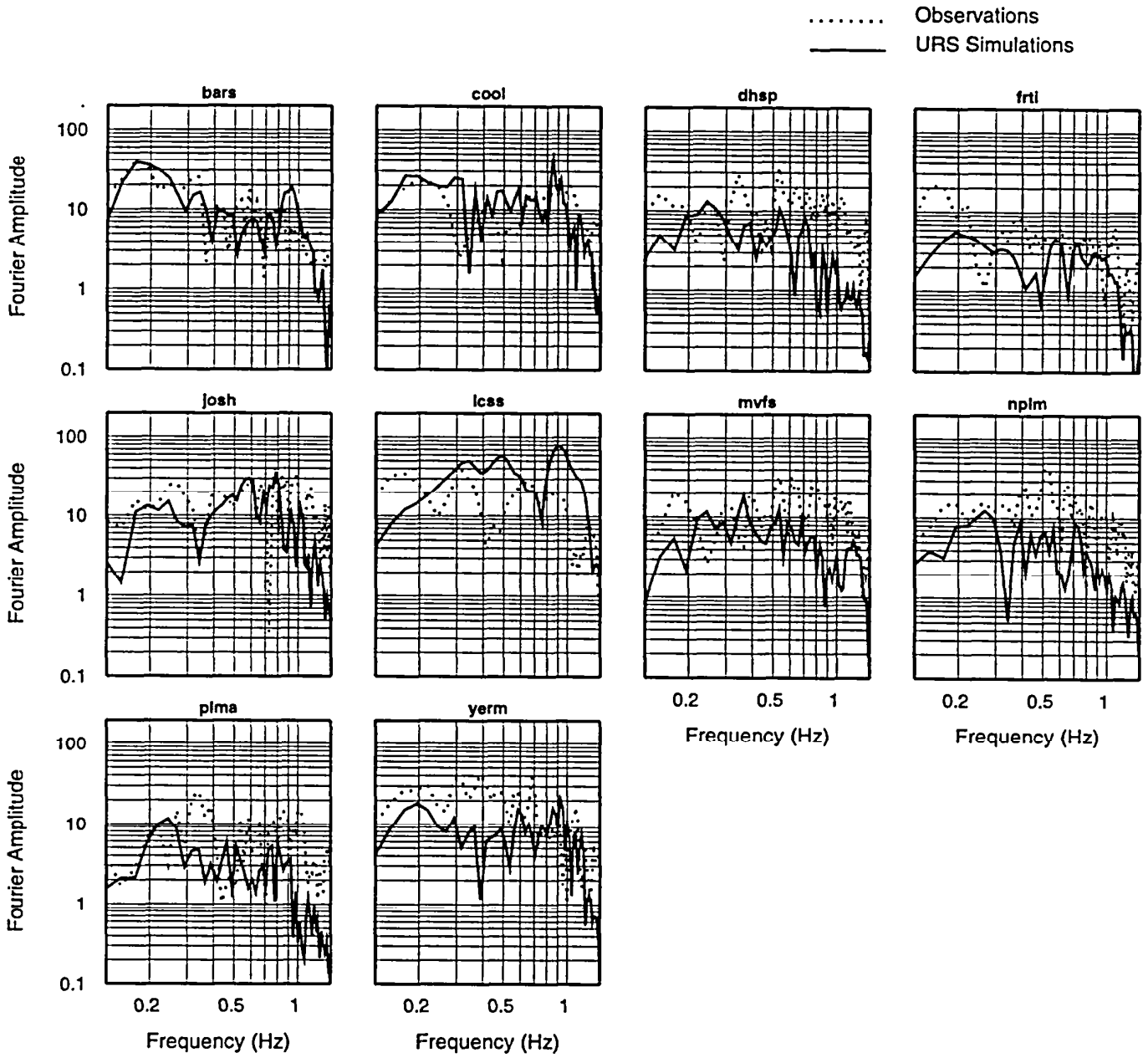

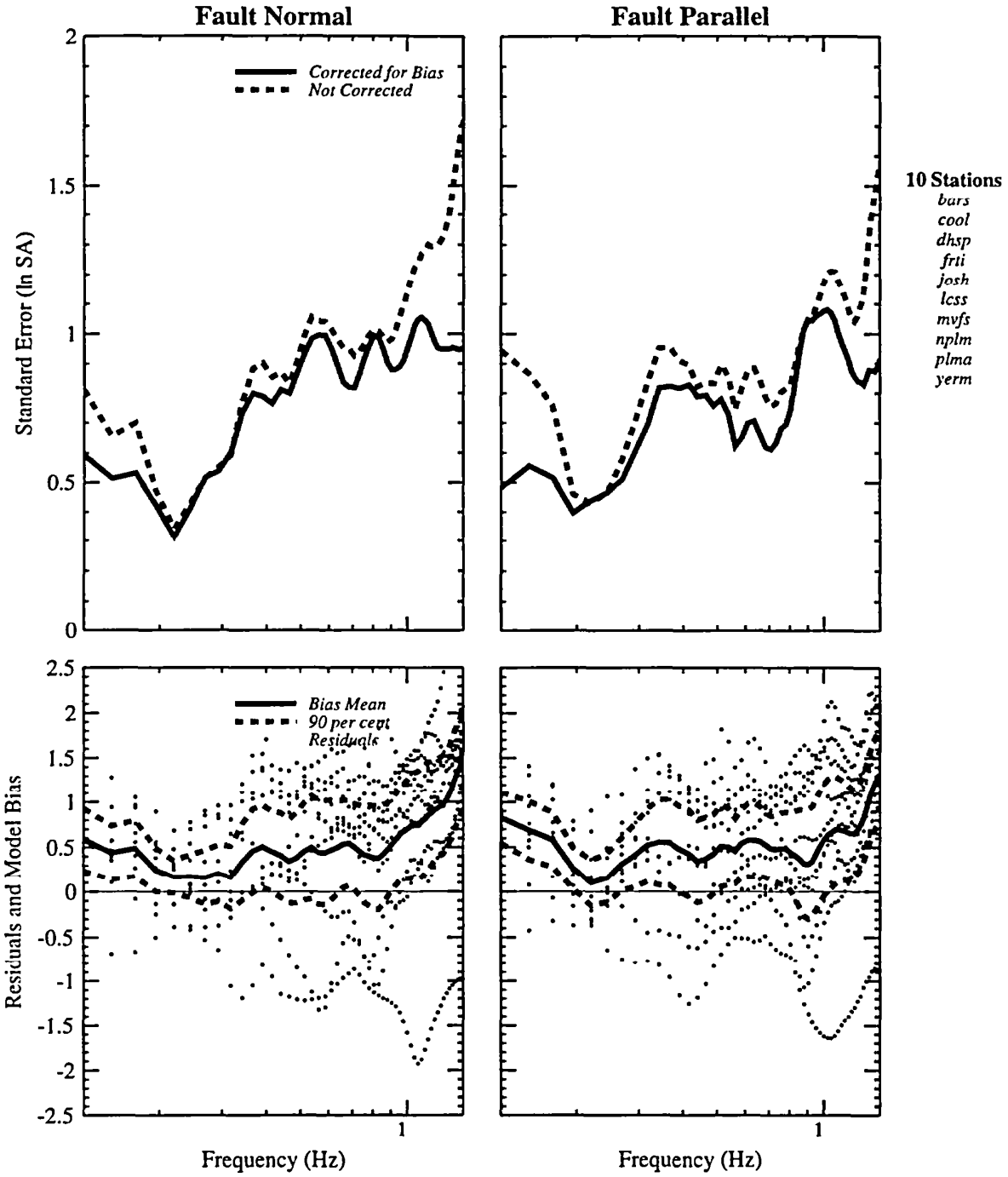

Landers Spectral Acceleration Goodness of Fit
Observed minus Synthetic (obs - sim)

n/smth0 Tue Aug 31 14:16:48 PDT 1999
/u2/mavy/PEER-5/Landers/GoodFit/mplot_goodfit.csh

Landers - Filter 0.125-1.43 Hz, Norma BB Sims - josh

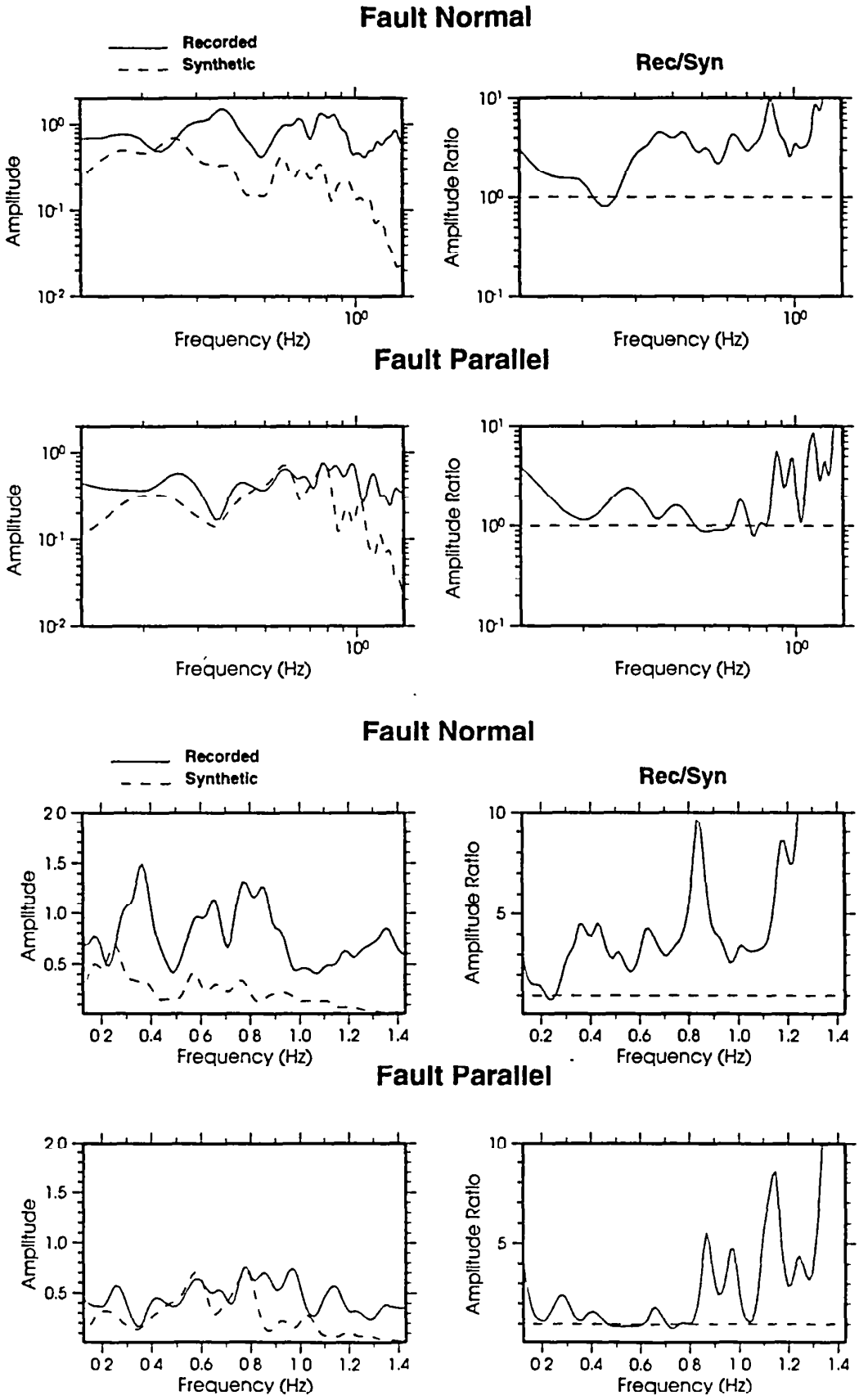

GMT Aug 24 15 26:24 1999 /net/coda/u2/arben/landers/shells

Landers - Filter 0.125-1.43 Hz, Norma BB Sims - frti

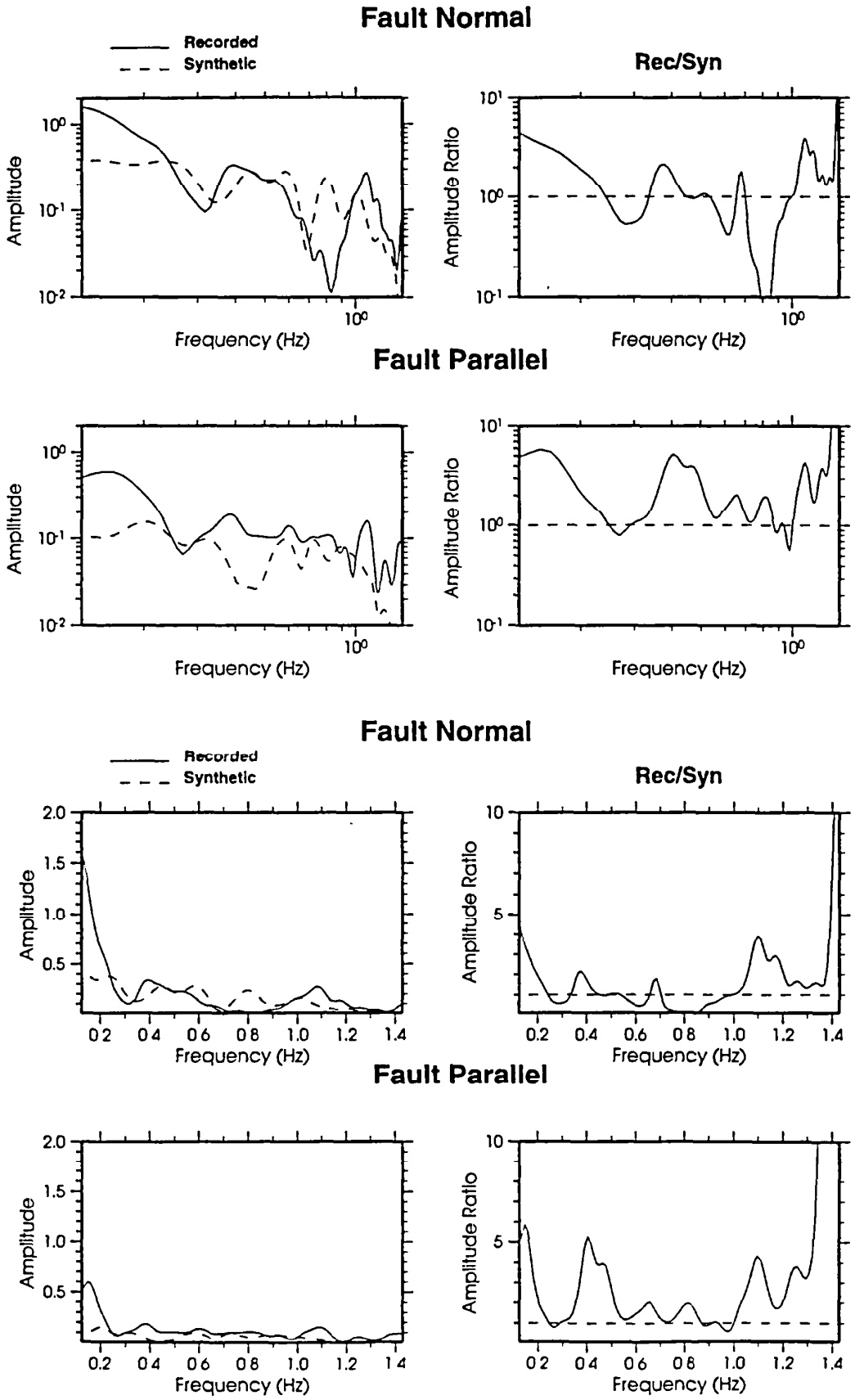

GMT Aug 24 15:25.58 1999 /net/coda/u2/arben/landers/shells

Landers - Filter 0.125-1.43 Hz, Norma BB Sims - cool

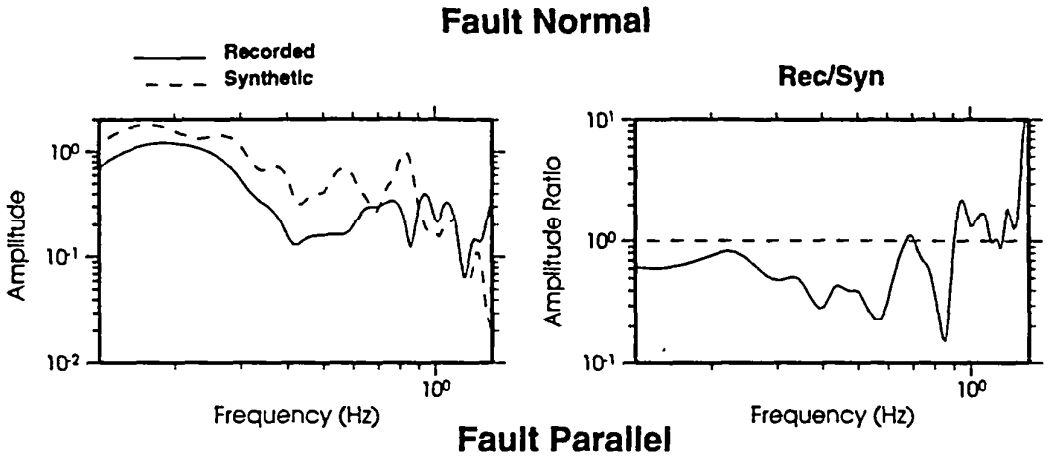

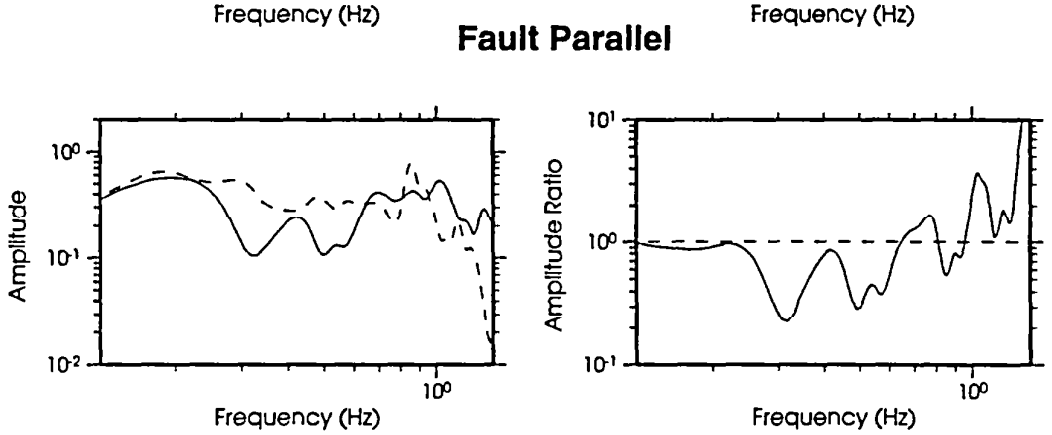

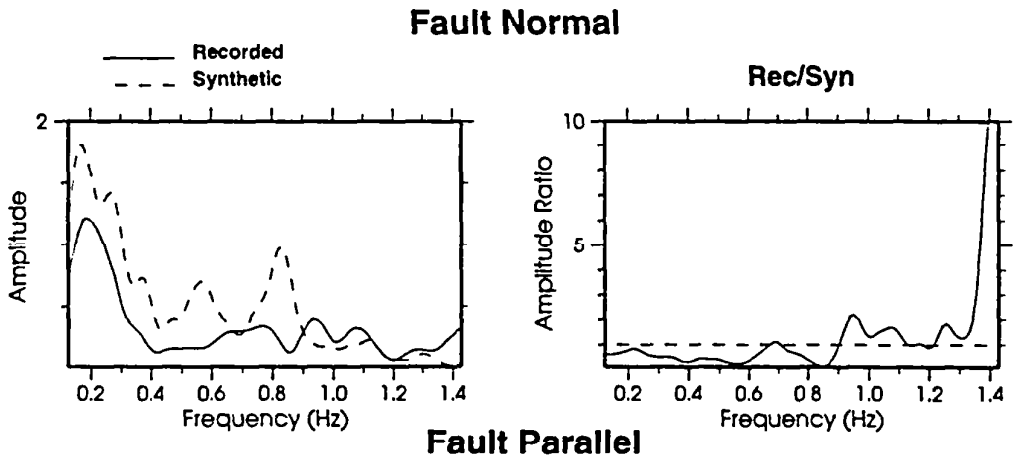

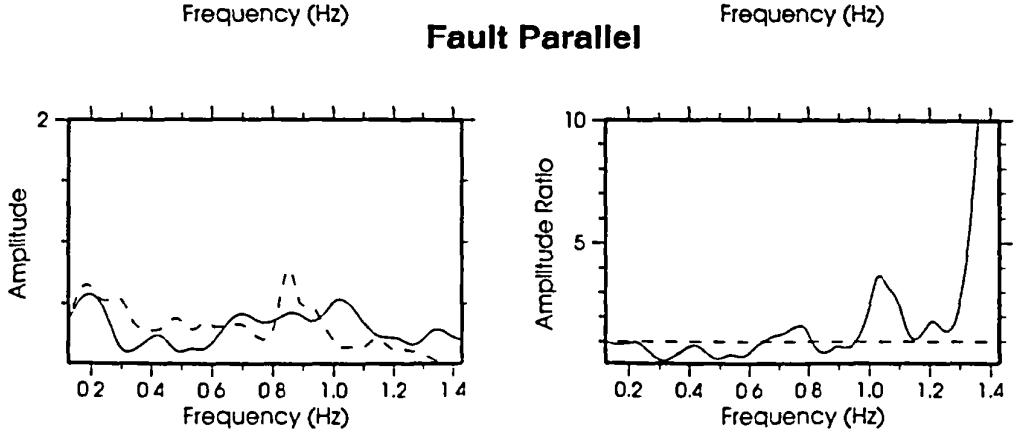

GMT Aug 24 15:25:04 1999 /net/coda/u2/arben/landers/shells

Landers - Filter 0.125-1.43 Hz, Norma BB Sims - bars

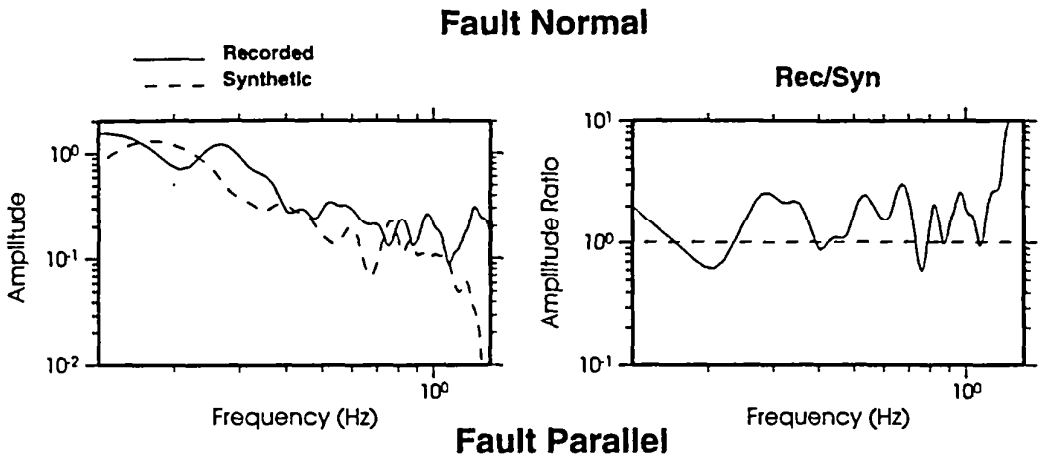

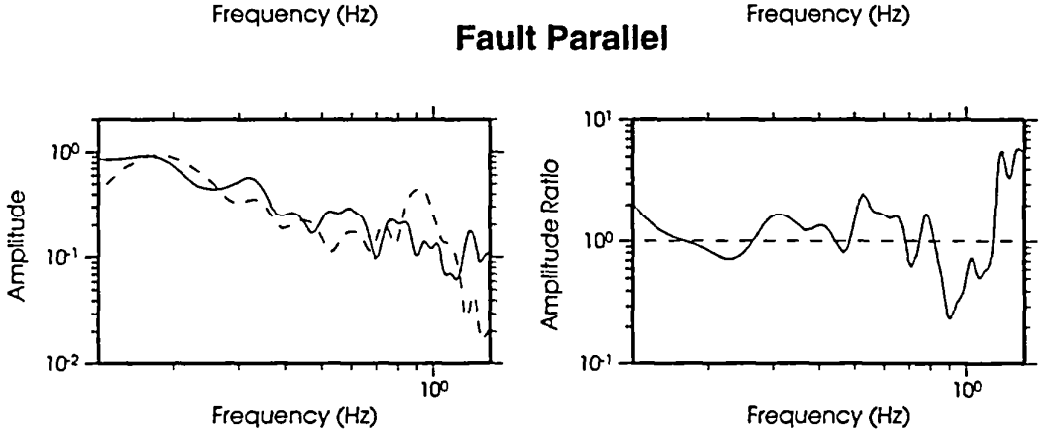

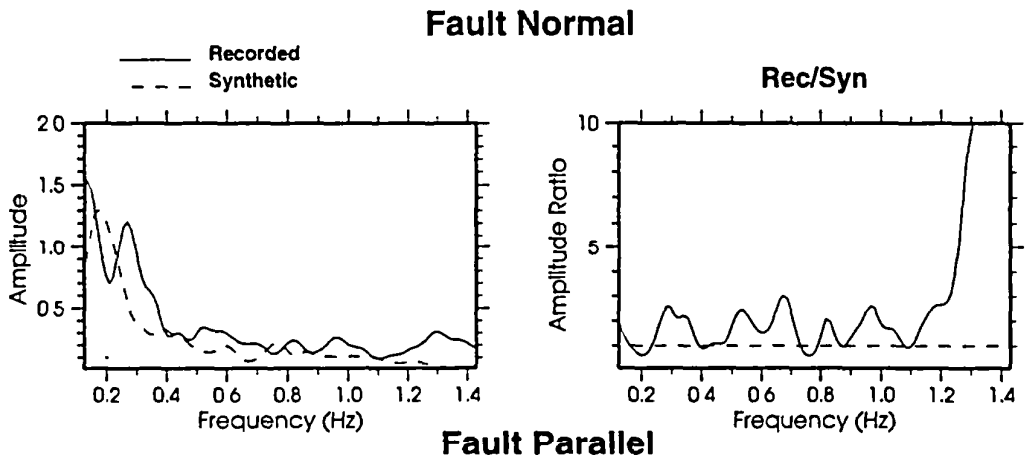

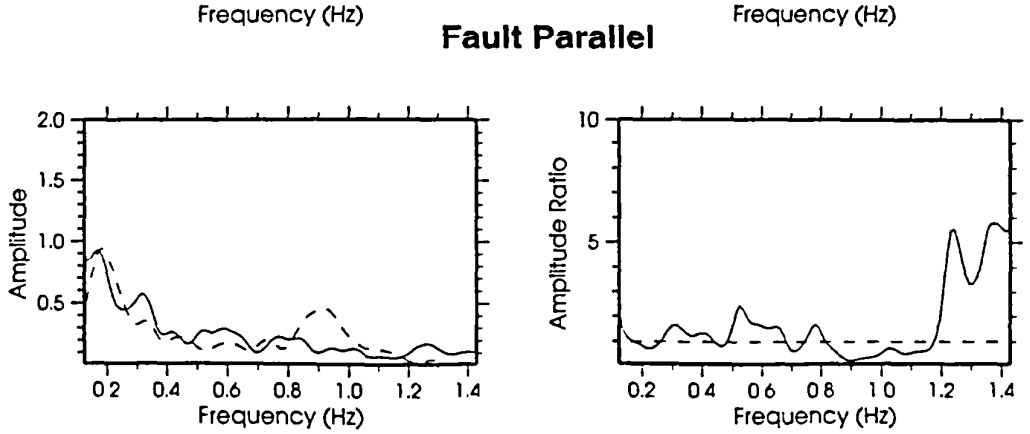

GMT Aug 24 15:24 38 1999 /net/coda/u2/arben/landers/shells

Landers - Filter 0.125-1.43 Hz, Norma BB Sims - yerm

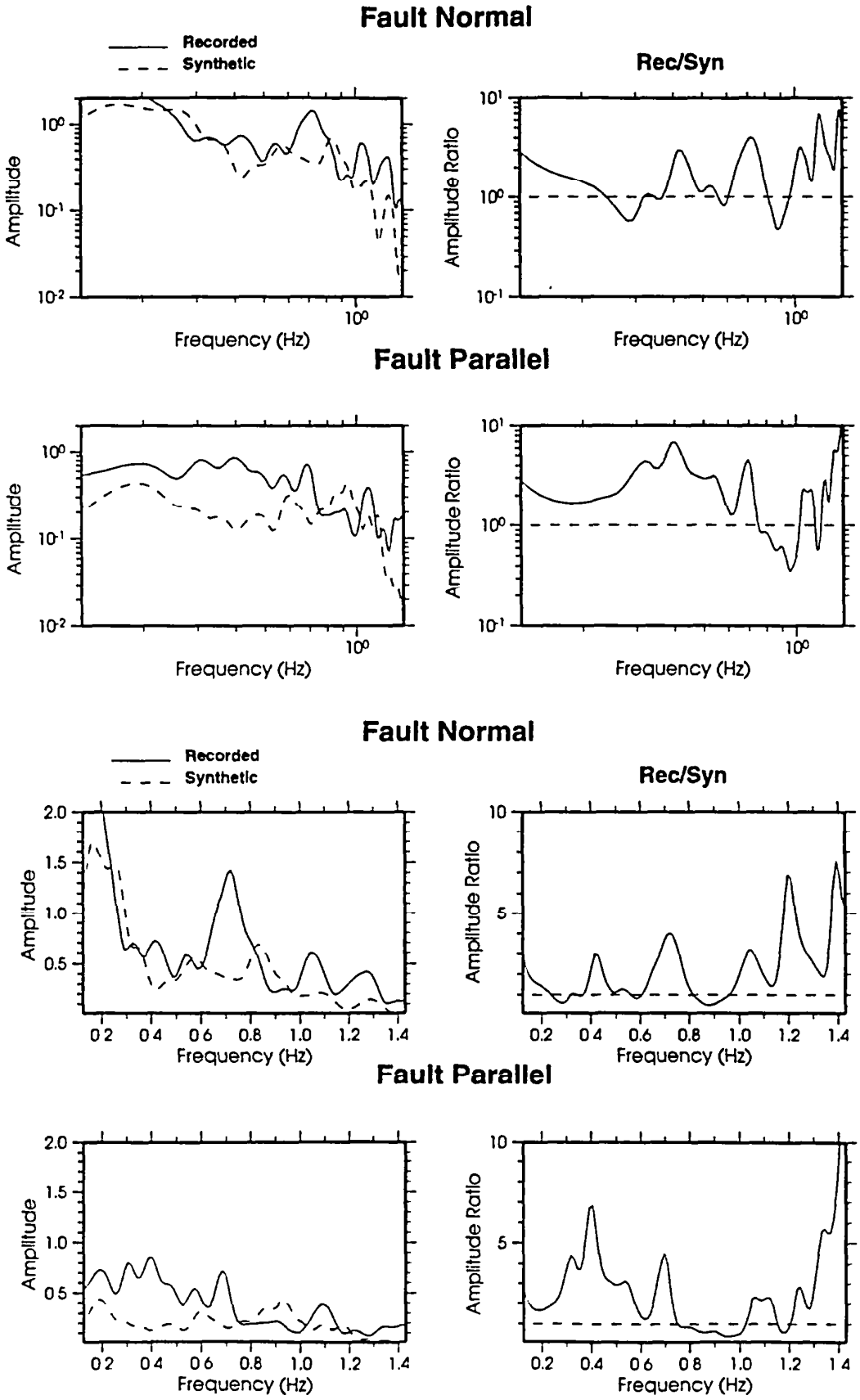

GMT Aug 24 15 28 18 1999 /net/coda/u2/arben/landers/shells

Landers - Filter 0.125-1.43 Hz, Norma BB Sims - lcss

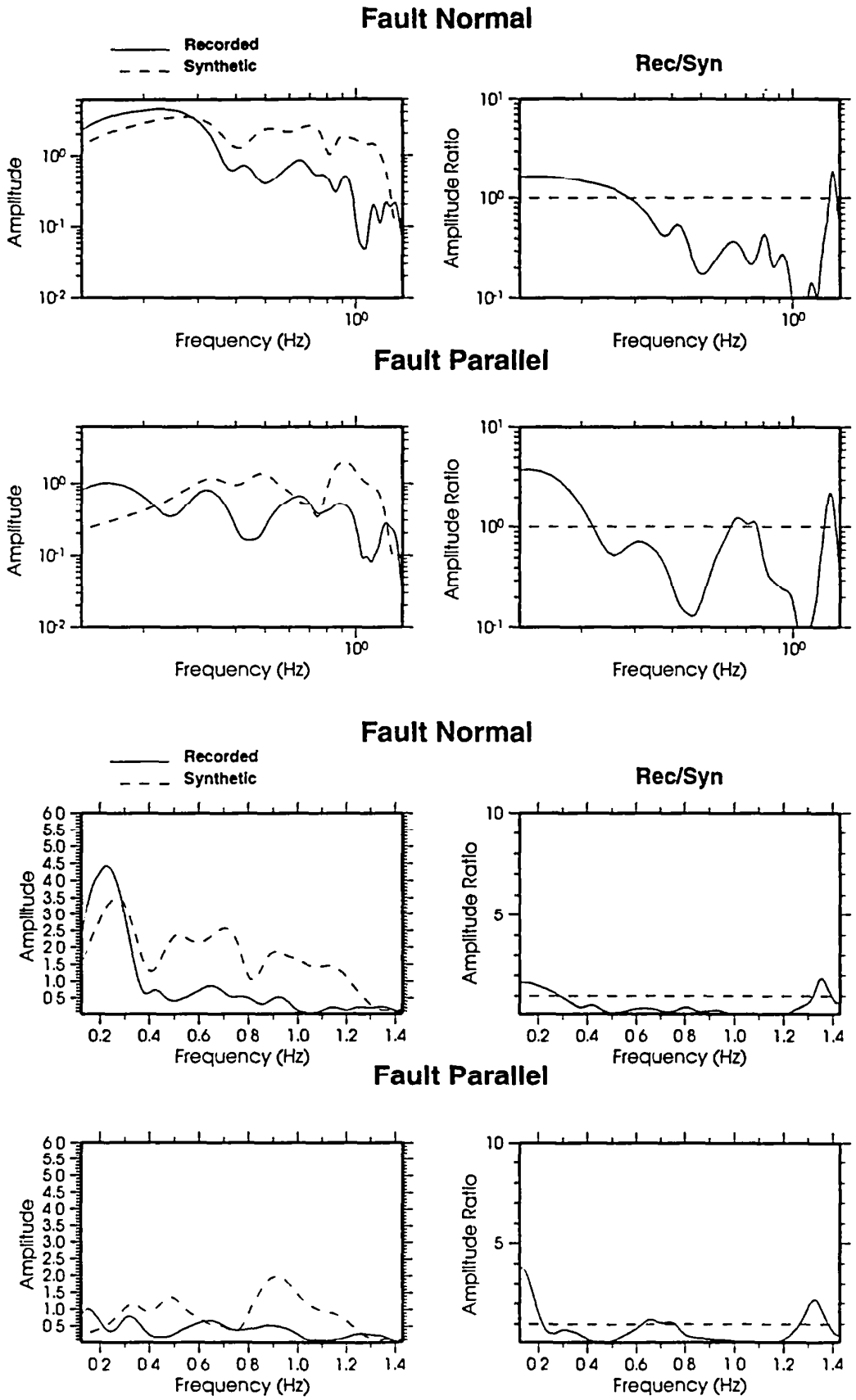

GMT Aug 24 15 23 47 1999 /net/coda/u2/arben/landers/shells

Landers - Filter 0.125-1.43 Hz, Norma BB Sims - dhsp

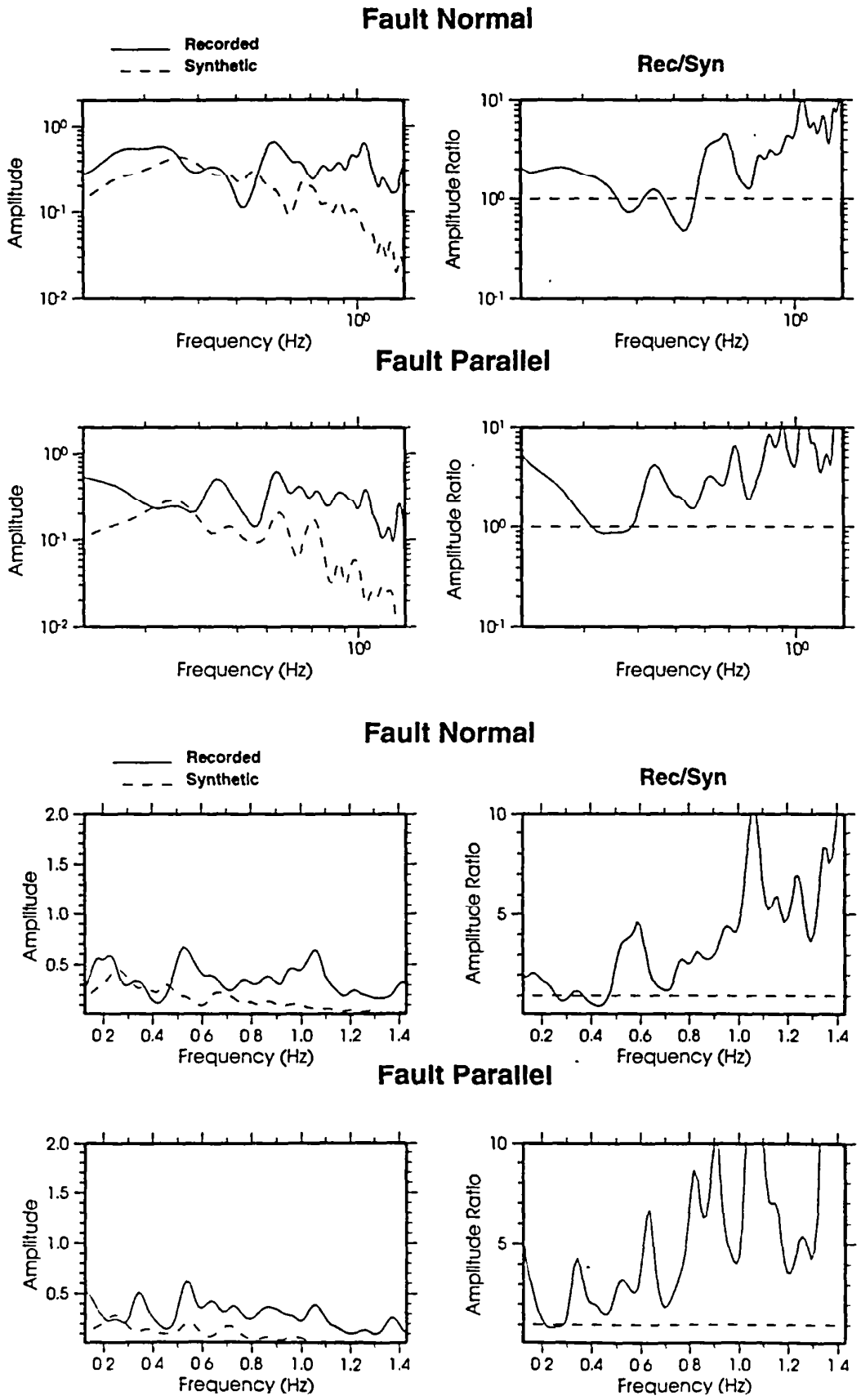

GMT Aug 24 15 25.30 1999 /net/coda/u2/arben/landers/shells

Landers - Filter 0.125-1.43 Hz, Norma BB Sims - plma

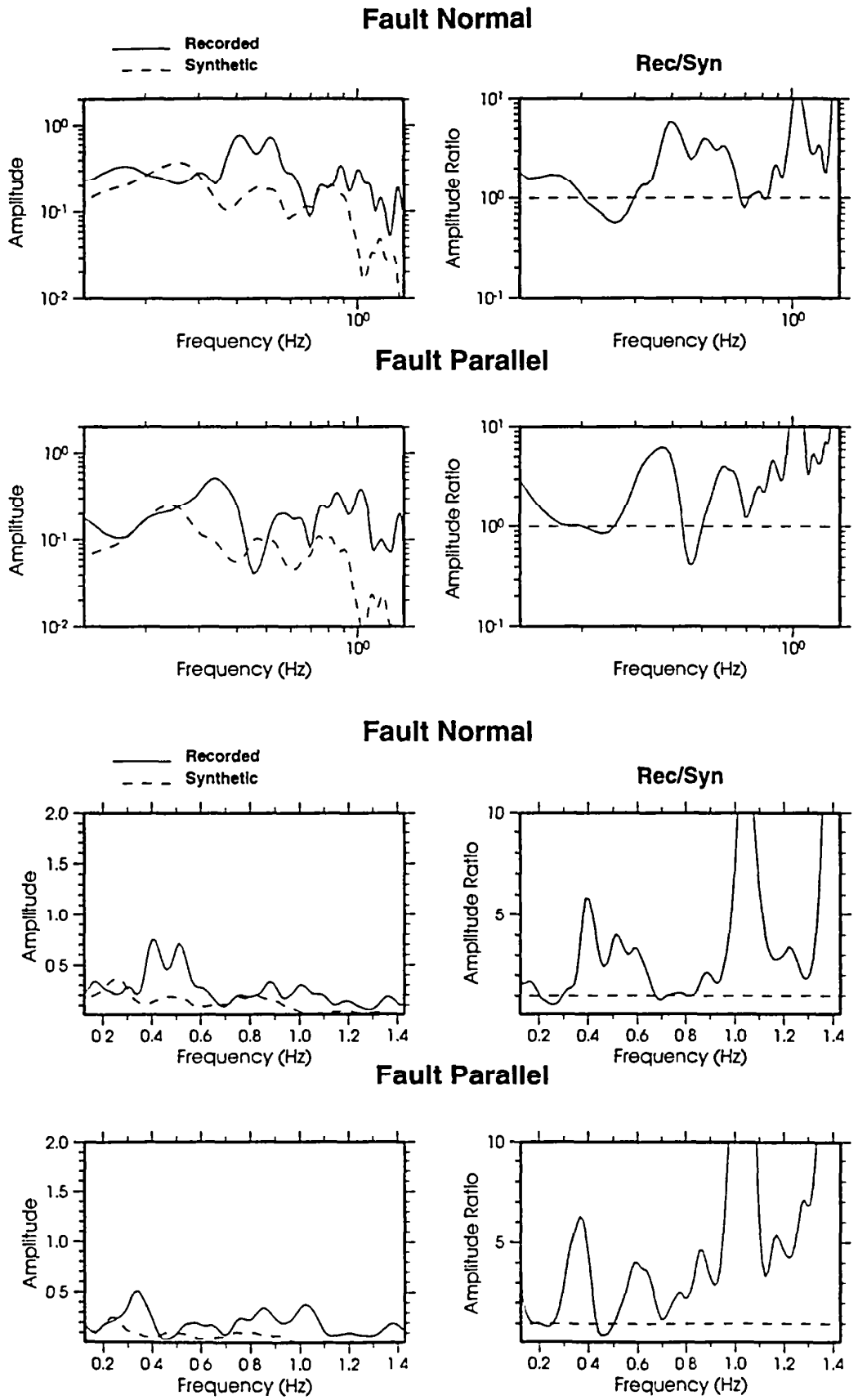

GMT Aug 24 15:27.48 1999 /net/coda/u2/arben/landers/shells

Landers - Filter 0.125-1.43 Hz, Norma BB Sims - nplm

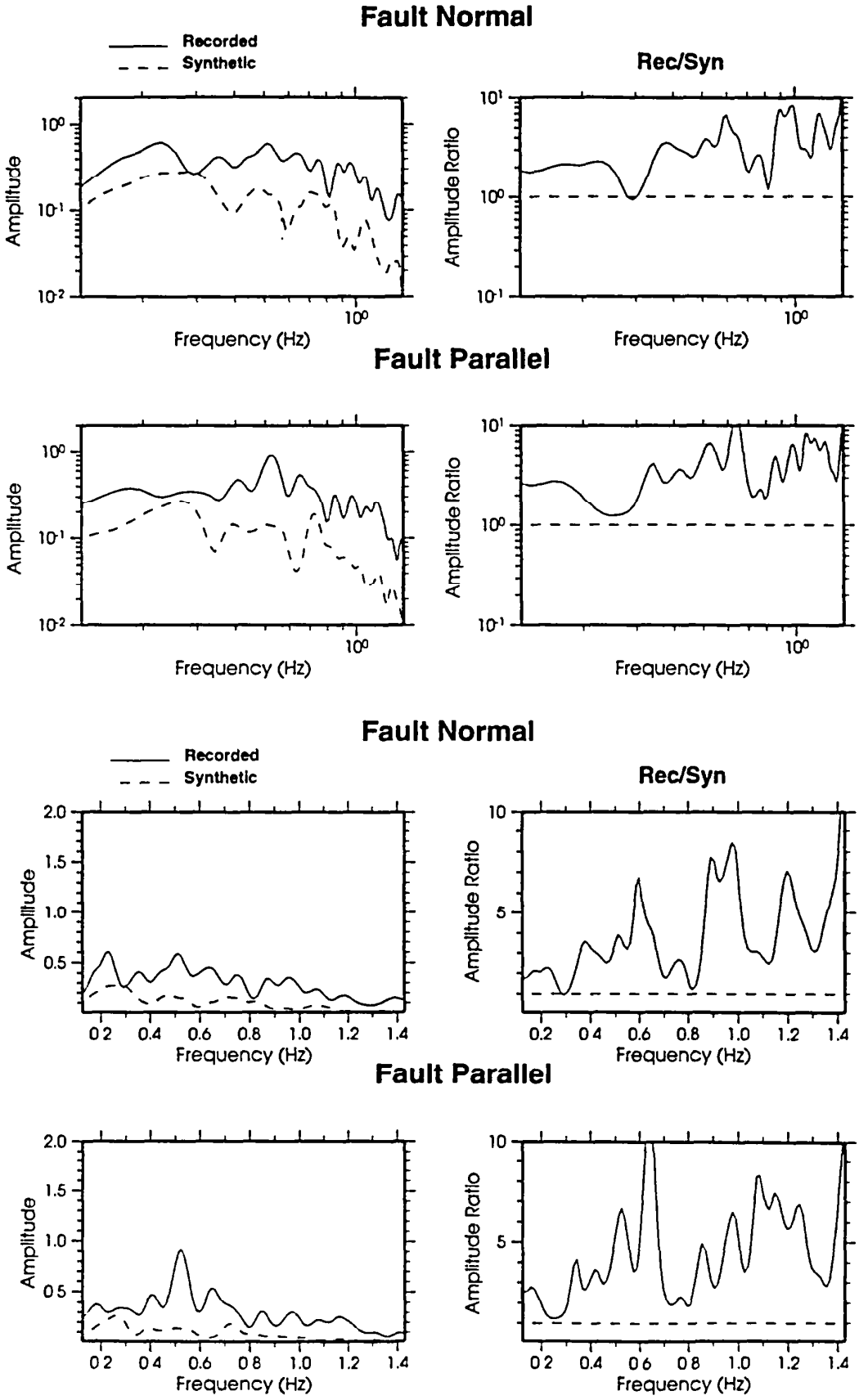

GMT Aug 24 15:27:19 1999 /net/coda/u2/arben/landers/shells

Landers - Filter 0.125-1.43 Hz, Norma BB Sims - mvfs

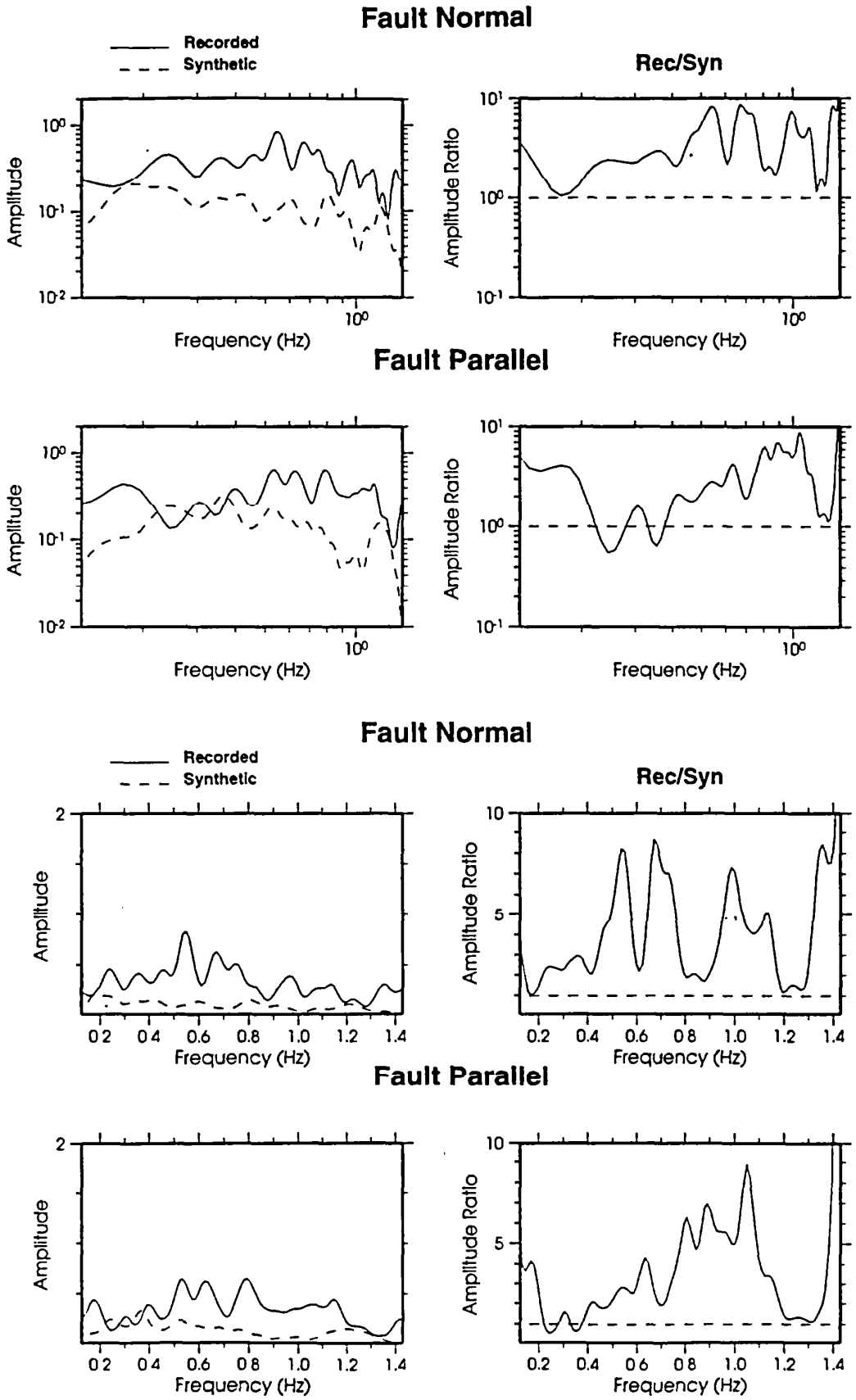

GMT Aug 24 15 26:51 1999 /net/coda/u2/arben/landers/shells

Landers Earthquake - Fault Normal

SA at 5.0 sec

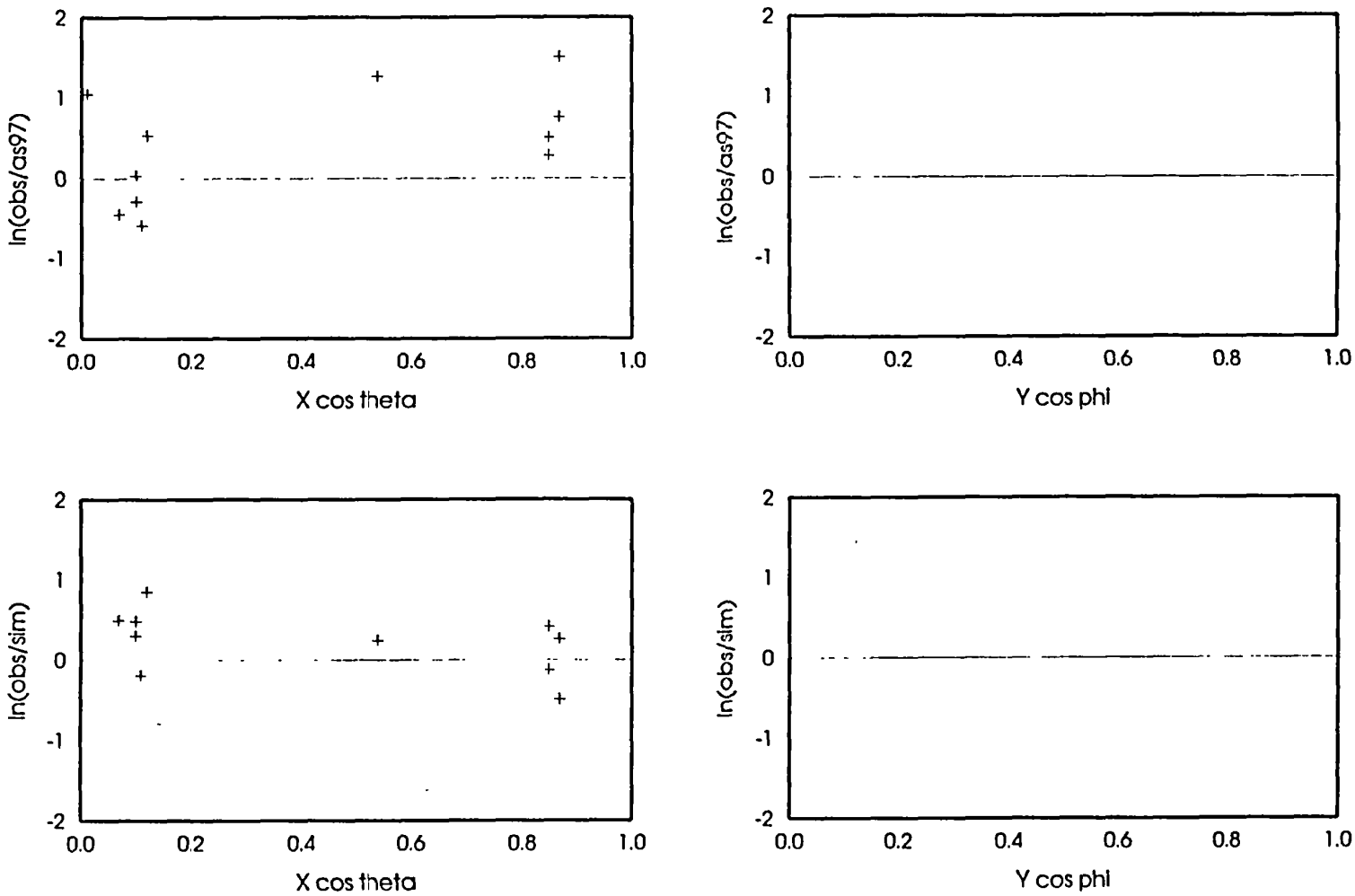

GMT Aug 24 15:26:32 1999 /net/coda/u2/arben/landers/Comparisons/Resid_plots

Landers Earthquake - Fault Parallel

SA at 5.0 sec

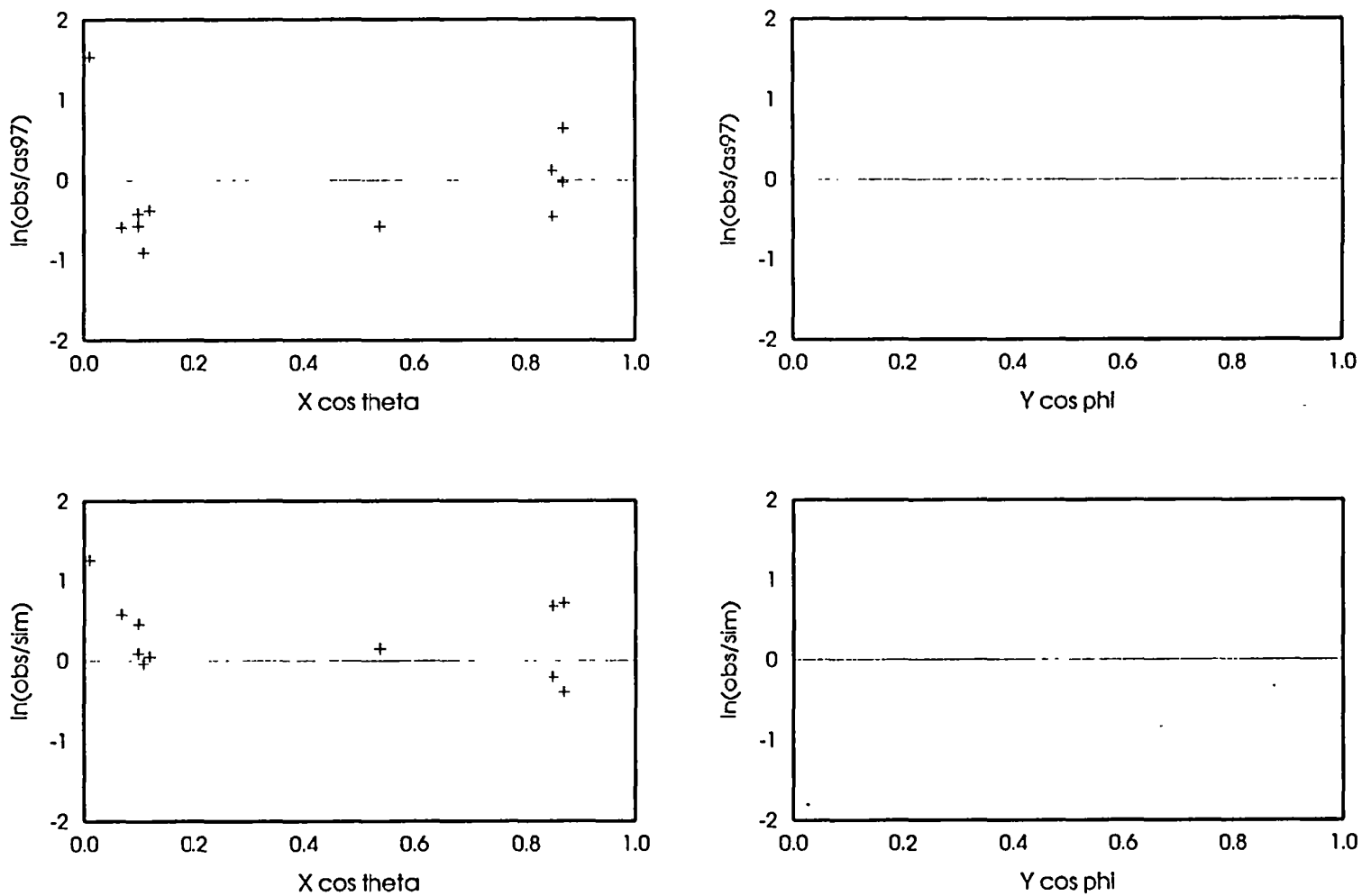

GMT Aug 24 15:26:34 1999 /net/coda/u2/arben/landers/Comparisons/Resid_plots

Landers Earthquake - Fault Normal

SA at 4.0 sec

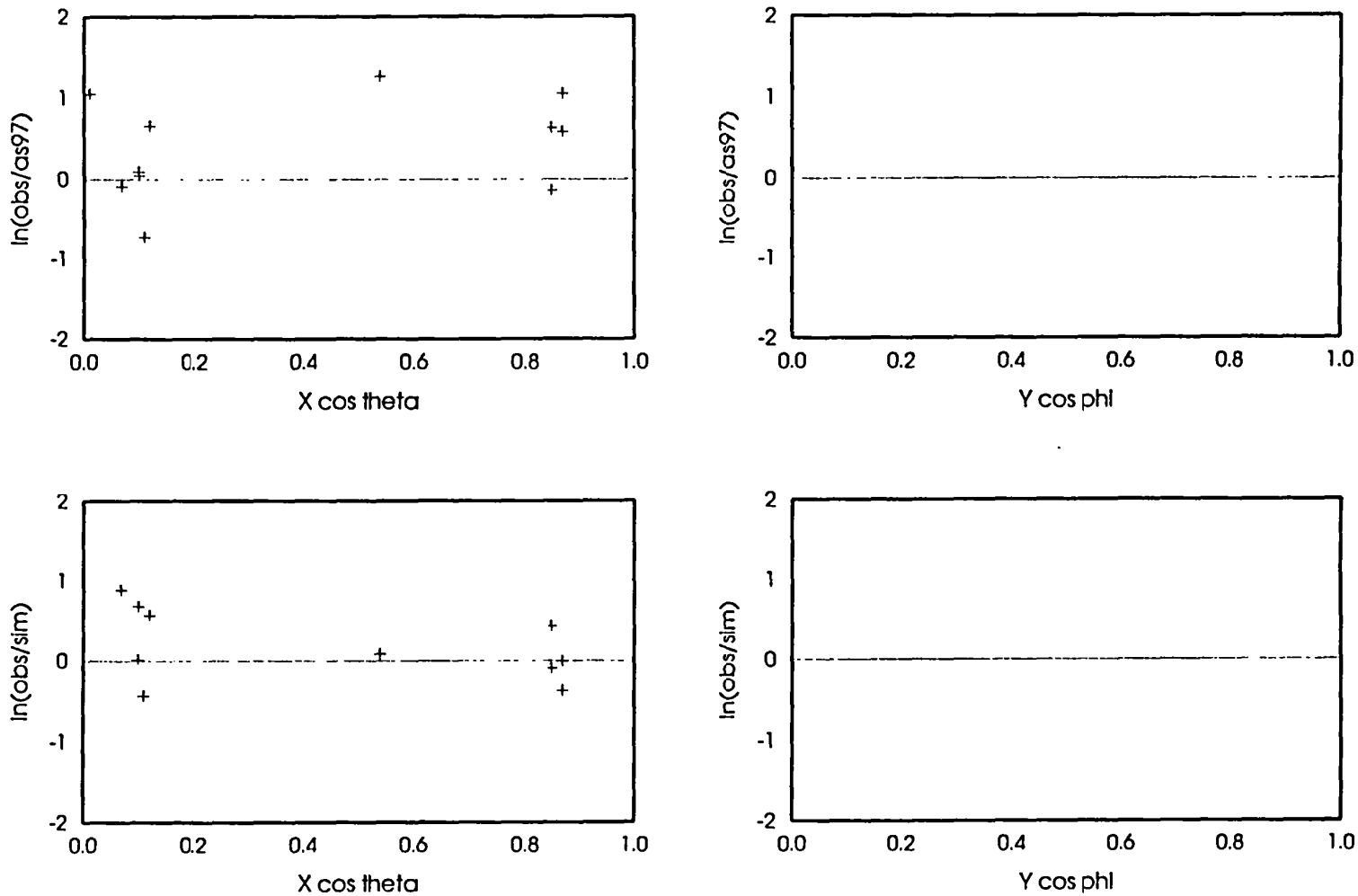

GMT Aug 24 15:26:37 1999 /net/coda/u2/arben/landers/Comparisons/Resid_plots

Landers Earthquake - Fault Parallel

SA at 4.0 sec

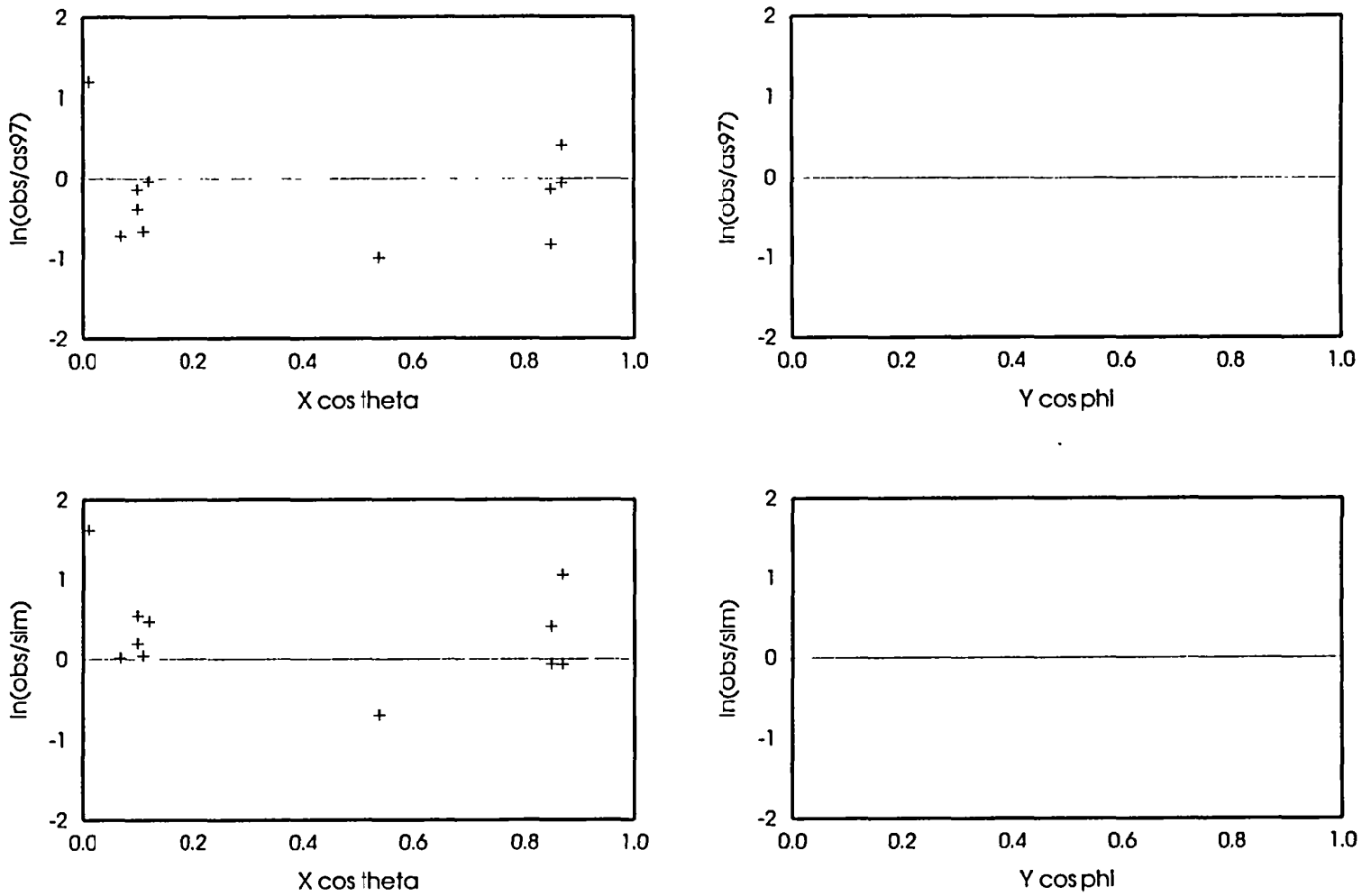

GMT Aug 24 15:26:39 1999 /nel/coda/u2/arben/landers/Comparisons/Resid_plots

Landers Earthquake - Fault Normal

SA at 3.0 sec

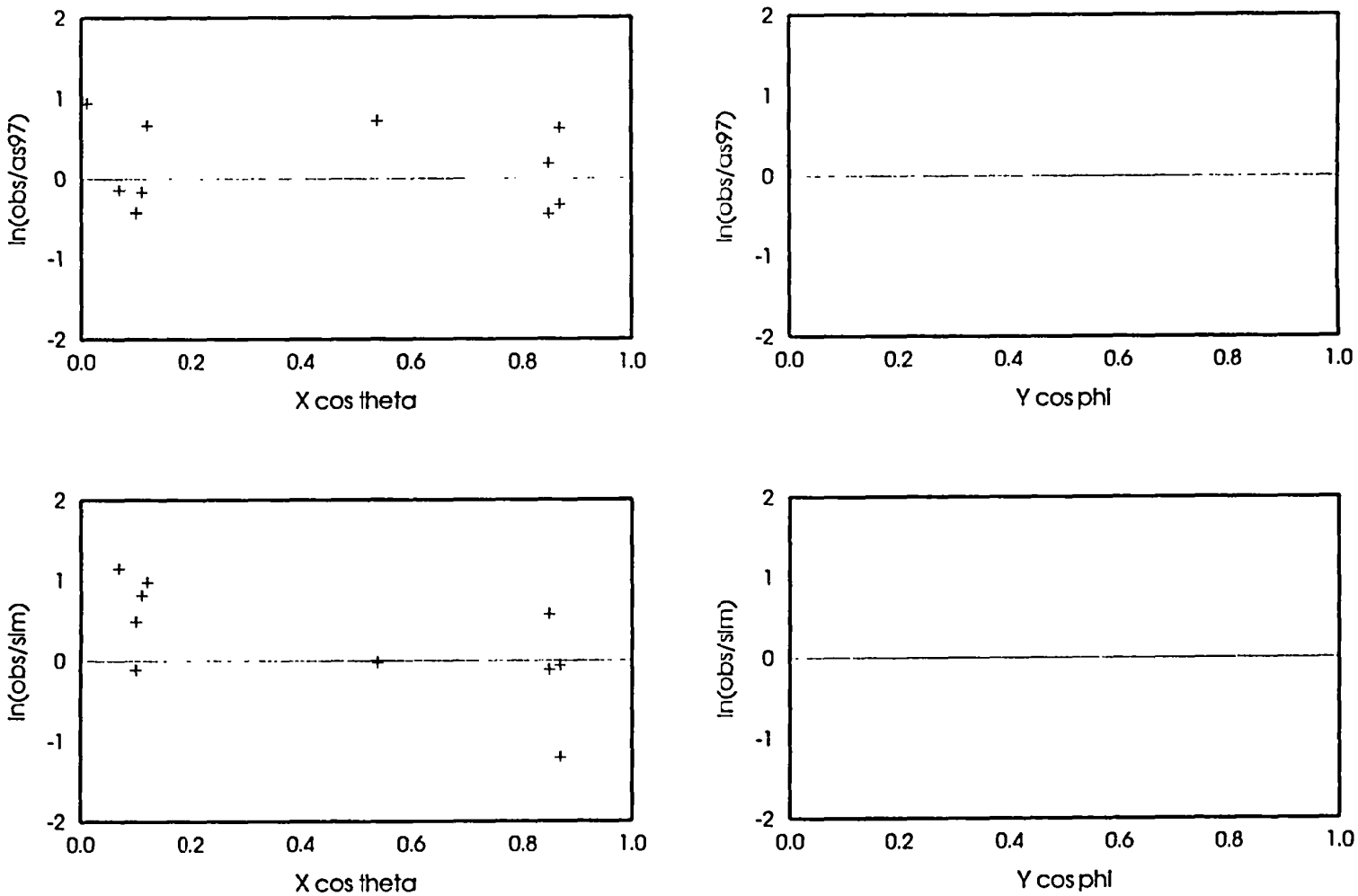

GMT Aug 24 15:26:41 1999 /net/coda/u2/arben/landers/Comparisons/Resid_plots

Landers Earthquake - Fault Parallel

SA at 3.0 sec

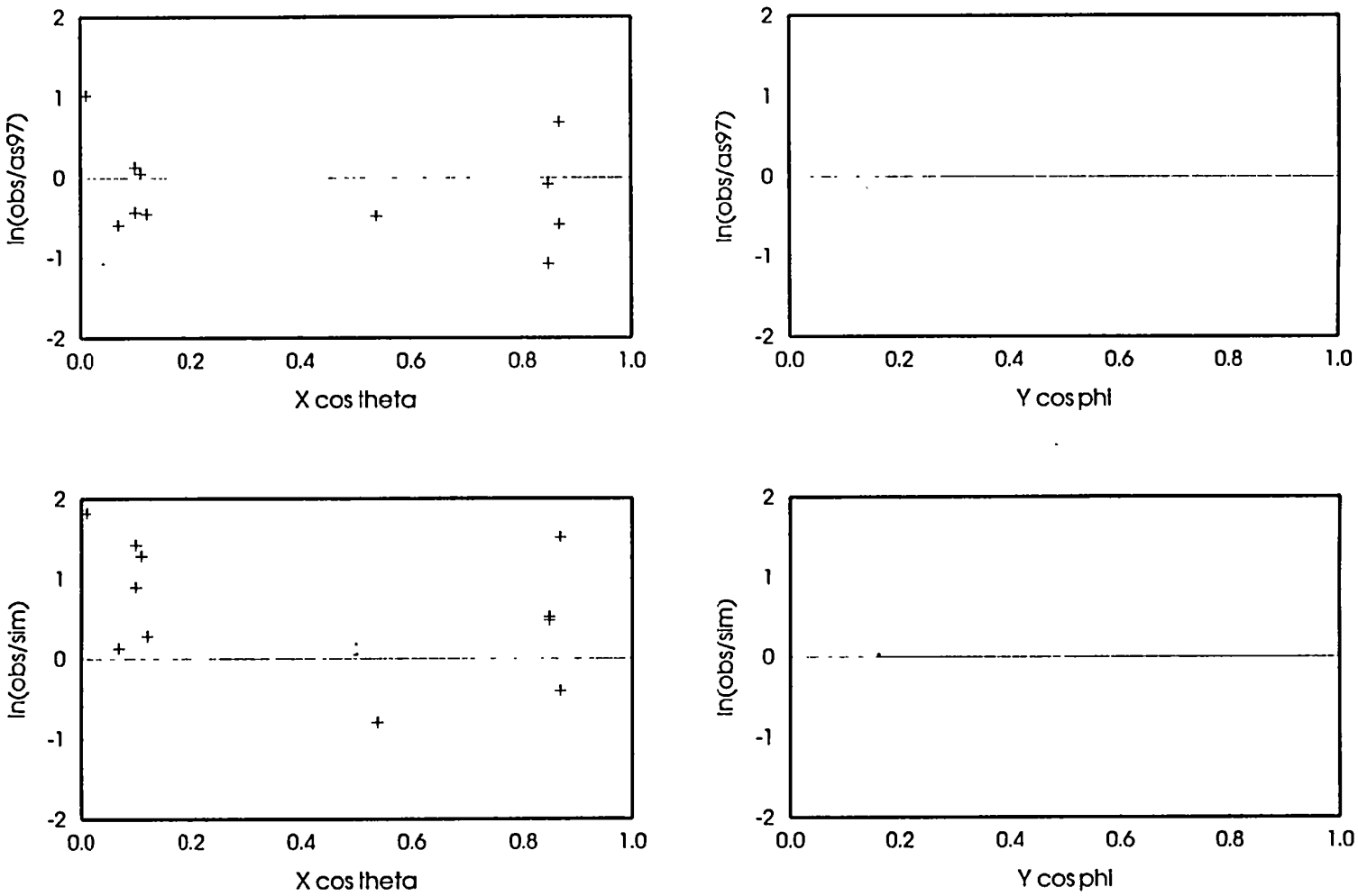

GMT Aug 24 15:26:44 1999 /net/coda/u2/arben/landers/Comparisons/Resid_plots

Landers Earthquake - Fault Normal

SA at 2.0 sec

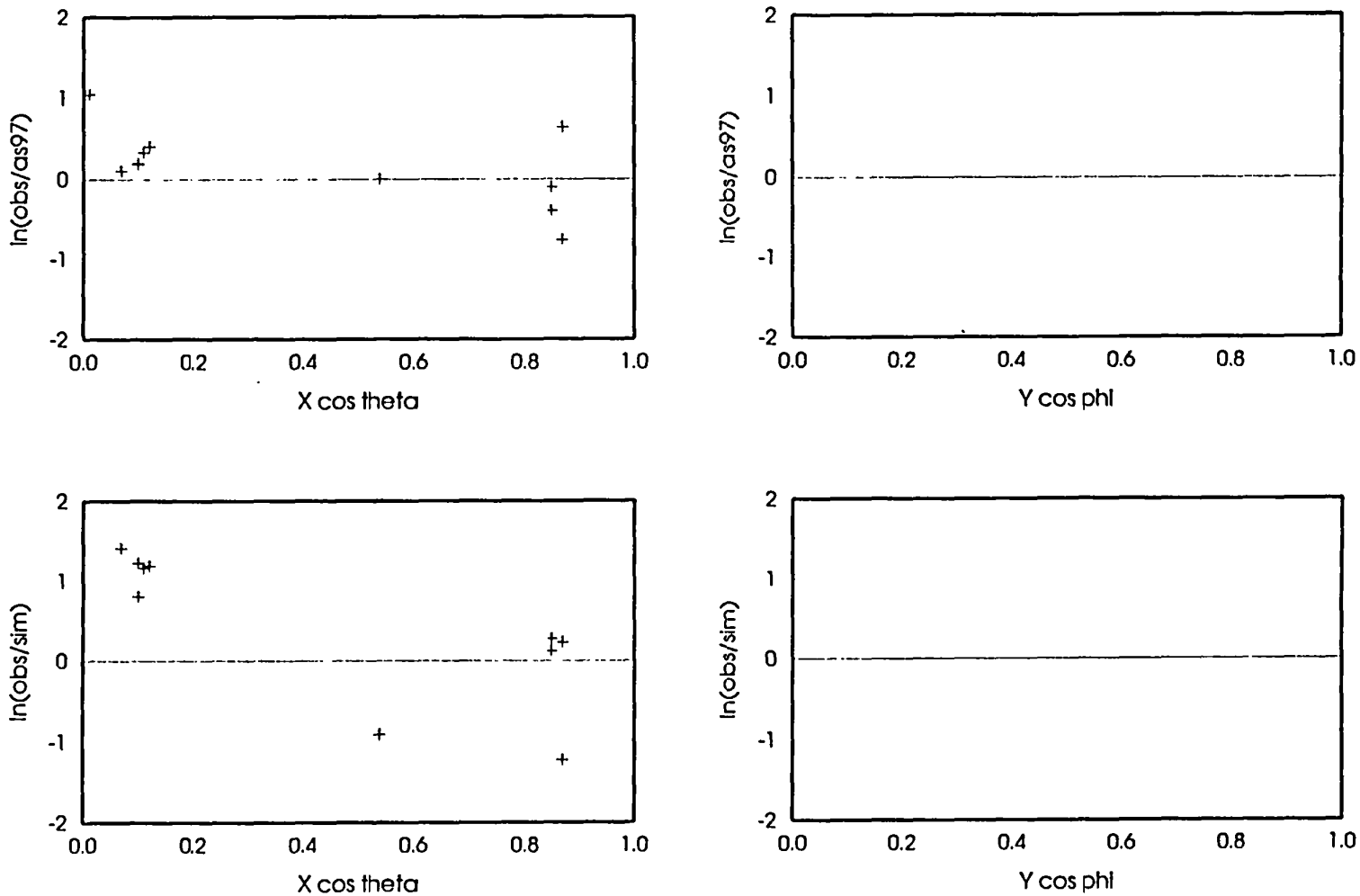

GMT Aug 24 15:26:46 1999 /net/coda/u2/arben/landers/Comparisons/Resid_plots

Landers Earthquake - Fault Parallel

SA at 2.0 sec

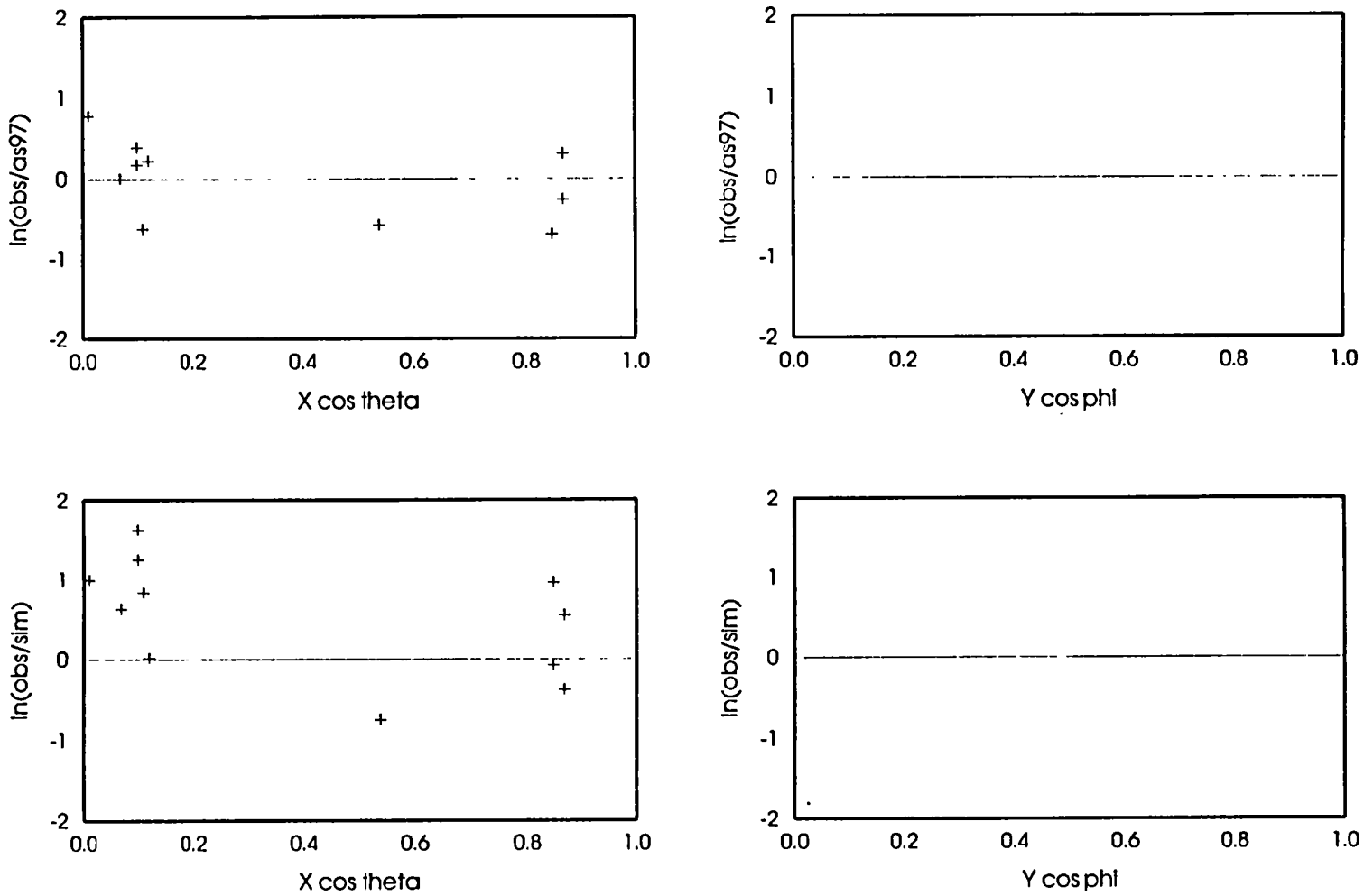

GMT Aug 24 15:26:48 1999 /net/coda/u2/arben/landers/Comparisons/Resid_plots

Landers Earthquake - Fault Normal

SA at 1.5 sec

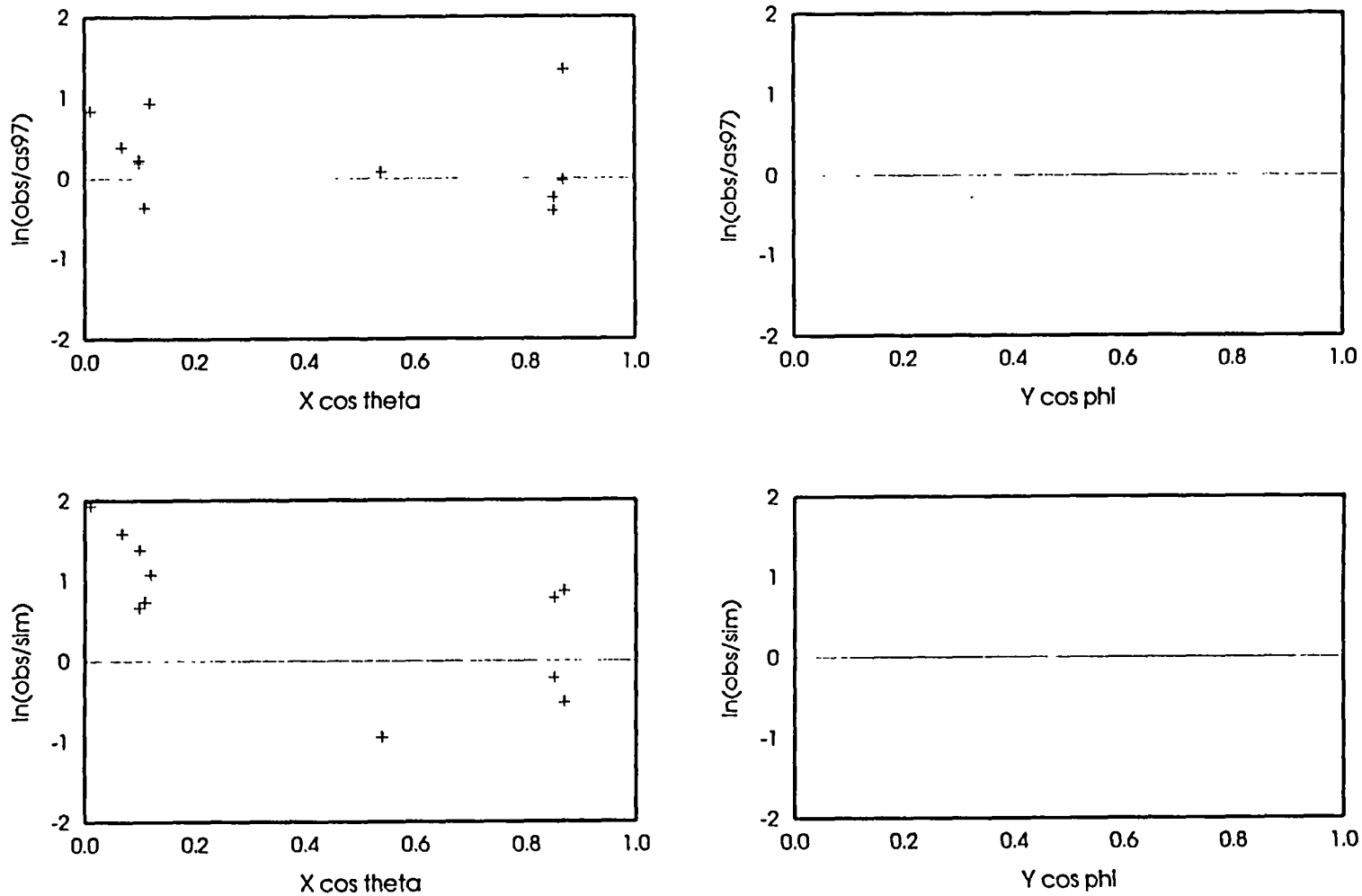

GMT Aug 24 15:26:51 1999 /net/coda/u2/arben/landers/Comparisons/Resid_plots

Landers Earthquake - Fault Parallel

SA at 1.5 sec

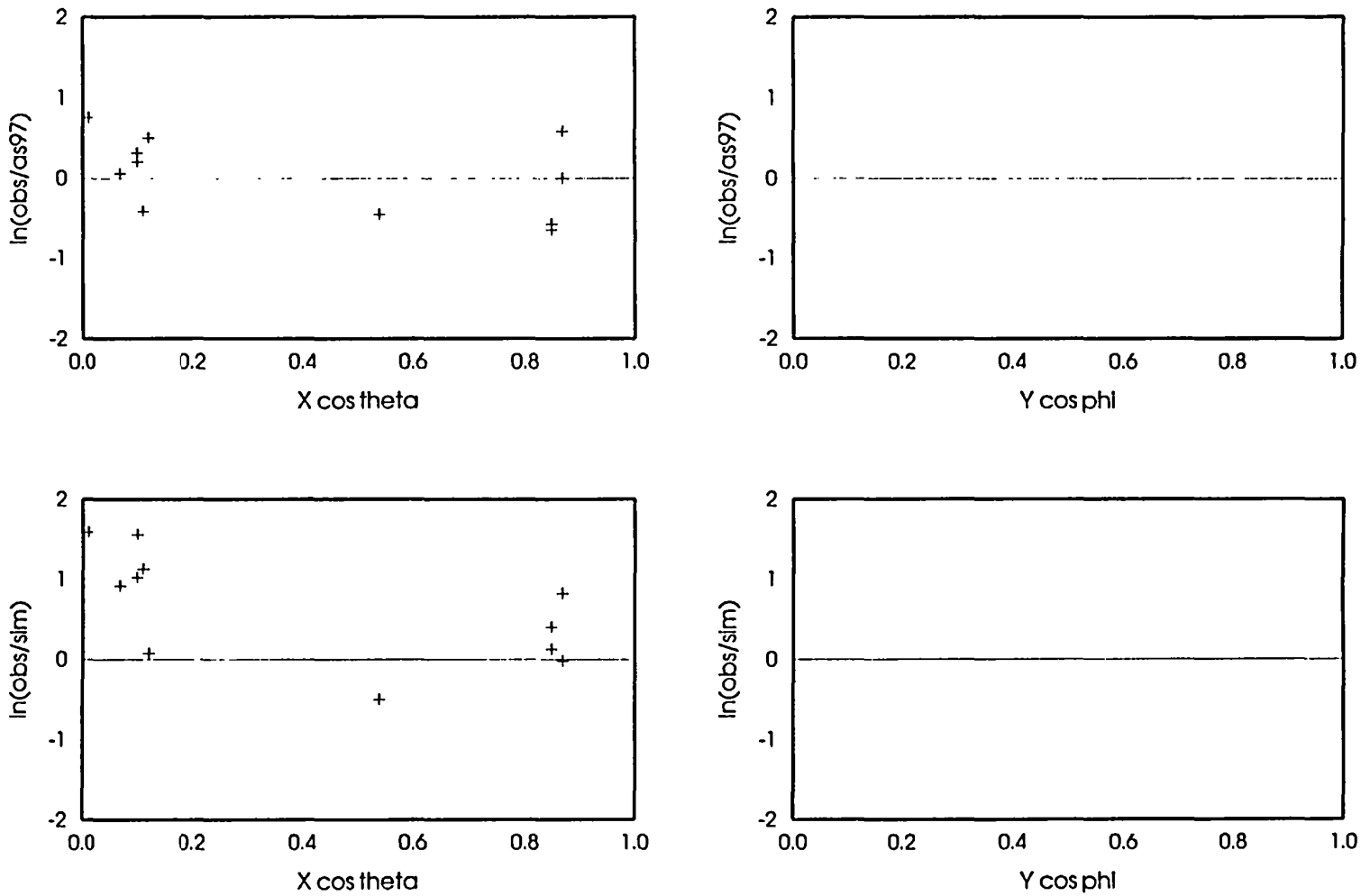

GMT Aug 24 15:26:55 1999 /net/coda/u2/arben/landers/Comparisons/Resid_plots

Landers Earthquake - Fault Normal

SA at 1.0 sec

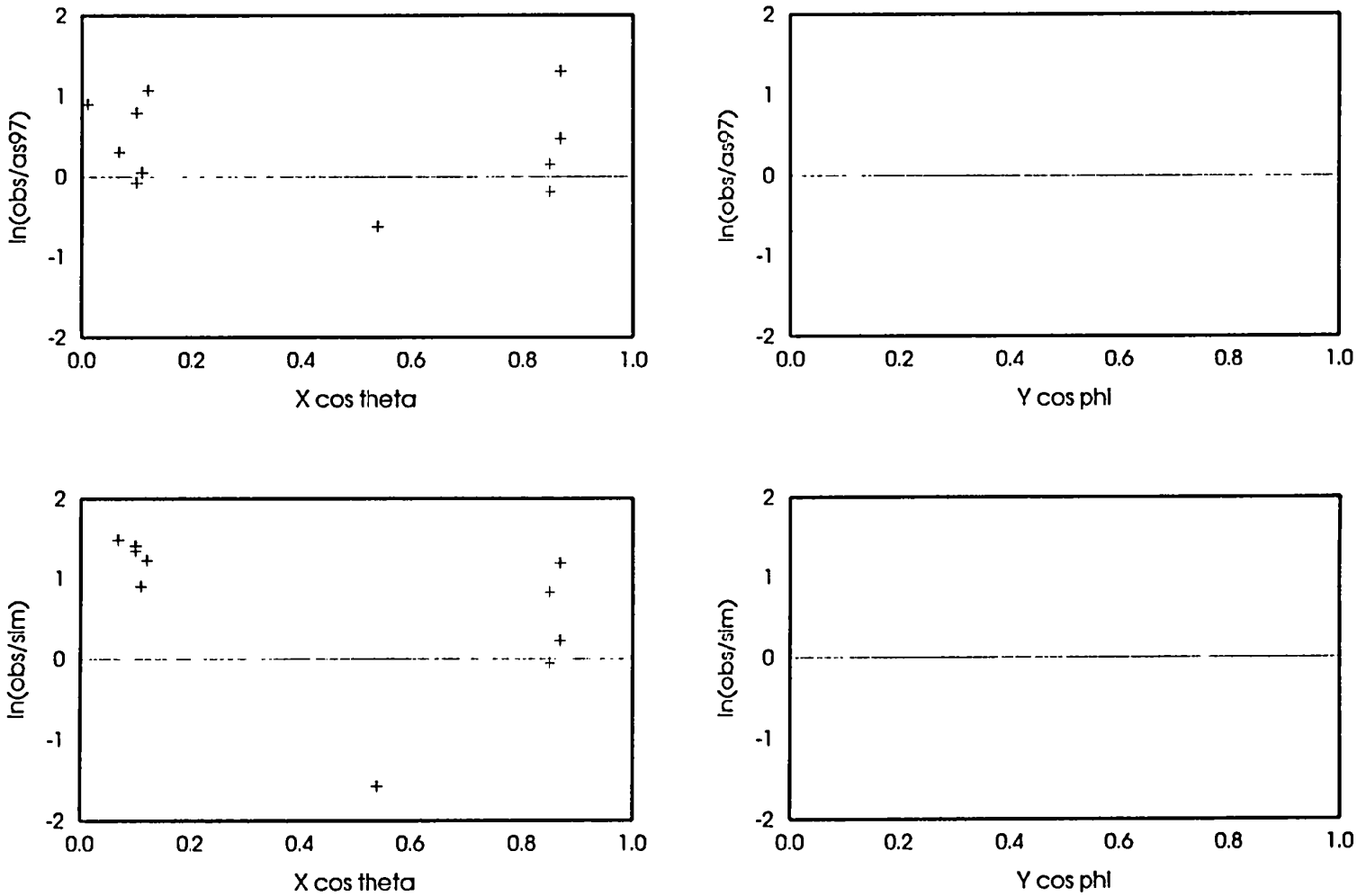

GMT Aug 24 15:26:59 1999 /net/coda/u2/arben/landers/Comparisons/Resid_plots

Landers Earthquake - Fault Parallel

SA at 1.0 sec

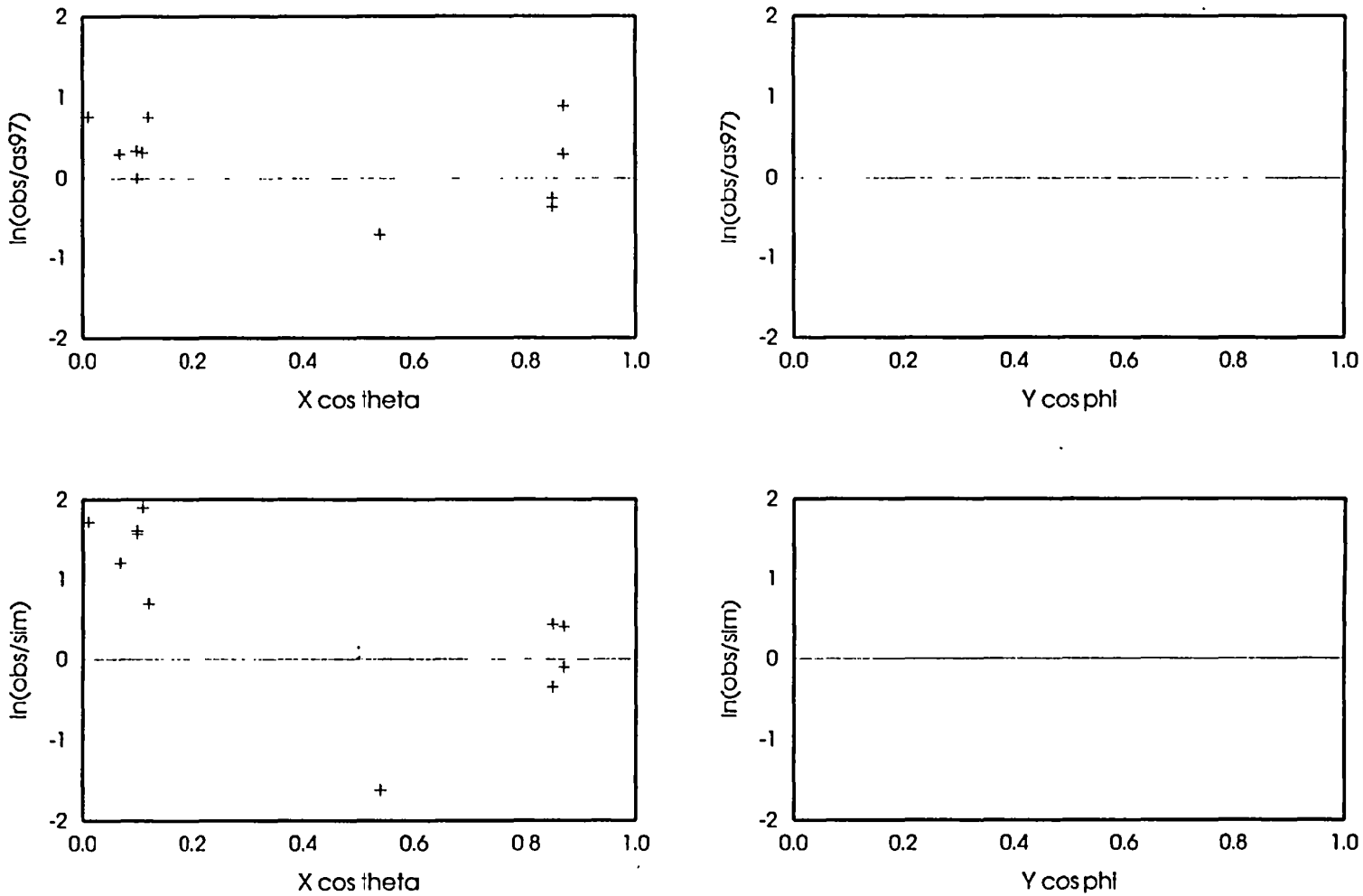

GMT Aug 24 15:27:01 1999 /net/coda/u2/arben/landers/Comparisons/Resid_plots

/u1/nancy/PEER-5/Northridge/Comparisons.990823/Tabulate
tableout

Station	Correlation FN	Correlation FP	Least Squares FN	Least Squares FP	Response Spectra FN	Response Spectra FP	Fourier Spectra FN	Fourier Spectra FP
cnpk	0.402		0.053		0.355	-0.610	0.583	-0.094
jeng	0.594	0.593	0.169	0.183	0.195	0.185	0.536	0.049
kagc	0.483		0.104		0.122	0.631	0.381	0.649
newh	0.760		0.348		0.172	-0.035	0.161	0.284
nord	0.493	0.764	0.058	0.338	0.010	0.069	-0.015	0.237
pacd	0.796		-0.393		-0.736	-0.205	-0.569	-0.057
rosc	0.476		0.052		0.117	0.553	0.153	0.633
rrs	0.717	0.819	0.255	0.424	0.736	0.061	0.683	0.143
sati	0.431	0.519	0.096	0.143	0.820	0.500	0.733	0.737
scs	0.668		0.254		0.344	0.233	0.571	0.370
scse	0.696	0.857	0.230	0.462	-0.011	0.040	0.108	0.003
ssus	0.391		-0.583		-0.628	0.078	-0.611	0.222
sylm	0.818	0.586	0.408	0.189	0.364	0.310	0.323	0.096
Average	0.594	0.690	0.081	0.290	0.143	0.139	0.234	0.252
Sigma	0.156	0.243	0.279	0.357	0.424	0.380	0.602	0.498
Sigma Mean	0.043	0.099	0.077	0.146	0.118	0.105	0.167	0.138

Northridge - Fault Normal

Simulations and Data Band Pass Filtered 0.125-1.43 Hz

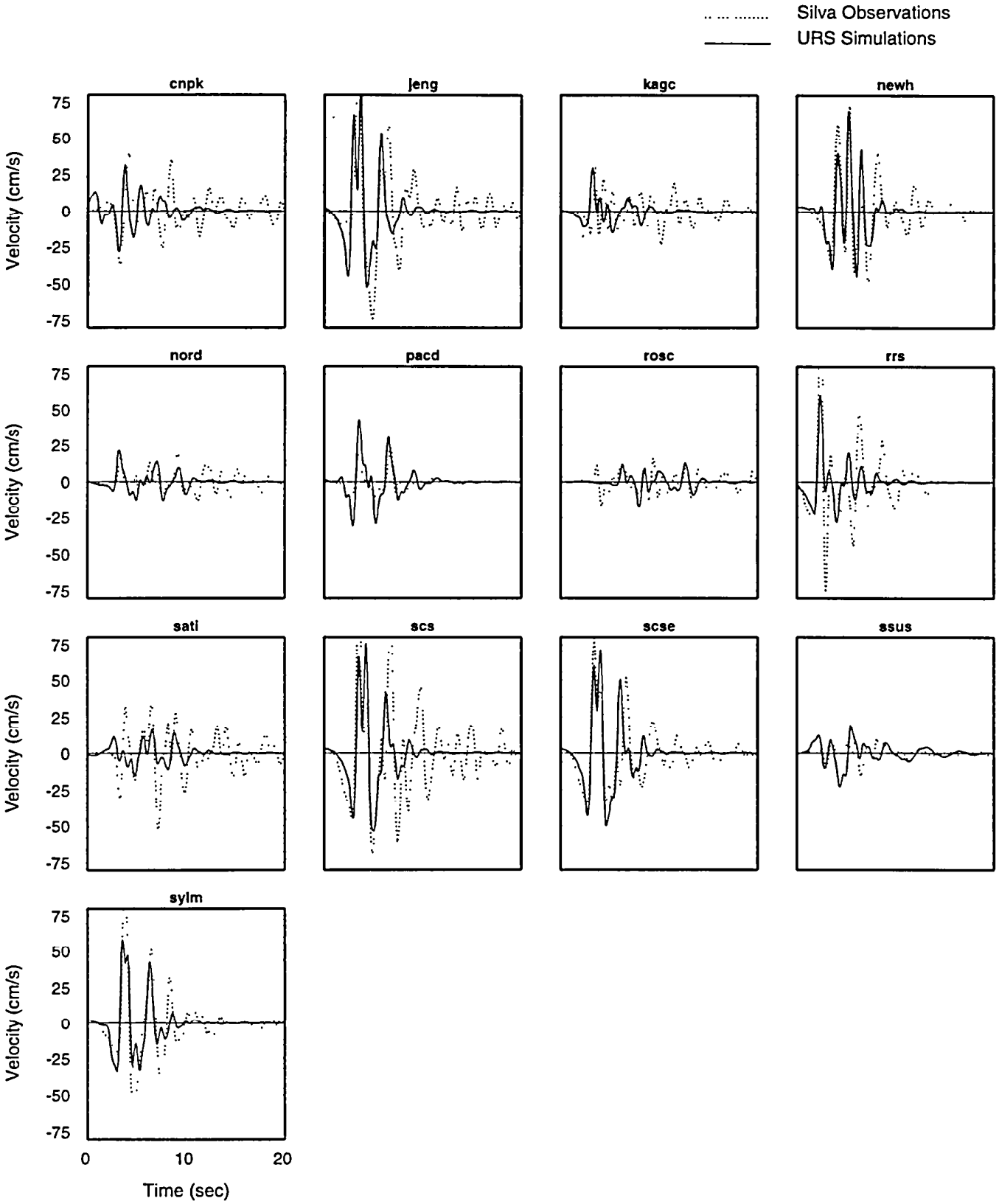

GMT Aug 31 11:04:15 1999 /u1/nancy/PEER-5/Northridge/Comparisons.990823/ExtraPlots

Northridge - Fault Parallel

Simulations and Data Band Pass Filtered 0.125-1.43 Hz

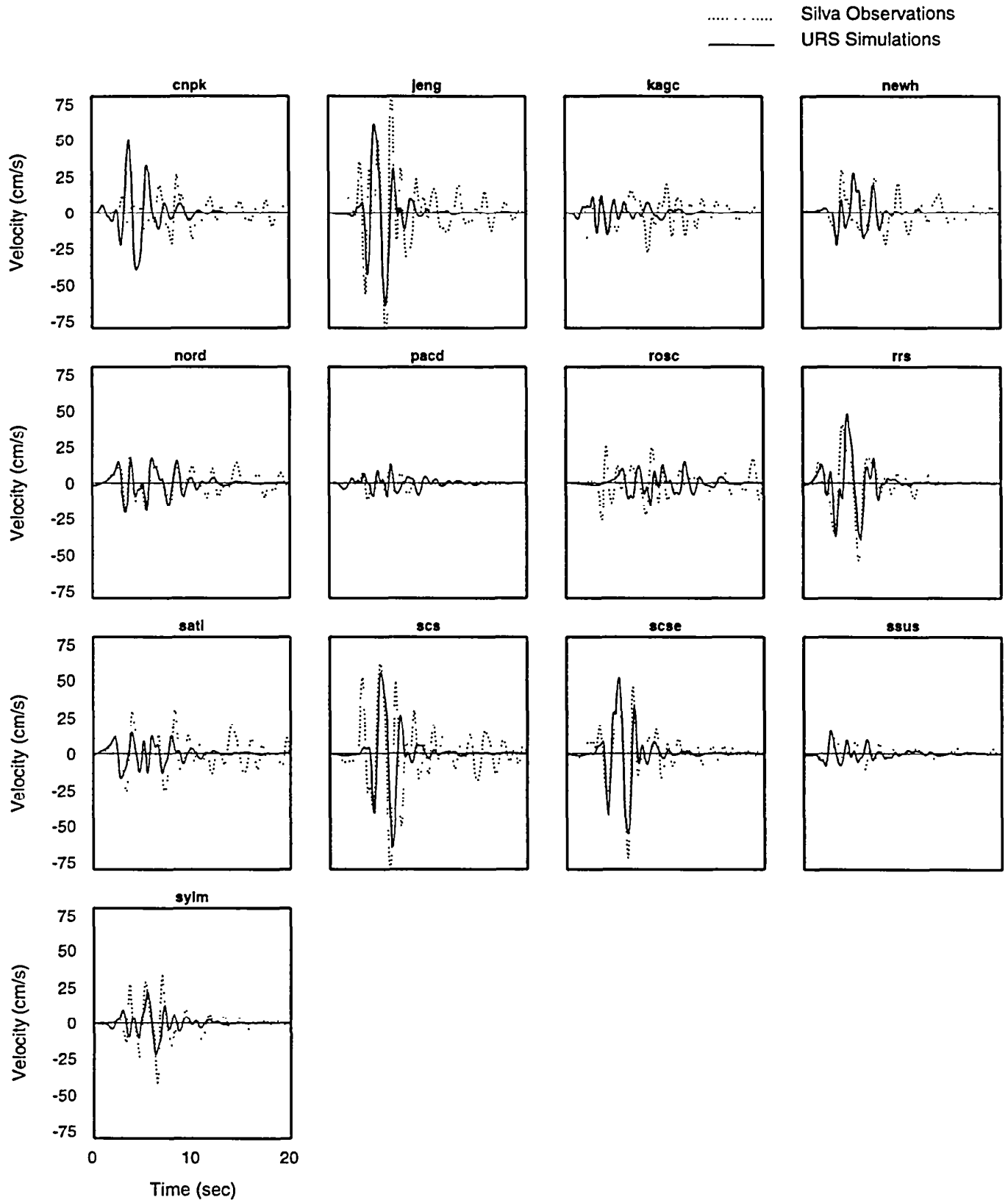

GMT Aug 31 11:04:40 1999 /u1/nancy/PEER-5/Northridge/Comparisons.990823/ExtraPlots

Northridge - Fault Normal

Simulations and Data

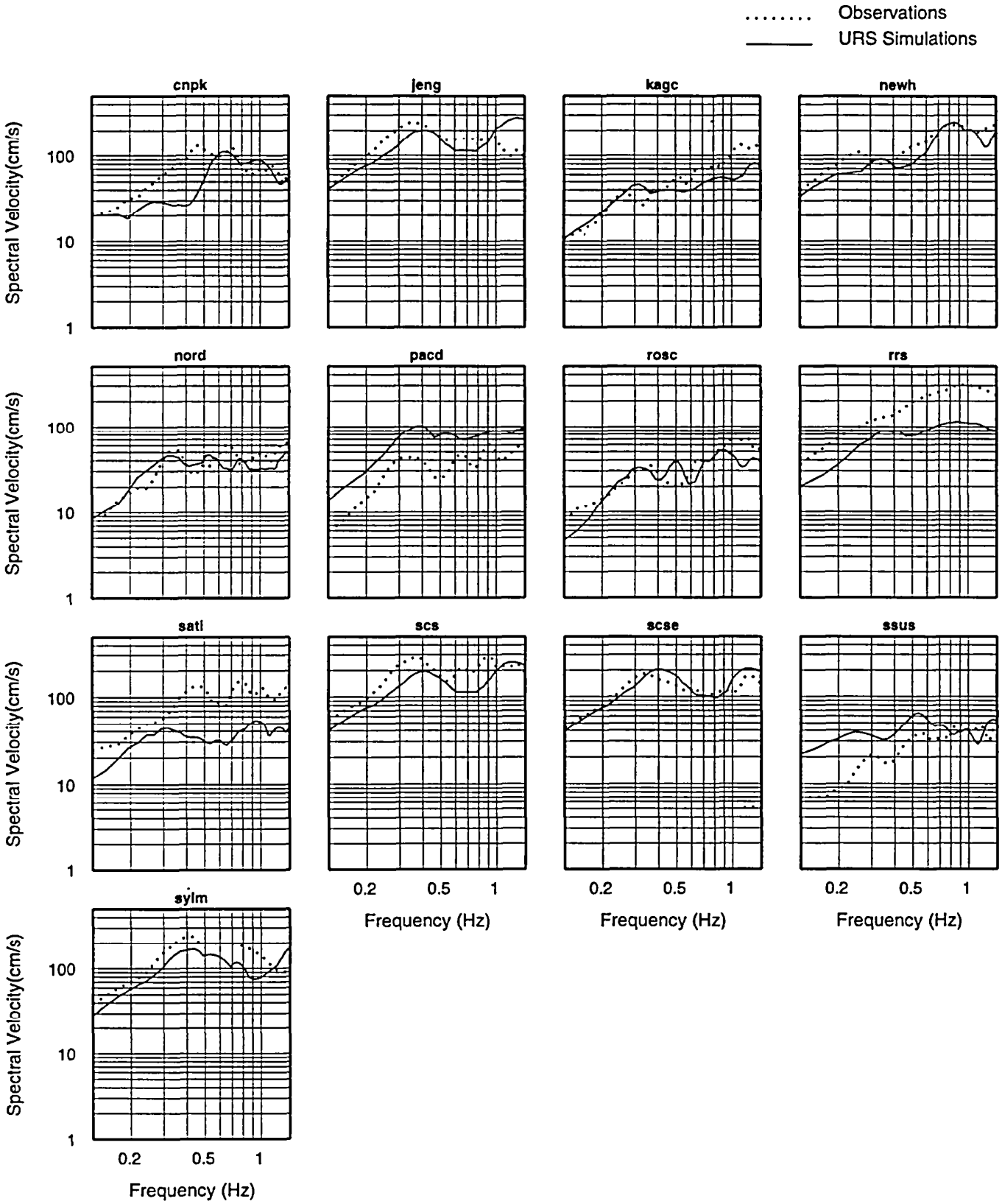

GMT Aug 31 15:56:15 1999 /u1/nancy/PEER-5/Northridge/Comparisons.990823/ExtraPlots

Northridge - Fault Parallel

Simulations and Data

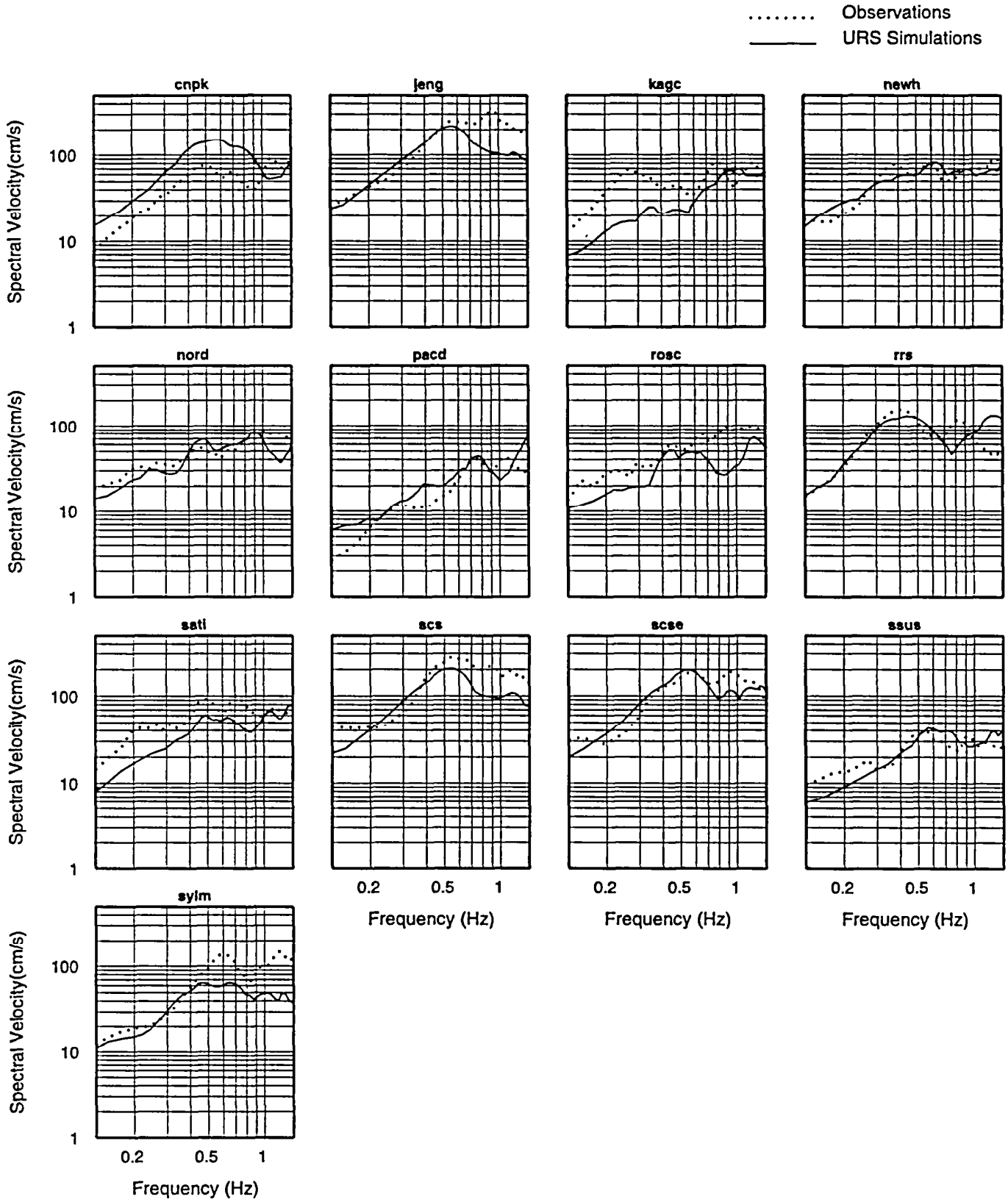

GMT Aug 31 15:56:49 1999 /u1/nancy/PEER-5/Northridge/Comparisons.990823/ExtraPlots

Northridge - Fault Normal

Simulations and Data Band Pass Filtered 0.125-1.43 Hz

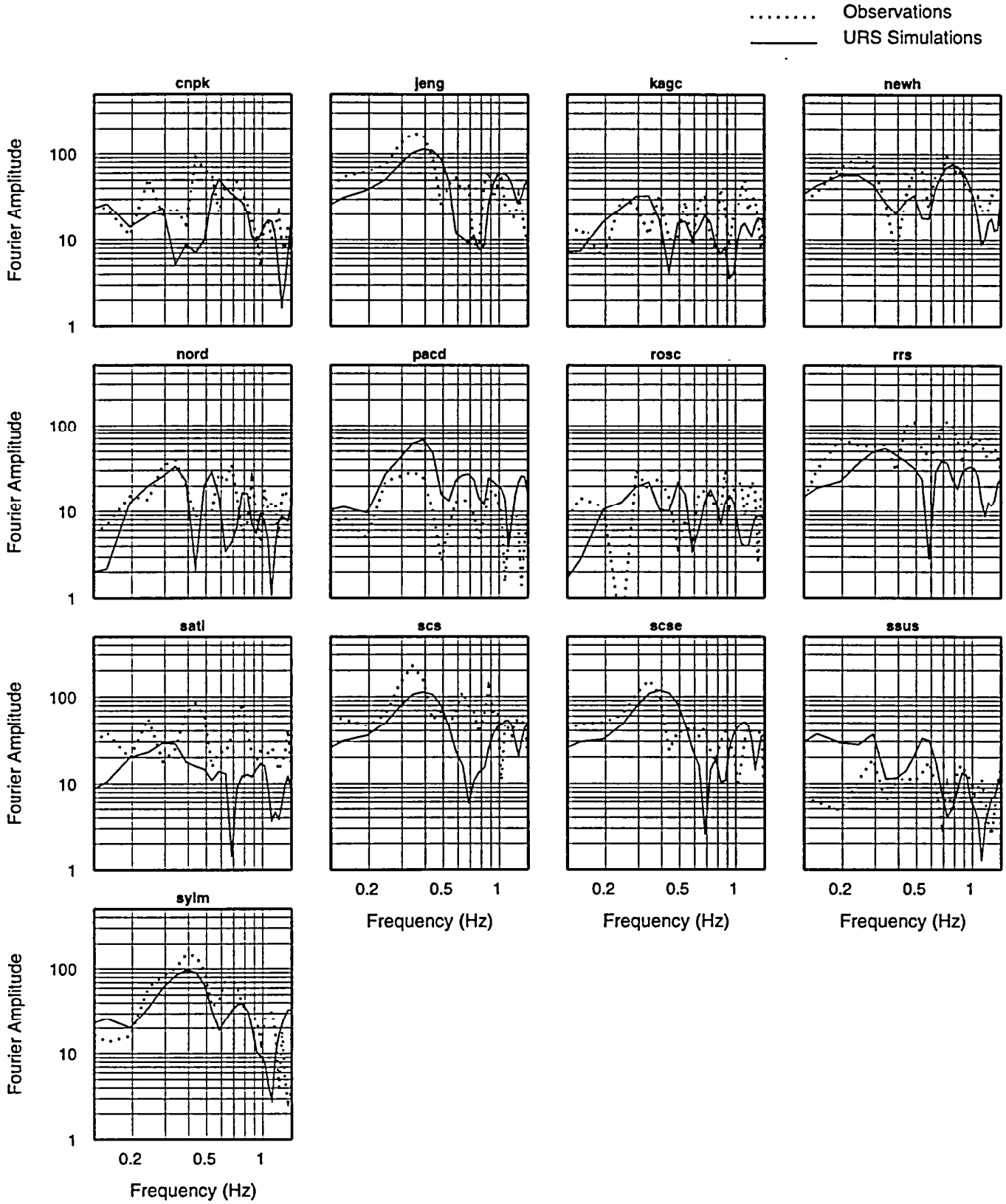

GMT Aug 31 15:49:28 1999 /u1/nancy/PEER-5/Northridge/Comparisons.990823/ExtraPlots

Northridge - Fault Parallel

Simulations and Data Band Pass Filtered 0.125-1.43 Hz

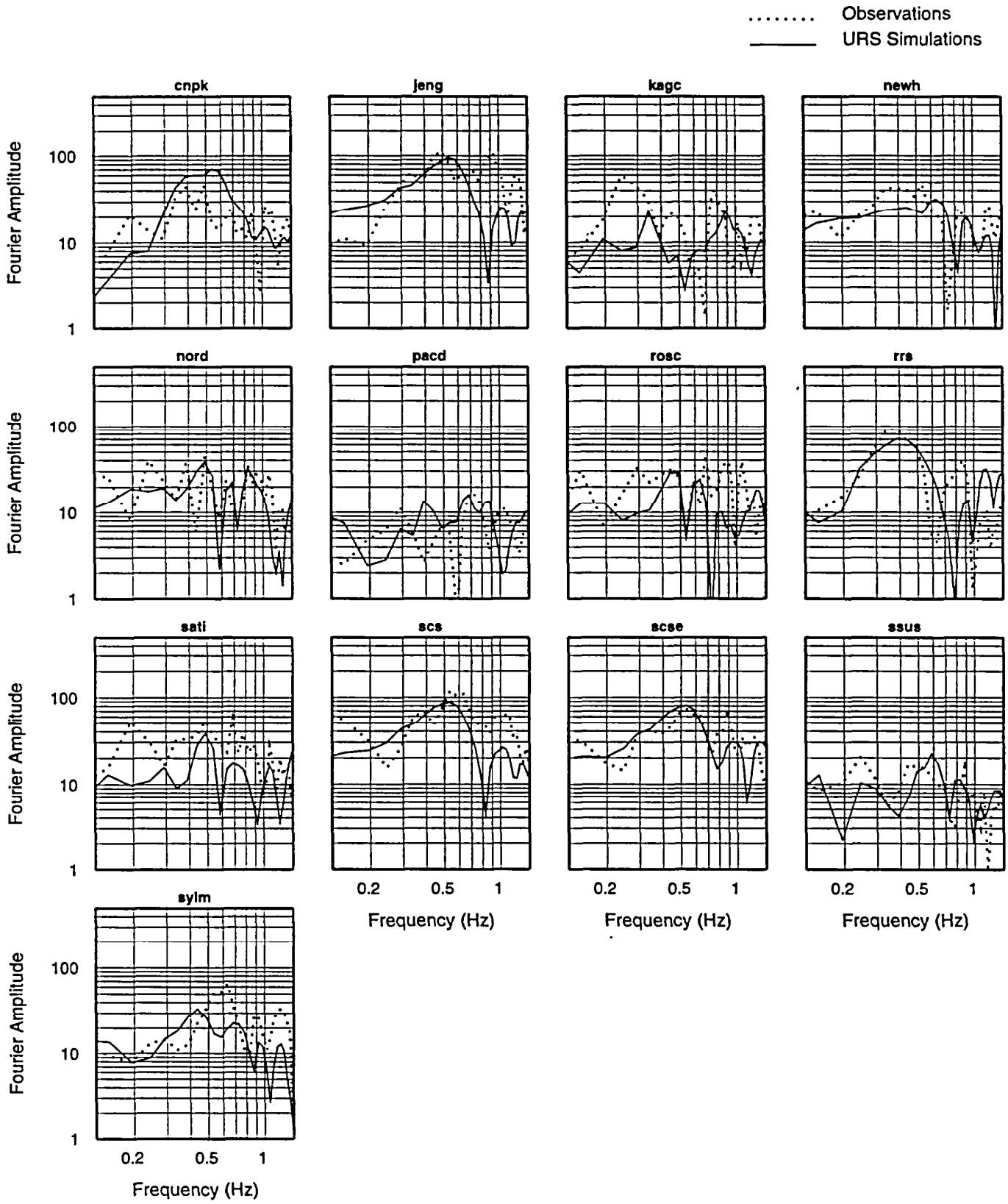

GMT Aug 31 15:50:23 1999 /u1/nancy/PEER-5/Northridge/Comparisons.990823/ExtraPlots

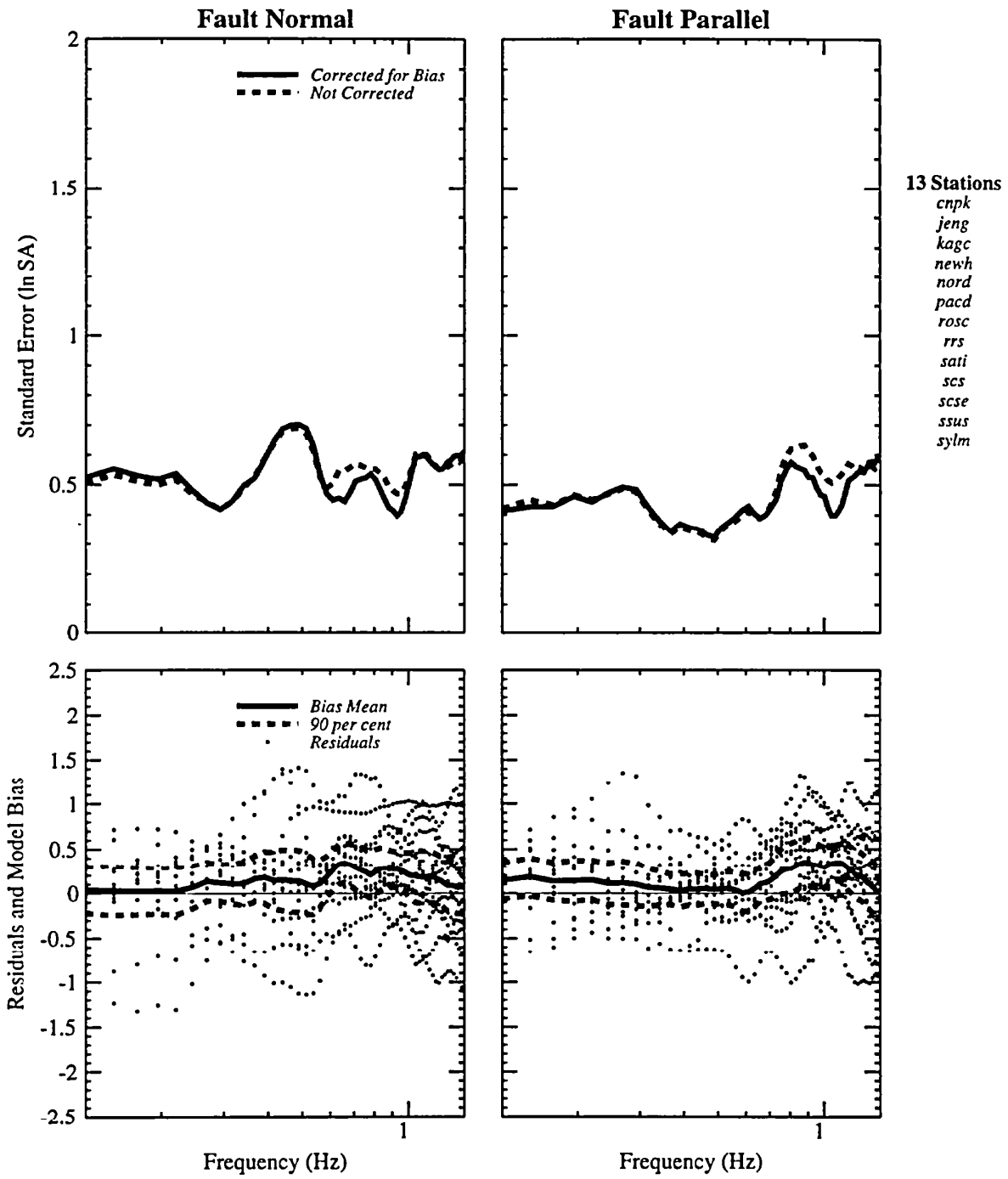

Northridge Spectral Acceleration Goodness of Fit
Observed minus Synthetic (obs - sim)

nfsmith0 Tue Aug 31 14:04:10 PDT 1999
/u1/nancy/PEER-5/Northridge/GoodFit/mplot_goodfit.csh

Northridge - Filter 0.125-1.43 Hz, Pas 94 BB Sims - cnpk

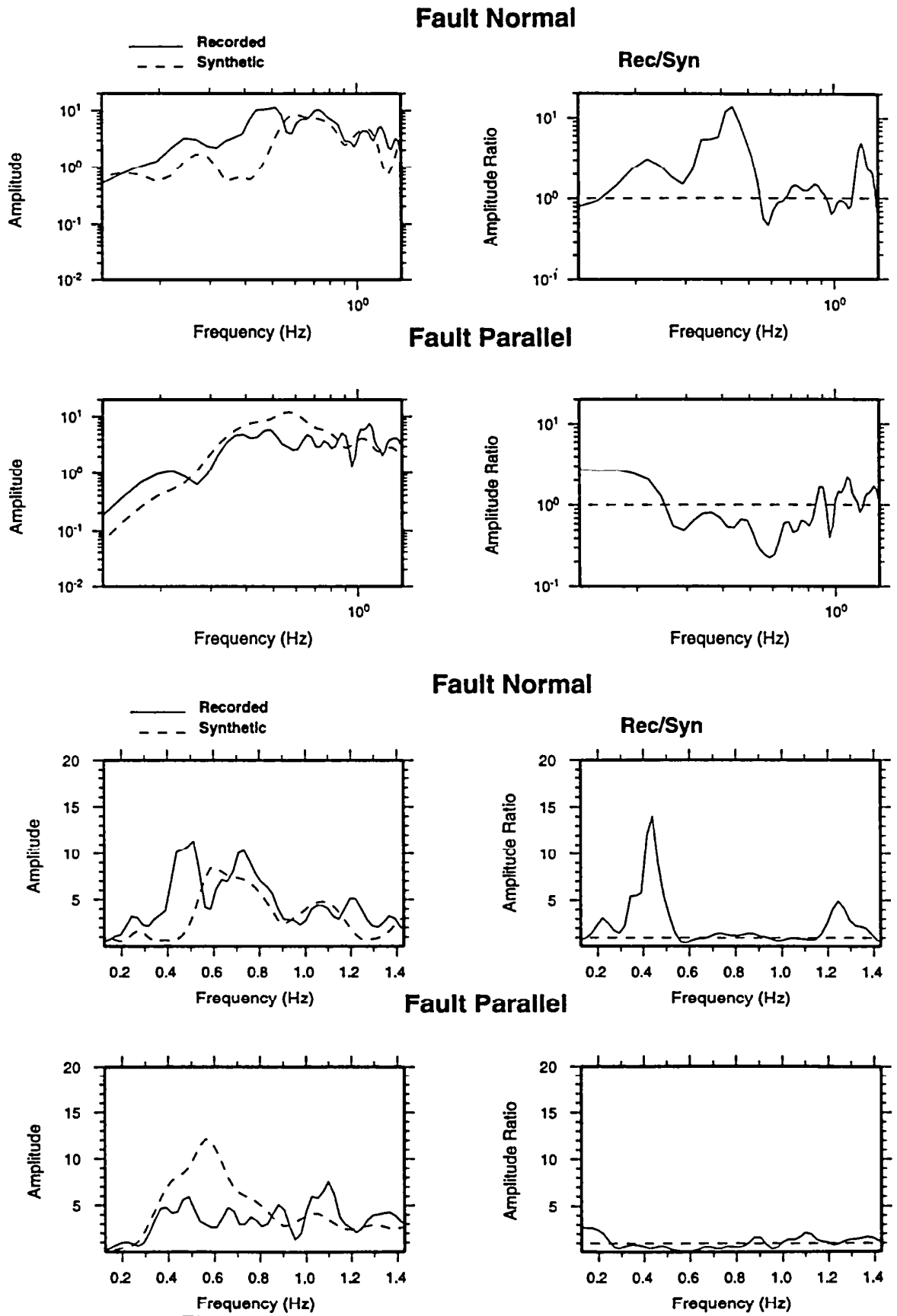

GMT Aug 23 13:57:01 1999 /u1/nancy/PEER-5/Northridge/Comparisons.990823/AP_fspec

Northridge - Filter 0.125-1.43 Hz, Pas 94 BB Sims - jeng

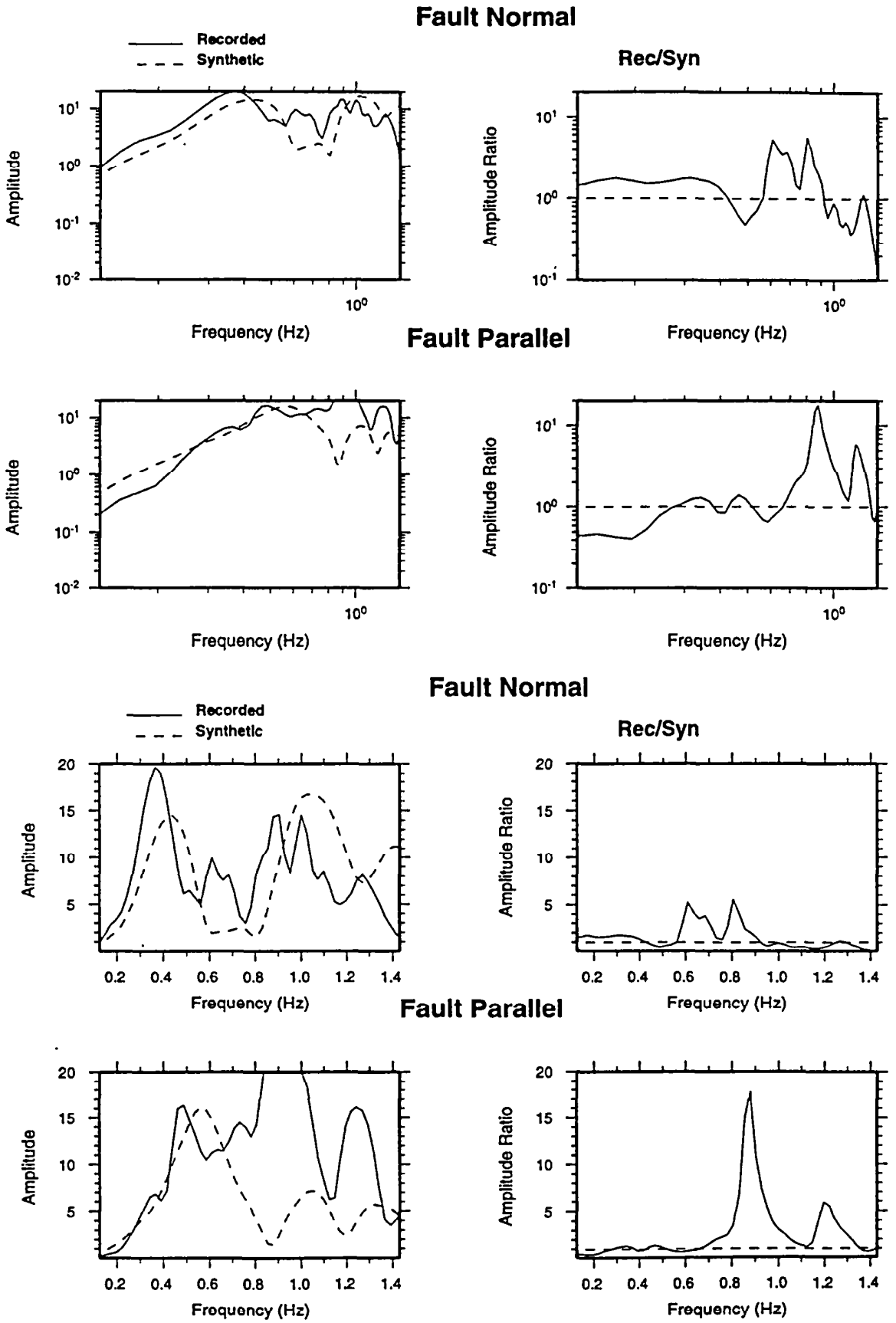

GMT Aug 23 13:57:21 1999 /u1/nancy/PEER-5/Northridge/Comparisons.990823/AP_fspec

Northridge - Filter 0.125-1.43 Hz, Pas 94 BB Sims - kagc

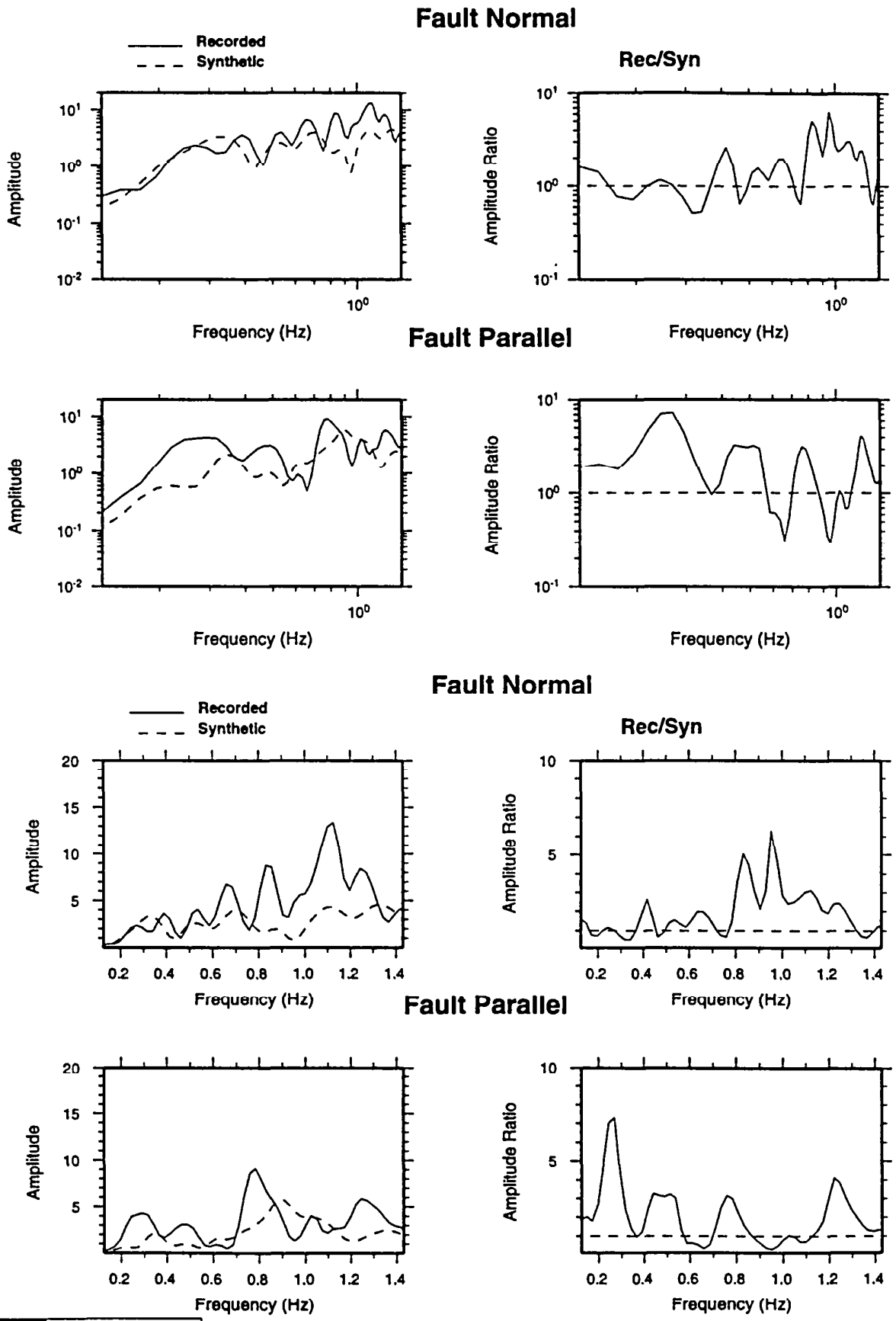

Northridge - Filter 0.125-1.43 Hz, Pas 94 BB Sims - newh

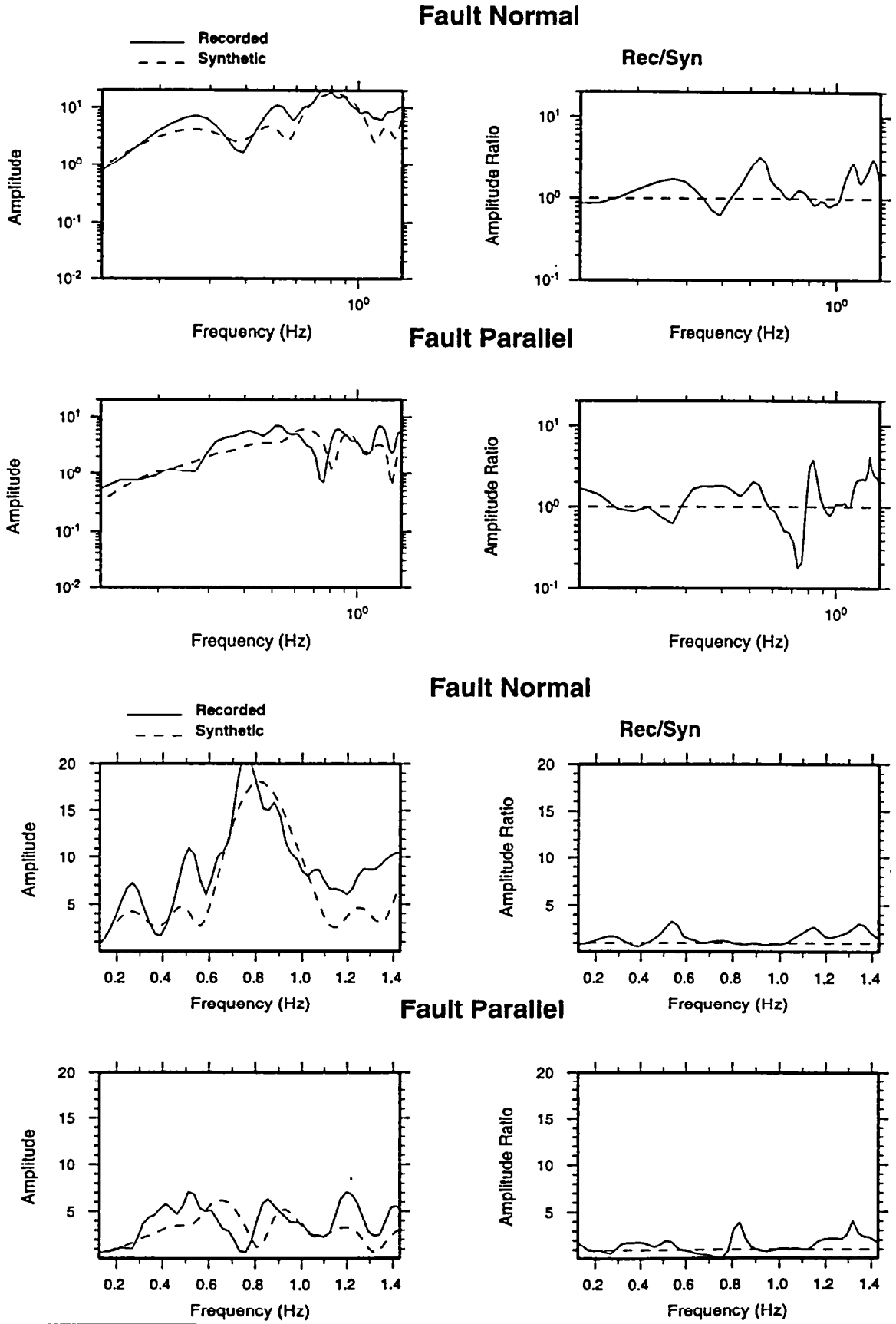

GMT Aug 23 13:58:01 1999 /u1/nancy/PEER-5/Northridge/Comparisons.990823/AP_fspec

Northridge - Filter 0.125-1.43 Hz, Pas 94 BB Sims - nord

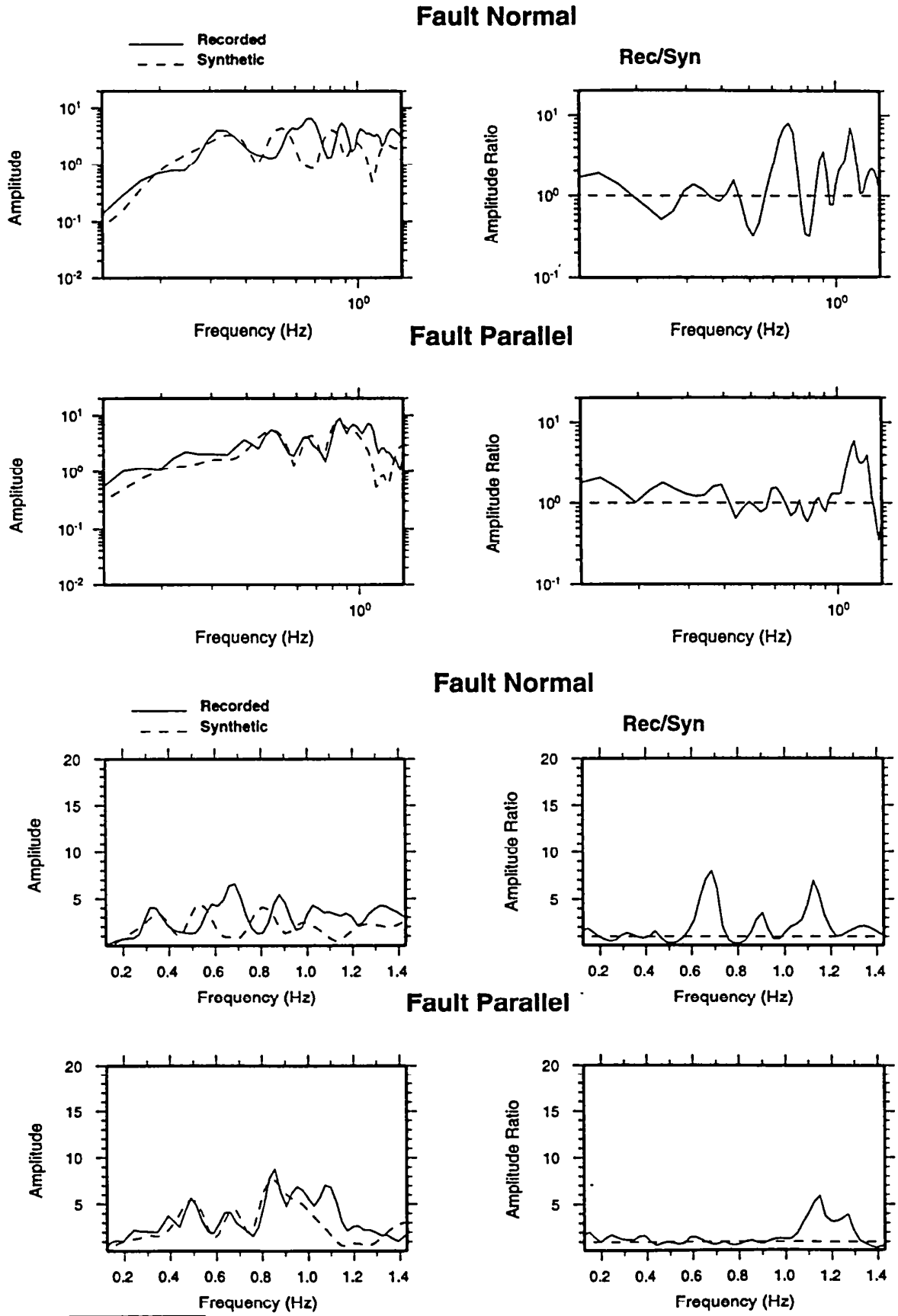

GMT Aug 23 13:58:21 1999 /u1/nancy/PEER-5/Northridge/Comparisons.990823/AP_fspec

Northridge - Filter 0.125-1.43 Hz, Pas 94 BB Sims - pacd

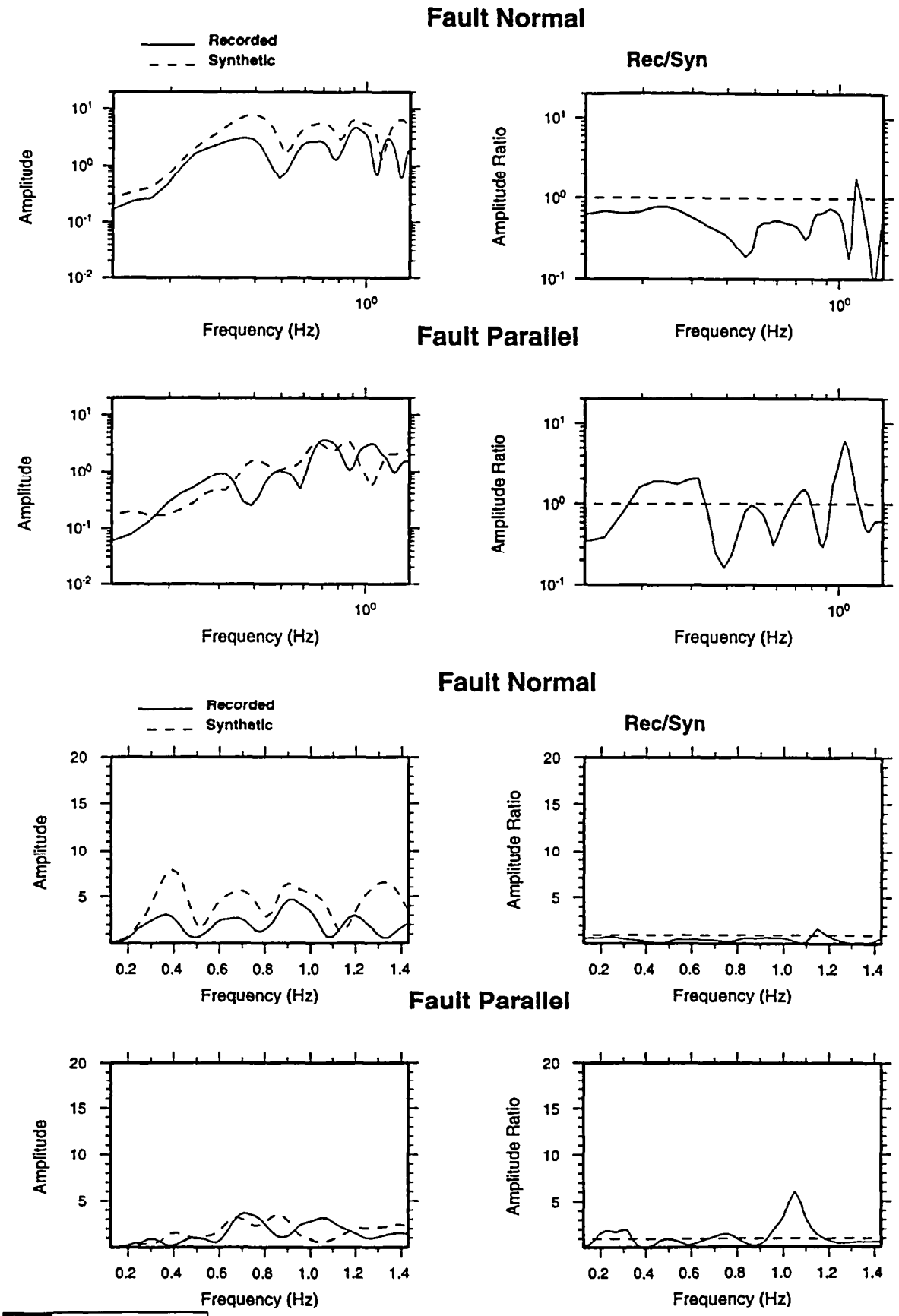

GMT Aug 23 13:58:41 1999 /u1/nancy/PEER-5/Northridge/Comparisons.990823/AP_fspec

Northridge - Filter 0.125-1.43 Hz, Pas 94 BB Sims - rosc

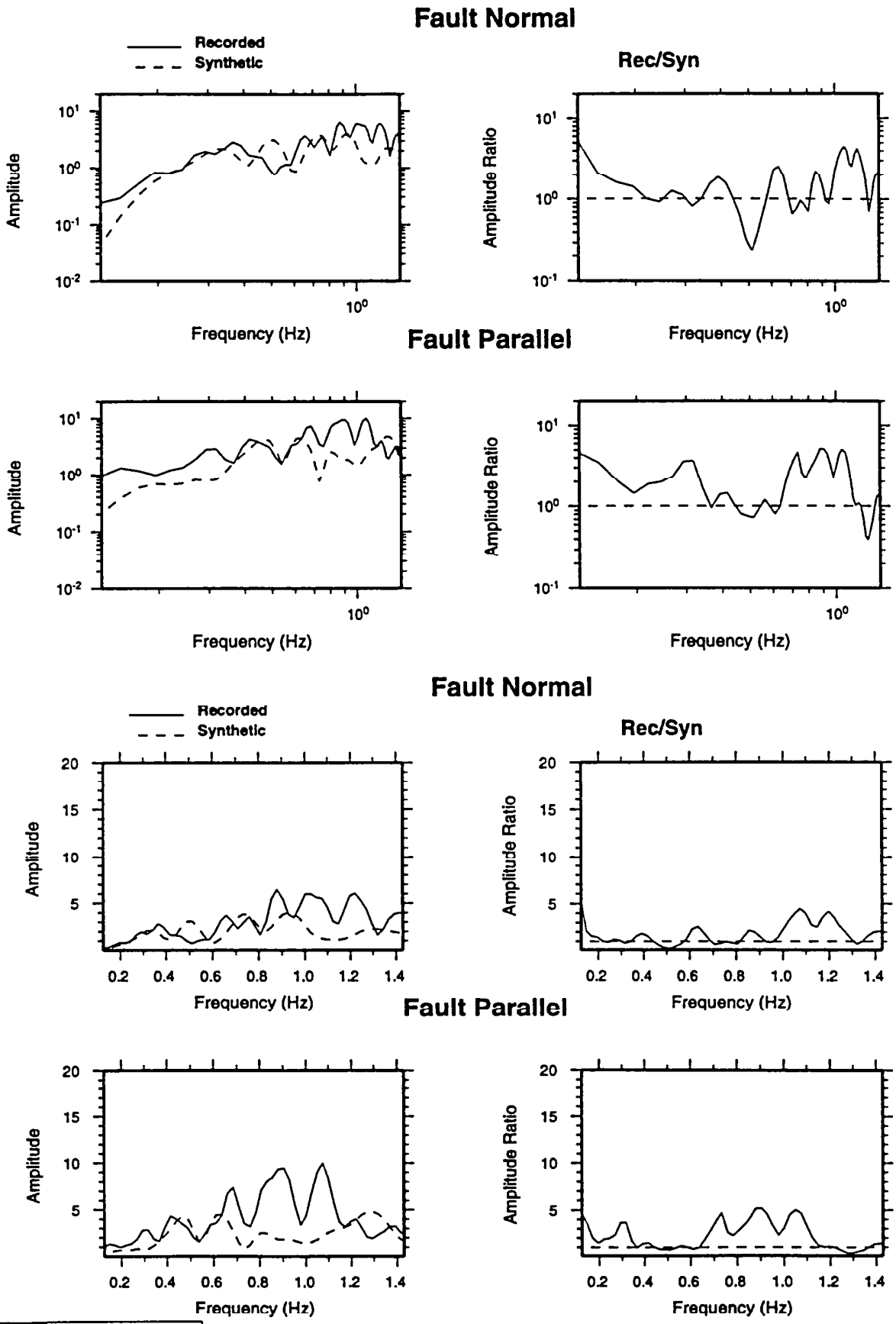

GMT Aug 23 14:00:08 1999 /u1/nancy/PEER-5/Northridge/Comparisons.990823/AP_fspec

Northridge - Filter 0.125-1.43 Hz, Pas 94 BB Sims - rrs

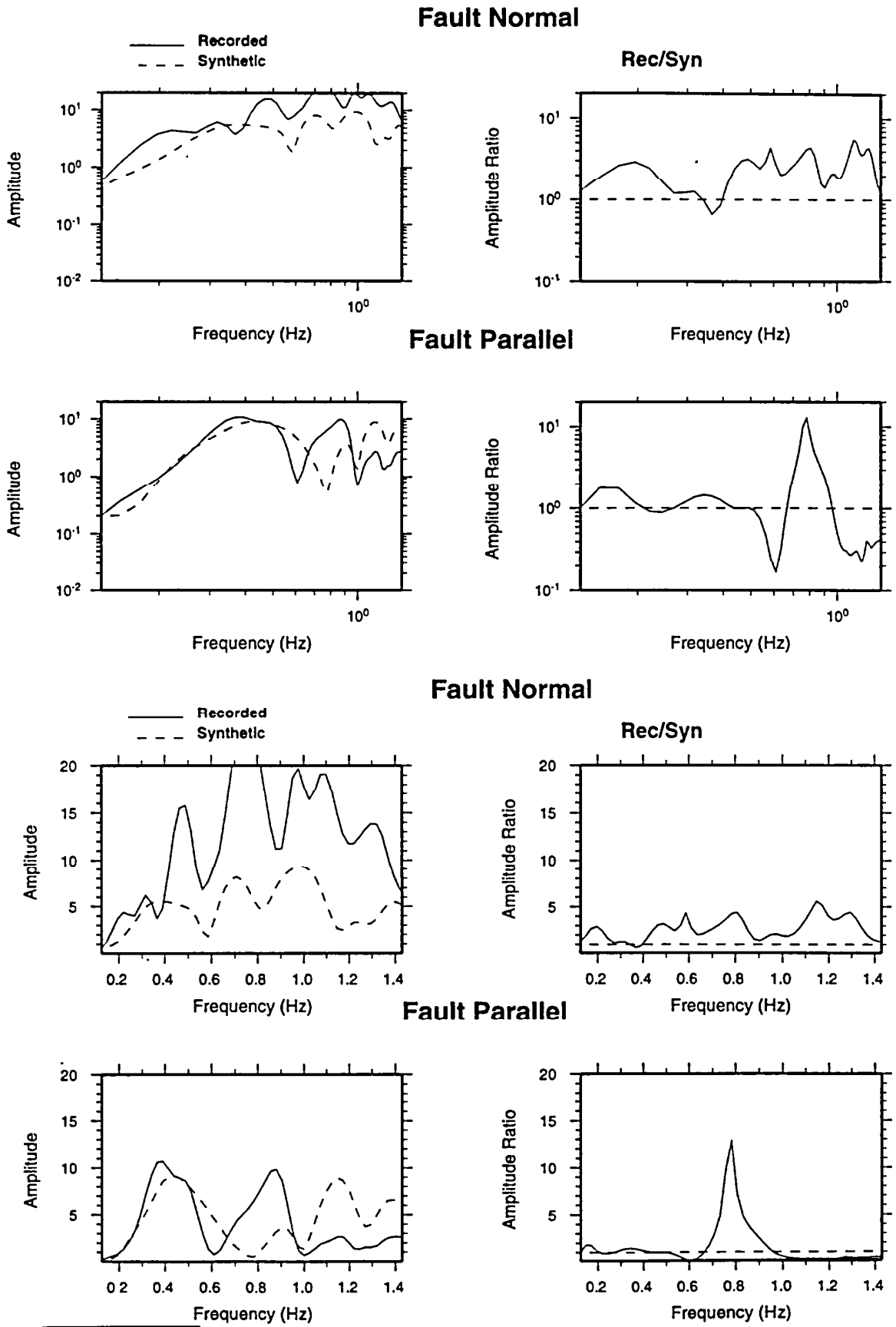

GMT Aug 24 10:56:58 1999 /u1/nancy/PEER-5/Northridge/Comparisons.990823/AP_fspec

Northridge - Filter 0.125-1.43 Hz, Pas 94 BB Sims - sati

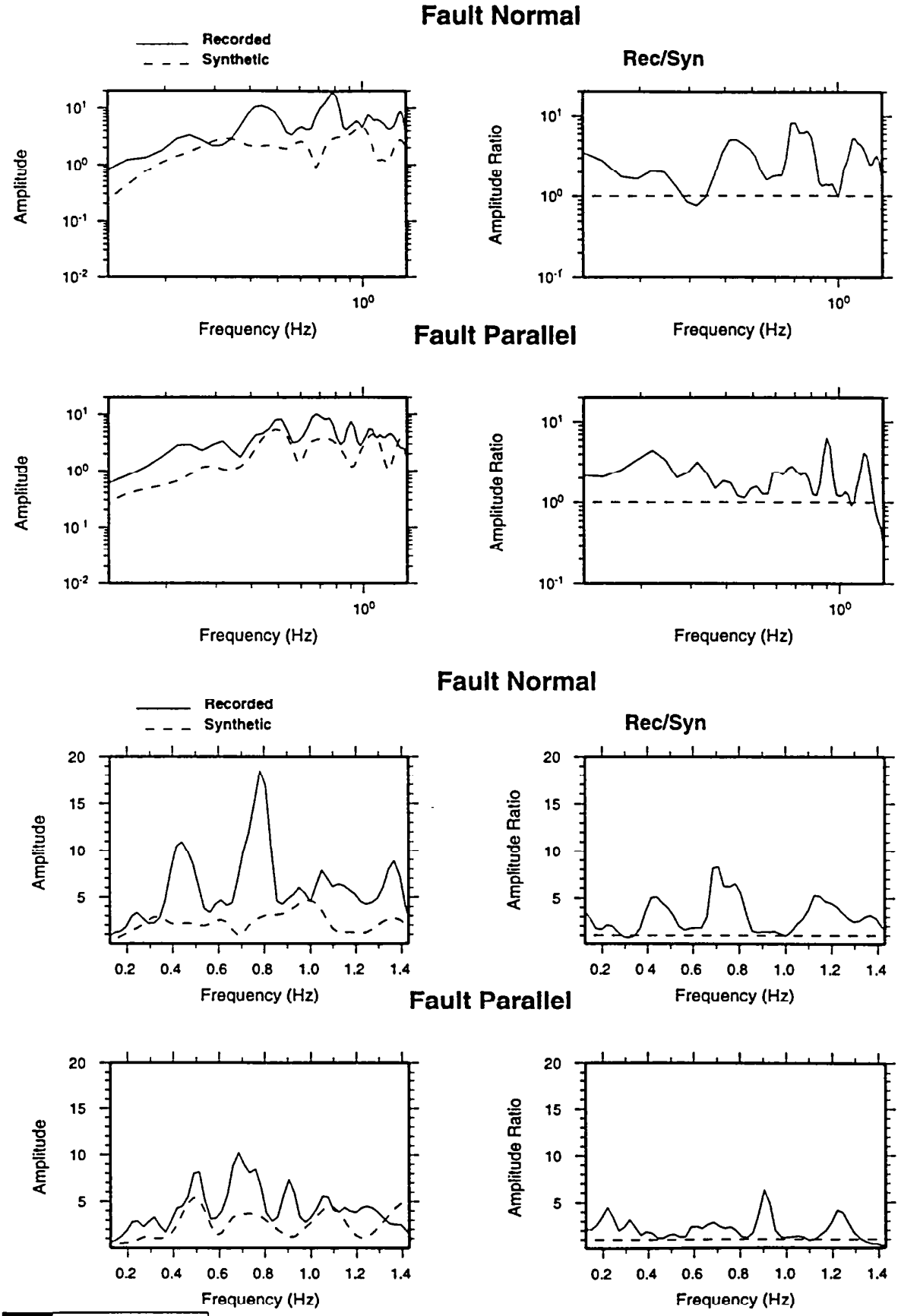

GMT Aug 24 10:57:31 1999 /u1/nancy/PEER-5/Northridge/Comparisons.990823/AP_fspec

Northridge - Filter 0.125-1.43 Hz, Pas 94 BB Sims - scs

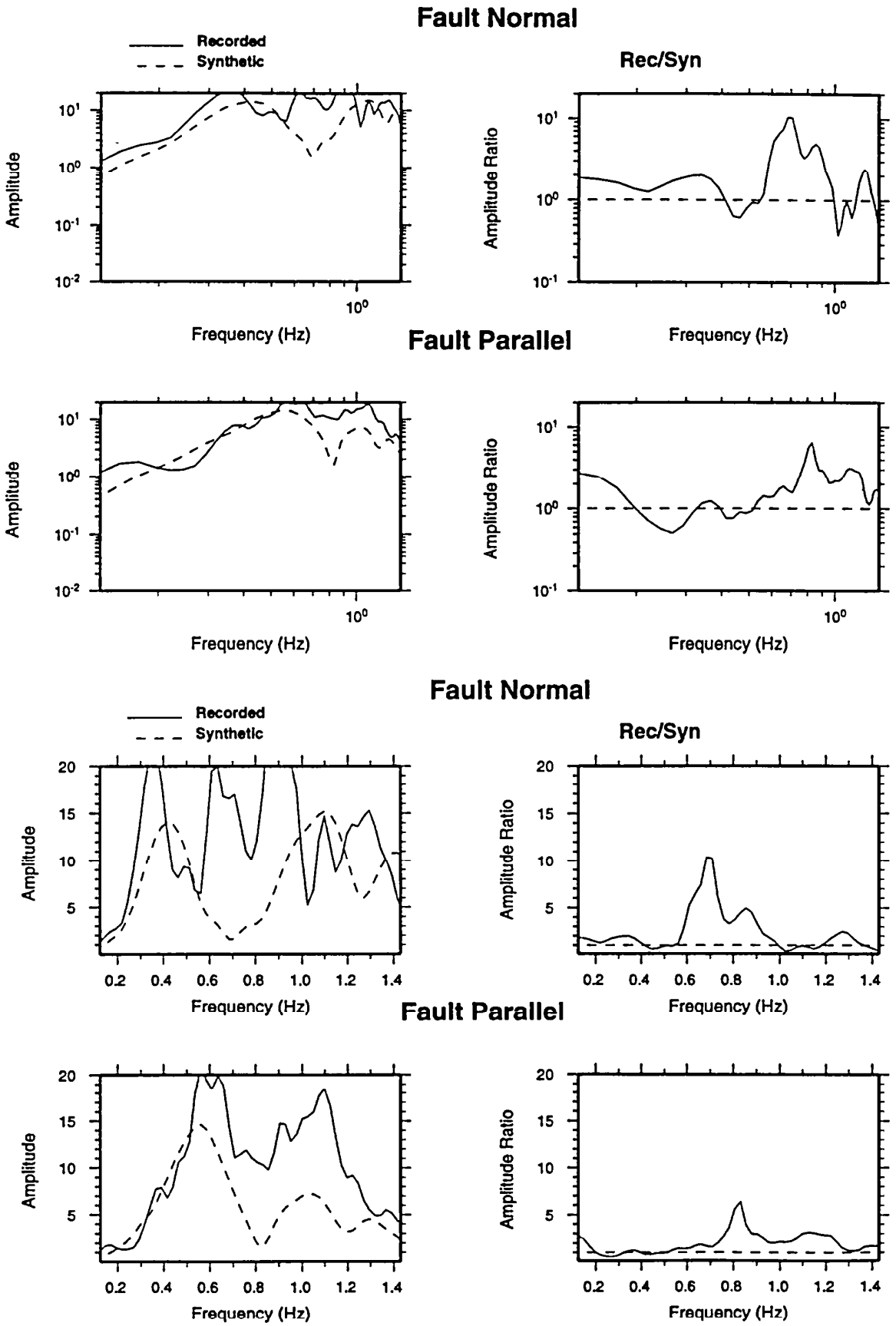

GMT Aug 23 14:01:09 1999 /u1/nancy/PEER-5/Northridge/Comparisons.990823/AP_fspec

Northridge - Filter 0.125-1.43 Hz, Pas 94 BB Sims - scse

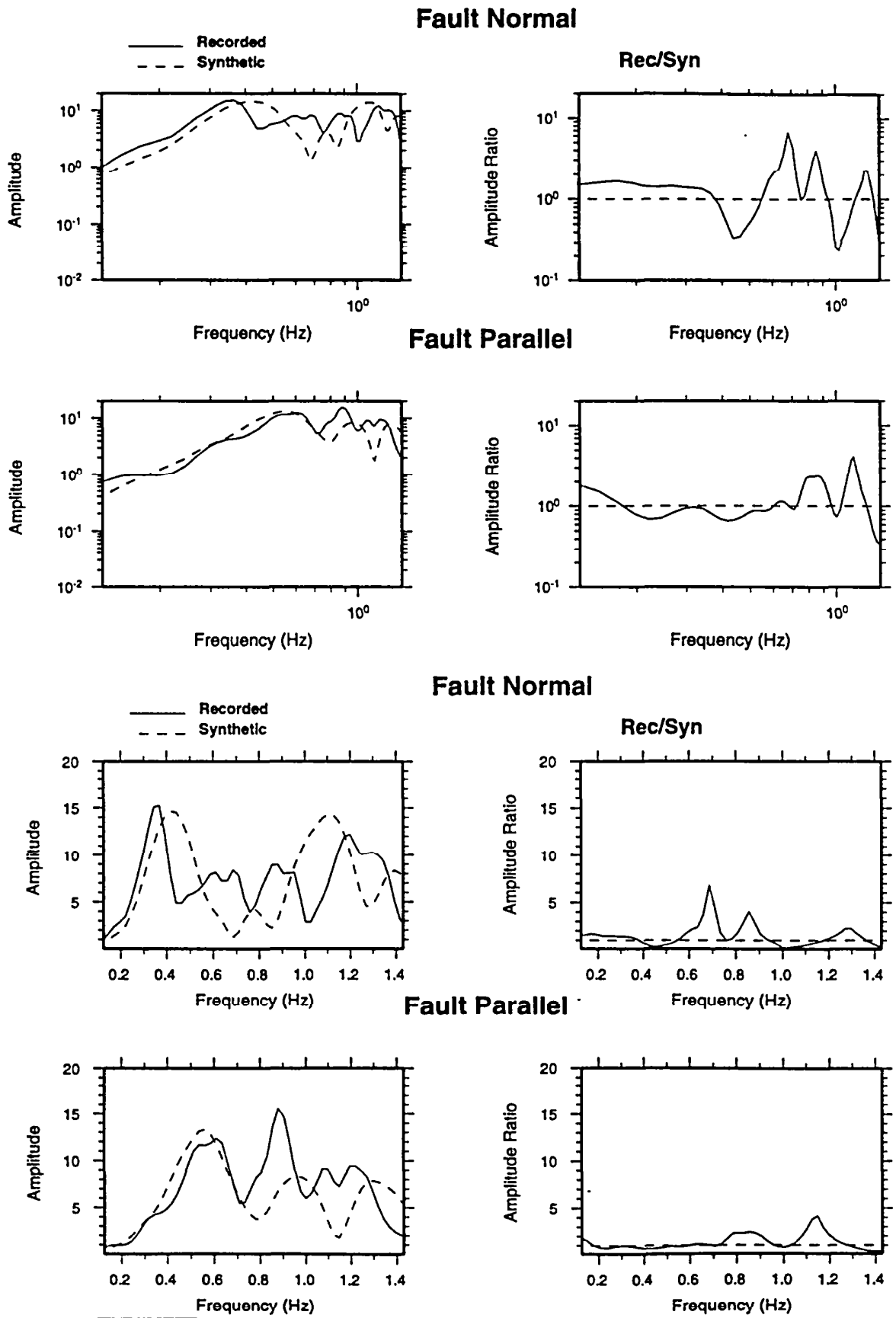

GMT Aug 23 14:01:29 1999 /u1/nancy/PEER-5/Northridge/Comparisons.990823/AP_fspec

Northridge - Filter 0.125-1.43 Hz, Pas 94 BB Sims - ssus

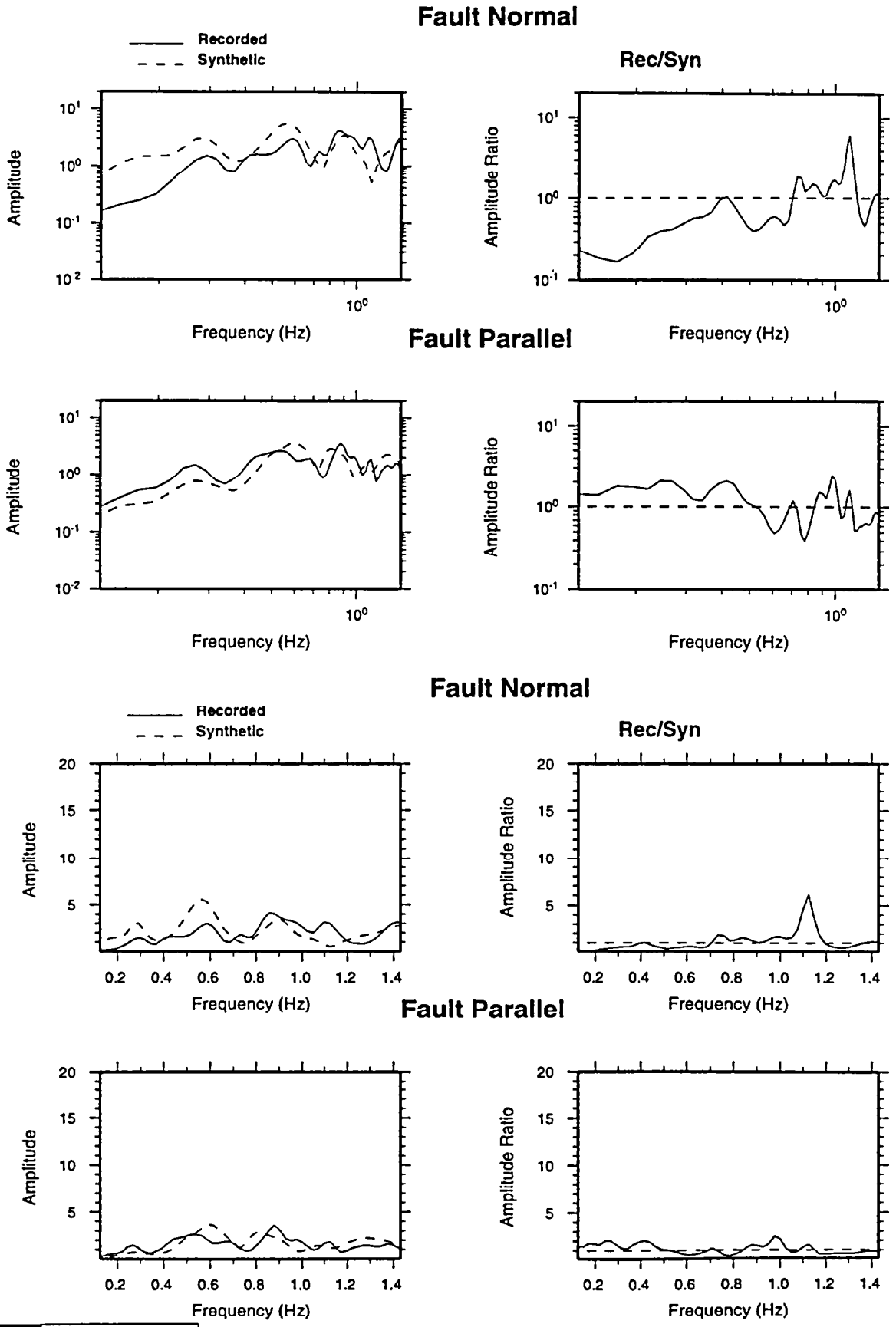

GMT Aug 24 10.58.40 1999 /u1/nancy/PEER-5/Northridge/Comparisons.990823/AP_fspec

Northridge - Filter 0.125-1.43 Hz, Pas 94 BB Sims - sylm

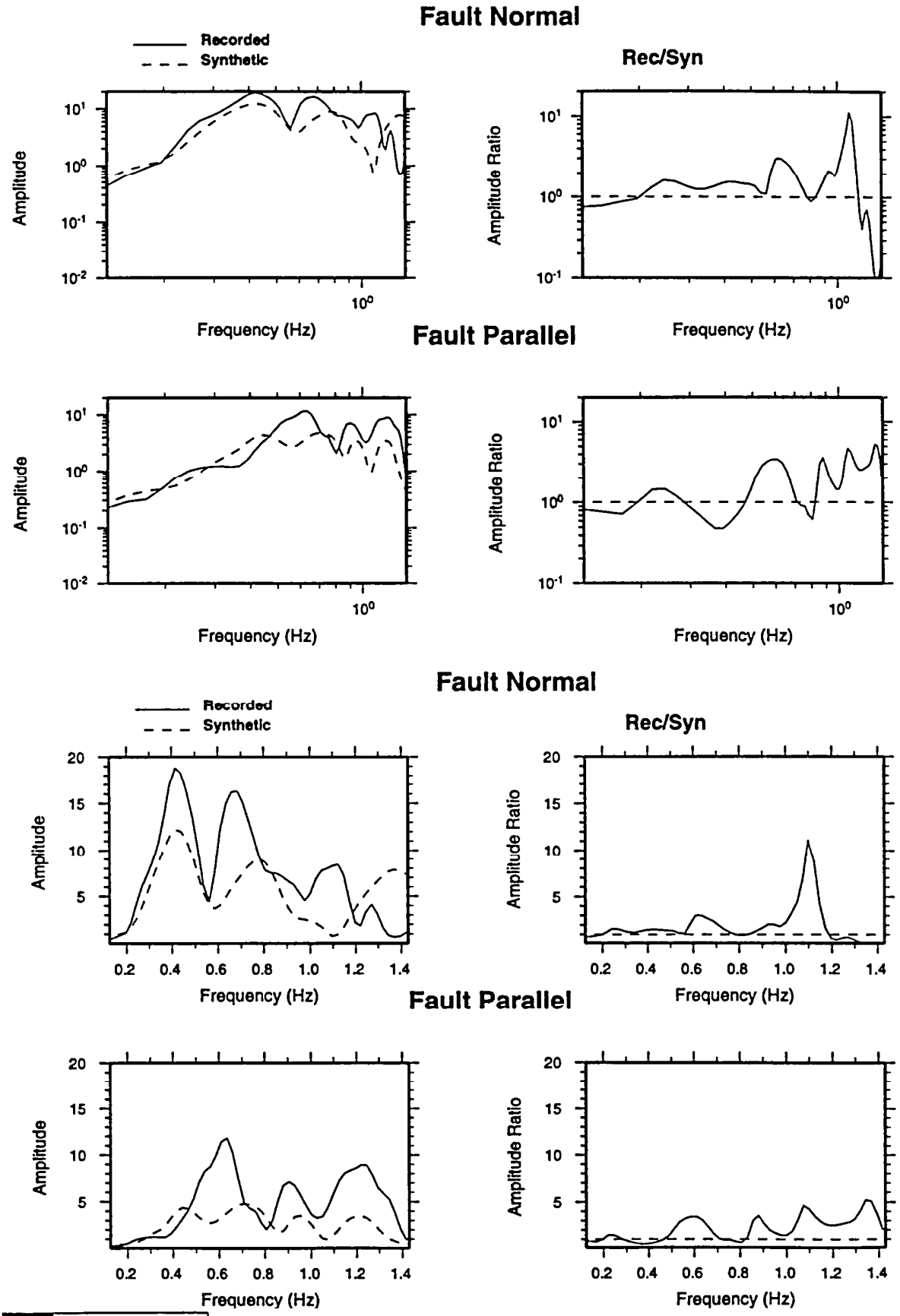

GMT Aug 23 14:02:09 1999 /u1/nancy/PEER-5/Northridge/Comparisons.990823/AP_fspec

Northridge - Fault Normal

SA at 7.0 sec

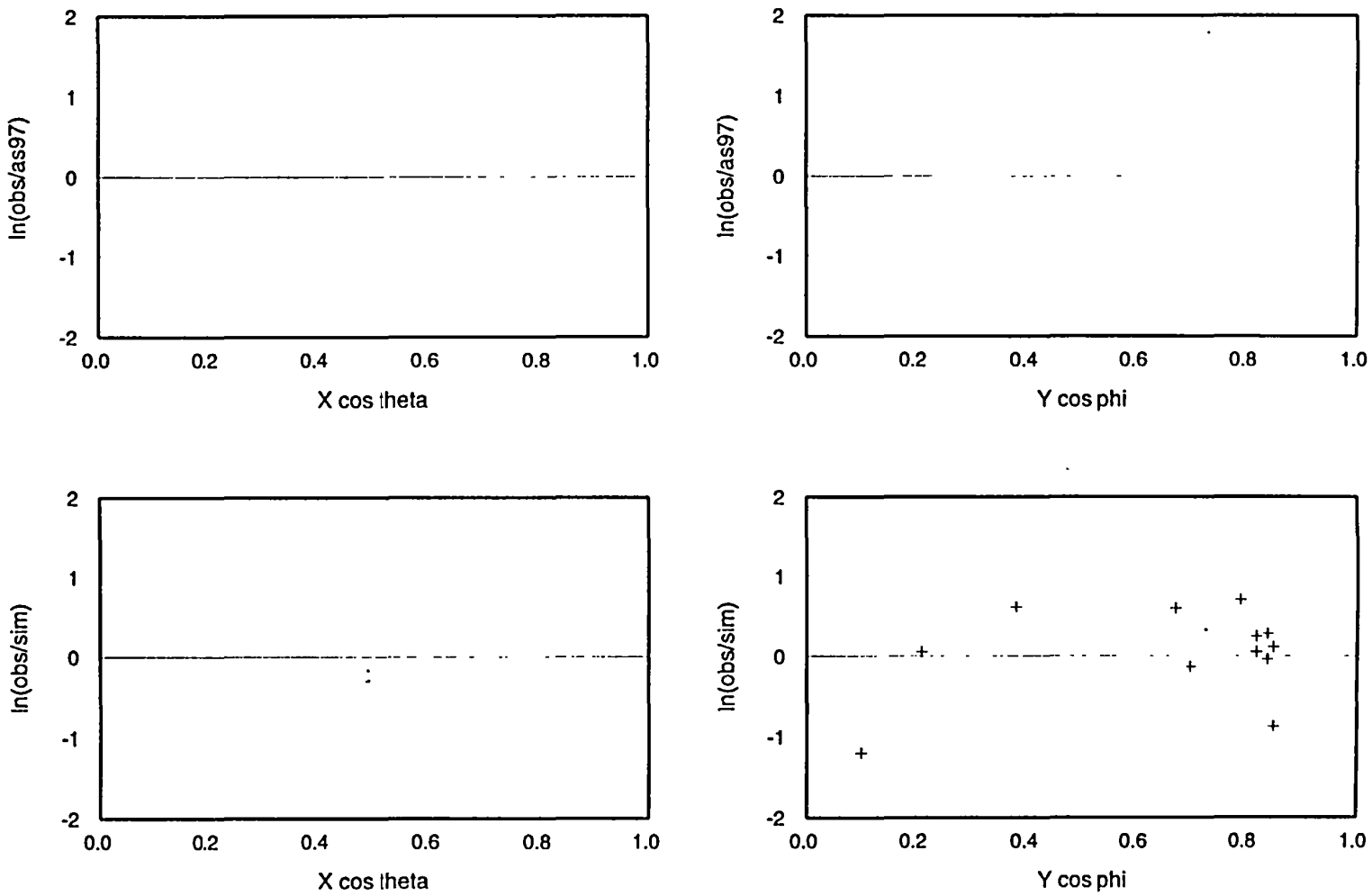

GMT Aug 24 11:15:05 1999 /u1/nancy/PEER-5/Northridge/Comparisons.990823/Resid_plots

Northridge - Fault Parallel

SA at 7.0 sec

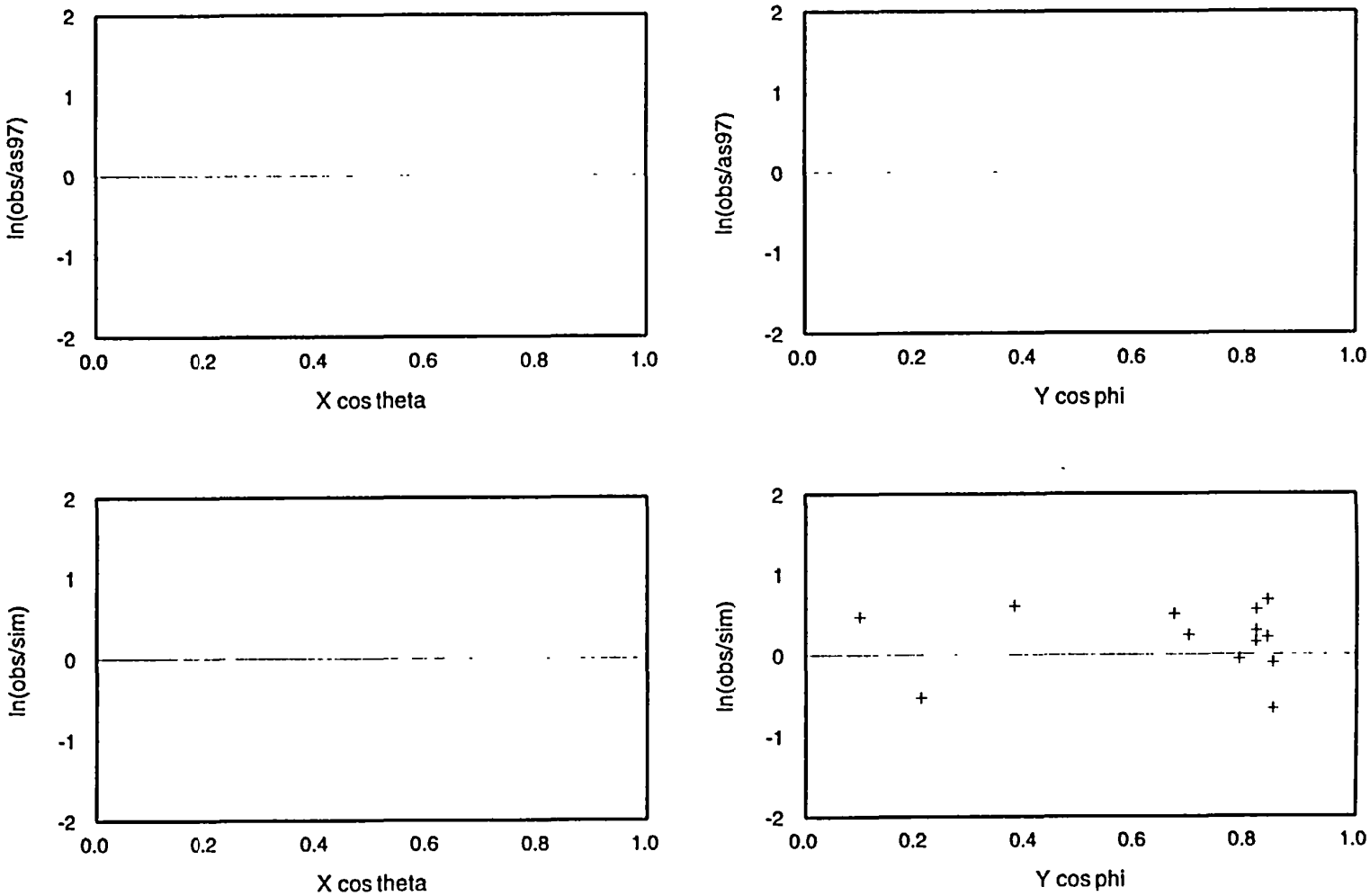

GMT Aug 24 11:15:30 1999 /u1/nancy/PEER-5/Northridge/Comparisons.990823/Resid_plots

Northridge - Fault Normal

SA at 6.0 sec

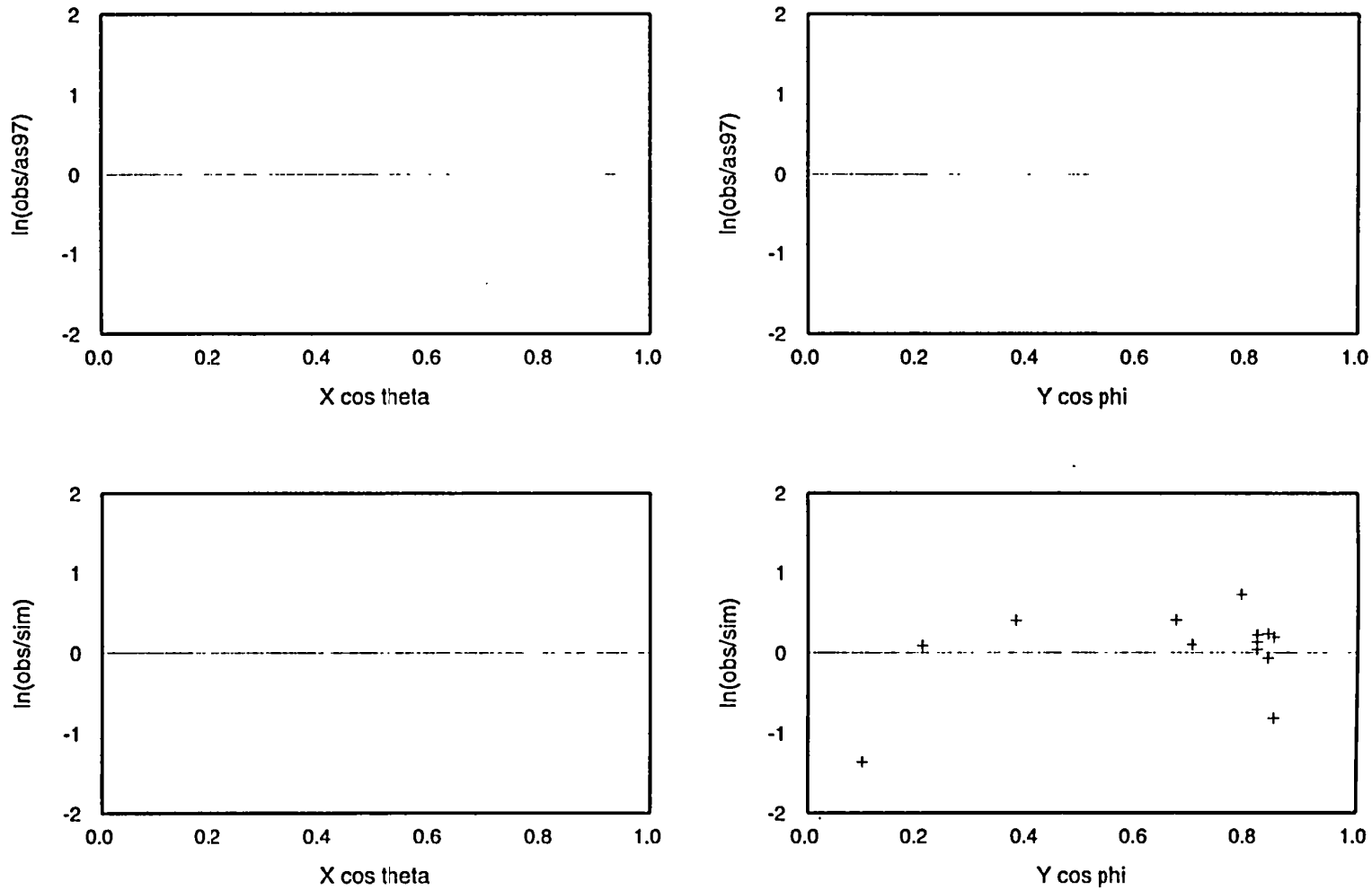

GMT Aug 24 11:15:56 1999 /u1/nancy/PEER-5/Northridge/Comparisons.990823/Resid_plots

Northridge - Fault Parallel

SA at 6.0 sec

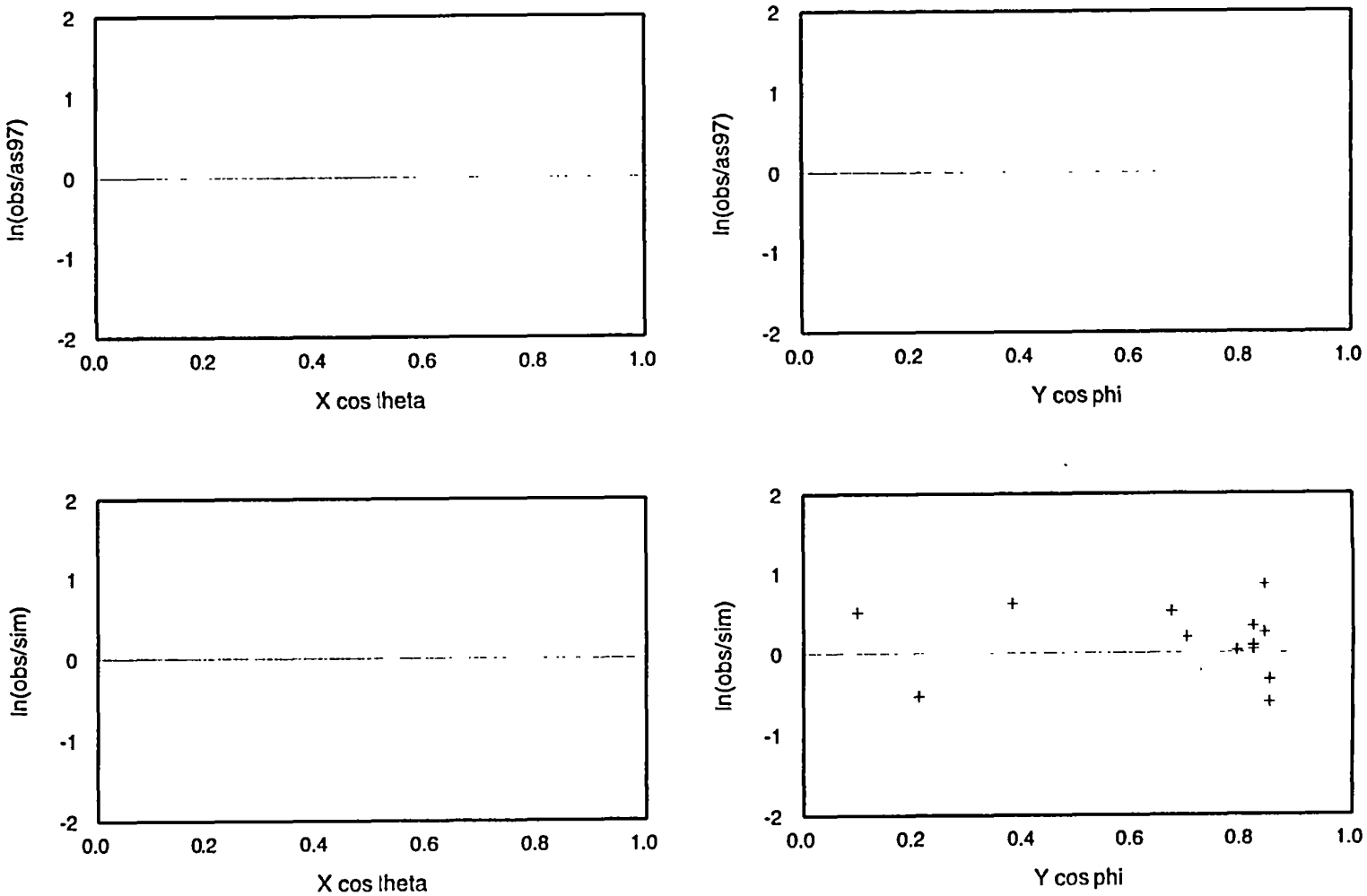

GMT Aug 24 11:16:09 1999 /u1/nancy/PEER-5/Northridge/Comparisons.990823/Resid_plots

Northridge - Fault Normal

SA at 5.0 sec

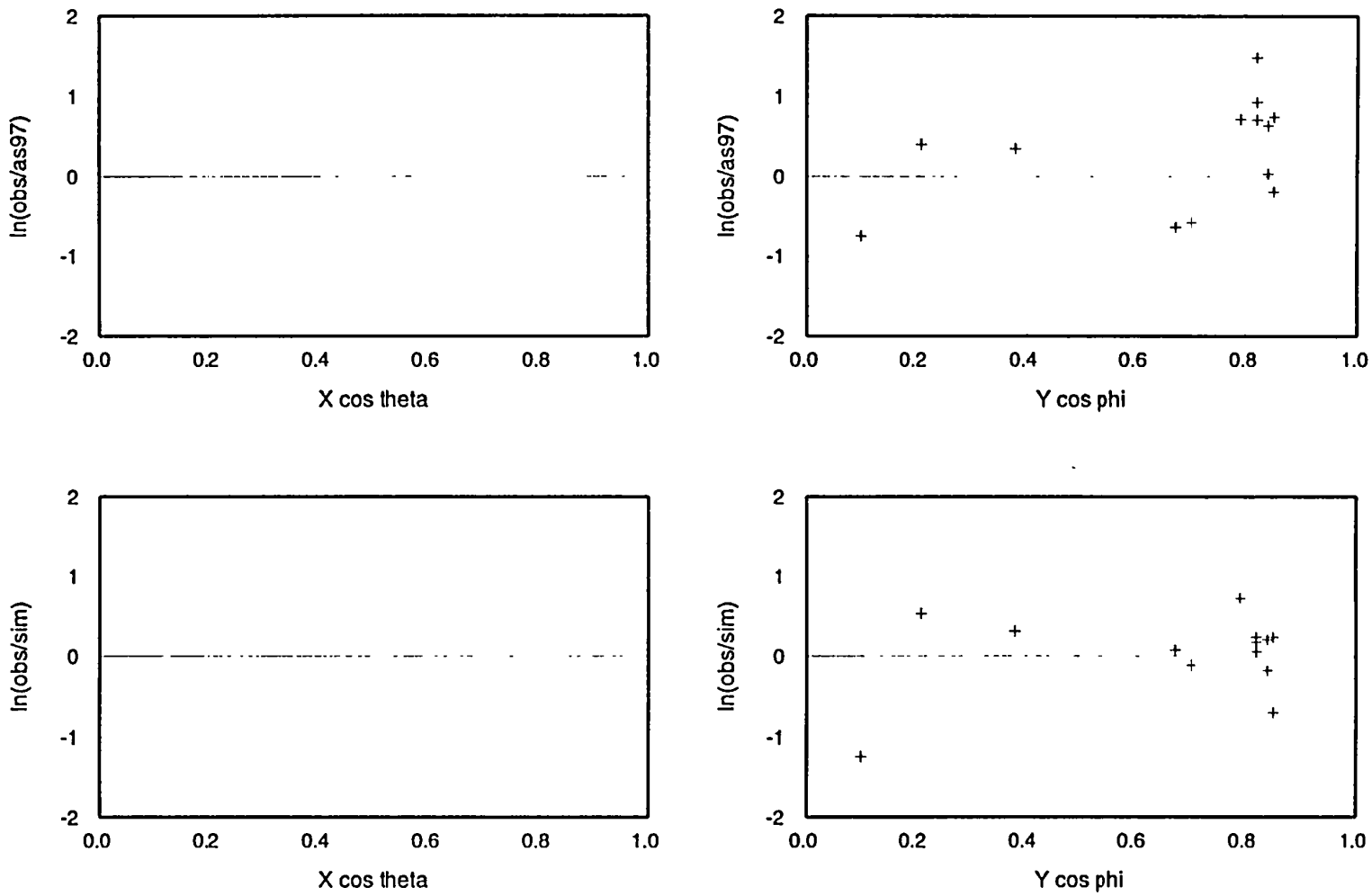

GMT Aug 24 11:16:19 1999 /u1/nancy/PEER-5/Northridge/Comparisons.990823/Resid_plots

Northridge - Fault Parallel

SA at 5.0 sec

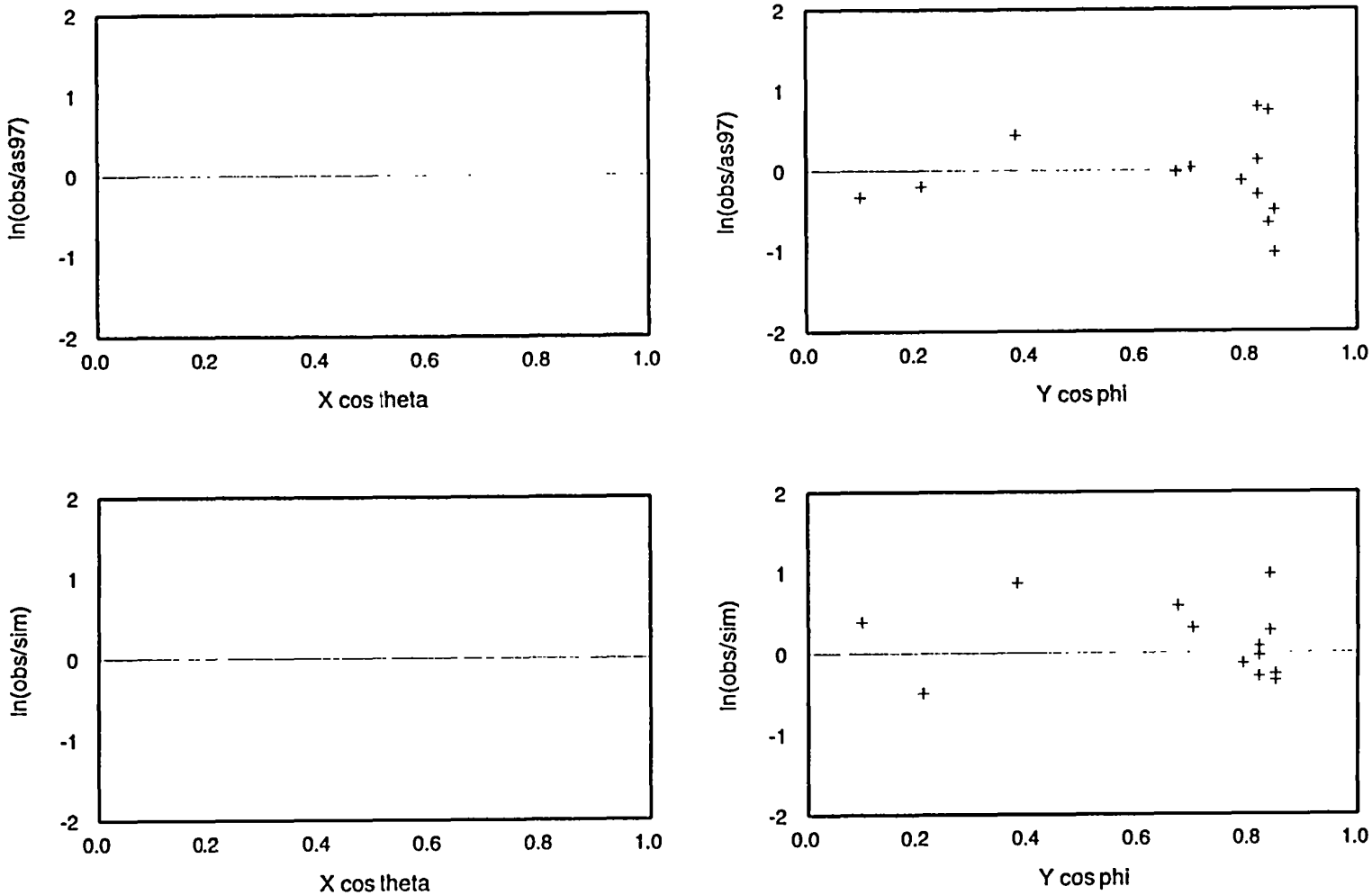

GMT Aug 24 11:16:35 1999 /u1/nancy/PEER-5/Northridge/Comparisons.990823/Resid_plots

Northridge - Fault Normal

SA at 4.0 sec

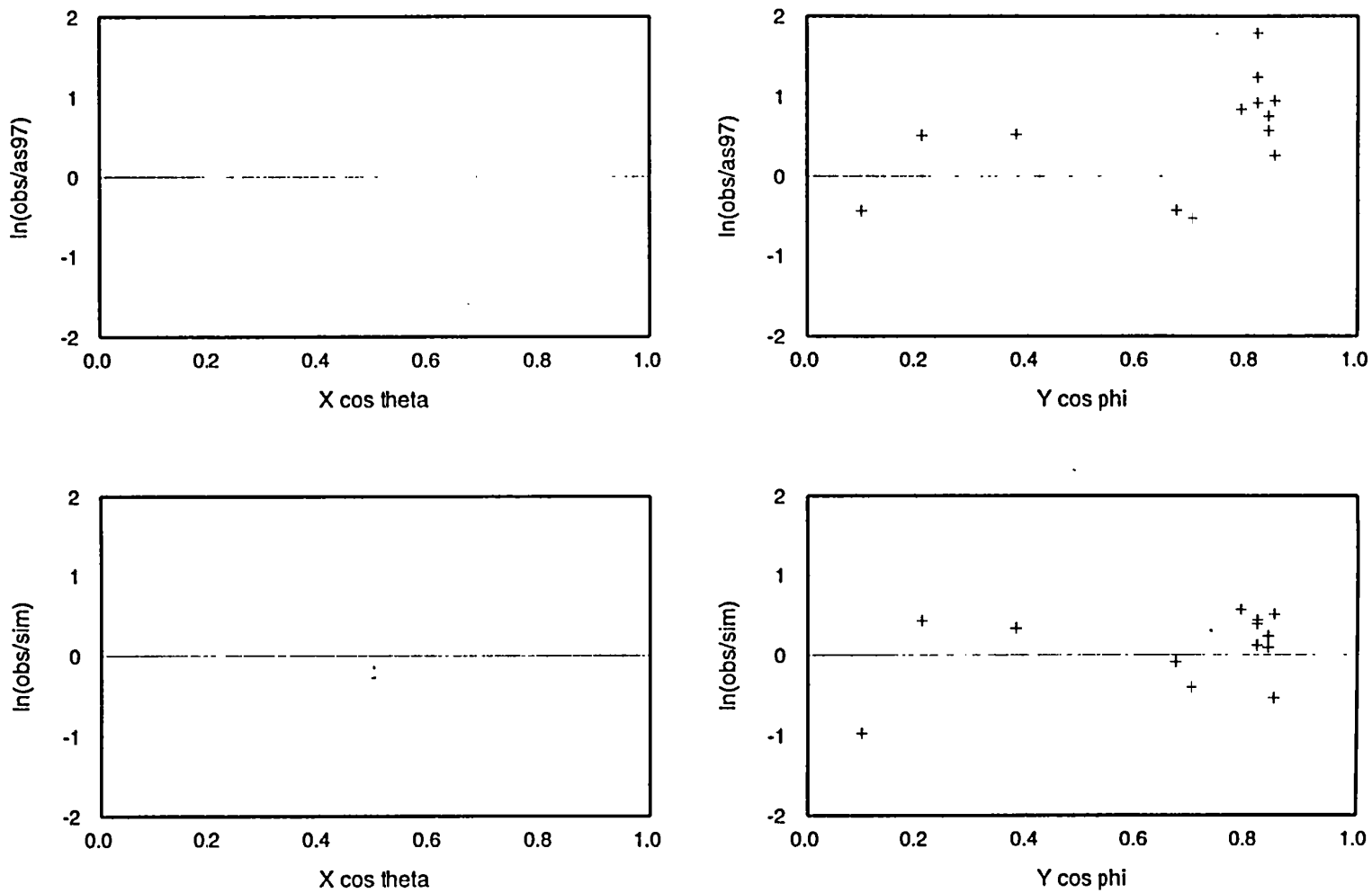

GMT Aug 24 11:16:46 1999 /u1/nancy/PEER-5/Northridge/Comparisons.990823/Resld_plots

Northridge - Fault Parallel

SA at 4.0 sec

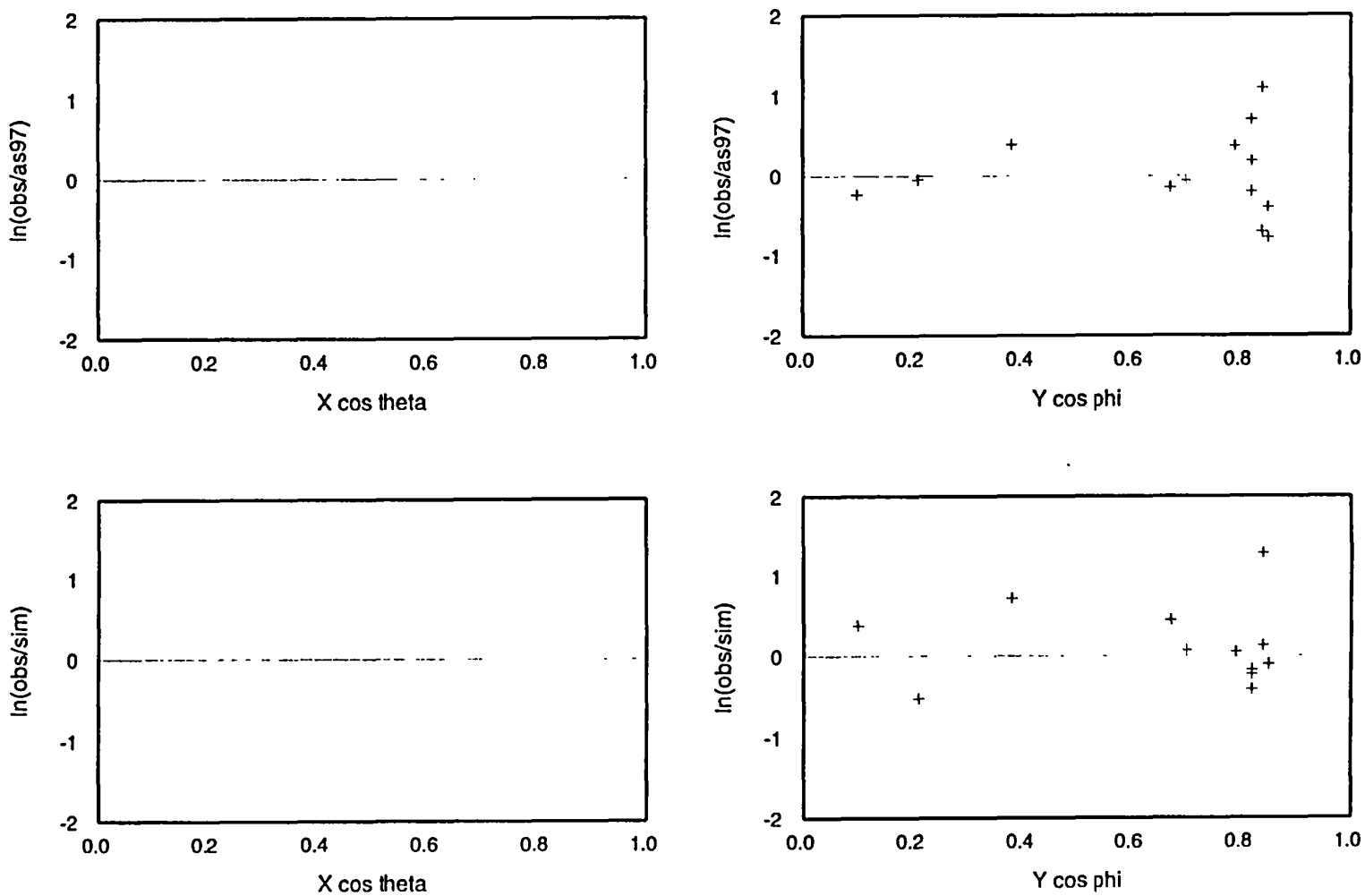

GMT Aug 24 11:18:05 1999 /u1/nancy/PEER-5/Northridge/Comparisons.990823/Resid_plots

Northridge - Fault Normal

SA at 3.0 sec

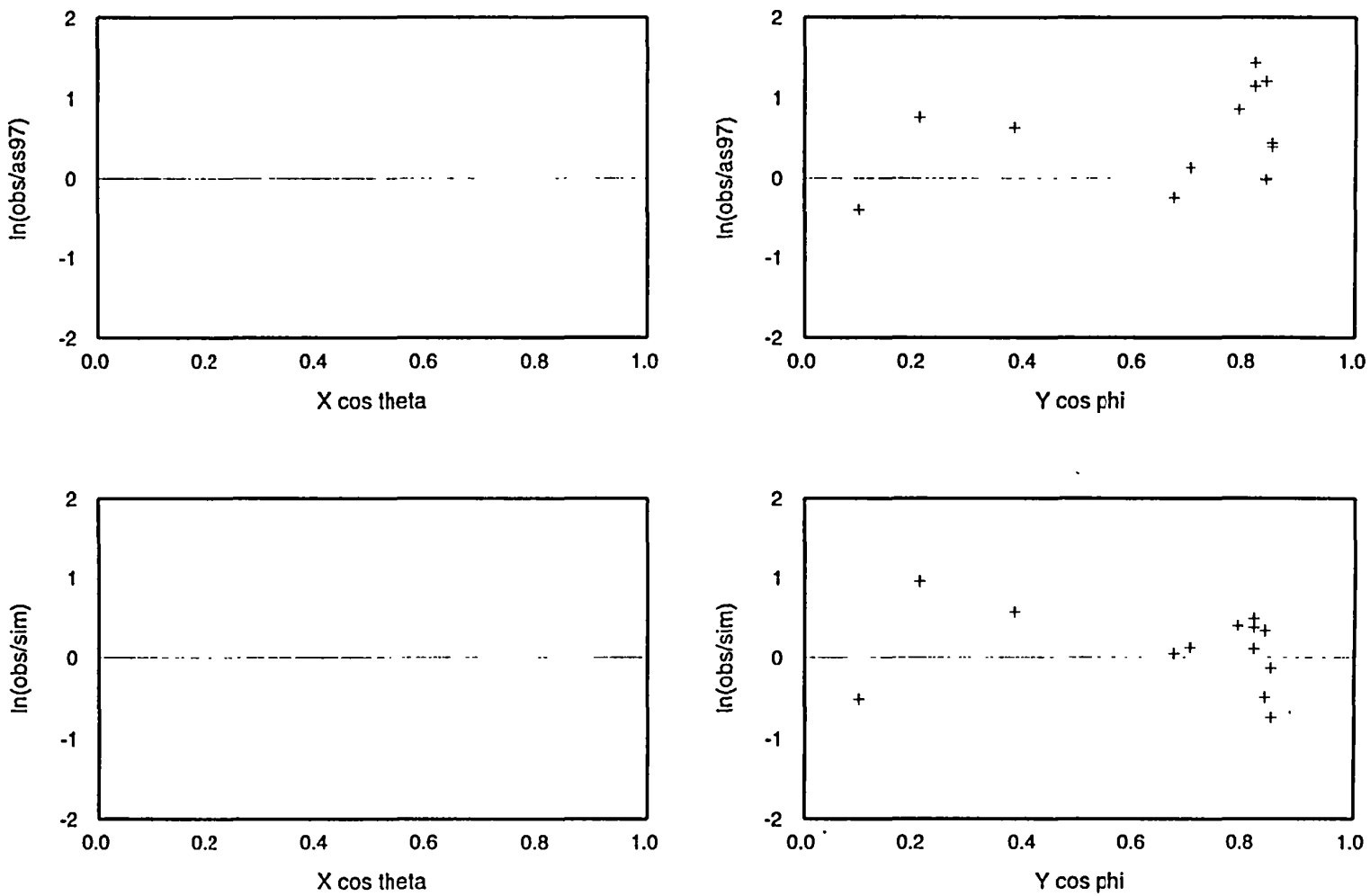

GMT Aug 24 11:18:18 1999 /u1/nancy/PEER-5/Northridge/Comparisons.990823/Resid_plots

Northridge - Fault Parallel

SA at 3.0 sec

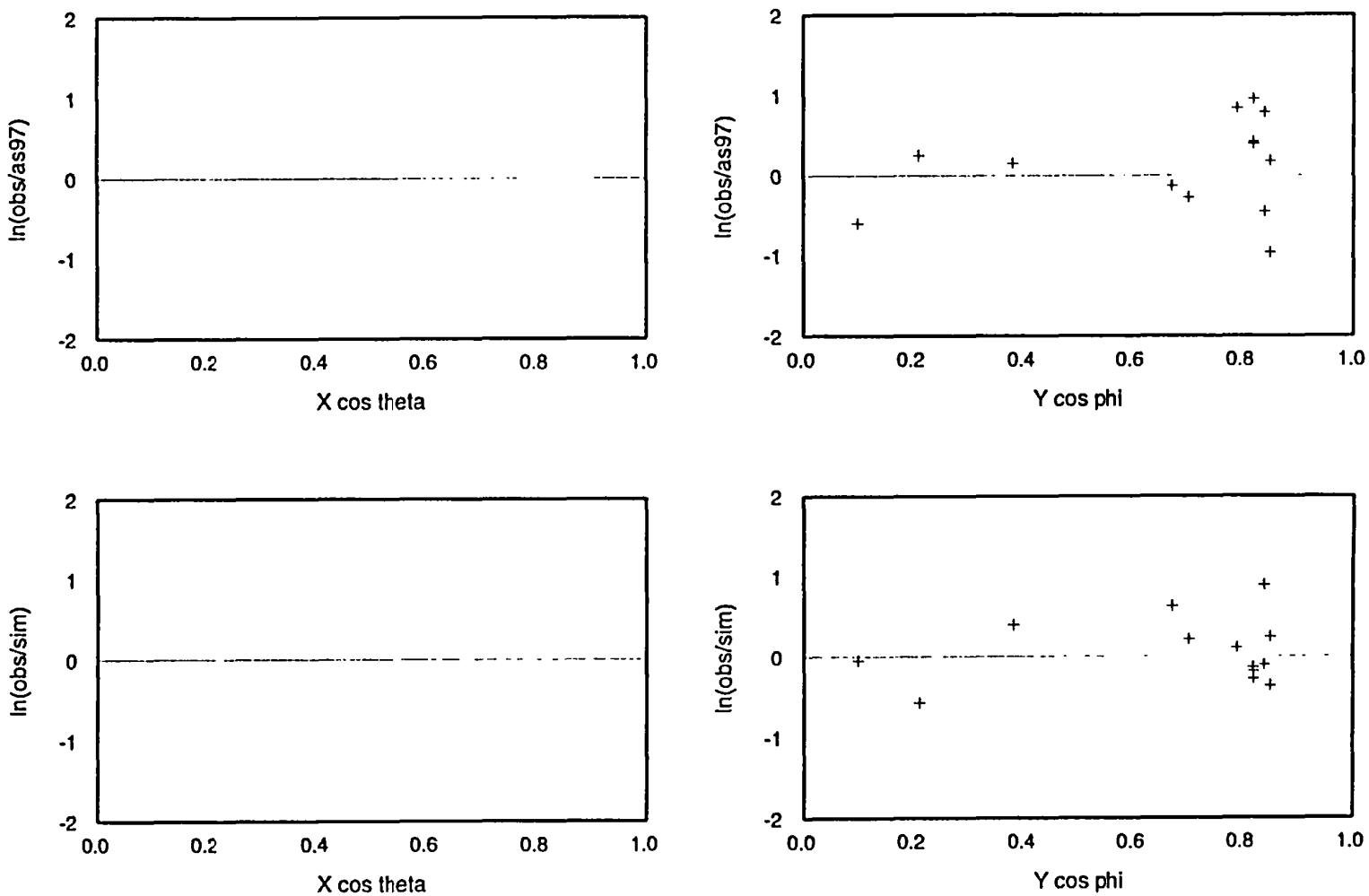

GMT Aug 24 11:19:27 1999 /u1/nancy/PEER-5/Northridge/Comparisons.990823/Resid_plots

Northridge - Fault Normal

SA at 2.0 sec

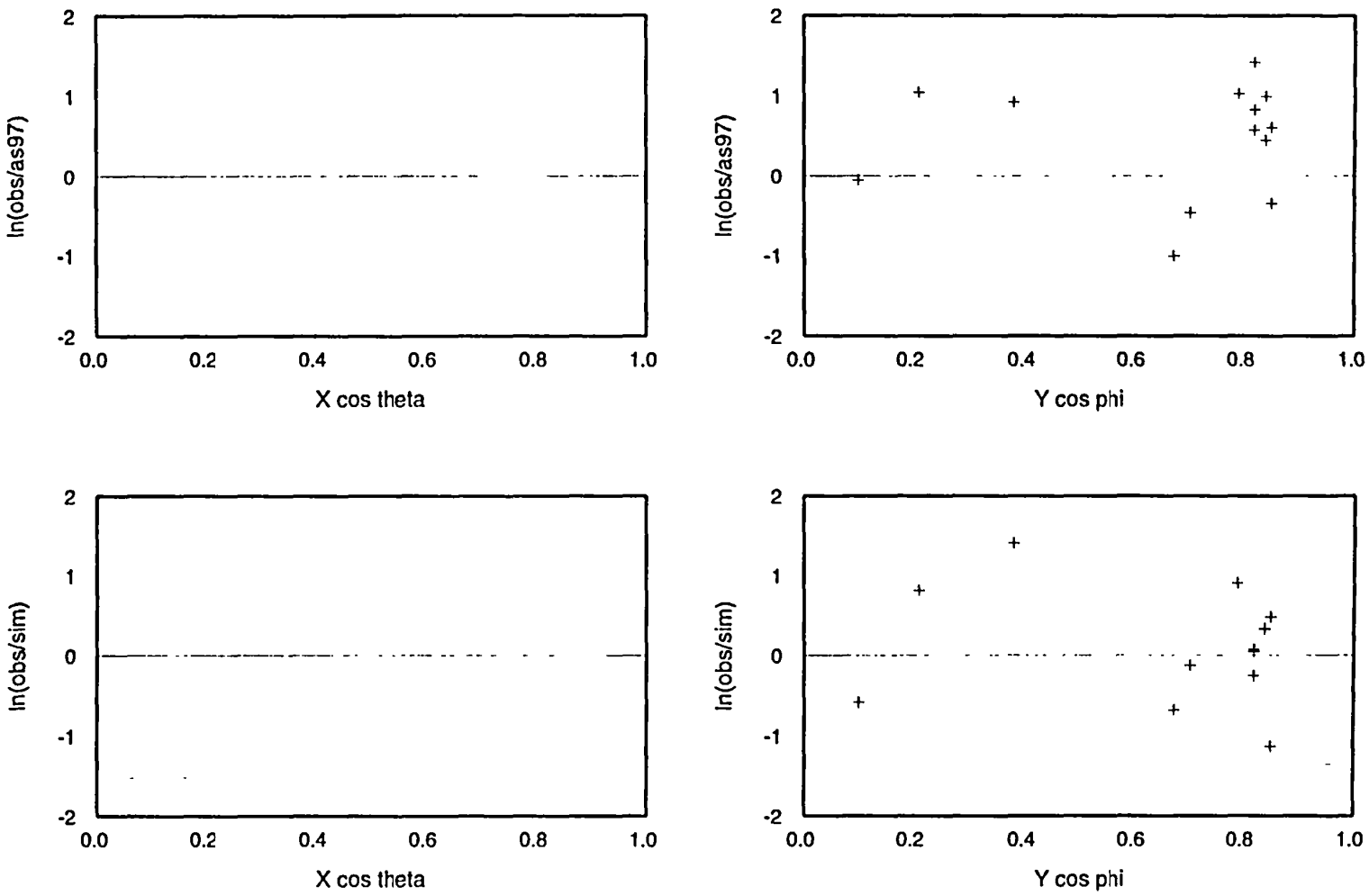

GMT Aug 24 11:19:50 1999 /u1/nancy/PEER-5/Northridge/Comparisons.990823/Resid_plots

Northridge - Fault Normal

SA at 1.5 sec

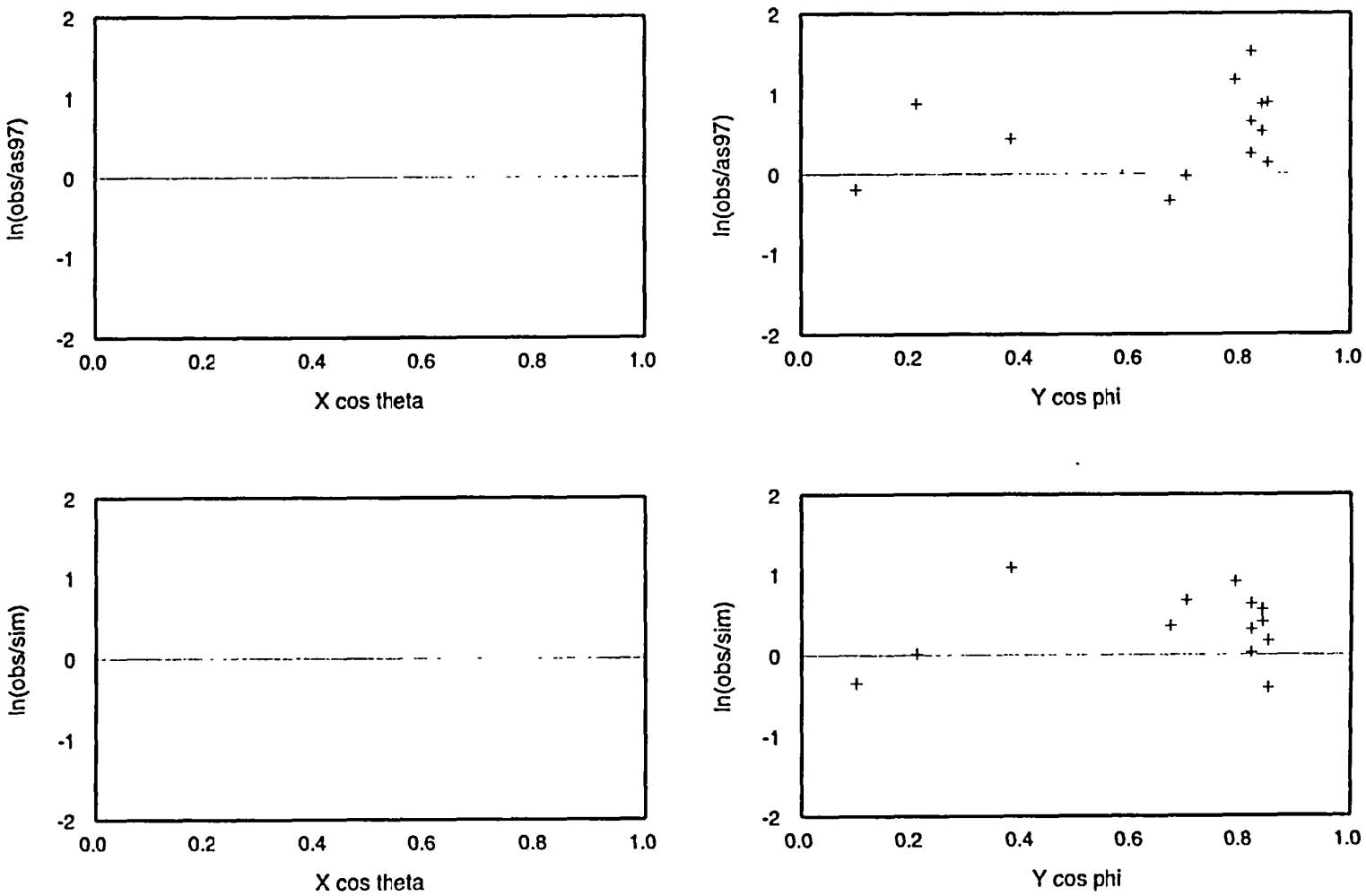

GMT Aug 24 11:21:53 1999 /u1/nancy/PEER-5/Northridge/Comparisons.990823/Resid_plots

Northridge - Fault Parallel

SA at 1.5 sec

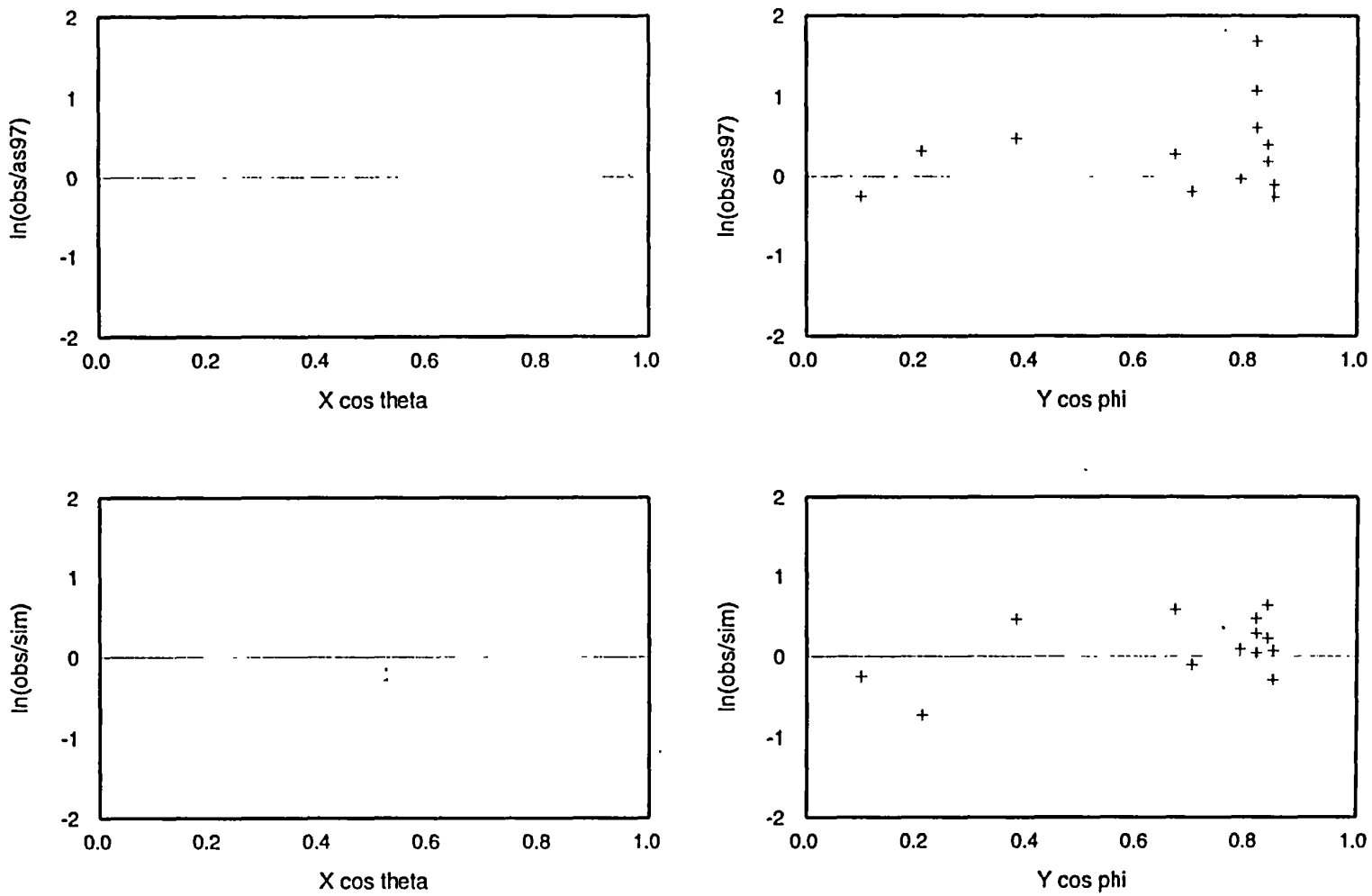

GMT Aug 24 11:22:02 1999 /u1/nancy/PEER-5/Northridge/Comparisons.990823/Resid_plots

Northridge - Fault Normal

SA at 1.0 sec

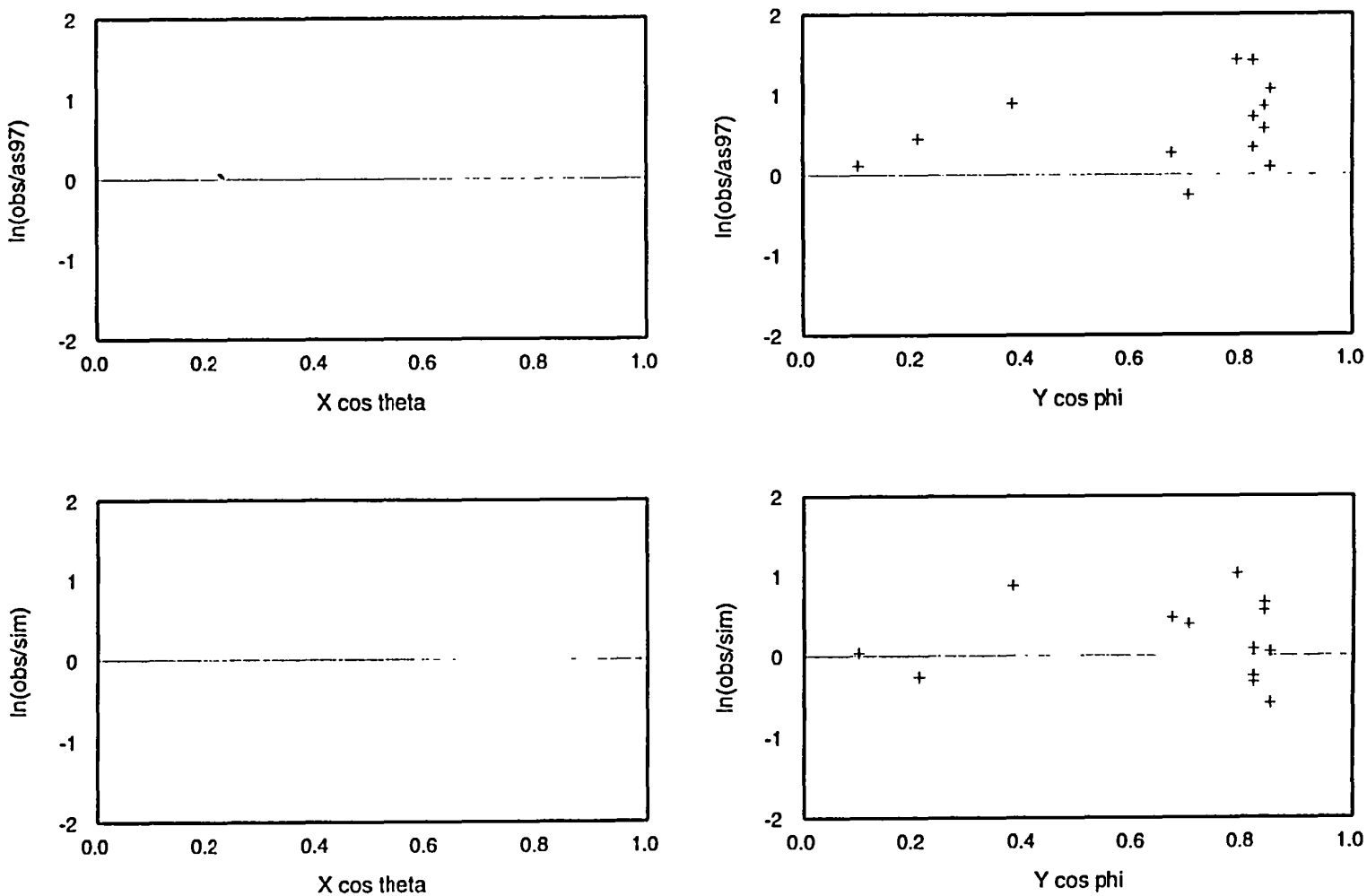

GMT Aug 24 11:22:12 1999 /u1/nancy/PEER-5/Northridge/Comparisons.990823/Resid_plots

Northridge - Fault Parallel

SA at 1.0 sec

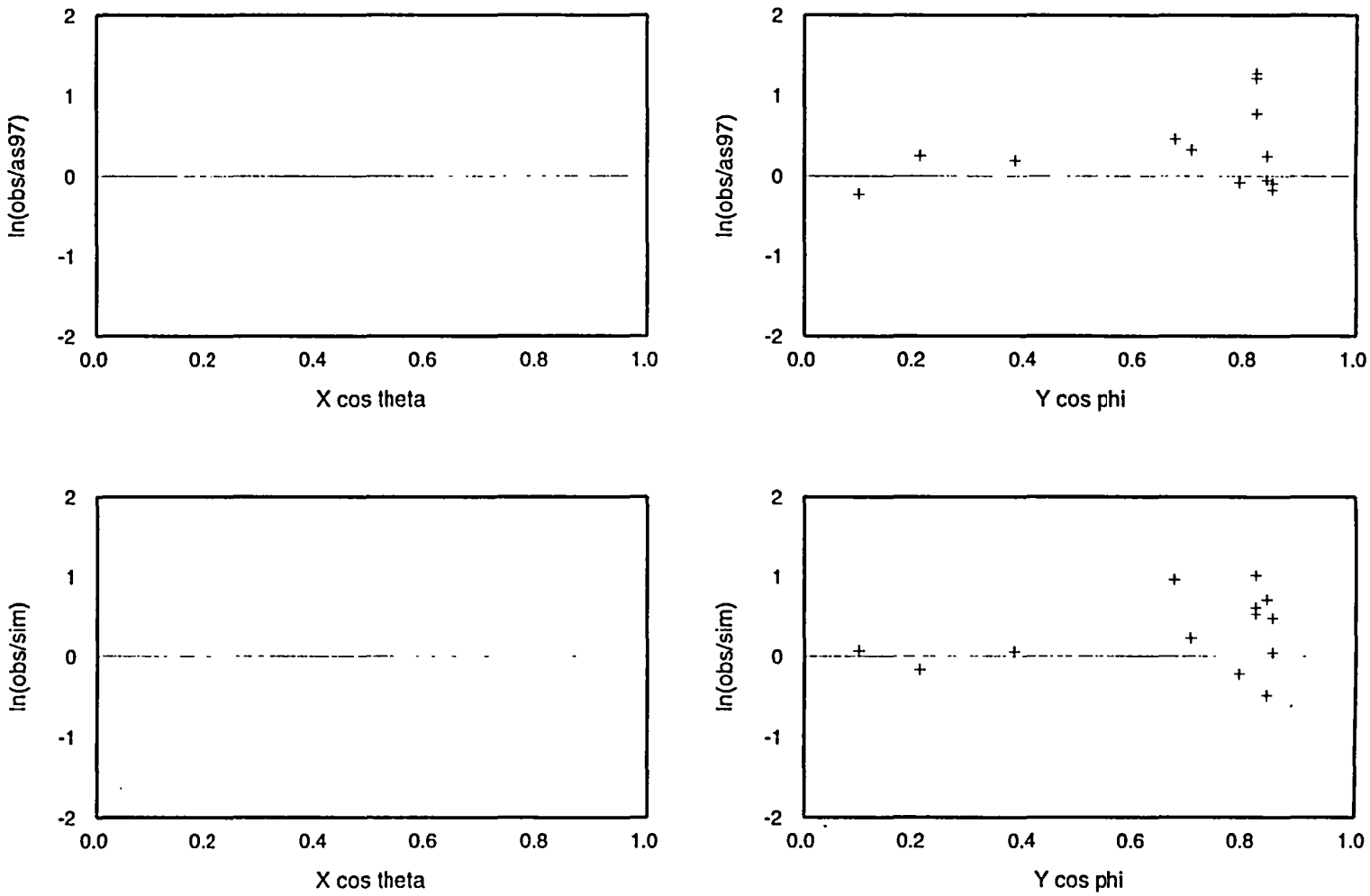

GMT Aug 24 11:22:24 1999 /u1/nancy/PEER-5/Northridge/Comparisons.990823/Resid_plots

/u1/nancy/PEER-5/Kobe/Comparisons/Tabulate
tableout

Station	Correlation FN	Correlation FP	Least Squares FN	Least Squares FP	Response Spectra FN	Response Spectra FP	Fourier Spectra FN	Fourier Spectra FP
abn	0.617		-1.297		0.069	0.473	-0.139	0.398
ama	0.403		0.084		0.568	0.213	0.535	0.346
fka2	0.688		0.107		-0.072	-0.476	-0.336	-0.561
fks	0.387		0.078		0.692	0.835	0.422	0.681
kbu2	0.836		0.383		-0.177	-0.402	-0.020	-0.592
kob2	0.565		-0.011		-0.234	-0.541	-0.456	-0.766
mot2	0.828		0.340		-0.229	-0.174	-0.042	-0.106
mrg	0.455		0.103		0.413	0.447	0.212	-0.040
osa	0.483		0.078		0.229	0.401	-0.302	-0.160
ski	0.675		0.153		0.171	0.529	0.231	0.345
tkt2	0.300		0.017		0.391	0.372	0.097	0.152
Average	0.567		0.003		0.166	0.152	0.018	-0.028
Sigma	0.179		0.448		0.582	0.786	1.028	1.199
Sigma Mean	0.054		0.135		0.176	0.237	0.310	0.362

Kobe - Fault Normal

Simulations and Data Band Pass Filtered 0.125-1.43 Hz

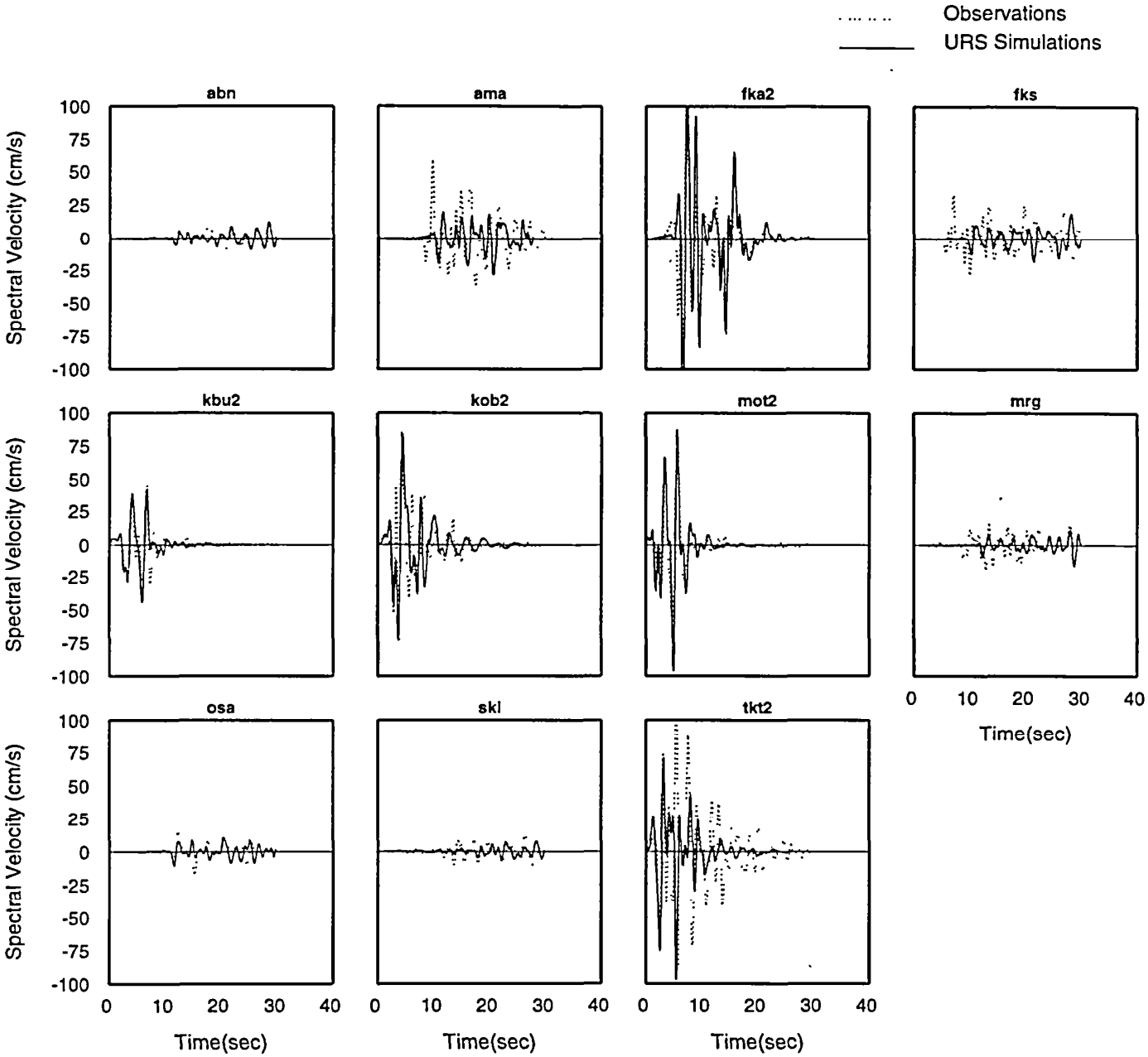

Kobe - Fault Parallel

Simulations and Data Band Pass Filtered 0.125-1.43 Hz

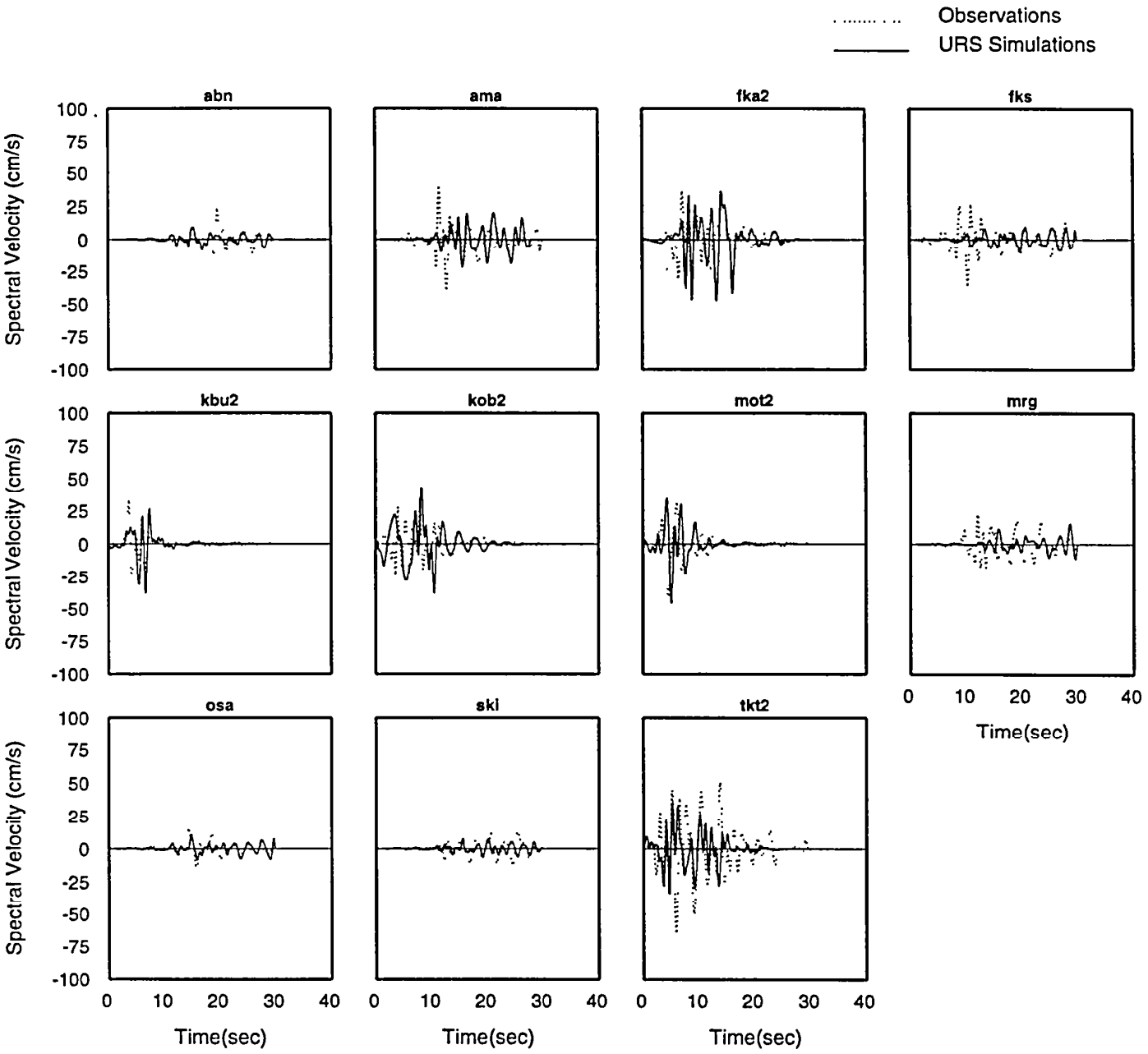

GMT Aug 31 12.26:06 1999 /u1/nancy/PEER-5/Kobe/Comparisons/Extra_plots

Kobe - Fault Normal

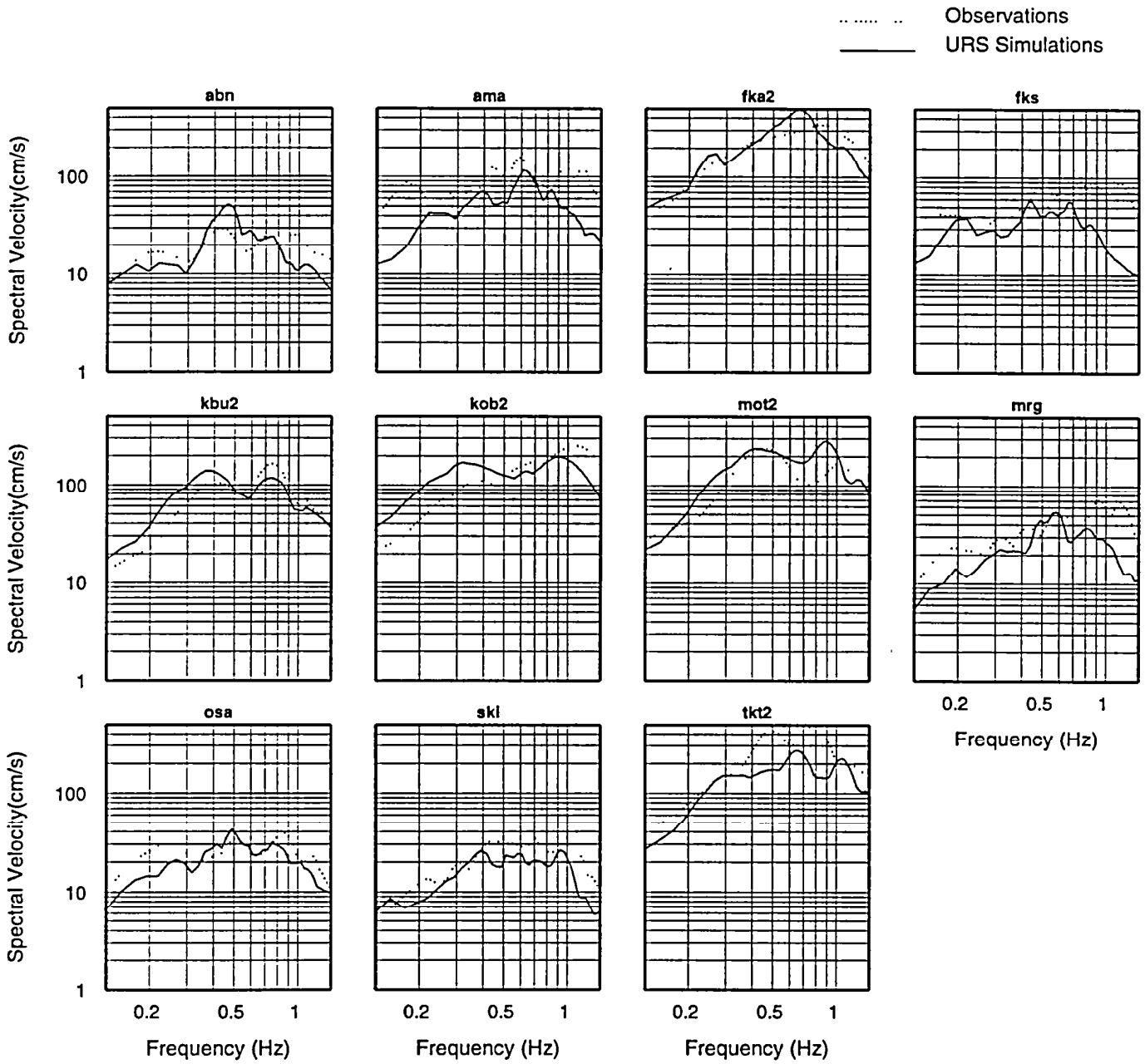

Kobe - Fault Parallel

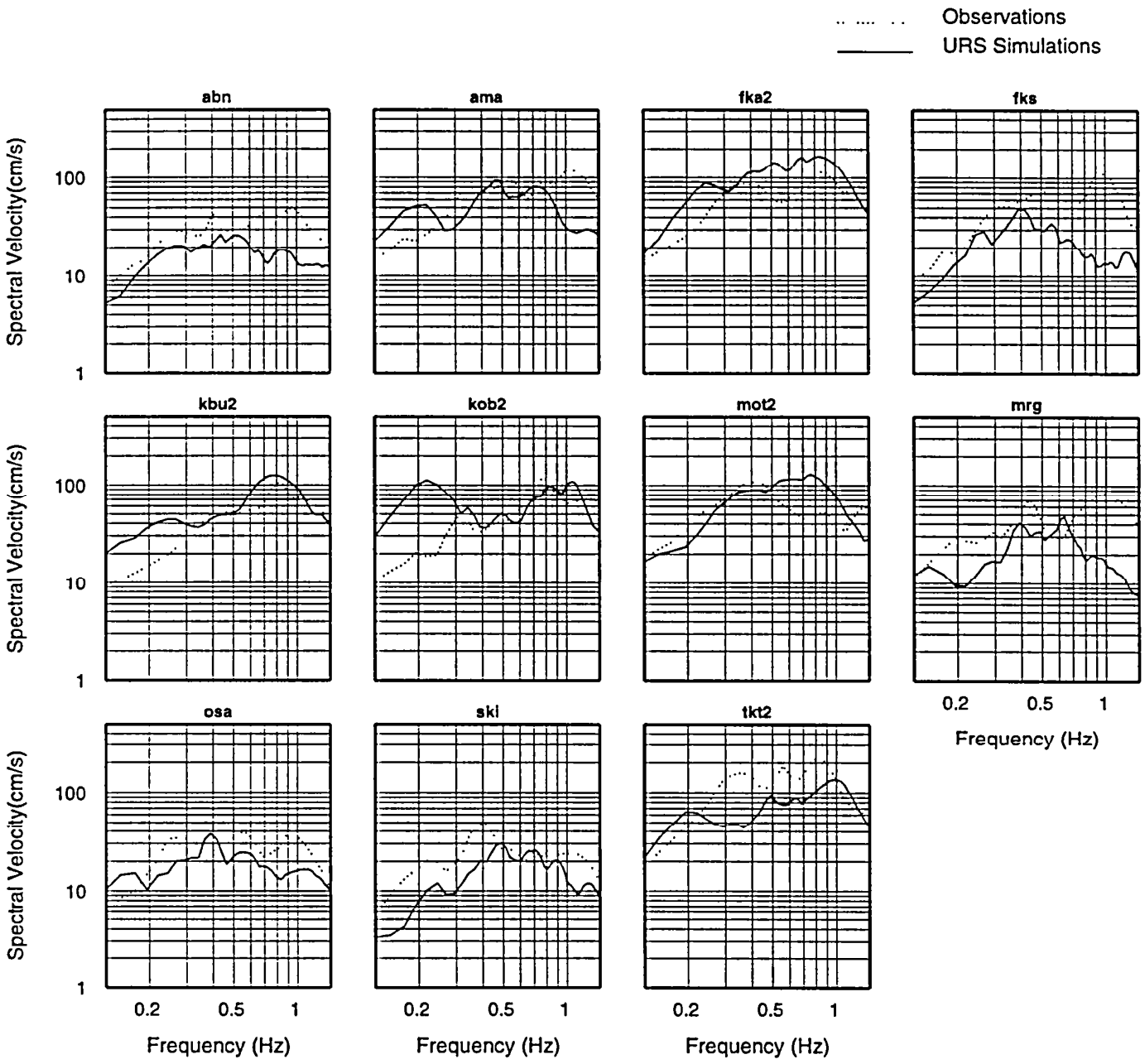

Kobe - Fault Normal

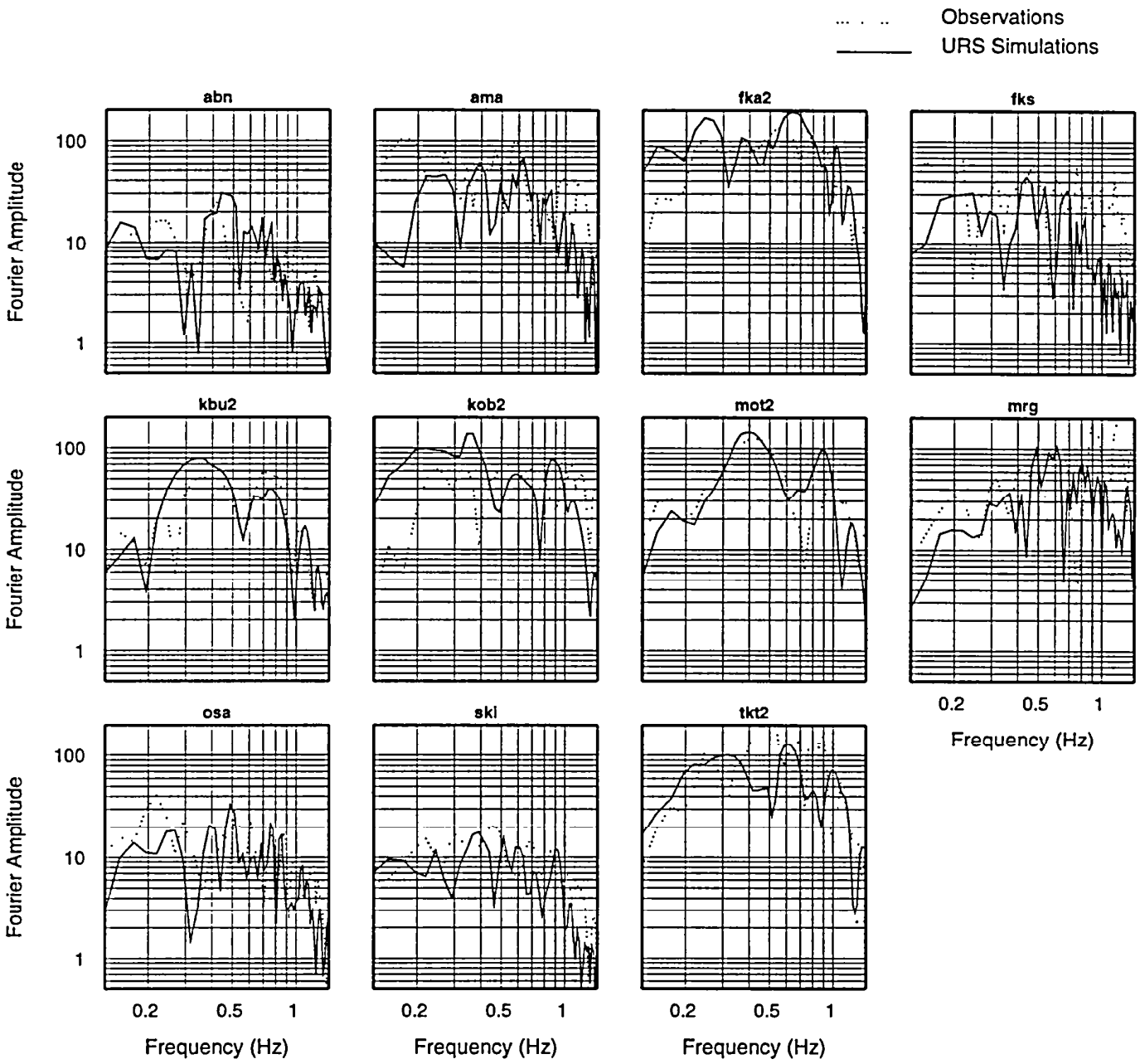

Kobe - Fault Parallel

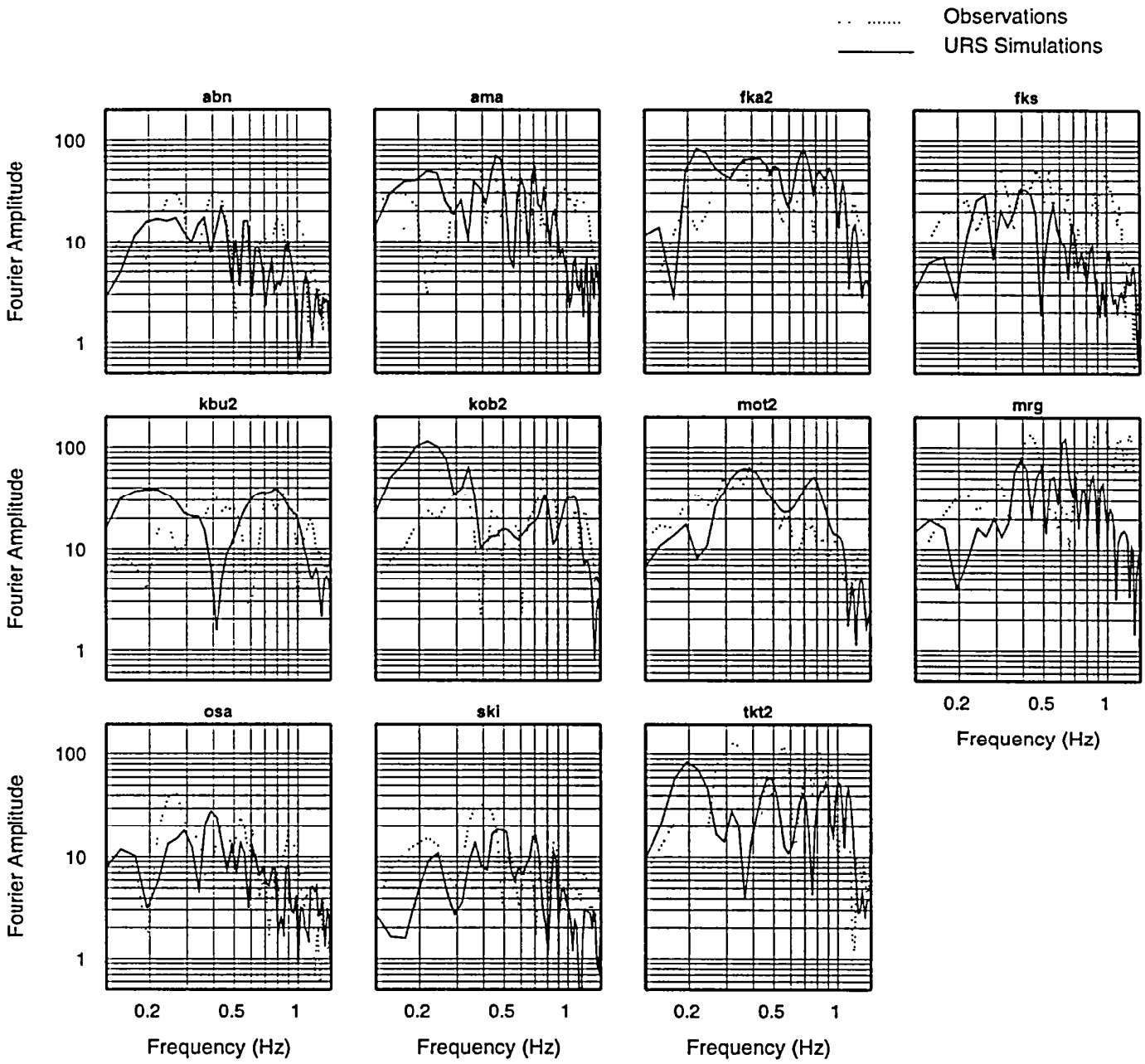

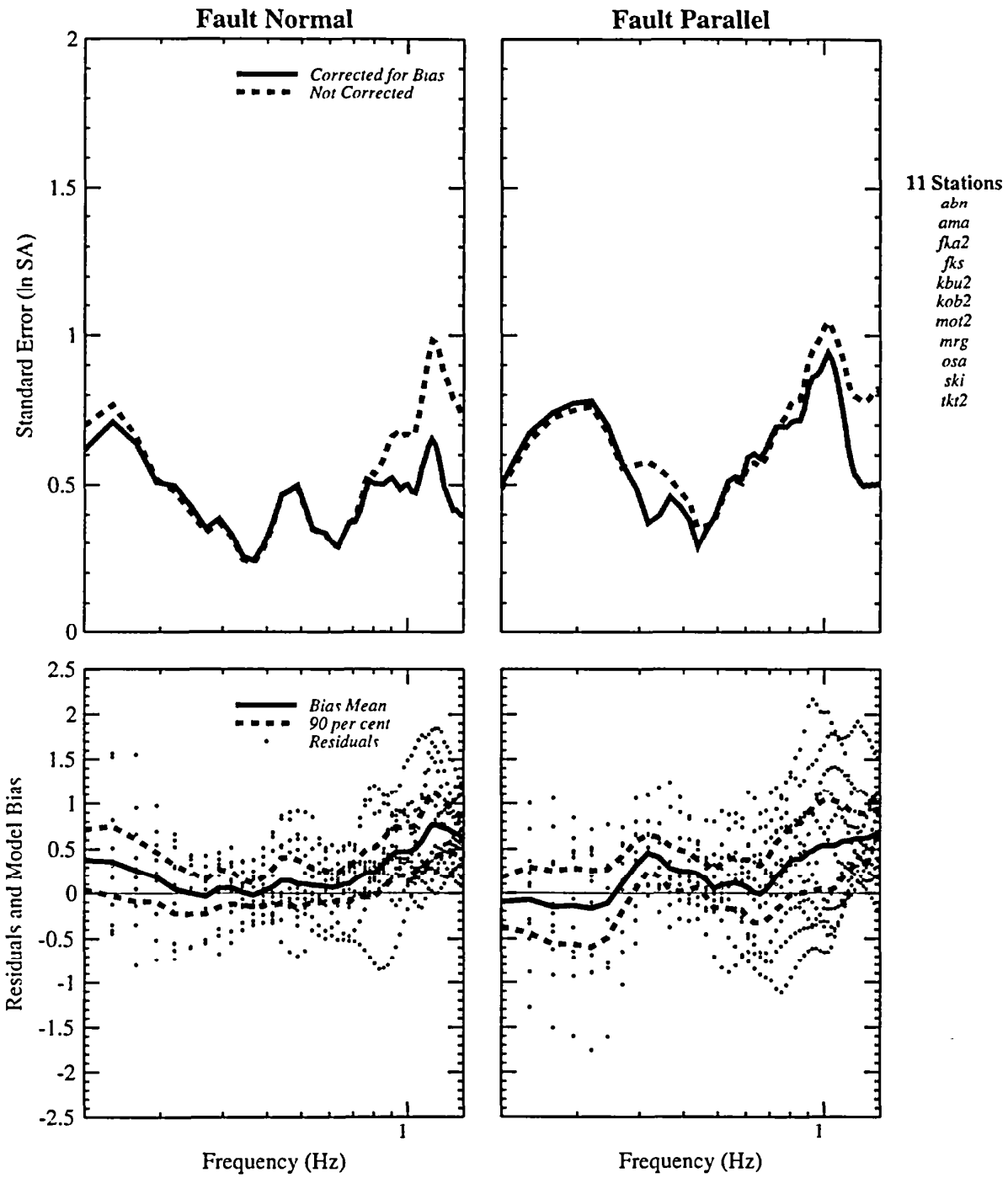

Kobe Spectral Acceleration Goodness of Fit
Observed minus Synthetic (obs - sim)

Kobe - Filter 0.125-1.43 Hz, HYBRID BB Sims - fka

Fault Normal

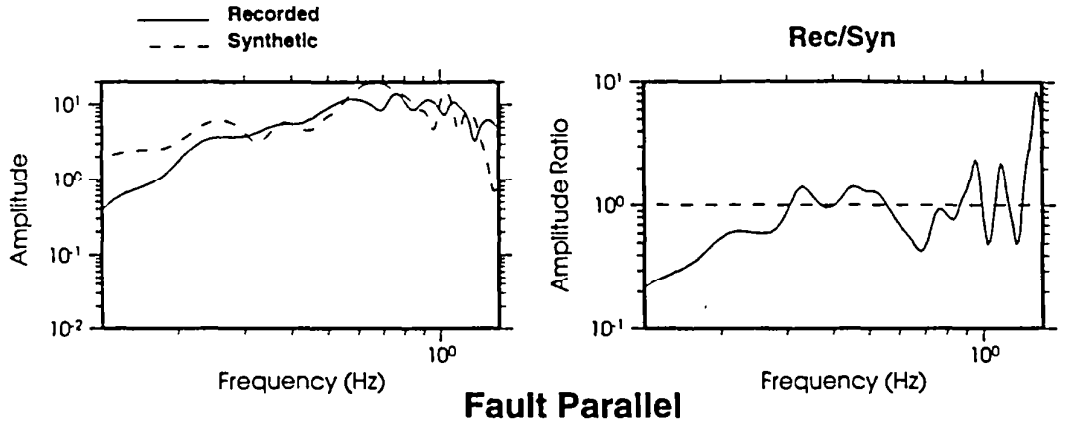

Fault Parallel

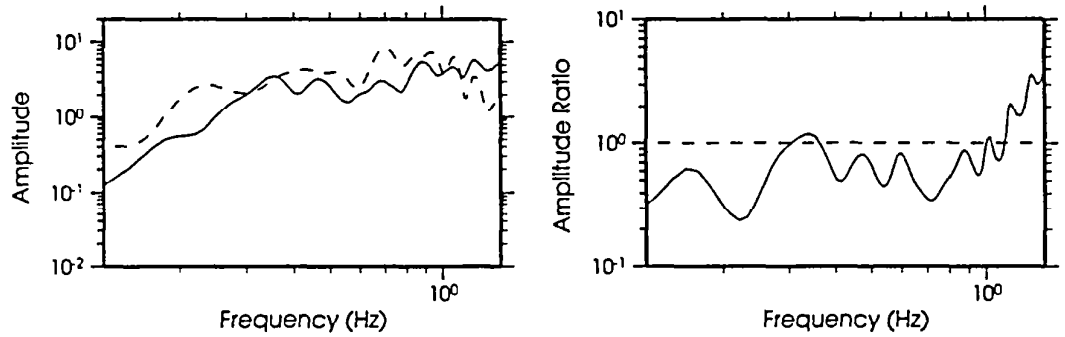

Fault Normal

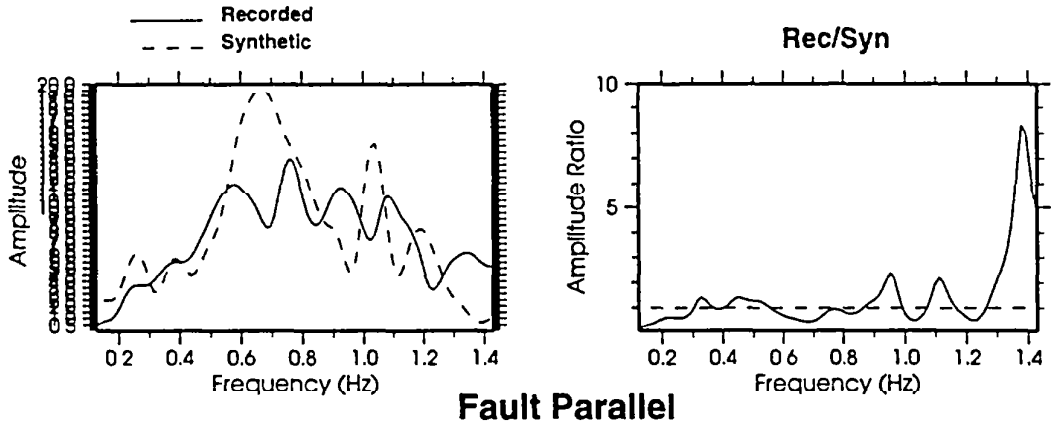

Fault Parallel

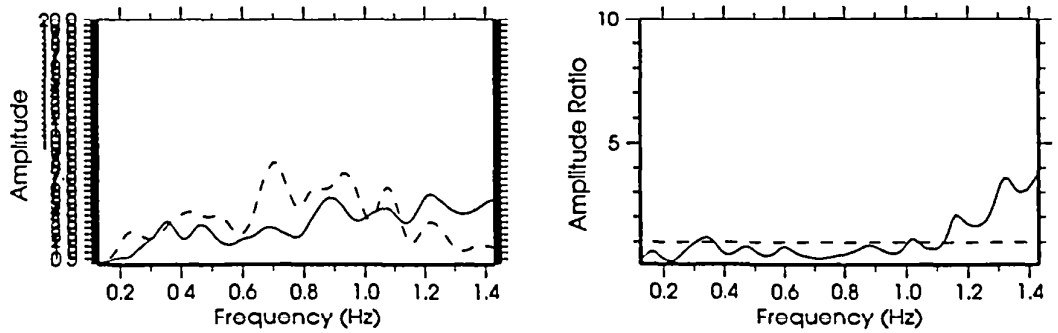

GMT Aug 24 16:23 57 1999 /net/coda/u2/arben/Kobe/shells

Kobe - Filter 0.125-1.43 Hz, HYBRID BB Sims - kbu

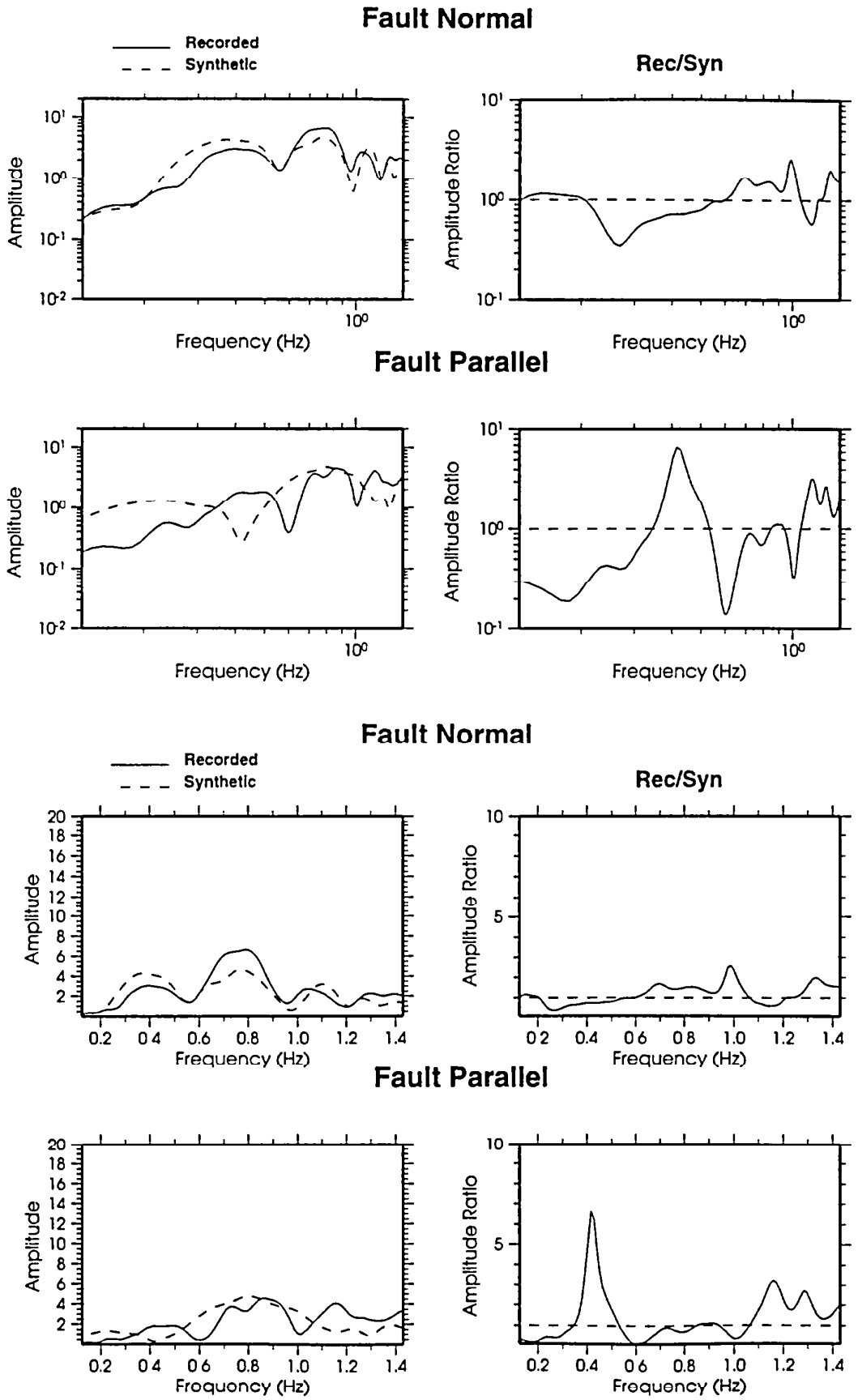

GMT Aug 24 16.24:23 1999 /net/coda/u2/arben/Kobe/shells

Kobe - Filter 0.125-1.43 Hz, HYBRID BB Sims - kob

Fault Normal

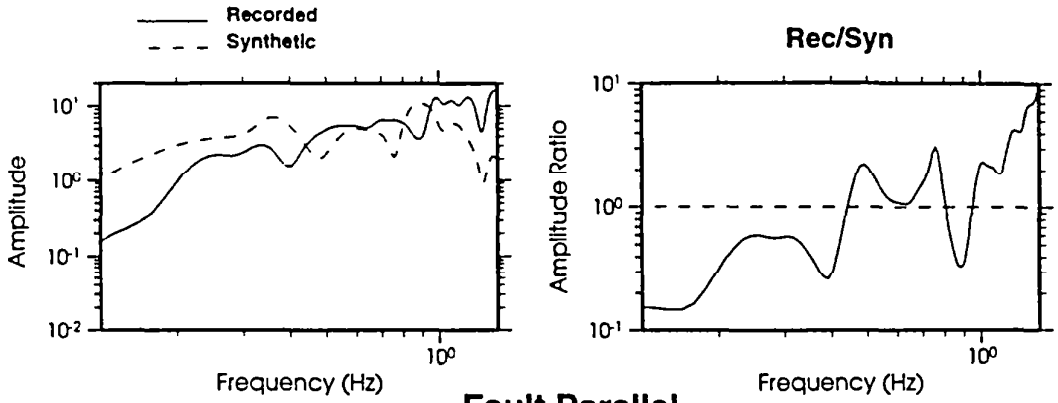

Fault Parallel

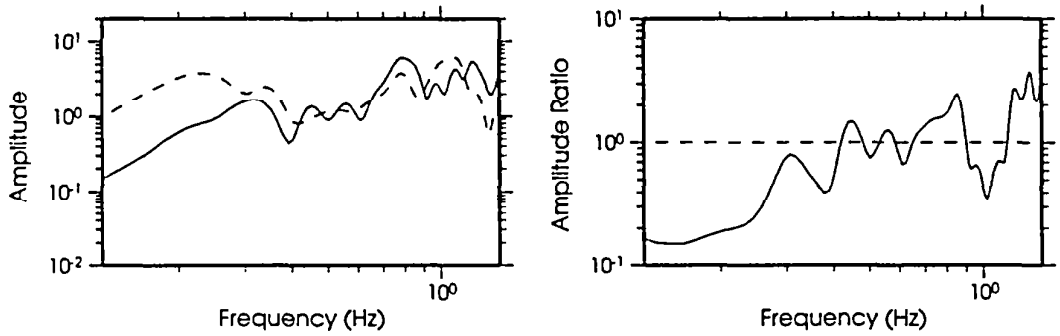

Fault Normal

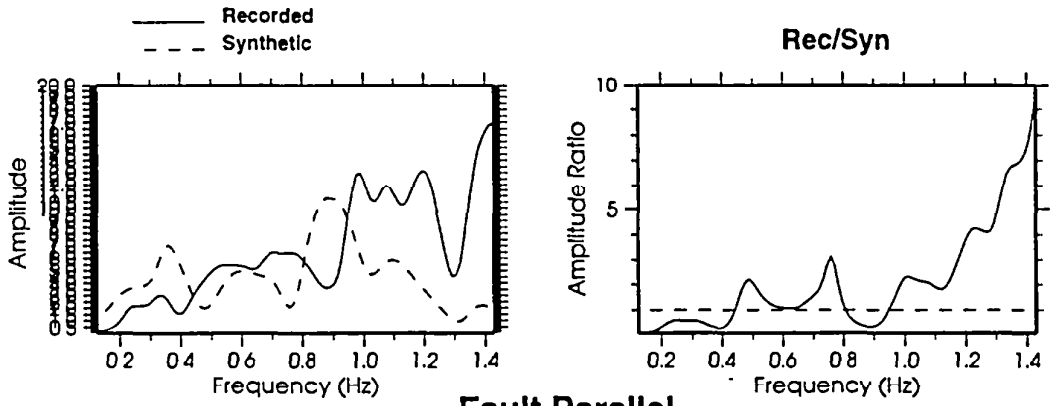

Fault Parallel

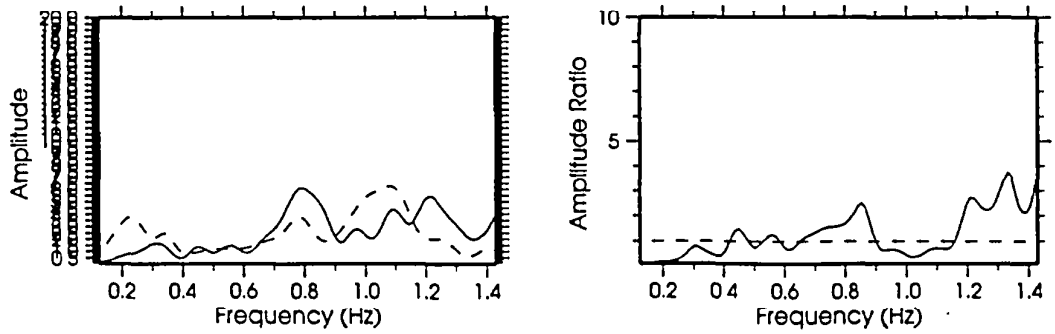

Kobe - Filter 0.125-1.43 Hz, HYBRID BB Sims - mot

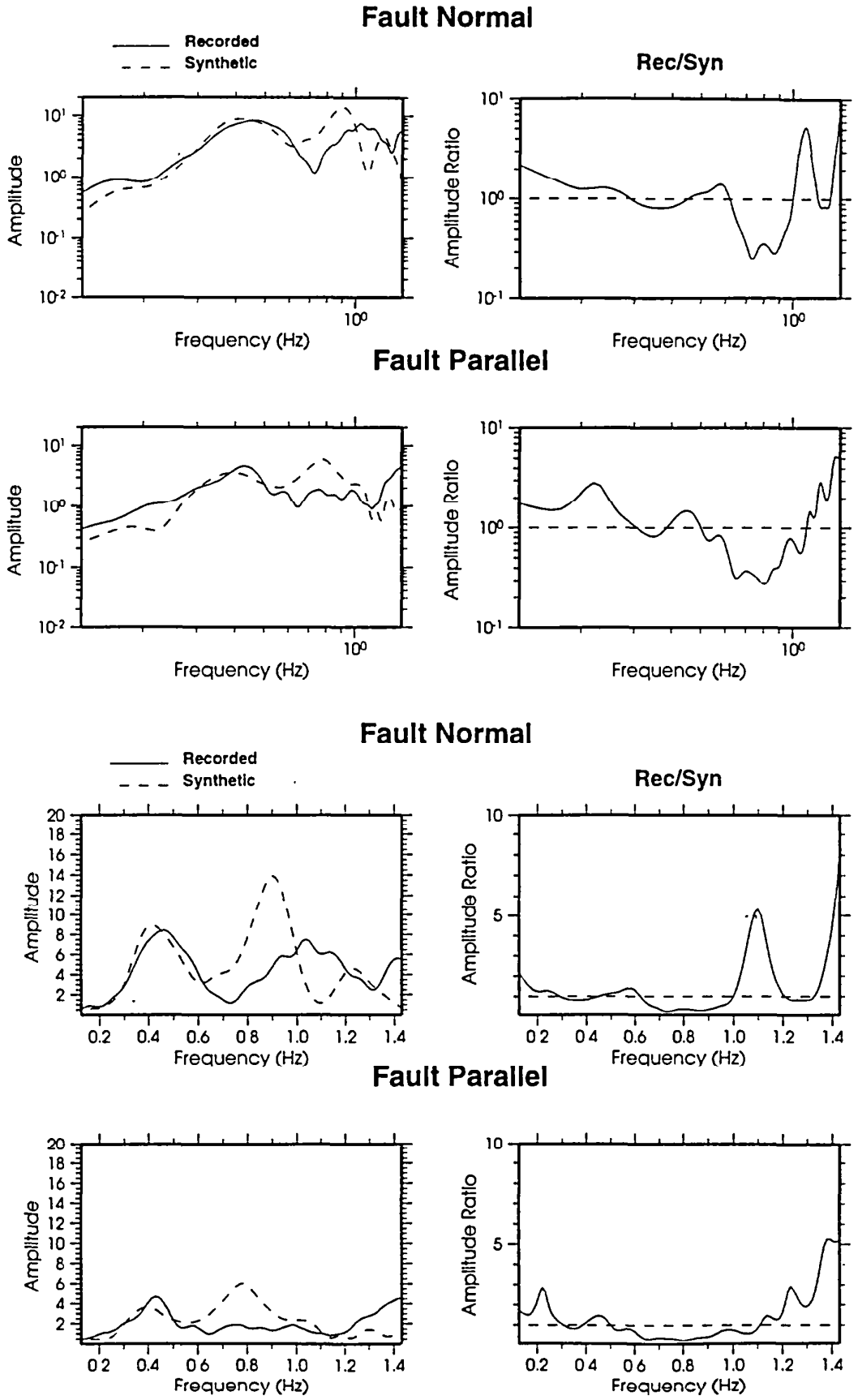

GMT Aug 24 16 25:14 1999 /net/coda/u2/arben/Kobe/shells

Kobe - Filter 0.125-1.43 Hz, HYBRID BB Sims - tkt

Fault Normal

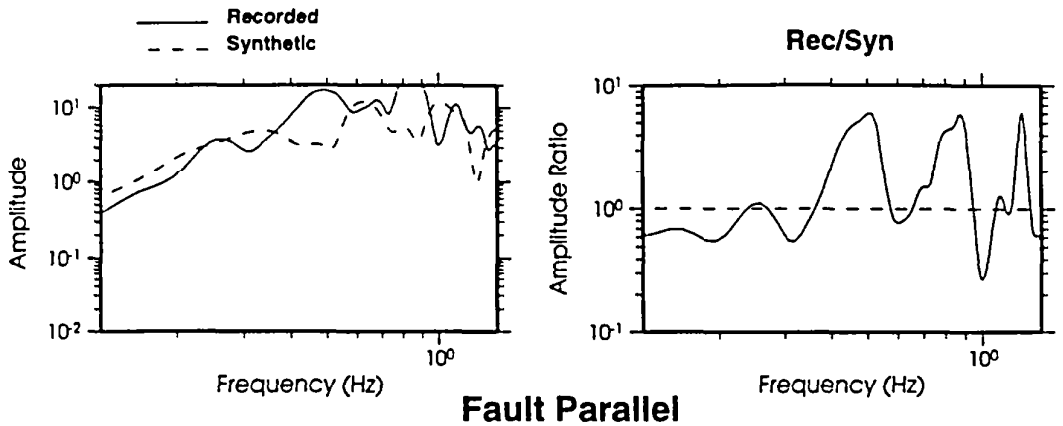

Fault Parallel

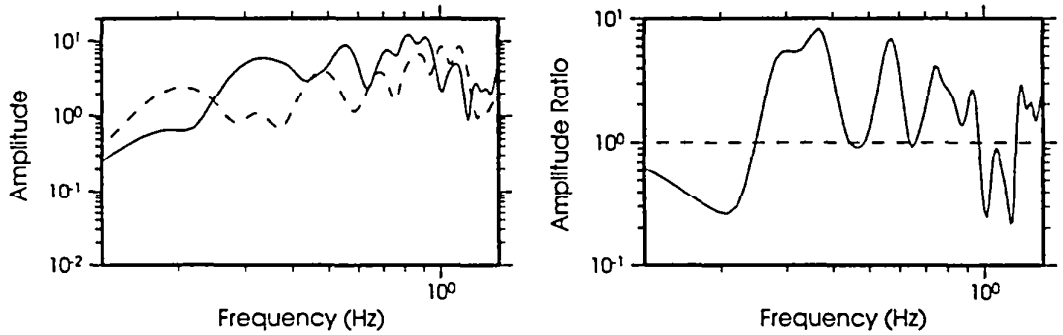

Fault Normal

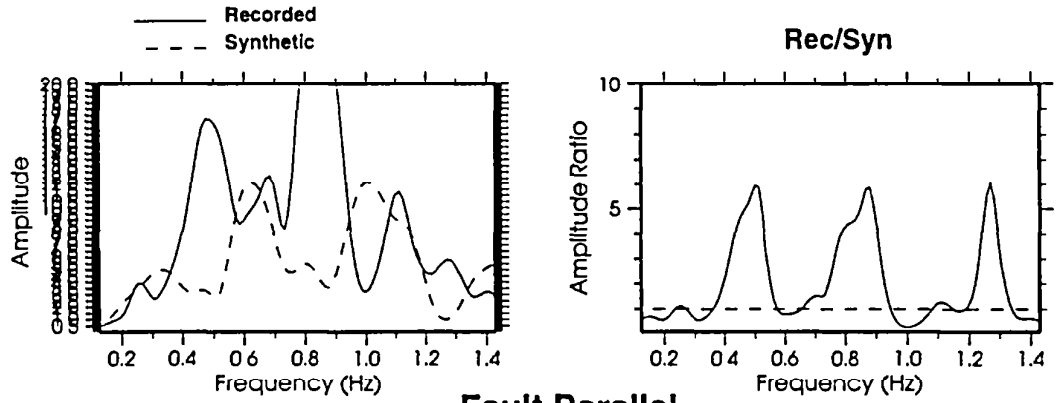

Fault Parallel

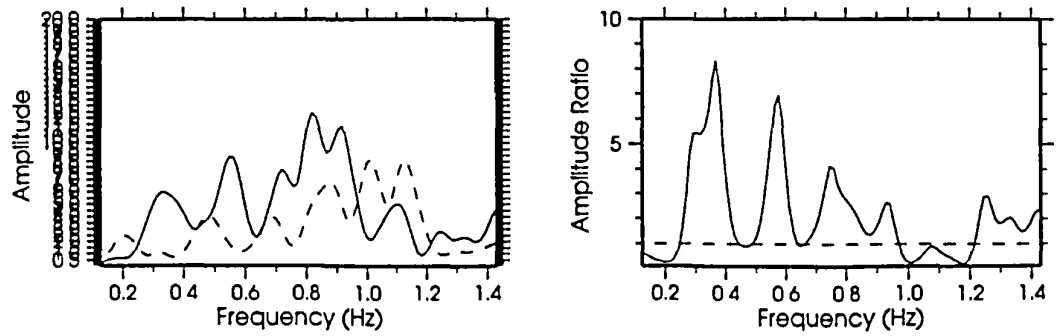

GMT Aug 24 16:25:40 1999 /net/coda/u2/arben/Kobe/shells

Kobe - Filter 0.125-1.43 Hz, Norma BB Sims - ski

Fault Normal

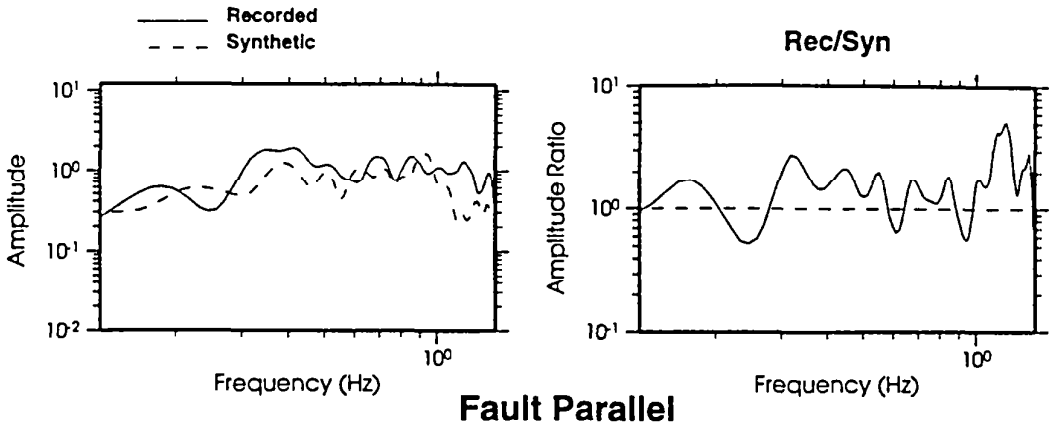

Fault Parallel

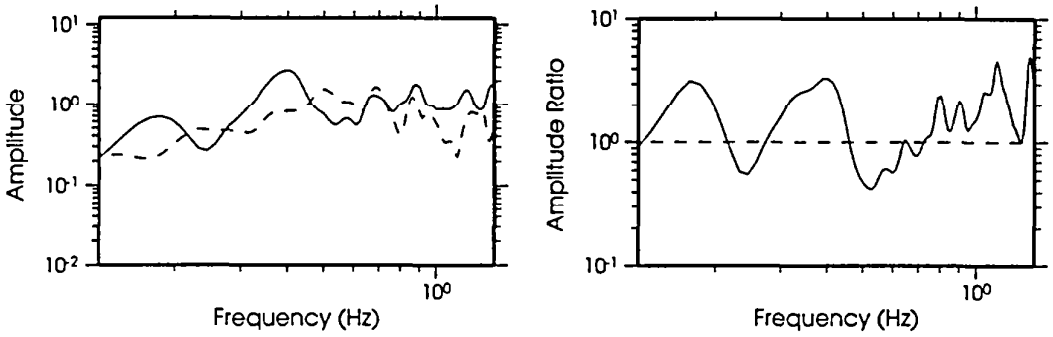

Fault Normal

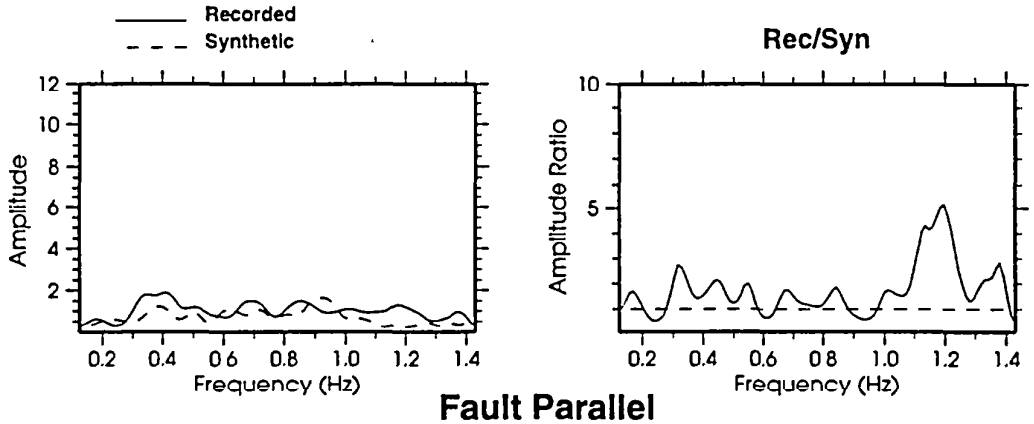

Fault Parallel

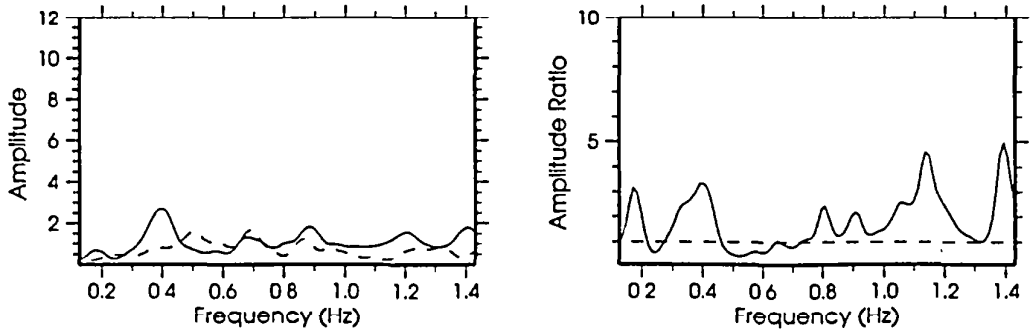

Kobe - Filter 0.125-1.43 Hz, Norma BB Sims - osa

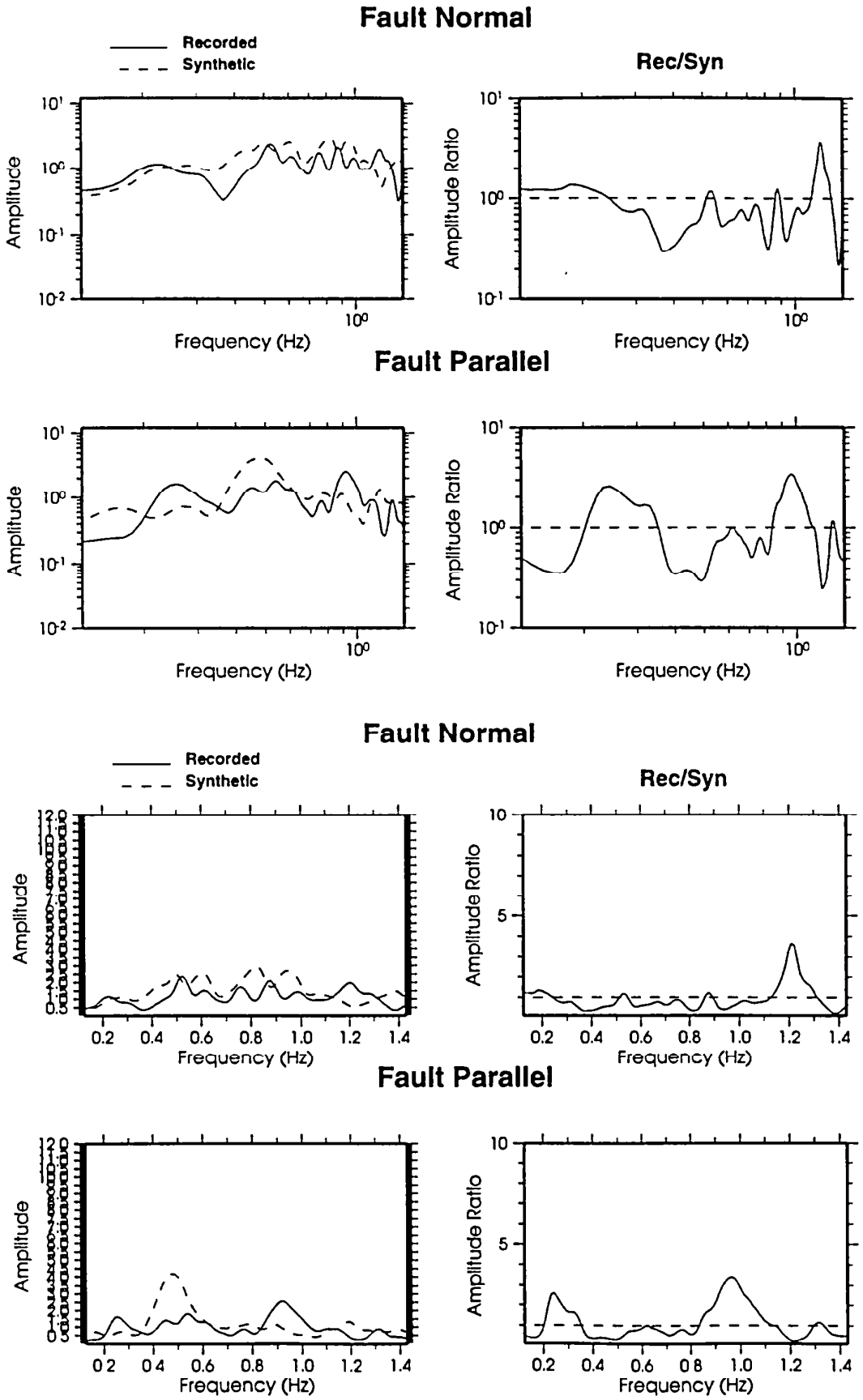

GMT Aug 24 18:14:19 1999 /net/coda/u2/arben/Kobe/shells

Kobe - Filter 0.125-1.43 Hz, Norma BB Sims - mrg

Fault Normal

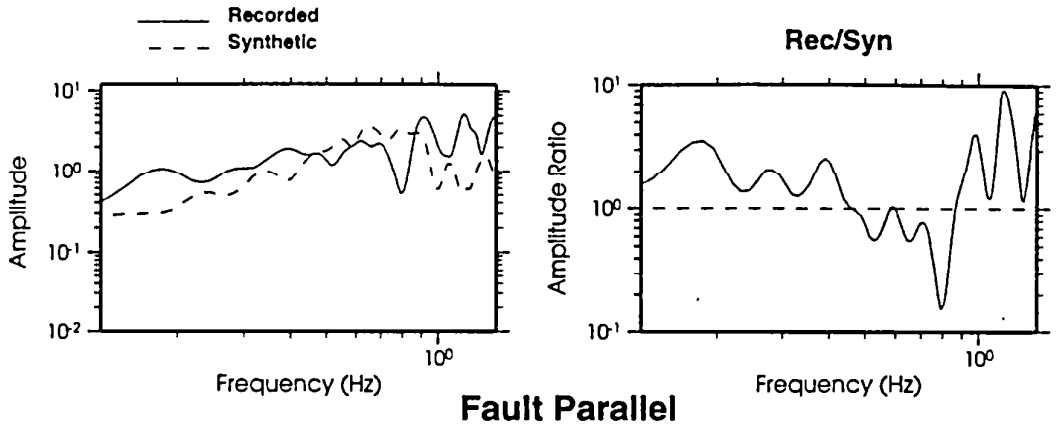

Fault Parallel

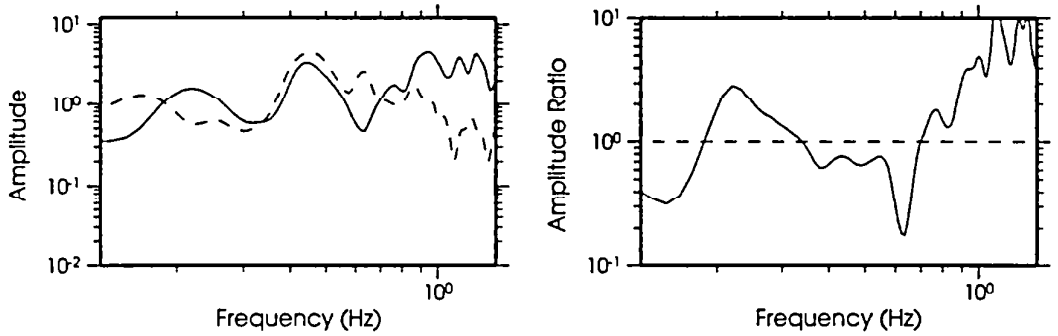

Fault Normal

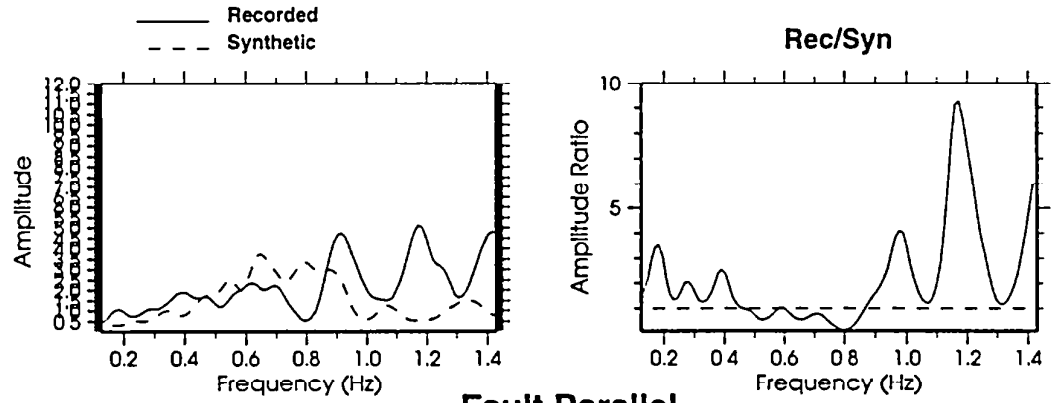

Fault Parallel

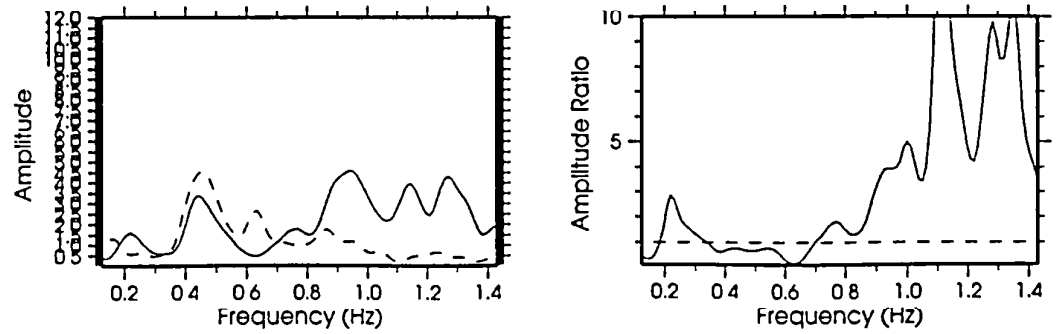

Kobe - Filter 0.125-1.43 Hz, Norma BB Sims - fks

Fault Normal

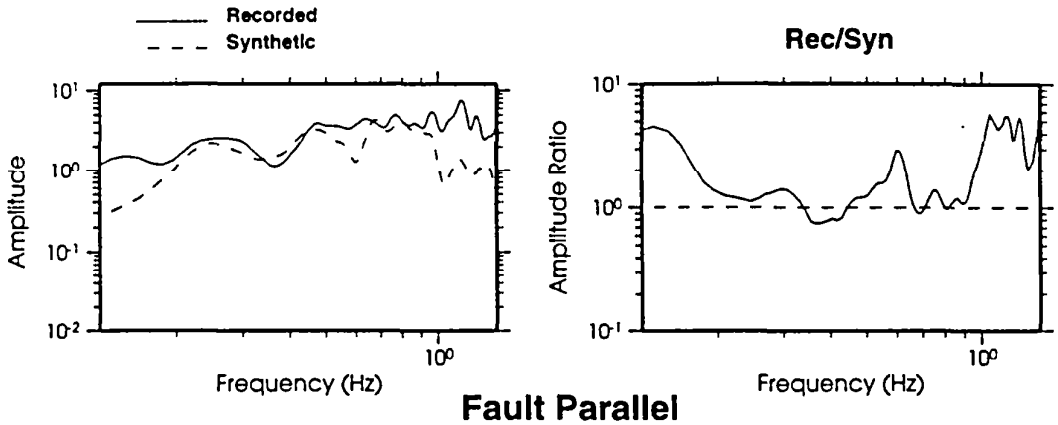

Fault Parallel

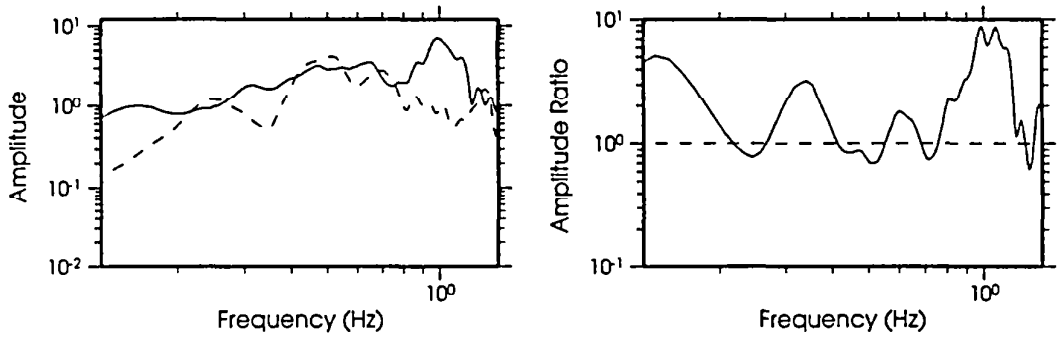

Fault Normal

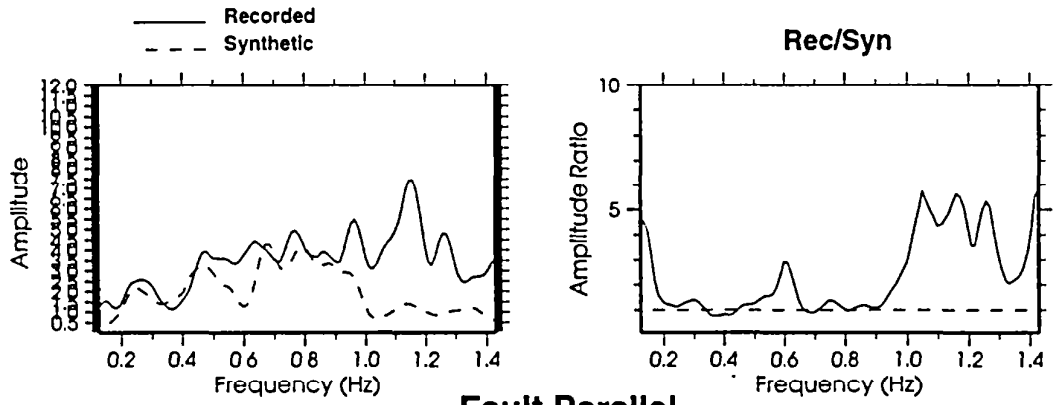

Fault Parallel

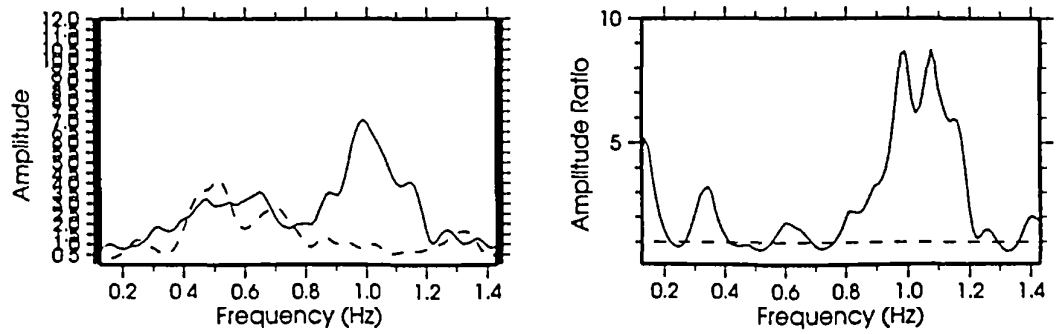

GMT Aug 24 18:13.55 1999 /net/coda/u2/arben/Kobe/shells

Kobe - Filter 0.125-1.43 Hz, Norma BB Sims - ama

Fault Normal

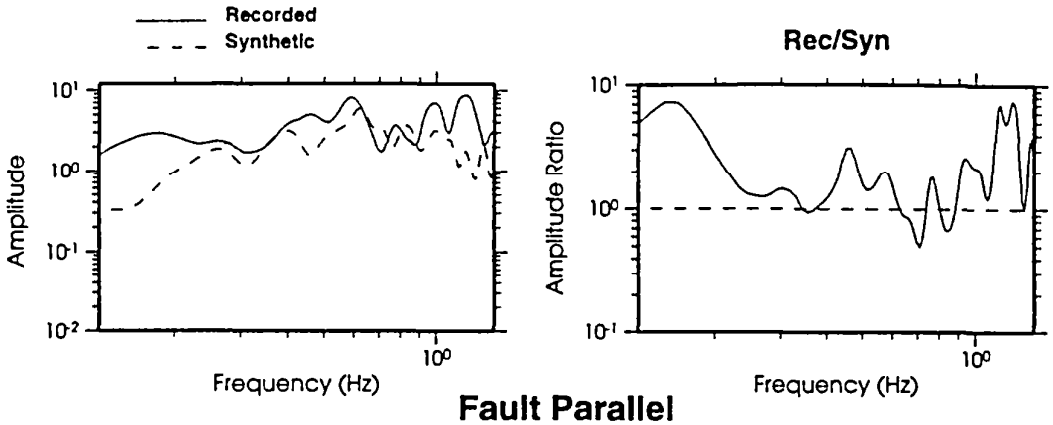

Fault Parallel

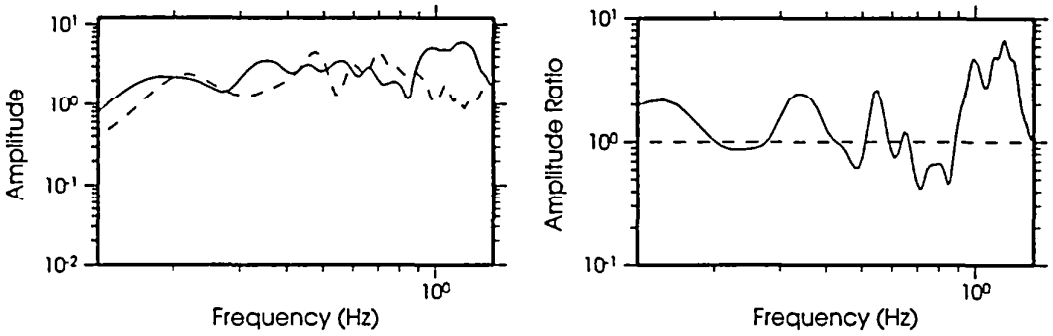

Fault Normal

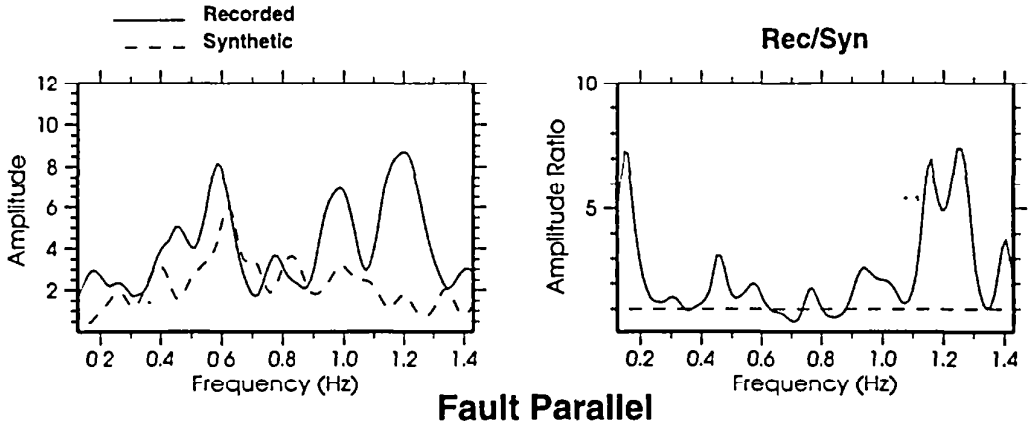

Fault Parallel

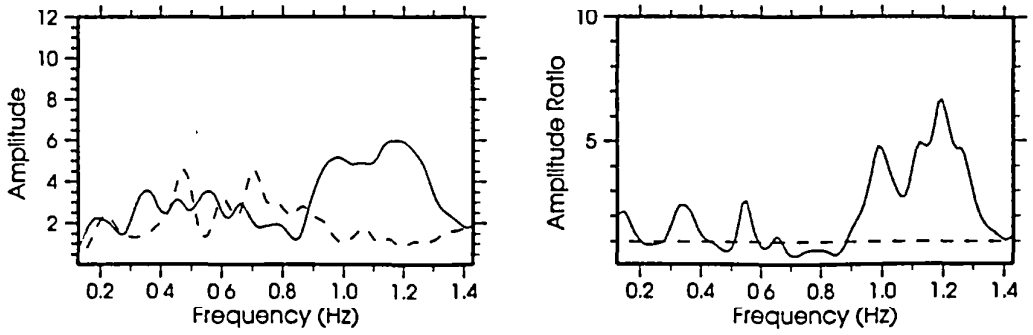

Kobe - Filter 0.125-1.43 Hz, Norma BB Sims - abn

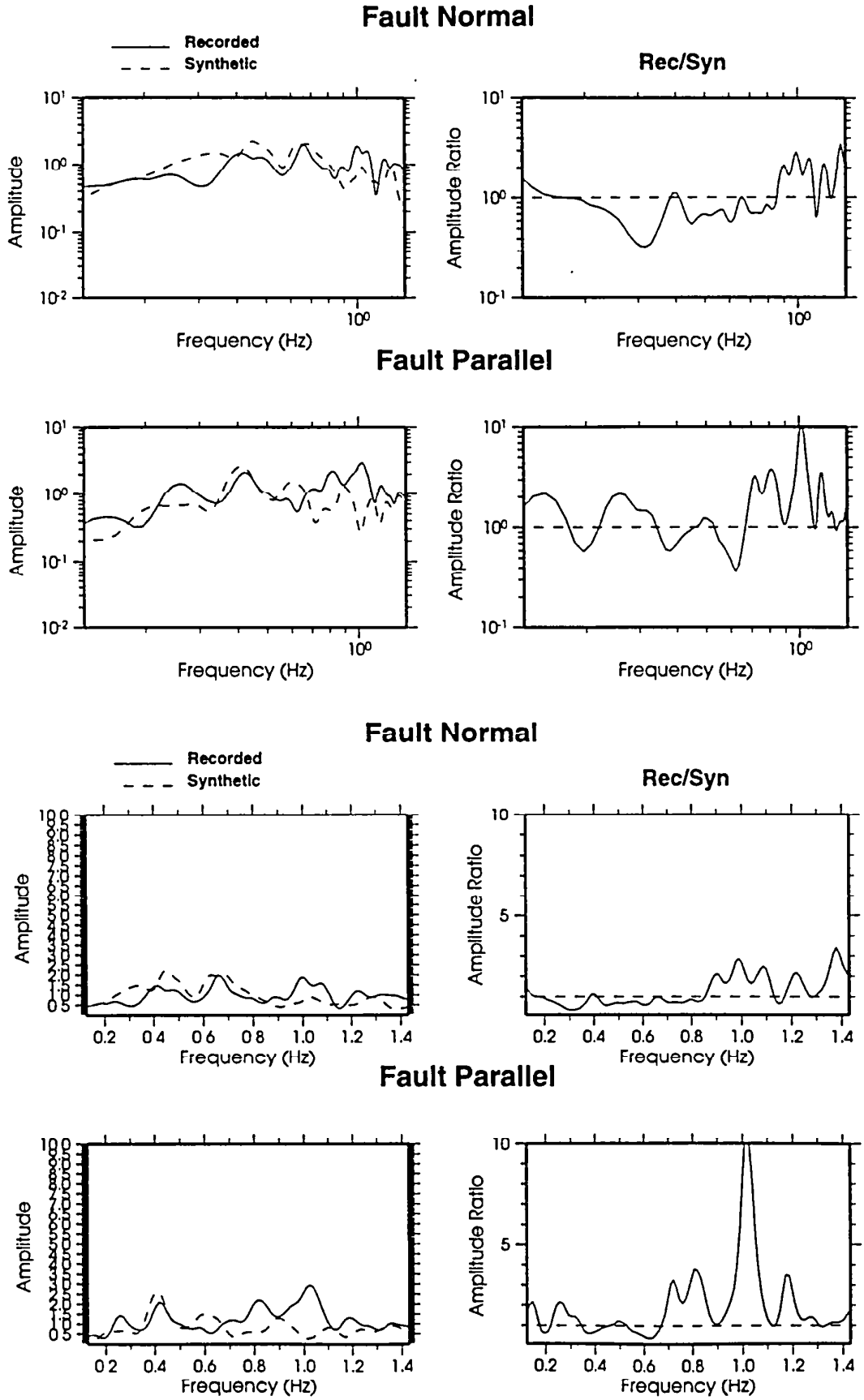

GMT Aug 24 18:13:44 1999 /net/coda/u2/arben/Kobe/shells

Kobe - Fault Normal

SA at 5.0 sec

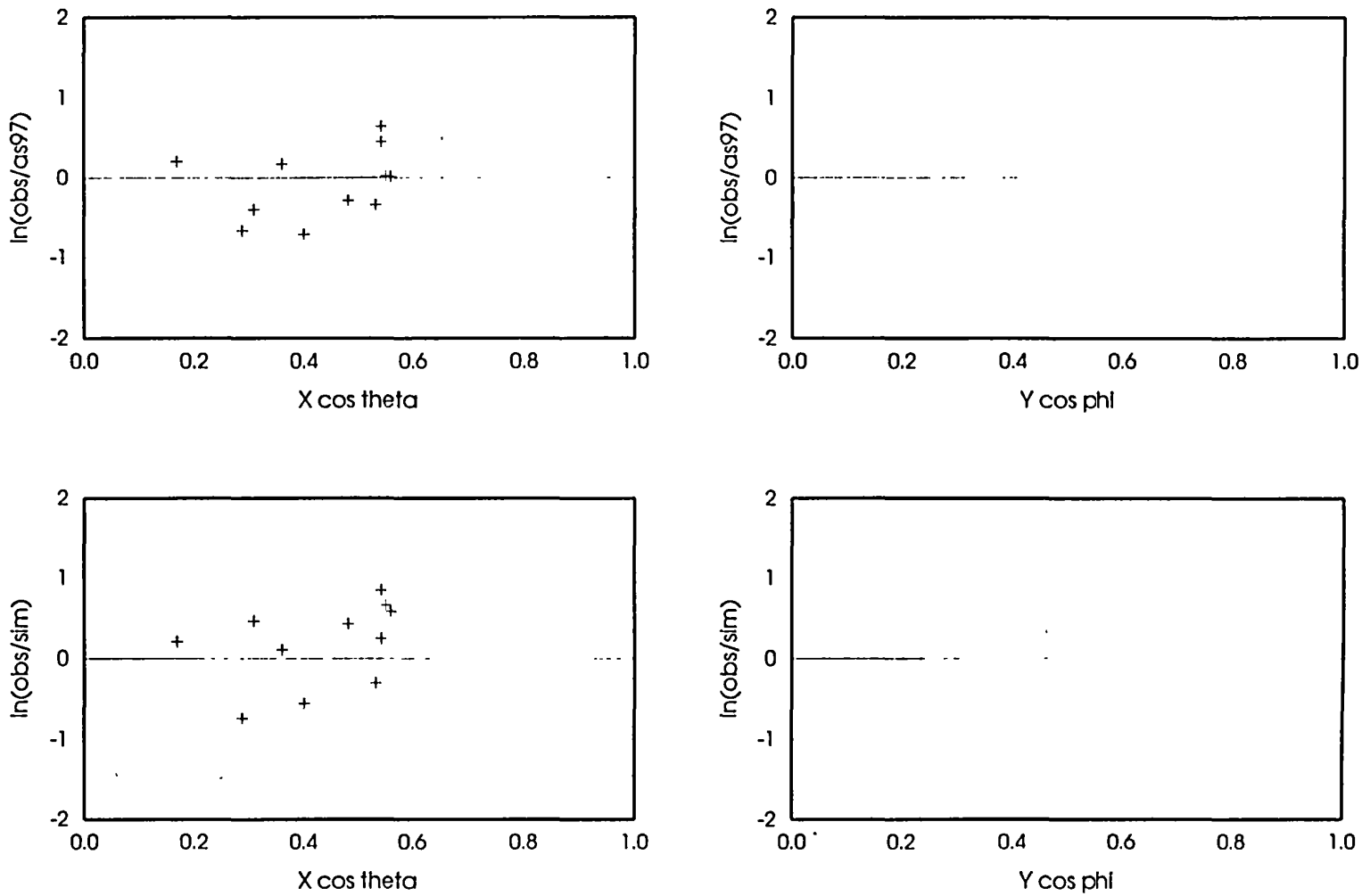

GMT Aug 24 17:56:17 1999 /net/coda/u2/arben/Kobe/Comparisons/Resid_plots

Kobe - Fault Parallel

SA at 5.0 sec

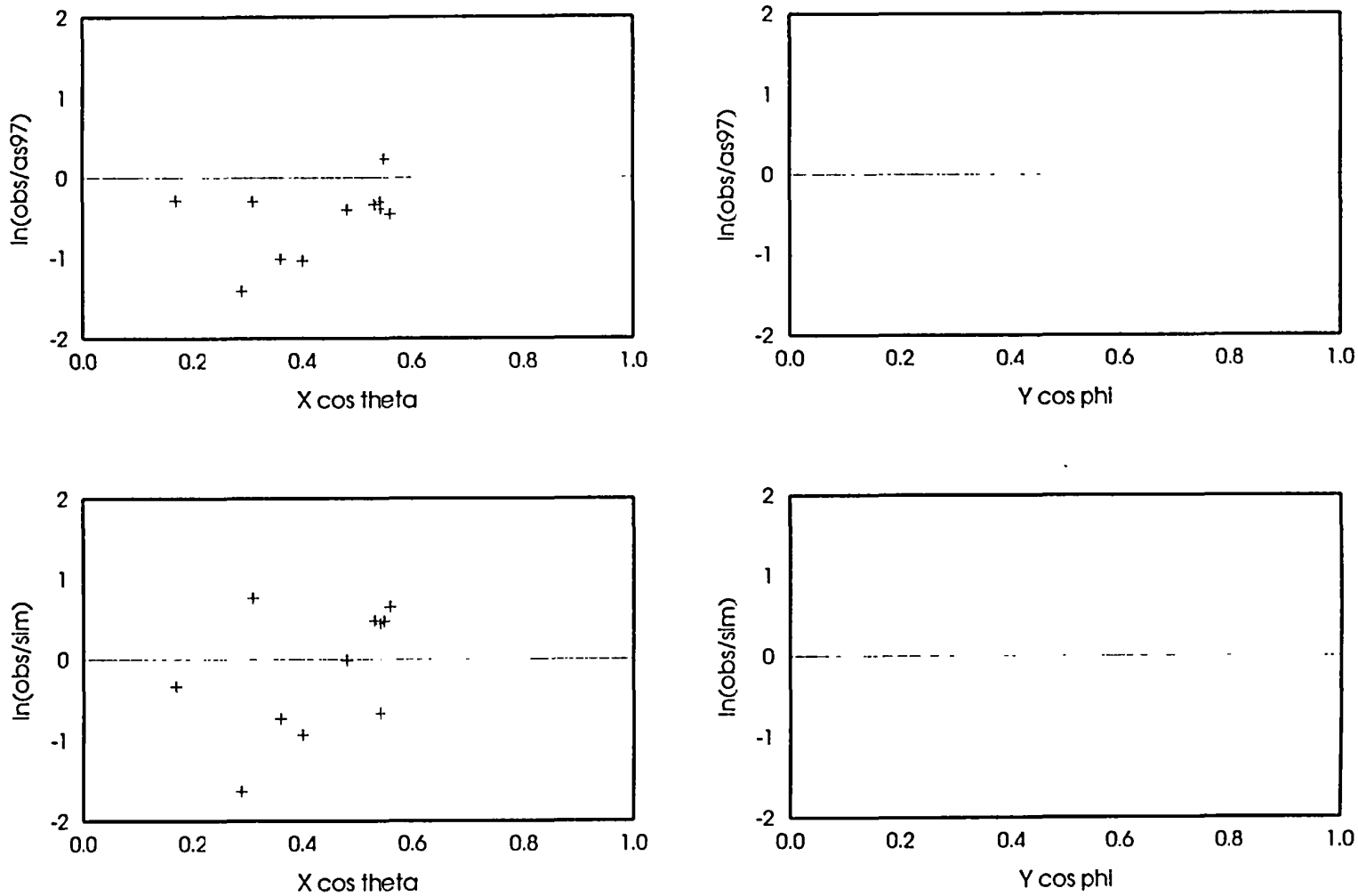

GMT Aug 24 17:56:19 1999 /net/coda/u2/arben/Kobe/Comparisons/Resid_plots

Kobe - Fault Normal

SA at 4.0 sec

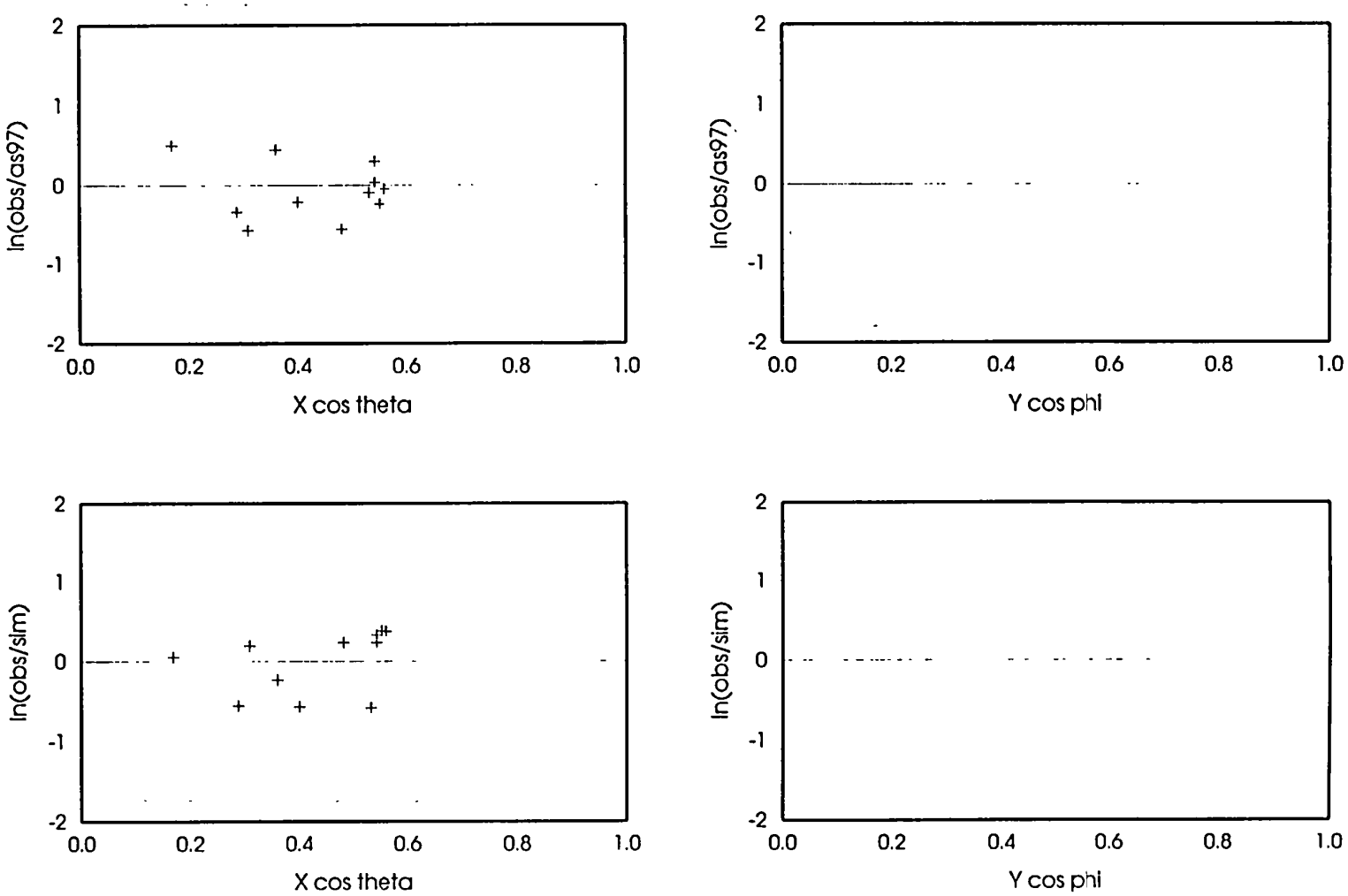

GMT Aug 24 17:56:21 1999 /net/coda/u2/arben/Kobe/Comparisons/Resid_plots

Kobe - Fault Parallel

SA at 4.0 sec

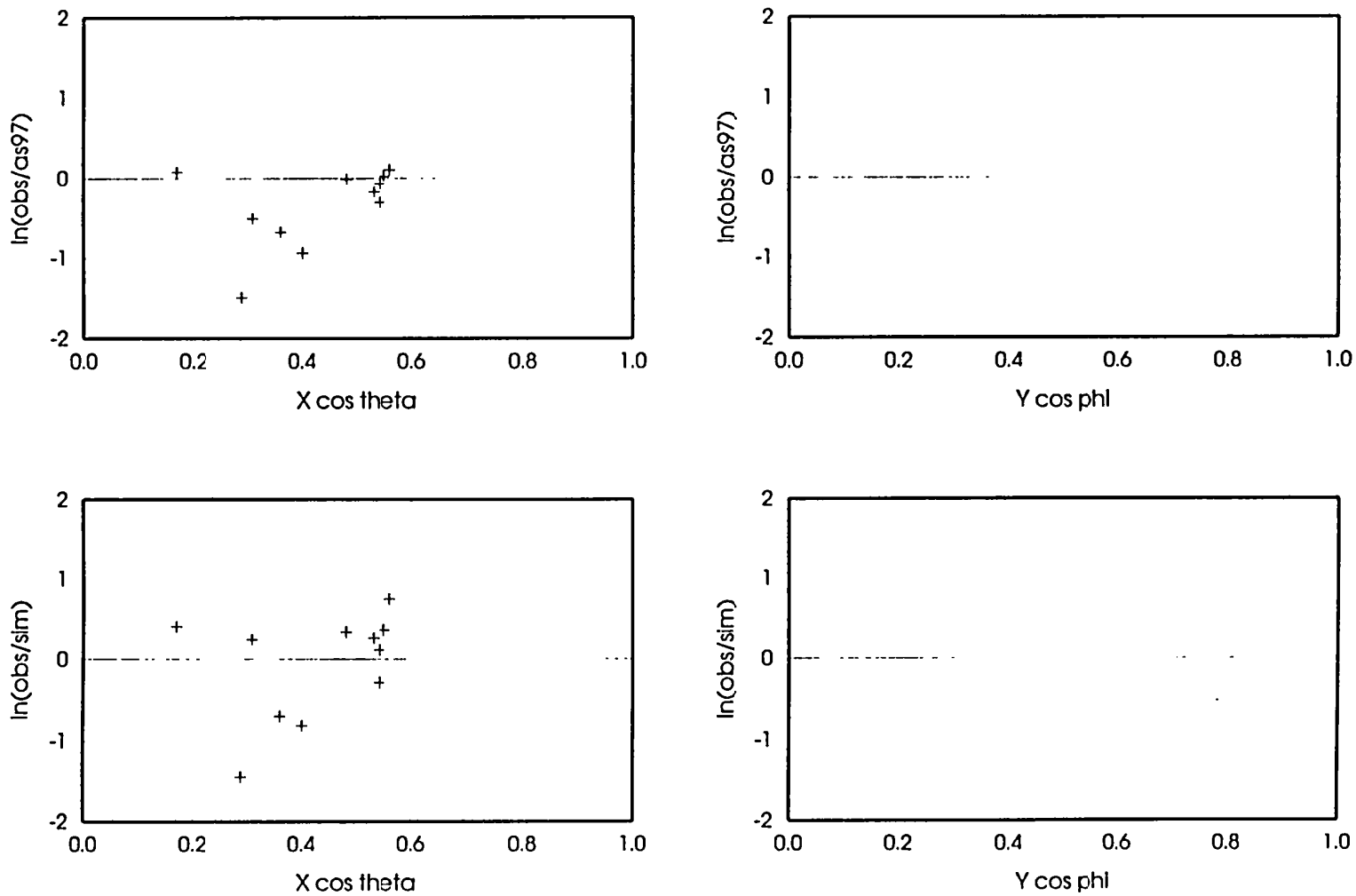

GMT Aug 24 17:56:23 1999 /net/coda/u2/arben/Kobe/Comparisons/Resid_plots

Kobe - Fault Normal

SA at 3.0 sec

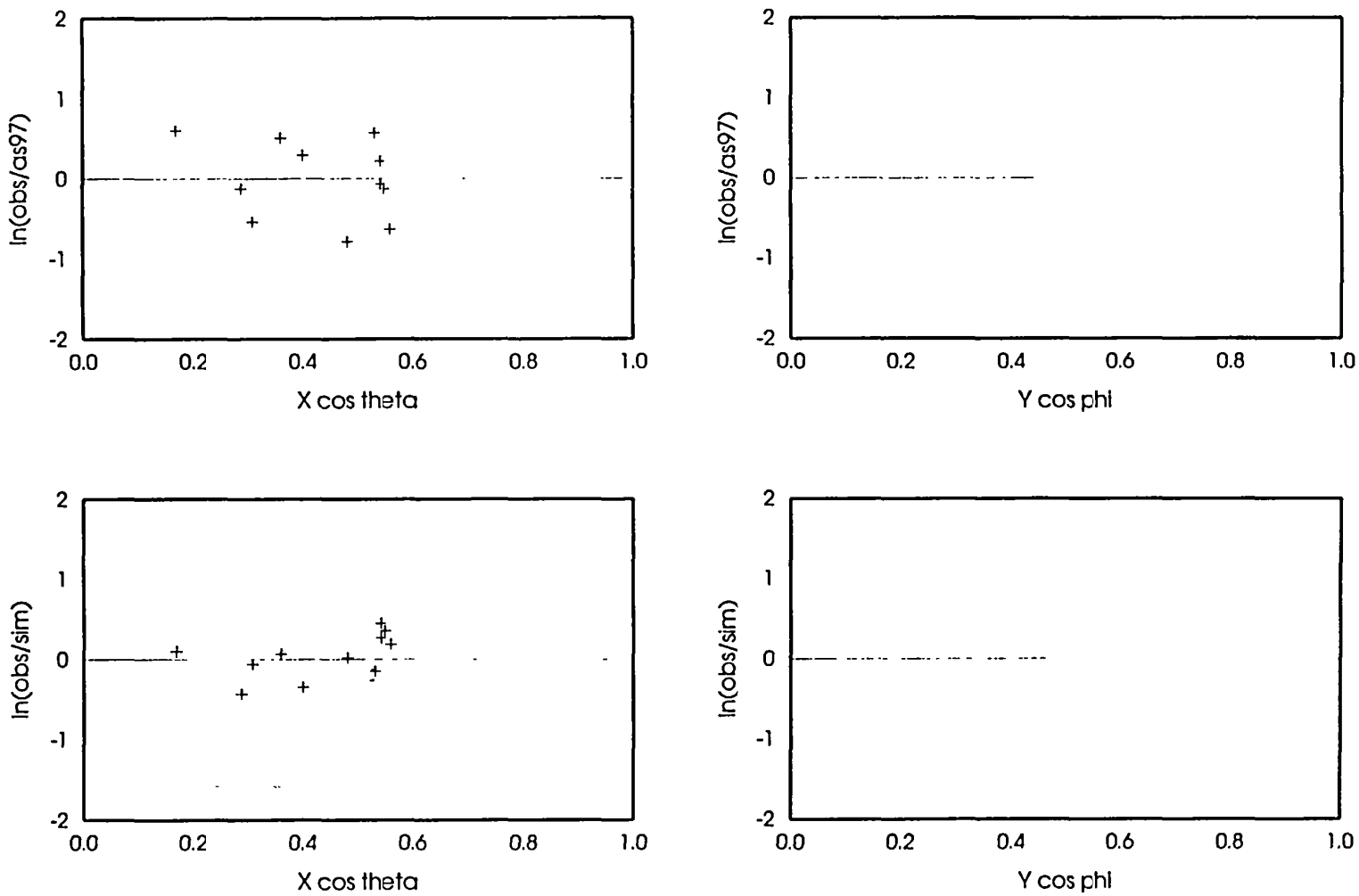

GMT Aug 24 17:56:26 1999 /net/coda/u2/arben/Kobe/Comparisons/Resid_plots

Kobe - Fault Parallel

SA at 3.0 sec

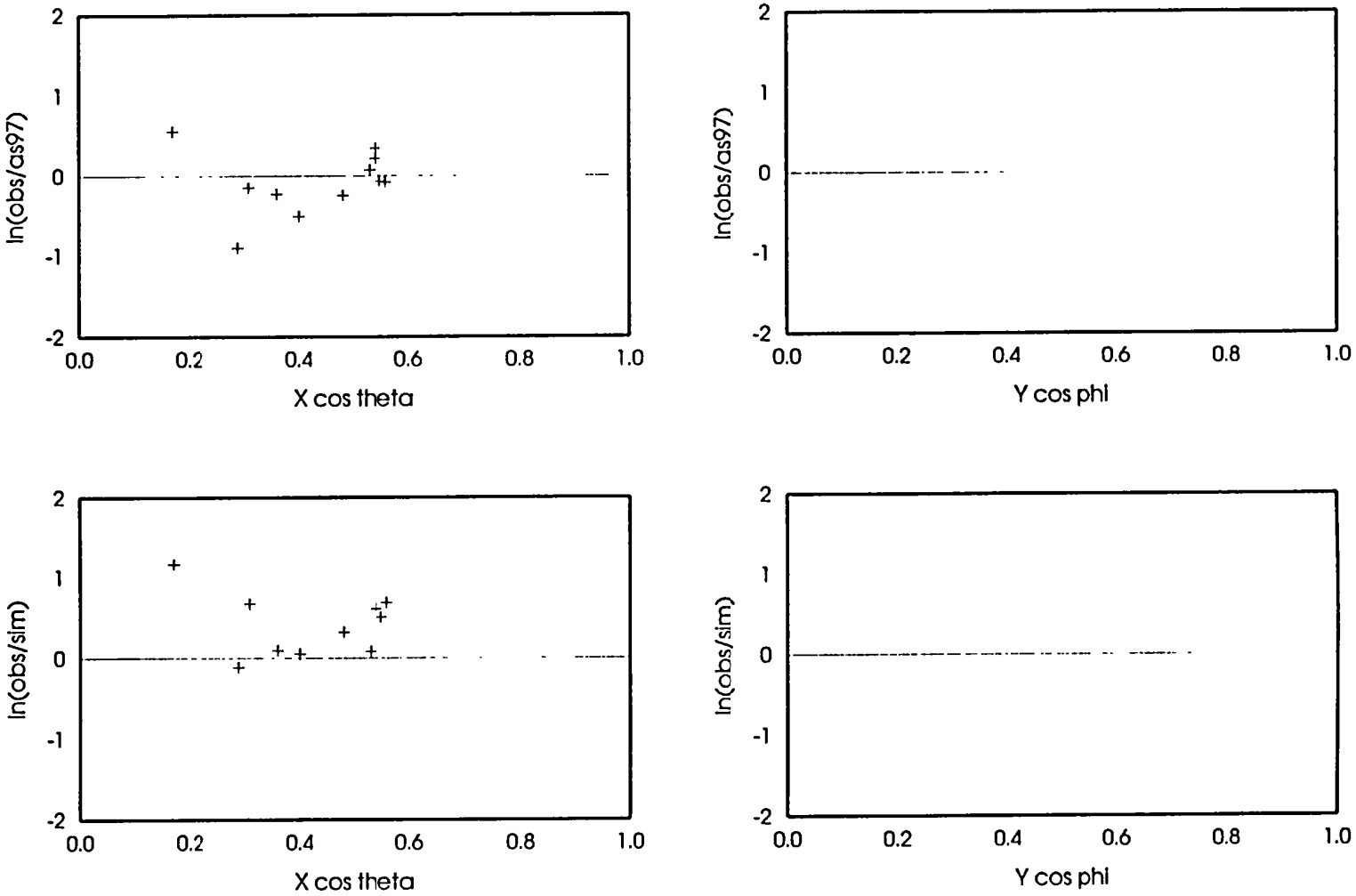

GMT Aug 24 17:56:28 1999 /net/coda/u2/arben/Kobe/Comparisons/Resid_plots

Kobe - Fault Normal

SA at 2.0 sec

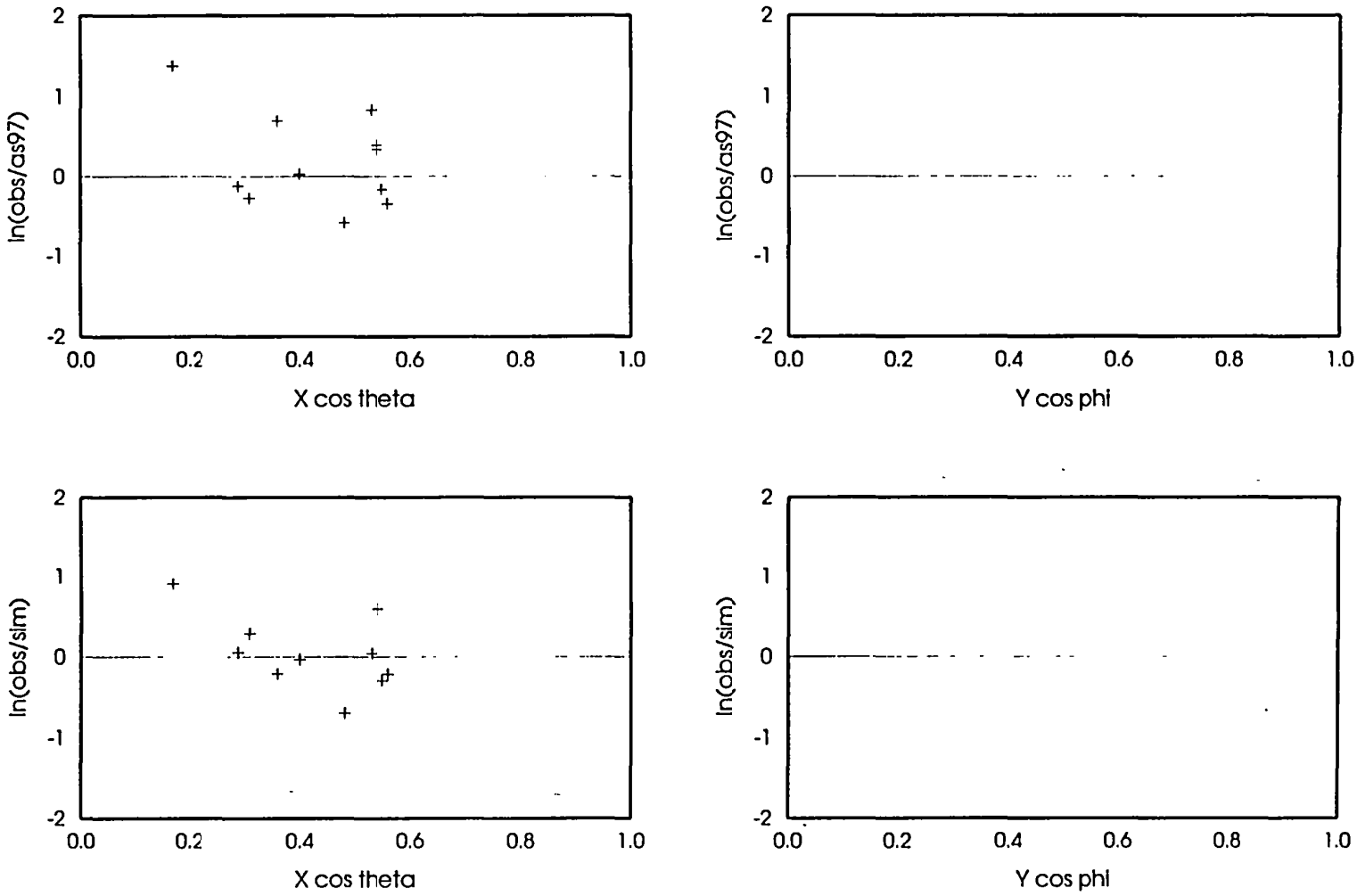

GMT Aug 24 17:56:30 1999 /net/coda/u2/arben/Kobe/Comparisons/Resid_plots

Kobe - Fault Parallel

SA at 2.0 sec

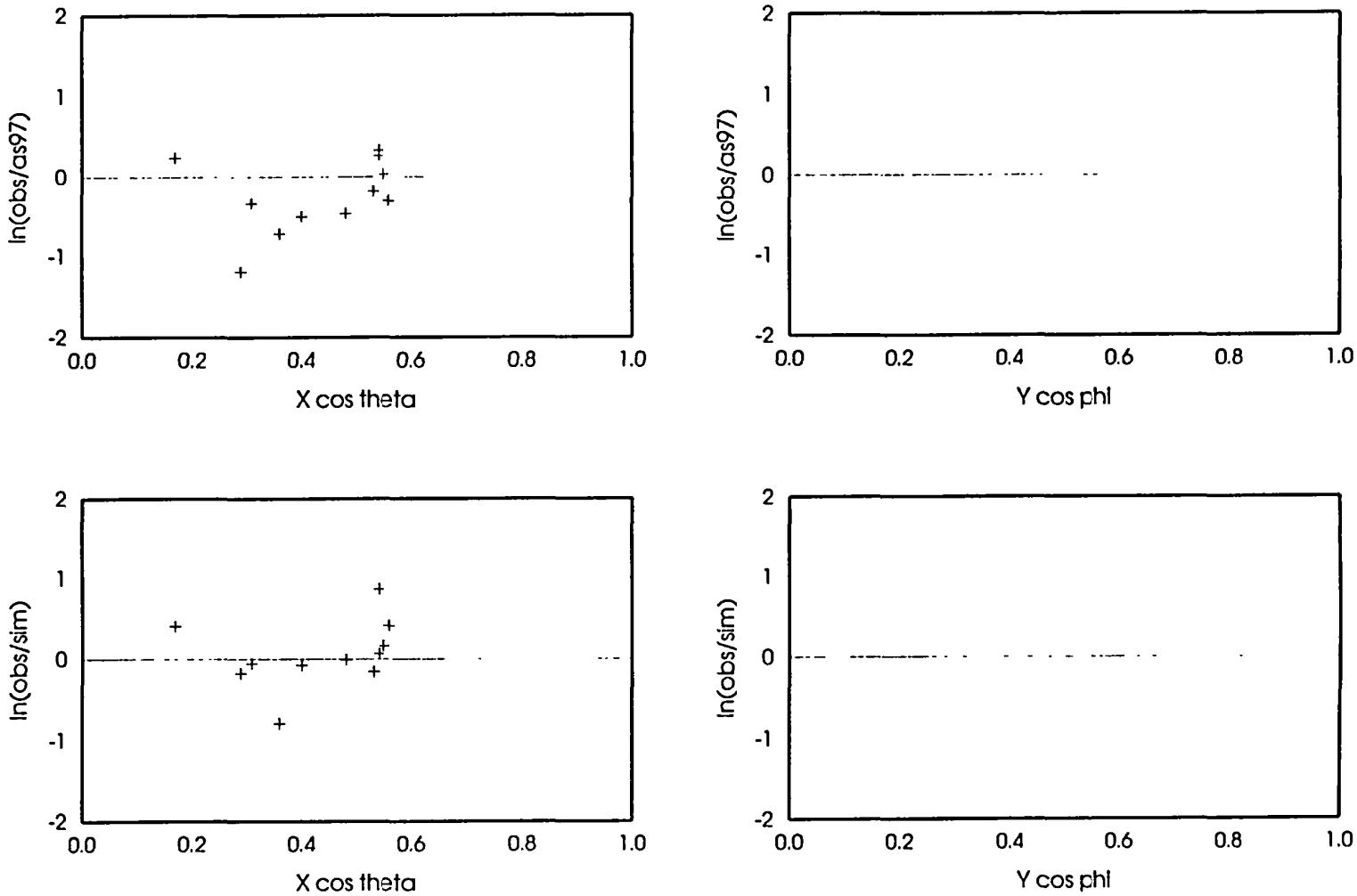

GMT Aug 24 17:56:32 1999 /net/coda/u2/arben/Kobe/Comparisons/Resid_plots

Kobe - Fault Normal

SA at 1.5 sec

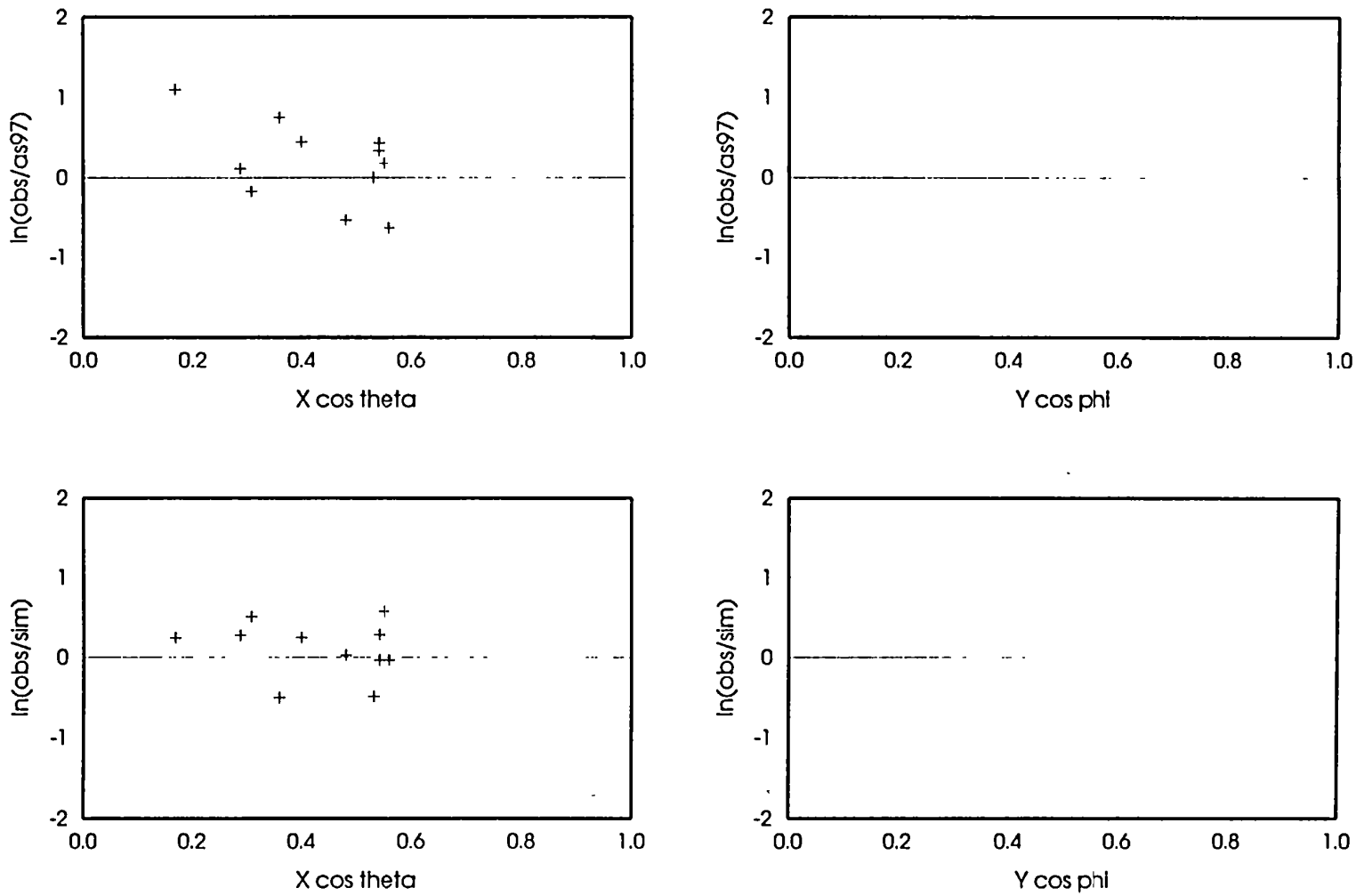

GMT Aug 24 17:56:34 1999 /net/coda/u2/arben/Kobe/Comparisons/Resid_plots

Kobe - Fault Parallel

SA at 1.5 sec

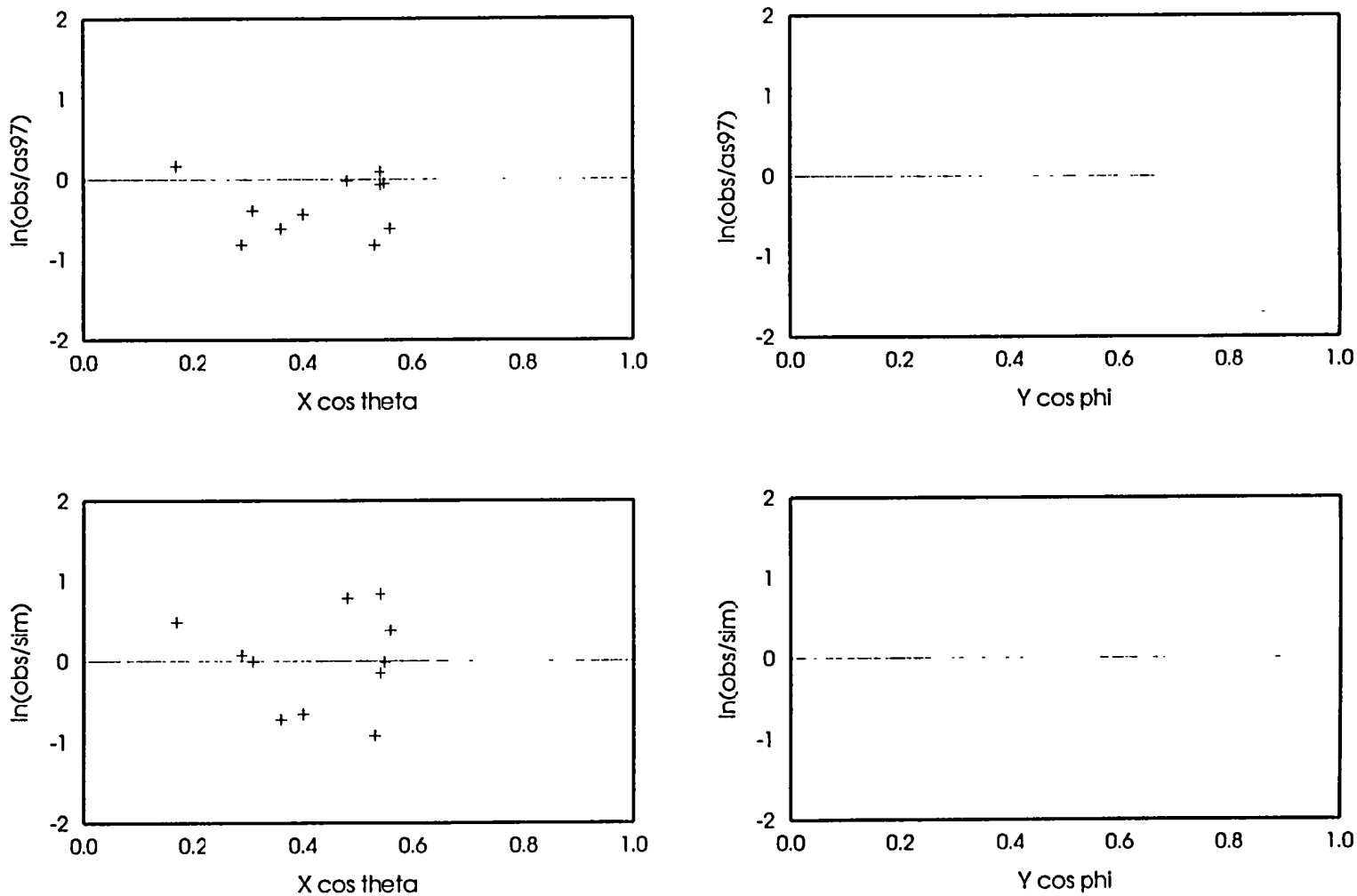

GMT Aug 24 17:56:36 1999 /net/coda/u2/arben/Kobe/Comparisons/Resid_plots

Kobe - Fault Normal

SA at 1.0 sec

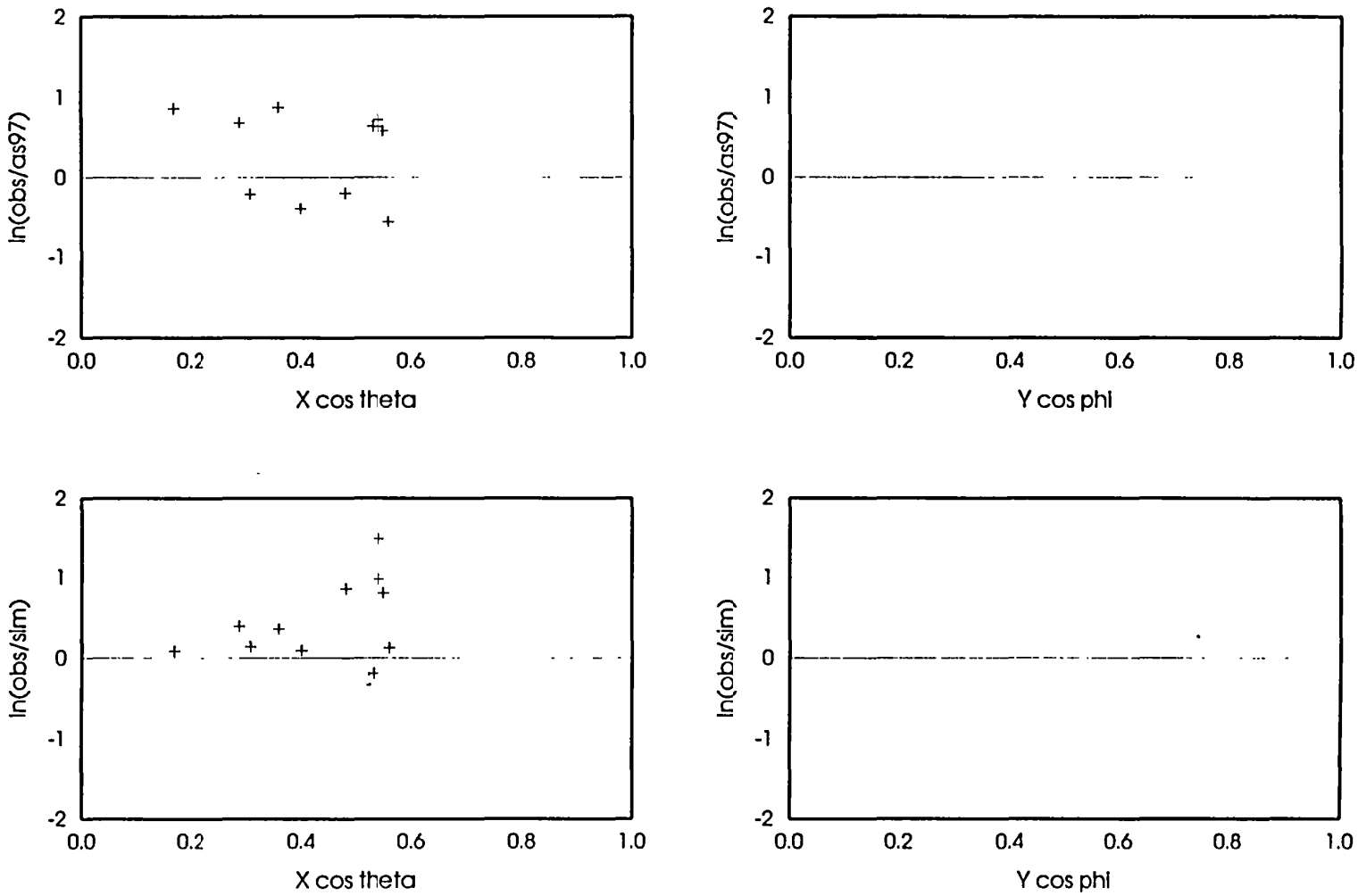

GMT Aug 24 17:56:38 1999 /net/coda/u2/arben/Kobe/Comparisons/Resid_plots

Kobe - Fault Parallel

SA at 1.0 sec

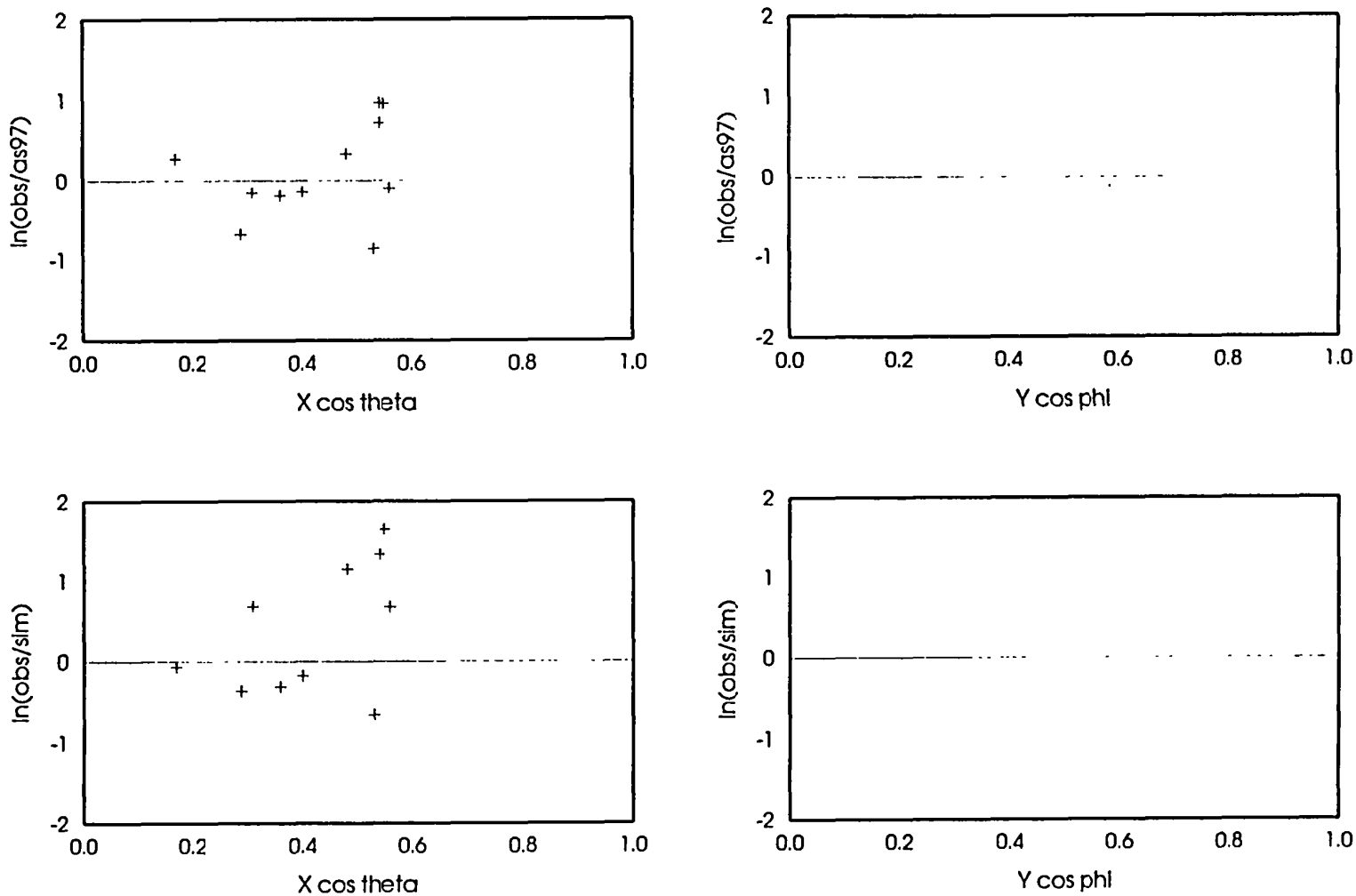

GMT Aug 24 17:56:40 1999 /net/ccda/u2/arben/Kobe/Comparisons/Resid_plots